Exploring the substrate range of selected myxobacterial cytochromes P450 from *Sorangium cellulosum* So ce56

Kumulative Dissertation

zur Erlangung des Grades

des Doktors der Naturwissenschaften

der Naturwissenschaftlich-Technischen Fakultät III

Chemie, Pharmazie, Bio- und Werkstoffwissenschaften

der Universität des Saarlandes

von

Dipl. Chem. Martin Litzenburger

Saarbrücken

2016

Tag des Kolloquiums:	12.05.2016
Dekan:	Prof. Dr. Dirk Bähre
Berichterstatter:	Prof. Dr. Rita Bernhardt
	Prof. Dr. Andreas Speicher
Vorsitz:	Prof. Dr. Claus Jacob
Akad. Mitarbeiter:	Dr. Michael Kohlstedt

Scientific contributions

This work is based on three original research papers reproduced in Chapter 2. The original manuscripts are printed with the kind of permissions from The American Society for Pharmacology and Experimental Therapeutics (Litzenburger *et al.* (2015)), Wiley-VCH Verlag GmbH&Co. KGaA (Schifrin *et al.* (2015)) and Springer Science and Business Media (Litzenburger *et al.* (2016)). The fourth manuscript was under review during the release of this thesis.

2.1 Litzenburger *et al.* (2015)

The author performed all experiments with the enzymes CYP109C1, CYP109C2, CYP109D1, CYP206A1, CYP260B1, CYP264A1 and CYP264B1 (*in vitro* conversions, whole-cell conversions, product purification and analyses of the NMR spectra) and drafted the manuscript. Fredy Kern performed all experiments with CYP267A1 and CYP267B1 and participated in writing the manuscript. The plasmids encoding the corresponding P450s as well as purified CYP109C1, CYP109C2, CYP109D1 and CYP264B1 were provided by Dr. Yogan Khatri. Furthermore, he participated in writing the manuscript. The project was supervised by Prof. Dr. Rita Bernhardt.

2.2 Schifrin *et al.* (2015)

The author performed the whole-cell conversions of cedrenol and zerumbone with CYP260A1 as well as the purification of the corresponding products. Furthermore, the author participated in writing the manuscript.

2.3 Litzenburger *et al.* (2016)

The author planed and performed all experiments and wrote the manuscript. The project was supervised by Prof. Dr. Rita Bernhardt.

2.4 Kern *et al.* (2016), submitted to Drug metabolism and Disposition

The author participated in the establishment of the analytical methods, expressed and purified CYP267B1 and performed the inhibition experiments. Furthermore, the author participated in writing the manuscript.

Content

Abstract:

Cytochromes P450 are highly versatile biocatalysts due to their ability to introduce molecular oxygen into a non-activated C-H bond. In this work, nine P450 enzymes from *Sorangium cellulosum* So ce56 were investigated concerning their substrate range and catalytic biodiversity. Hence, terpenes, terpenoids, carotenoid-derived aroma compounds, aromatic compounds and drugs were tested as potential substrates for CYP109C1, CYP109C2, CYP109D1, CYP260A1, CYP260B1, CYP264A1, CYP264B1, CYP267A1 and CYP267B1. Those systems showing a highly selective product pattern towards a single product were chosen to be scaled up in an *E. coli* based whole-cell system for the formation of sufficient amounts of products for structure elucidation via NMR spectroscopy. During these studies, tricyclic psychotherapeutic drugs, ionones, damascones as well as terpenes and terpenoids were identified as novel substrates for some the tested P450s and several of their products were characterized. For the carotenoid-derived aroma compounds and sesquiterpenes, novel products such as the hydoxylated derivatives of allyl-ionones and δ-damascone or the oxyfunctionalized derivatives of zerumbone and cedrenol were identified, whereas the conversion of tricyclic drugs led to the same metabolites as those produced by human P450s. These results demonstrate the high diversity towards the substrate range and reaction types performed by the myxobacterial P450s and, therefore, their potential biotechnological applications.

Zusammenfassung:

Cytochrome P450 sind vielseitig einsetzbare Biokatalysatoren, da sie molekularen Sauerstoff in eine nicht aktivierte C-H Bindung einbauen können. In dieser Arbeit wurden neun P450 Enzyme von *Sorangium cellulosum* So ce56 bezüglich ihrer Substratspezifität und katalytischen Vielfalt untersucht. Aus diesem Grund wurden Terpene, Terpenoide, Norisoprenoide, aromatische Moleküle und pharmazeutische Wirkstoffe als potentielle Substrate für CYP109C1, CYP109C2, CYP109D1, CYP260A1, CYP260B1, CYP264A1, CYP264B1, CYP267A1 und CYP267B1 untersucht. Die Substrate, deren Produktmuster eine hohe Selektivität für ein einzelnes Hauptprodukt zeigen, wurden mit Hilfe eines Ganzzellsystems im großen Maßstab umgesetzt, um eine ausreichende Menge an Produkt für die NMR Analyse zu erhalten. Dabei wurden trizyklische Psychopharmaka, Ionone, Damascone sowie verschiedene Terpene und Terpenoide als neue Substrate für einige dieser P450s identifiziert. Für die Norisoprenoide und Sesquiterpene wurden die hydroxylierten δ-Damascon- und Allyl-ionon-Derivate sowie die oxidierten Zerumbon- und Cedrenolderivative als neue Produkte identifiziert. Im Gegensatz dazu wurden die trizyklischen Wirkstoffe zu den gleichen Metaboliten umgesetzt, die schon von den humanen P450s bekannt sind. Diese Ergebnisse verdeutlichen die potentiellen biotechnologischen Anwendungsgebiete der myxobakteriellen P450s aufgrund ihres großen Substratspektrums sowie ihrer katalytischen Vielfältigkeit.

1. Introduction

1.1 Cytochromes P450

1.1.1 Background and nomenclature

In 1958, Garfinkel and Klingenberg discovered red pigments out of rat and pig livers, respectively (Garfinkel 1958; Klingenberg 1958). These pigments were named cytochrome P450 (P450) by Omura and Sato in 1962 due to their characteristic absorption maximum at 450 nm in the reduced and carbon monoxide bound form. In contrast, other hemo-proteins show a typical absorption maximum at 420 nm (Omura and Sato 1962). P450s contain a Fe^{3+}-ion that is coordinated by a protoporphyrin IX as well as water and cysteine as axial ligands, whereby cysteine causes the specific absorption maximum at 450 nm. In 1963, Estabrook, Cooper and Rosenthal discovered their enzymatic activity in the metabolism of steroids (Estabrook *et al.* 1963). One year later, Omura and Sato published the detailed spectroscopic properties as well as the location of P450s in mitochondria of adrenal cortex (Omura and Sato 1964a; Omura and Sato 1964b). The electron transfer proteins adrenodoxin reductase and adrenodoxin as well as the reconstitution of a NADPH-dependent steroid 11β-hydroxylase activity of a P450 were discovered in 1966 (Omura *et al.* 1966). The first bacterial P450 was found in *Rhizobium* bacteroids and, in contrast to the mammalian P450s, the *Rhizobium* P450 was soluble (Appleby 1967). Since that time, P450s were discovered in all domains of life and over 21,000 different P450s (http://drnelson.uthsc.edu/CytochromeP450.html) were already identified (Nelson 2011). They were found in mammalians, bacteria, archaea, fungi, plants and in 2009 the first viral P450 was discovered (Lamb *et al.* 2009). To classify this variety of P450s, a systematic nomenclature was introduced in 1987 (Nebert *et al.* 1987). The abbreviation CYP stands for cytochrome P450 while the first number gives the membership of the family (over 40% identity of the amino acid sequence). The first letter indicates the subfamily (over 55% identity of the amino acid sequence) and the last number represents the specific isoenzyme. The following figure shows the example of CYP260A1 from *Sorangium cellulosum* So ce56.

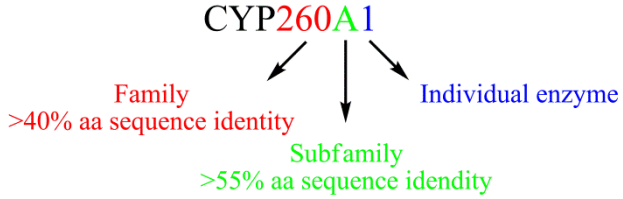

Figure 1: Nomenclature of the P450s exemplified by CYP260A1 from *Sorangium cellulosum* So ce56.

1.1.2 Functions and reactions

P450s belong to the class of oxidoreductases, enzymes that catalyze the electron transfer from one molecule to another one. P450s are monooxygenases and catalyze the activation of molecular oxygen, whereby one oxygen atom can insert into a non-activated C-H bond, whereas the other oxygen atom is reduced to water. The required electrons are provided by a cofactor such as NAD(P)H and delivered to the P450 by electron transfer proteins. Thus, the oxyfunctionalization of organic compounds is performed by P450s as shown in Figure 2.

The physiological roles of many P450s, especially for those found in bacteria, fungi and plants, are not discovered yet. In contrast, the physiological function of many human P450s has been identified, albeit there are still some orphan P450s (Guengerich and Cheng 2011). Human P450s are mainly involved in the biosynthesis of steroids, prostaglandins, vitamin D_3 or fatty acids as well as in the metabolism of drugs and other xenobiotics (Bernhardt 2006). The steroid hormone biosynthesis takes place in the adrenal cortex, whereby 6 P450s are capable of the formation of mineralocorticoids, glucocorticoids and sexual hormones. In contrast, the clearance of drugs is mainly performed in the liver and about 75% of all drugs are metabolized by P450s. Thereby, about 90% of the P450 catalyzed reactions can be accounted to CYP1A2, CYP2C9, CYP2C19, CYP2D6, and CYP3A4. The CYP3A enzymes play the most important role by performing about 45% of all P450 catalyzed reactions (Rendic and Guengerich 2014). In general, the liver P450s and steroidogenic P450s belong to the best characterized human P450s since steroidal P450s were discovered first and the characterization of drug metabolizing P450s is required by the pharmaceutical industry.

$$RH + NAD(P)H + H^+ + O_2 \xrightarrow{P450} ROH + NAD(P)^+ + H_2O$$

Figure 2: General reaction catalyzed by P450s

There are several different reaction types performed by P450s and still new types of reactions are being discovered (Coelho *et al.* 2013; Ren *et al.* 2015). The most common reactions catalyzed by these P450s are hydroxylation, epoxidation, N-, O- and S-dealkylation, the oxidation of heteroatoms as well as the oxidation of olefins and acetylenes. Besides these typical examples, there are several uncommon reactions catalyzed such as reduction, desaturation, oxidative ester cleavage, ring expansion, ring formation, aldehyde scissions, dehydration, one electron oxidation, coupling reactions, isomerization and several more (Guengerich 2001). These various types of reactions show the high diversity and importance of the P450s for the production of structurally diverse compounds. Also the substrate range differs for the various P450s. For example, the liver

P450 CYP3A4 is capable of the metabolism of about 27% of all drugs indicating its very broad substrate range (Rendic and Guengerich 2014). In contrast, other P450s like the steroid hydroxylase family CYP11B are very selective concerning their substrate range (Schiffer *et al.* 2015a). This substrate diversity is caused by the substrate recognition sites (see Figure 6) and turns the identification of novel or natural substrates to a challenging process.

1.1.3 Catalytic cycle

The catalytic cycle of P450s was first postulated in 1968 and several improvements were done since that time (Gunsalus *et al.* 1975). The analysis of intermediates involved in this cycle is challenging caused by some instable intermediates whose presence is short-time. Nevertheless, spectroscopic and crystallographic methods enabled the elucidation of several intermediates and it is postulated that there are eight intermediates involved in the catalytic reaction of P450s as shown in Figure 3 (Denisov *et al.* 2005). The cycle begins with water as sixth distal ligand to stabilize the low spin state of the ferric Fe^{3+} (1). Then the water is displaced by the substrate and the five coordinated heme iron shifts to the high-spin state (2). This spin shift causes a change in the redox potential and Fe^{3+} can be reduced to Fe^{2+} by the uptake of an electron (3). Molecular oxygen and carbon monoxide are strong ligands for the Fe^{2+} resulting either in the CO-bound form or in the case of the catalytic cycle in the oxy-ferrous state (4). This state is further reduced to a ferric peroxoanion (5a) leading to the ferric hydroperoxo intermediate (compound 0; 5b) after the uptake of a proton. This intermediate can release a water molecule after the acceptance of a further proton forming an iron-oxo state (compound I; 6). Compound I is highly reactive and can, therefore, interact with the substrate to form the oxygenated product. The exact mechanism of the hydroxylation step is not yet clarified, however, a two-state reactivity mechanism (TSR), in which compound I abstracts a hydrogen followed by a rebound of the alkyl radical, is proposed (Shaik *et al.* 2002). The newly formed product is then released and the cycle can restart. Besides the “typical” cycle, there are some uncoupling pathways like the autooxidation shunt, peroxide shunt or oxidase shunt (grey dashed arrows). These shunts decrease the catalytic efficiency by the unproductive consumption of NAD(P)H (Meunier *et al.* 2004).

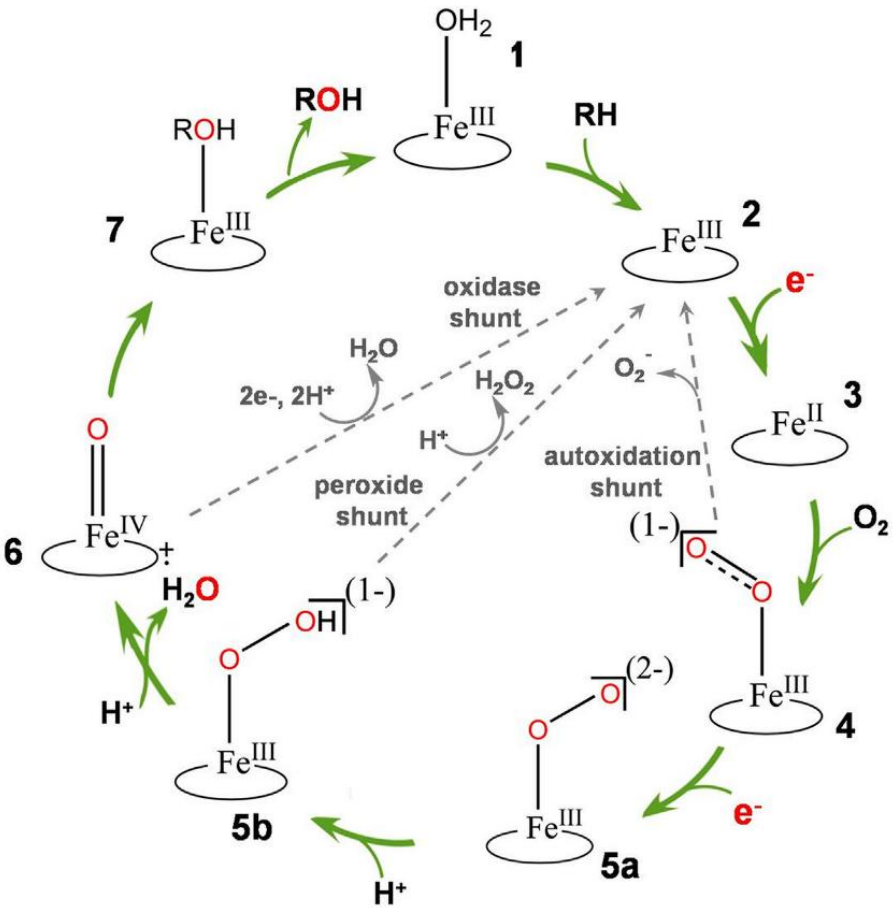

Figure 3: Catalytic cycle of the P450 mechanism. Figure was adopted from (Kiss *et al.* 2015).

The changes of the spin- and oxidation-state can be investigated by spectroscopic measurements. The carbon monoxide difference spectroscopy leads to the determination of the protein concentration (Omura and Sato 1964a; Omura and Sato 1964b). Additionally, binding studies of either substrates or inhibitors can be performed by studying the spin state shift of the heme iron. The high spin state is represented by an absorption maximum at 390-394 nm, whereas a maximum at 415-417 nm represents the low spin state. By adding a substrate to the protein solution, water is displaced as sixth ligand and the equilibrium shifts to the high spin state. The result is a typical type-I spectrum with a maximum at about 390-394 nm and a minimum at 415-417 nm. By adding an inhibitor, a typical type-II spectrum is obtained with a maximum at about 415-417 nm and a minimum at 390-394 nm (Meunier *et al.* 2004; Luthra *et al.* 2011).

1.1.4 Electron transfer partners

As shown in the cycle before, P450s need electrons from an external source to catalyze the oxyfunctionalization. The most common provider for electrons is NAD(P)H, however P450s are not able to interact with this cofactor in a direct way. As a result, additional electron transfer

proteins are required to enable the electron transfer between NAD(P)H and the P450. There are several classes of electron transport chains, whereby the mitochondrial and microsomal systems are the most prominent ones. The mitochondrial system in mammalians consists of a membrane anchored reductase possessing FAD as prosthetic group, and a soluble ferredoxin containing an iron sulfur cluster. On the other hand, the mammalian microsomal system consists of a single electron transport protein called NADPH cytochrome P450 reductase (CPR). The CPR is also membrane anchored and possesses both, a FAD and a FMN domain to transfer the electrons. The FAD domain interacts thereby as electron acceptor for NAD(P)H, whereas the FMN domain delivers electrons to the P450 (Wang *et al.* 1997). These two systems do not only exist in mammals but also in bacteria with the difference that all redox partners as well as the P450 are soluble in bacterial systems. There are several other classes of electron transfer systems known for the bacterial system including fusion proteins having the P450 and reductase components fused into a single polypeptide chain. CYP102A1 ($P450_{BM3}$) from *Bacillus megaterium* is the most prominent example of such a self-sufficient P450. Due to this specific property, $P450_{BM3}$ can directly interact with NAD(P)H and deliver the electrons to the iron of the heme domain (Hannemann *et al.* 2007).

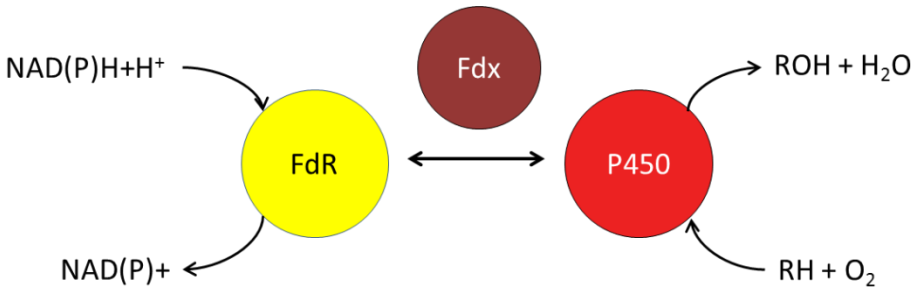

Figure 4: Class 1 electron transfer system of bacteria. The ferredoxin reductase (FdR), ferredoxin (Fdx) and P450 are soluble. The electrons are provided by the cofactor NAD(P)H, transferred to FdR and shuttled to the P450 by the ferredoxin.

The electron transfer proteins from *Sorangium cellulosum* So ce56 are analogous to the soluble class 1 system (see Figure 4). Two ferredoxin reductase genes and eight ferredoxin genes were identified in So ce56, whereby Fdr_A, Fdr_B, Fdx2 and Fdx8 were demonstrated as efficient electron transfer proteins for CYP260A1 (Ewen *et al.* 2009). Nevertheless, the application of autologous redox partners is not required, since several P450s are known for their interaction with heterologous electron transfer proteins (Hannemann *et al.* 2007). This can be explained by the highly conserved interaction domains of P450s as well as those of their redox partners (Hlavica 2015). Thereby, the application of heterologous redox partners is of interest for P450s whose natural redox partners are still not known. Additionally, replacing the redox partners by heterologous electron transfer proteins can lead to an increased product yield which is of

interest for biotechnological applications (Ringle *et al.* 2013; Brixius-Anderko *et al.* 2015; Kern *et al.* 2015). This might be explained by the higher activity of the heterologous redox partners, their solubility or their increased expression level. There is also a report about the altered reaction type after applying a fused or a non-fused hybrid redox system, respectively (Zhang *et al.* 2014). Hence, the choice of redox partners is a significant parameter regarding the efficiency of a catalytic system.

1.1.5 Structure of P450s

Although having an amino acid sequence identity frequently lower than 20%, P450s show a similar structural fold (Graham and Peterson 1999). In general, they usually possess 4 β-sheets and 12 α-helices (A-L) (see Figure 5). Thereby, the core is highly conserved showing a four helix bundle composed by the helices D, L, I and the antiparallel helix E, the helices J and K as well as two β-sheets and a coil called "meander" (Werck-Reichhart and Feyereisen 2000). The prosthetic heme group is confined between the distal I helix and proximal L helix and bound to the adjacent Cys-heme-ligand loop containing the P450 signature amino acid sequence FxxGx(H/R)xCxG. The cysteine residue as fifth ligand of the heme iron is conserved in all P450s and responsible for the characteristic 450 nm Soret band. The I-helix forms a wall of the heme pocket and contains the signature amino acid sequence (A/G)-Gx(E/D)T. Moreover, the highly conserved threonine is positioned in the active site and seems to be involved in the catalysis (Denisov *et al.* 2005).

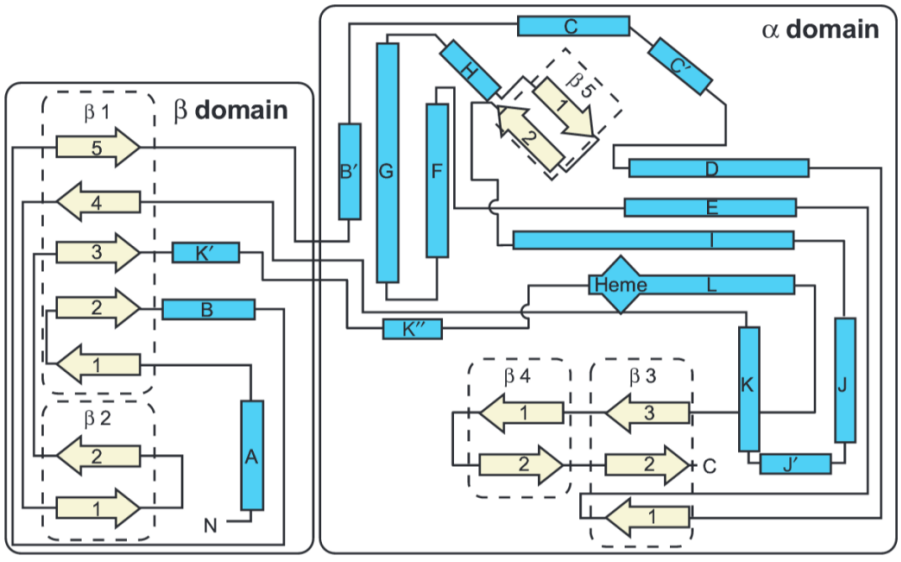

Figure 5: Topology diagram showing the secondary structure of CYP102. Blue boxes represent the α-helices and the cream arrows represent the β-sheets. Figure was adopted from (Werck-Reichhart and Feyereisen 2000).

Despite their structural similarity, the substrate range and selectivity differ for all P450s. There are six substrate recognition sites (SRS) capable of the predetermination of the substrate

specifity (see Figure 6). The SRSs consist of the B' helix (SRS1), parts of the F, G and I helices (SRS2, SRS3 and SRS4), the β4 hairpin (SRS5) and the K helix β2 connecting site (SRS6). The SRSs are more flexible protein regions and, therefore, involved in the substrate recognition and orientation (Gotoh 1992).

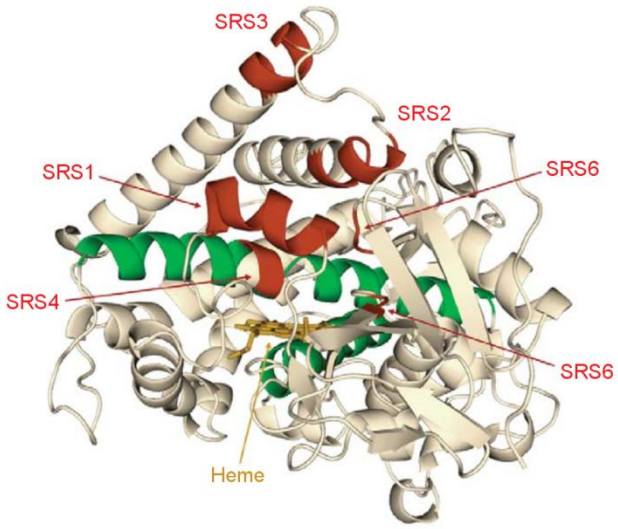

Figure 6: Model of the tertiary structure of a P450 monooxygenase. The heme is colored in orange, the substrate recognition sites (1-6) are colored in red and the heme coordinating helices I and L are shown in green. Figure was adopted from (Urlacher and Eiben 2006).

1.2 Bacterial P450s

1.2.1 General aspects

The first bacterial P450 was identified in *Bradyrhizobium japonicum* in 1967 but its natural function was not elucidated (Appleby 1967). P450cam (or CYP101) from *Pseudomonas putida* was described a little bit later and catalyzes the oxidation of camphor and was, therefore, the first bacterial P450 with a known functionality (Katagiri *et al.* 1968). This enzyme was also the first P450 for which the crystal structure was obtained (Poulos *et al.* 1985). In the last two decades, various sequencing projects revealed the appearance of P450 genes in diverse bacteria. The identification of the strictly conserved heme-binding domain signature is used for that purpose (Nelson 1999). So far, over 1,000 bacterial P450s were already identified (Kelly and Kelly 2013). For example, *Streptomyces avermitilis* has 33 P450 genes, *Sorangium cellulosum* So ce56 21, whereas *Escherichia coli* has none P450 genes (Kelly *et al.* 2003; Khatri *et al.* 2010b). The absence of P450s proves that these enzymes are not needed in all organisms, however, P450s seem to be essential for organisms with a higher complexity (Kelly *et al.* 2003).

The physiological role of many bacterial P450s is not identified yet; however, their biodiversity is often bound up with using different carbon sources for growth (Kelly and Kelly 2013). The bacterial P450 177A1 permits growth on hexahydro-1,3.5-trinitro-1,3.5-triazin (RDX) and subsequent phytoremediation (Rylott *et al.* 2006). Furthermore, *Candida tropicalis* is able to grow on oil, whereby P450s are involved in the metabolism of this carbon source (Lebeault *et al.* 1971). Besides their functions as carbon source metabolizer, there are several more natural functions elucidated. They are involved in the catabolism of camphor, fatty acids or cholesterol as well as in the biosynthesis of antifungal, antibacterial or anti-tumor agents such as nystatin, novobiocin or epothilone (Kelly and Kelly 2013). Nevertheless, the determination of their natural function is a challenging task even if the CYPome is known. Operons can give first clues for their enzymatic activities as well as experiments such as gene knock-outs or conversions of specific substrates with purified enzymes. However, organisms, where P450s are not associated with an operon or lacking of information about the metabolomics hinder the elucidation of the physiological roles of these P450s (Kelly and Kelly 2013).

Nevertheless, their unique catalytic activities towards structurally diverse compounds as well as their valuable properties, like high selectivity or expression rates turn these P450s in a promising tool for the oxyfunctionalization of organic compounds. Additionally, their solubility facilitates the handling of the microbial P450s compared with mammalian P450s (Bernhardt 2006). The solubility is not only accounting for the P450s but also for their natural redox partners influencing the catalyzed reactions in a significant manner (Ringle *et al.* 2013; Brixius-Anderko *et al.* 2015). Since there are bacterial P450s containing a fused electron transfer domain, the utilization of external redox partners is no longer required in these systems (Hannemann *et al.* 2007). The best characterized bacterial fusion P450 is CYP102A1 ($P450_{BM3}$) from *Bacillus megaterium*. It was discovered in 1987 and since that time the substrate free as well as several substrate-bound crystal structures were published. Besides the crystallographic characterization, it is also one of the best studied P450s towards protein engineering (Whitehouse *et al.* 2012). $P450_{BM3}$ and its mutants are capable of the conversion of structurally diverse classes of substrates ranging from fatty acids (Munro *et al.* 2002), over terpenes (Whitehouse *et al.* 2012) to drugs (Ren *et al.* 2015). Thereby, several reaction types like hydroxylation, epoxidation, dealkylation (Jung *et al.* 2011) as well as some novel reactions such as the formation of a protected imine from an amine (Ren *et al.* 2015) or the cyclopropantion by the $P411_{BM3}$ variant (Coelho *et al.* 2013) were observed.

1.2.2 Myxobacterial P450s from *Sorangium cellulosum* So ce56

Sorangium cellulosum So ce56 belongs to the group of myxobacteria, a group of gram-negative, unicellular bacteria with rod-shaped vegetative cells. Their specific characteristics are the gliding movement and the formation of fruiting bodies under starvation conditions (Shimkets *et al.* 2006). Myxobacteria are important producers of novel classes of secondary metabolites, like the anti-tumor agents epothilone A and B produced by the strain So ce90 (Gerth *et al.* 1996). Such metabolites may be used as drugs or might serve as lead structures for the development of novel drugs and, hence, attract the attention of the pharmaceutical industry (Newman and Cragg 2012). The involvement of P450s in the production of these complex molecules is known as shown for EpoK and its epoxidase activity towards epothilones C and D (Julien and Shah 2002). As a result, the investigation of myxobacteria as well as their P450s is of particular interest. The strain So ce56 has one of the largest genomes and was sequenced in 2007. Several polyketide synthases (PKS) and nonribosomal polypeptide synthetases (NPRS) were identified giving first insights into the secondary metabolism of this strain, whereby chivosazol, etnangien, myxochelin and flaviolin were characterized as products. Furthermore, there are additional PKS and NRPS domains whose products are not known as well as domains which are potentially involved in the carotenoid and terpenoid biosynthesis. Taken together, 17 unique loci involved in the secondary metabolism were identified (Schneiker *et al.* 2007).

Our laboratory investigated the CYPome of So ce56 and 21 P450 genes were identified, cloned and successfully expressed and purified (Khatri *et al.* 2010b). Moreover, the ferredoxins Fdx2 and Fdx8 as well as the reductases FdR_A and FdR_B were identified, expressed, purified and tested for their ability to transfer electrons to the myxobacterial P450s revealing their natural functionality (Ewen *et al.* 2009; Khatri *et al.* 2010b). Besides their natural redox partners, the non-physiological electron transfer partners adrenodoxin reductase (AdR) and adrenodoxin (Adx) as well as the truncated form $Adx_{4\text{-}108}$ from *Bos taurus* are also known for their efficient electron transfer (Khatri *et al.* 2010a). However, the physiological roles of these P450s are not known yet and also about potential substrates only little is known. Several substrate classes were already tested and fatty acids (Khatri *et al.* 2010b), carotenoid-derived aroma compounds (Khatri *et al.* 2010a; Ly *et al.* 2012), terpenes, terpenoids (Ewen *et al.* 2009; Schifrin *et al.* 2015) and steroids (Khatri *et al.* 2015) were found to act as substrates for some of the P450s.

To determine the reaction type and selectivity of the catalyzed reactions, the product(s) need to be analyzed. The most common techniques to elucidate the structures are mass spectrometry with database comparison of the fragment pattern, nuclear magnetic resonance spectroscopy or the comparison with an authentic standard. If standards are not available, MS or NMR analyses

are necessary for product identification. During MS analyses, the compounds are fragmented and the fragment patterns are compared with a database. Hence, an efficient database is required since it is very challenging to characterize novel compounds solely by their specific fragments. For that reason, NMR spectroscopy is preferred to elucidate the structure of novel compounds; however, higher amounts of products are necessary for NMR analysis. Sufficient amounts of products can be either obtained by scaling up the *in vitro* reaction or the application of a whole-cell system. Since the *in vitro* reactions require high amounts of purified enzymes (P450 and redox partners) and the expensive cofactor NADPH, the application of a scaled up *in vitro* system is limited. To overcome this problem, an *E. coli* based whole-cell system was established for some of the myxobacterial P450s (Ringle *et al.* 2013).

1.3 P450s as biocatalysts for biotechnological applications

The regio-, and stereoselective oxyfunctionalization of a non-activated C-H bond is a challenging task in the organic chemistry. In contrast, P450s are known for their highly selective catalytic activity under mild conditions. The lack of organic solvents and the absence of toxic chemicals like heavy metals is especially beneficial (Koeller and Wong 2001; Roiban and Reetz 2015). Furthermore, their diverse reaction types and broad substrate range is advantageous for biotechnological applications. However, the low activity, the utilization of redox partners, the requirement of the expensive cofactor NAD(P)H and uncoupling reactions limit their possible range of applications. Many of these limitations can be overcome by using techniques like protein engineering, optimization of the redox chain or the application of a cofactor regenerating system (Julsing *et al.* 2008; Bernhardt and Urlacher 2014). The increasing number of P450s with novel biotechnological properties, efforts in protein engineering techniques and improvements in whole-cell biocatalysis are helpful to turn P450s into a valuable tool for the green chemistry (Julsing *et al.* 2008). Besides employing them as single catalysts, there are also examples of combining P450s with synthetic chemistry in chemo-enzymatic approaches or the utilization of multiple enzymes in a cascade reaction (Rentmeister *et al.* 2009; Schulz *et al.* 2015).

P450s can be applied as biocatalysts for the production of fine chemicals and pharmaceutically active compounds (Kumar 2010). Terpenes and their oxygenated derivatives (terpenoids) represent an interesting group of fine chemicals that is of importance for the flavor and fragrance industry (Kraft *et al.* 2000). For example, $P450_{BM3}$ mutants are involved in the regioselective epoxidation of α-pinene and the optimization of the production process led to the formation of 1 g/l after 4h (Urlacher and Girhard 2012). Another interesting compound is (+)-nootkatone, a grapefruit flavour, formed by the oxidation of (+)-valencene. Urlacher and coworkers firstly used CYP109B1 from *Bacillus subtilis* to form the desired product nootkatone

out of valencene in a direct way. The utilization of a two liquid phase system to increase the yield led to a production of 120 mg/l with *cis*- and *trans*-nootkatol as side-products. However, the formation of nootkatol as side-product decreases the yield of nootkatone (Girhard *et al.* 2009). To avoid these side-products, a cascade reaction consisting of a P450 hydroxylating valencene to nootkatol and an alcohol dehydrogenase oxidizing the alcohol *in situ* to the desired nootkatone was used. This multi-enzyme approach led to a yield of over 300 mg/l (Schulz *et al.* 2015). Metabolic engineering is another method to obtain terpenoids. Such an approach uses several enzymes representing the metabolic pathway to form the precursor which is then further oxygenated. For example, diverse enzymes were expressed in *E. coli* to produce the terpene precursor GPP followed by a terpene synthase forming limonene. The additional expression of a P450 (CYP153 from *mycobacterium* HXN 1500) led to the formation of perillylic alcohol out of simple sugars with yields up to 100 mg/l (Alonso-Gutierrez *et al.* 2013). Besides the formation of terpenoids, there are several other classes of substrates which can be used for the production of fine chemicals such as fatty acids or alkanes (Picataggio *et al.* 1992; Liu *et al.* 2004).

The production of pharmaceutical and medicinal compounds is also of considerable interest, since P450s are involved in the metabolism of drugs. Drug metabolites might have adverse effects and a possible toxicity must be determined. Hence, the Food and Drug administration as well as the European Medicines agency presented their guidelines concerning the safety testing of drug metabolites. Drug metabolites formed at greater than 10% of the parent drug systemic exposure at steady state or total drug-related exposure need to be tested in toxicological studies (FDA 2008; ICH 2009). Moreover, these metabolites might be used as authentic standards for analytical purposes or also used as drugs or lead structure to develop novel pharmaceutical compounds. The production of these metabolites can be performed by either mammalian or bacterial P450s, whereby engineering of the P450s is often necessary. Many bacterial P450s need to be engineered to enable the biotransformation of the non-natural substrates (Ren *et al.* 2015). In contrast, mammalian P450s are capable of the desired conversion but often show a low activity or the formation of multiple products and, hence, require improvements by protein engineering, too. However, bacterial P450s seem to be more suitable due to their high turnover rates, stability and expression levels (Urlacher *et al.* 2004; Julsing *et al.* 2008).

P450s are also capable of the oxyfunctionalization of structurally diverse compounds in the secondary metabolism of plants and bacteria (Podust and Sherman 2012). Between 1981 and 2010, 1334 drugs were approved of which 64 are natural products, 202 have a biological origin, 299 are derivatives of natural products and 323 are synthetics mimicking a natural product (Newman and Cragg 2012). This distribution shows the influence of secondary metabolites and

myxobacteria are known as top producers of such biologically active compounds (Reichenbach and Hofle 1993). Epothilones are produced by the myxobacterium So ce90 and these compounds attract the attention of the pharmaceutical industry due to their anti-tumor activity (Gerth *et al.* 1996). There are already examples of the biotechnological application of P450s in the biosynthesis of secondary metabolites such as the anticancer drug taxol or artemisinin, an agent for the treatment of malaria (Ajikumar *et al.* 2010; Paddon *et al.* 2013). Additionally, in the biosynthetic pathway for the production of the anti-cholesterol drug pravastatin, P450sca from *streptomyces carbophilus* is used (Matsuoka *et al.* 1989). These applications of P450s for the formation of biologically active secondary metabolites show the significance of these enzymes for the regio-, and stereoselective oxyfunctionalization of complex molecules.

Due to their involvement in the steroid hormone biosynthesis, P450s are also employed in the biotechnological production of steroids and their derivatives. An article about the screening of bacterial P450s for their selective hydroxylase activity towards testosterone was published in 2006 and shows the activity of such P450s for the highly selective formation of a single main product (Agematu *et al.* 2006). Two reviews about the microbial biotransformation of steroidal compounds were published in 2012, showing the significance of these enzymes towards steroid conversion (Bhatti and Khera 2012; Donova and Egorova 2012). However, microbial conversions employing whole organisms lack the information about the specific enzyme that is capable of the desired reaction. Furthermore, the probability of a multi-hydroxylation reaction caused by the involvement of more than one enzyme is much higher. But this screening approach is the fastest way to identify new product patterns. Thereby, novel hydroxylase activities are of high interest, since the introduction of a hydroxyl-group alters the chemo-physical properties of the molecule. The influence of such a functional group can be shown for steroids hydroxylated in position 11 and their resulting anti-inflammatory effect (Ruhmann and Berliner 1967). A novel hydroxylase activity was recently found for a P450 from So ce56, where CYP260A1 acts as 1α-hydroxylase for C19 steroids, however, the functions of these new compounds were not investigated yet (Khatri *et al.* 2015).

Taken together, P450s are valuable tools in the biotechnological production of fine chemicals and biologically active compounds, whereby investigations of novel or improved activities are a promising field of research.

1.4 Aims and scope

The aim of this work is the investigation of myxobacterial P450s from *Sorangium cellulosom* So ce56 towards their substrate range and biodiversity. Their physiological roles and, hence, their substrate range are not identified yet. About potential substrates and performed reactions only little is known and, as a result, several classes of substrates should be tested for their ability to act as a substrate for these P450s. For that purpose, terpenes, terpenoids, carotenoid-derived aroma compounds, small aromatic compounds and diverse drugs, which are known to serve as substrates for other P450s, were chosen. Initially, all substrates should be tested in a reconstituted *in vitro* system with the P450s CYP109C1, CYP109C2, CYP109D1, CYP260A1, CYP260B1, CYP264A1, CYP264B1, CYP267A1 and CYP267B1. To perform such *in vitro* reactions, the expression and purification of the corresponding P450s as well as the redox partners, adrenodoxin and adrenodoxin reductase, is necessary. Moreover, efficient extraction methods need to be established for each substrate class to recover the substrates as well as their corresponding products. The conversions should then be analyzed by HPLC-DAD or GC-MS depending on the physical properties of the analytes such as UV-absorption or volatility. For this purpose, substrate class dependent HPLC- and GC-methods are required.

Those systems showing a selective product pattern during the *in vitro* conversions should be further analyzed to elucidate the structures of the products. For that reason, the reactions need to be scaled up by utilizing an *E. coli* based whole-cell system harboring the corresponding P450 as well as the redox partners Fpr and Adx. Using such an approach, sufficient amounts of products of at least 5 mg should be obtained to enable the structure identification via NMR-spectroscopy. To fulfill that requirement, the whole-cell systems need optimizations towards the yields by testing diverse conversion conditions like performing the reaction with growing cells or resting cells in buffer. Furthermore, the utilization of additives such as cell permeabilizing agents like EDTA is often necessary to reach the desired productivity. Before the products can be characterized, individual purification strategies based on either preparative HPLC or column chromatography with silica gel need to be developed for each class of compounds. The purified products should then be characterized by HPLC-DAD and GC-MS as well as by several NMR techniques such as ^{1}H, ^{13}C, HSQC, HMBC, COSY and NOESY to identify the reaction types performed by these P450s. Furthermore, the corresponding structures should give insights into the regio- and stereoselectivity of the catalyzed reactions.

The elucidated products should then be compared with the products formed by other P450s to check if the myxobacterial P450s are capable of some unique reaction types or showing certain

regio- and stereoselectivities. Moreover, the substrate range and the biocatalytic activities of the myxobacterial P450s should lead to some speculations about their potential natural functions.

2. Scientific articles

The results of this work were published in the articles listed below:

2.1 Conversions of tricyclic antidepressants and antipsychotics with selected P450s from *Sorangium cellulosum* So ce56
Martin Litzenburger, Fredy Kern, Yogan Khatri, and Rita Bernhardt

2.2 New Sesquiterpene Oxidations with CYP260A1 and CYP264B1 from *Sorangium cellulosum* So ce56
Alexander Schifrin, Martin Litzenburger, Michael Ringle, Thuy TB Ly, and Rita Bernhardt

2.3 Selective oxidation of carotenoid-derived aroma compounds by CYP260B1 and CYP267B1 from *Sorangium cellulosum* So ce56
Martin Litzenburger and Rita Bernhardt

2.4 CYP267A1 and CYP267B1 from *Sorangium cellulosum* So ce56 are highly versatile drug metabolizers (submitted to Drug metabolism and Disposition)
Fredy Kern, Yogan Khatri, Martin Litzenburger, and Rita Bernhardt

2.1 Conversions of tricyclic antidepressants and antipsychotics with selected P450s from *Sorangium cellulosum* So ce56

Martin Litzenburger, Fredy Kern, Yogan Khatri, and Rita Bernhardt

Drug Metabolism and Disposition, 2015 Mar, 43(3), 392-399

doi: 10.1124/dmd.114.061937

Supplemental material to this article can be found at:
http://dmd.aspetjournals.org/content/suppl/2014/12/30/dmd.114.061937.DC1.html

1521-009X/43/3/392–399$25.00
DRUG METABOLISM AND DISPOSITION

http://dx.doi.org/10.1124/dmd.114.061937
Drug Metab Dispos 43:392–399, March 2015

DRUG METABOLISM & DISPOSITION

Conversions of Tricyclic Antidepressants and Antipsychotics with Selected P450s from *Sorangium cellulosum* So ce56 [S]

Martin Litzenburger, Fredy Kern, Yogan Khatri, and Rita Bernhardt

Institut für Biochemie, Universität des Saarlandes, Saarbruecken, Germany (M.L., F.K., Y.K., R.B.)

Received November 13, 2014; accepted December 30, 2014

ABSTRACT

Human cytochromes P450 (P450s) play a major role in the biotransformation of drugs. The generated metabolites are important for pharmaceutical, medical, and biotechnological applications and can be used for derivatization or toxicological studies. The availability of human drug metabolites is restricted and alternative ways of production are requested. For this, microbial P450s turned out to be a useful tool for the conversion of drugs and related derivatives. Here, we used 10 P450s from the myxobacterium *Sorangium cellulosum* So ce56, which have been cloned, expressed, and purified. The P450s were investigated concerning the conversion of the antidepressant drugs amitriptyline, clomipramine, imipramine, and promethazine; the antipsychotic drugs carbamazepine, chlorpromazine, and thioridazine, as well as their precursors, iminodibenzyl and phenothiazine. Amitriptyline, chlorpromazine, clomipramine, imipramine, and thioridazine are efficiently converted during the in vitro reaction and were chosen to upscale the production by an *Escherichia coli*–based whole-cell bioconversion system. Two different approaches, a whole-cell system using M9CA medium and a system using resting cells in buffer, were used for the production of sufficient amounts of metabolites for NMR analysis. Amitriptyline, clomipramine, and imipramine are converted to the corresponding 10-hydroxylated products, whereas the conversion of chlorpromazine and thioridazine leads to a sulfoxidation in position 5. It is shown for the first time that myxobacterial P450s are efficient to produce known human drug metabolites in a milligram scale, revealing their ability to synthesize pharmaceutically important compounds.

Introduction

Cytochromes P450 (P450s) are heme-thiolate monooxygenases. They are present in nearly all organisms and belong to one of the largest superfamilies of enzyme proteins (Nelson, 2011). P450s are involved in the degradation and detoxification of drugs and xenobiotics, as well as in the metabolism of steroid hormones, lipids, and antibiotics (Bernhardt, 2006; Bernhardt and Urlacher, 2014). In general, P450s catalyze the insertion of a molecular oxygen atom into organic molecules while the other oxygen atom is reduced to water. Beside the hydroxylation, they catalyze a broad range of reactions such as sulfoxidation, epoxidation, deamination, dehalogenation, and N-, O-, and S-dealkylation (Sono et al., 1996; Bernhardt and Urlacher, 2014). To catalyze such reactions, these enzymes are dependent on redox partners, either homologous or heterologous, which provide electrons from NAD(P)H via an electron transfer chain (Hannemann et al., 2007).

Human P450s play a major role in the metabolism of drugs. The human liver P450s CYP3A4/5, CYP2D6, CYP2C9, CYP1A2, and CYP2C19 are responsible for the conversion of about 80% of all drugs (Zanger and Schwab, 2013). One important group of pharmaceuticals is psychotherapeutic drugs. Antipsychotic drugs and tricyclic antidepressants are used for the treatment of psychiatric disorders. In 1952, these psychotherapeutic drugs started with the discovery of chlorpromazine and since that time many drugs, mainly based on phenothiazine or iminodibenzyl, have been discovered and are used for psychiatric medication (Shen, 1999; Owens, 2014). The involvement of human liver P450s in the phase I biotransformation of these psychotherapeutics is well studied (Tanaka and Hisawa, 1999). Most of the drug metabolites are produced by P450s (see Table 1), with the exception of N-oxide products that are formed by the flavin-containing monooxygenases (Ziegler, 1993). Since some of the drug metabolites might have adverse effects, the U.S. Food and Drug Administration (FDA) published the guidance for safety testing of drug metabolites. Any human metabolite representing >10% of the parent drug exposure at steady state has to be tested in safety studies (FDA, 2008). However, this FDA guidance is superseded by the guidelines of the International Conference on Harmonization (Frederick and Obach, 2010; Haglund et al., 2014). Concerning these guidelines, further safety testing is recommended for human metabolites that are observed at exposures >10% of total drug-related exposure and at significantly greater levels in humans than the maximum exposure seen in toxicity studies (European Medicines Agency, 2009). As a result, ways for the production of these drug metabolites are demanded by the pharmaceutical industry. Production of such metabolites for toxicological studies and further derivatization can be achieved either by chemical synthesis or biocatalysis. The enzymatic production has many benefits such as high selectivity or the absence of employing toxic chemicals (Koeller and Wong, 2001). Microbial enzymes play an increasing role in the production of known human drugs and secondary metabolites, which are used for drug development (Demain, 1999; Patel, 2002). In this respect, microbial P450s are often involved in the production of these metabolites (Urlacher and Girhard, 2012) due to their ability to hydroxylate inactive carbon-hydrogen bonds in complex molecules.

The work is supported by Deutsche Forschungsgemeinschaft (DFG 1343/23-1).
dx.doi.org/10.1124/dmd.114.061937.
[S] This article has supplemental material available at dmd.aspetjournals.org.

ABBREVIATIONS: Adx_{4-108}, adrenodoxin (truncated form); FDA, Food and Drug Administration; Fpr, ferredoxin-$NADP^+$ reductase; GC, gas chromatography; HPLC, high-performance liquid chromatography; MS, mass spectrometry; P450, cytochrome P450; RT, retention time.

TABLE 1

Overview of psychotherapeutic drugs, their metabolites, and the human P450s capable for the metabolism

Drug	Human P450	Main metabolite	Reference
Amitriptyline	CYP1A2, CYP3A4, CYP2B6, CYP2C8, CYP2C9, CYP2C19, CYP2D6	2-Hydroxyamitriptyline 3-Hydroxyamitriptyline 2,11-Dihydronortriptyline 10-Hydoxyamitriptyline 10-,11-Dihydroxyamitriptyline 10-Oxy-amitriptyline Amitriptyline-*N*-oxide Amitriptyline dihydrodiol Desmethylamitriptyline	Prox and Breyer-Pfaff, 1987; Venkatakrishnan et al., 2001
Carbamazepine	CYP1A2, CYP2A6, CYP3A4, CYP2B6, CYP2C8, CYP2E1	10-,11-Epoxycarbamazepine 2-Hydroxycarbamazepine 3-Hydroxycarbamazepine	Kerr et al., 1994; Pearce et al., 2002
Chlorpromazine	CYP1A2, CYP3A4, CYP2B6, CYP2C19, CYP2D6	7-Hydroxychlorpromazine Chlorpromazine-*N*-oxide Chlorpromazine sulfoxide Desmethylchlorpromazine Didesmethylchlorpromazine	Murray, 2006; Wójcikowski et al., 2010
Clomipramine	CYP1A2, CYP3A4, CYP2C19, CYP2D6	2-Hydroxyclomipramine 8-Hydroxyclomipramine 10-Hydroxyclomipramine Clomipramine-*N*-oxide Desmethylclomipramine	Nielsen et al., 1996; Yokono et al., 2001
Imipramine	CYP1A2, CYP3A4, CYP2C9, CYP2D6	2-Hydroxyimipramine 10-Hydroxyimipramine Desmethylimipramine Didesmethylimipramine Imipramine-*N*-oxide	Singh, 2012
Promethazine	CYP2B6, CYP2D6	3-Hydroxypromethazine 4-Hydroxypromethazine Desmethylpromethazine Promethazine sulfoxide	Nakamura et al., 1996
Thioridazine	CYP2D6	*N*-desmethylthioridazine 7-Hydroxythioridazine Mesoridazine Thioridazine-5-sulfoxide	Daniel et al., 2000

Myxobacteria are known for the production of pharmaceutically and chemically important compounds, which attracted the attention of the pharmaceutical industry (Weissman and Müller, 2010). In 2007, the myxobacterium *Sorangium cellulosum* So ce56 was sequenced and 21 P450 genes were identified (Schneiker et al., 2007; Khatri et al., 2010b). Although, the physiologic roles of those P450s are still not known, some of them are able to convert exogenous substrates such as terpenes and terpenoids or fatty acids (Khatri et al., 2010b; Ly et al., 2012). However, the potential for the conversion of pharmaceutically interesting compounds has not yet been tested.

In this study, 10 P450s (CYP109C1, CYP109C2, CYP109D1, CYP260A1, CYP260B1, CYP264A1, CYP264B1, CYP266A1, CYP267A1, and CYP267B1) from *S. cellulosum* So ce56 were selected and employed for the in vitro conversion of seven psychotherapeutic drugs and their precursors. Compounds showing significant in vitro conversion were further chosen for the conversion with an *Escherichia coli*–based whole-cell biotransformation system to upscale the production and facilitate structure elucidation via NMR spectroscopy. The purified compounds were compared with known human metabolites to check for specific derivatives and to elucidate possible new metabolites, which could be useful for further drug development.

Materials and Methods

Chemicals. Amitriptyline and thioridazine were provided by Dr. Stephan Lütz (Novartis, Basel, Switzerland). Isopropyl β-D-1-thiogalactopyranoside and 5-aminolevulinic acid were purchased from Carbolution Chemicals (Saarbruecken, Germany). Bacterial media were purchased from Becton Dickinson (Heidelberg, Germany). All other chemicals were obtained from standard sources in the highest purity available.

Strains. The *E. coli* strain Top 10 for cloning purpose was obtained from Invitrogen (San Diego, CA). The *E. coli* strain BL21(DE3) for the heterologous expression of the P450s and BL21-Gold(DE3) for the whole-cell conversions were purchased from Agilent Technologies (Santa Clara, CA).

Molecular Cloning and Preparation of Expression Vectors. The 10 P450s from *S. cellulosum* So ce56 (CYP109C1, CYP109C2, CYP109D1, CYP260A1, CYP260B1, CYP264A1, CYP264B1, CYP266A1, CYP267A1, and CYP267B1) were selected for this study. The genes of those P450s were cloned in pCWori$^+$ plasmids as described elsewhere (Khatri et al., 2010b). To improve the expression yield, the genes of the P450s (CYP109C1, CYP109C2, CYP109D1, CYP260A1, CYP260B1, CYP264A1, and CYP264B1) were excised from their corresponding pCWori$^+$ plasmids and cloned into a pET17b plasmid (Novagen, Darmstadt, Germany) (Ringle et al., 2013). Likewise, the genes of CYP266A1, CYP267A1, and CYP267B1 were excised and cloned into a pET22b plasmid (Novagen).

For the expression of the redox partners ferredoxin-NADP$^+$ reductase (Fpr) and adrenodoxin (truncated form) ($Adx_{4\text{-}108}$) in the *E. coli*–based whole-cell system, the pCDFDuet-1 (Merck, Darmstadt, Germany) vector with a streptomycin resistance marker gene was used. The DNA fragment encoding $Adx_{4\text{-}108}$ was amplified by Polymerase chain reaction (forward primer, 5′- AAT GAC ATG CTT GAT CTG GCC TAT GGA CTA ACA GAT AGA T -3′, and reverse primer, 5′- ATC TAT CTG TTA GTC CAT AGG CCA GAT CAA GCA TGT CAT T-3′) using pKKHC_$Adx_{4\text{-}108}$ as a template (Uhlmann et al., 1994). Then, the DNA fragment was inserted between NcoI and *Hind*III of the multiple cloning site MS-I of pCDFDuet-1 (Merck). The forward primer was used to delete the NdeI restriction site. The fragment encoding Fpr was amplified by Polymerase chain reaction (forward primer, 5′- CAT ATG GCT GAT TGG GTA ACA GGC AAA GTC ACT AAA GTG CAG AAC TGG -3′, and reverse primer, 5′- CGG GGT ACC TTA CCA GTA ATG CTC CGC TGT CAT GTG GCC CGG TCG GC-3′) using the pET16_Fpr plasmid as a template (Girhard et al., 2010). The fragment was subcloned in the pCR4 blunt vector and finally inserted between NdeI and KpnI, resulting in the pCDF_dFA expression vector.

Media and Buffers. For the heterologous expression of the related P450s, terrific broth medium (24 g yeast extract, 12 g peptone, 4 ml glycerol, 2.31 g K_2HPO_4, and 12.54 g KH_2PO_4 per liter H_2O) was used. The whole-cell conversion was performed in M9CA medium (6 g Na_2HPO_4, 3 g KH_2PO_4, 0.5 g NaCl, 1 g NH_4Cl, 4 g casamino acids, 4 g glucose, 50 μl 1M $CaCl_2$, 2 ml 1 M $MgSO_4$, 2 ml of trace elements solution per liter H_2O; Trace elements solution contained 2.5 g EDTA, 250 mg $FeSO_4$, 25 mg $ZnCl_2$ and 5 mg $CuSO_4$ per 50 ml H_2O). The conversion with resting cells was done in 50 mM potassium phosphate buffer (pH 7.4) containing 2% glycerol as the carbon source.

Expression and Purification of the Enzymes. The corresponding P450s were expressed and purified as described previously (Khatri et al., 2010b). The electron transfer partners $Adx_{4\text{-}108}$ and adrenodoxin reductase from *Bos taurus* were expressed and purified as described elsewhere (Sagara et al., 1993; Uhlmann et al., 1994).

In Vitro Conversions. A reconstituted in vitro system containing the corresponding P450 (0.5 μM), adrenodoxin reductase (1.5 μM), $Adx_{4\text{-}108}$ (10 μM), $MgCl_2$ (1 mM), and a cofactor regenerating system with glucose-6-phosphate (5 mM) and glucose-6-phosphate dehydrogenase (2 U ml^{-1}) in the end volume of 250 μl of potassium phosphate buffer (20 mM, pH 7.4) was used. The compounds (10 mM), except carbamazepine (MeOH), phenothiazine (EtOH), and iminodibenzyl (EtOH), were dissolved in water and added to an end-concentration of 200 μM. The reaction was started by the addition of NADPH (500 μM). After 3 hours at 30°C the reaction was quenched by adding chloroform (500 μl). The aqueous phase was extracted twice with chloroform (2 × 500 μl). A negative control in the absence of P450 in the reaction sample was employed for each substrate to verify the P450-dependent reaction.

Whole-Cell System Using M9CA. The experiments were performed with *E. coli* BL21(DE3) gold cells. The cells were transformed with two plasmids, one for the corresponding P450 (pET17b or pET22b) and the other one for the redox partners Fpr and $Adx_{4\text{-}108}$ (pCDF_dFA). The overnight culture was prepared in nutrient broth containing ampicillin (100 μg/ml) and streptomycin (50 μg/ml). The main culture with M9CA medium was inoculated with the overnight culture (dilution 1:100) and incubated at 37°C. The induction of the corresponding genes was initiated by adding 1 mM isopropyl β-D-1-thiogalactopyranoside and 0.5 mM 5-aminolevulinic acid when the optical density reached 0.9–1 and the culture was grown further at 28°C. After 21 hours of expression, the temperature was set to 30°C and the substrates [stock solution 50 mM in water except for carbamazepine (MeOH), phenothiazine (EtOH) and iminodibenzyl (EtOH)] were added to a final concentration of 200 μM. To permeabilize the cells, EDTA was also added to a final concentration of 20 mM. The reaction was carried out for 48 hours under the same conditions. Samples were harvested, quenched with the same volume of chloroform and extracted twice. The organic phase was collected, pooled, and evaporated to dryness. The extracts were stored at −20°C until purification.

Whole-Cell System Using Resting Cells. The overnight culture was prepared as described before. Terrific broth medium was inoculated with the overnight culture (dilution 1:100). The expression was induced by adding 1 mM isopropyl β-D-1-thiogalactopyranoside and 0.5 mM 5-aminolevulinic acid at an optical density of 0.7–0.8. After 24 hours of expression at 28°C, the cells were harvested by centrifugation for 20 minutes at 4500*g*. The cell pellet was resuspended and washed in the buffer [20 mM potassium phosphate buffer (pH 7.4) containing 2% glycerol] following the centrifugation step. The 2.4 g cell mass was suspended in 100 ml buffer containing 2% glycerol. The substrates (200 μM) and EDTA (20 mM) were added and the cells were incubated for 24 hours at 30°C. The reaction was stopped by adding the same volume of chloroform. The extraction was done as described previously. Until purification, the extracts were stored at −20°C.

Analysis of the In Vitro and Whole-Cell Conversions via High-Performance Liquid Chromatography (HPLC)-Diode Array Detector. HPLC analysis was performed on a system consisting of a PU-2080 HPLC pump, an AS-2059-SF autosampler, and a MD-2010 multi wavelength detector (Jasco, Gross-Umstadt, Germany). A Nucleodur 100-5 C18 column (125 × 4 mm; Macherey-Nagel, Düren, Germany) was used at 40°C. The mobile phase consisted of water containing 0.1% trifluoroacetic acid (A) and acetonitrile containing 0.1% trifluoroacetic acid (B). A gradient from 20% to 80% of B with a flow rate of 1 ml/min was used for the separation of the compounds. The detection wavelengths were substrate dependent: amitriptyline (215 nm), carbamazepine (288 nm), chlorpromazine (256 nm), clomipramine (252 nm), iminodibenzyl (288 nm), imipramine (252 nm), phenothiazine (252 nm), promethazine (252 nm), and thioridazine (264 nm).

Purification of the Products. The extracts produced by the whole-cell system were purified via HPLC with a Nucleodur 100-5 C18 column (250 × 5 mm; Macherey-Nagel). For the preparative column, a gradient from 20% to 80% of B was also used but the flow rate was increased to 1.5 ml/min. The fractions containing product were collected, pooled, and treated with the same volume of 1 M glycine buffer (pH 11.4). After four times of extraction with chloroform, the combined organic fractions were evaporated to dryness and prepared for the NMR analysis.

Analysis of the Products via Gas Chromatography-Mass Spectrometry (GC-MS). GC-MS analysis was performed on a system consisting of an AI/AS 3000 autosampler, a DSQII quadrupole, a Focus GC column oven (Thermo Fisher Scientific, Waltham, MA), and a DB-5 column with a length of 30 m, 0.25 mm i.d., and 0.25 μm film thickness (Agilent Technologies). The compounds were analyzed in an *m/z* range of 30–450. The starting oven temperature was 100°C for 1 minute, and then the temperature was ramped to 320°C for 20°C/min and held for 10 minutes with a flow rate of 1 ml/min. The EI-mass spectra were compared with the NIST Mass Spectral Library (version 2.0; Gaithersburg, MD).

NMR Analysis. The structures of the products were analyzed by NMR spectroscopy (Institut für Pharmazeutische Biologie, Universität des Saarlandes). The ^1H and ^{13}C NMR were recorded on a Bruker (Rheinstetten, Germany) 500 NMR spectrometer. Two-dimensional NMR spectra were recorded as gs-HH-COSY, gs-HSQC, and gs-HMBC. All chemical shifts are relative to $CDCl_3$ (δ = 77.00 for ^{13}C-NMR; δ = 7.24 for ^1H-NMR) using the standard δ notion in parts per million.

Results

In Vitro Conversions. Initially, 10 P450s were used for the in vitro conversion of seven drugs (amitriptyline, carbamazepine, chlorpromazine, clomipramine, imipramine, promethazine, and thioridazine) and two precursors (iminodibenzyl and phenothiazine) to evaluate their ability for the conversion of those compounds. As shown in Table 2, CYP260A1, CYP264A1, CYP267A1, and CYP267B1 were able to convert some of the compounds; however, the remaining six enzymes did not show any conversion. CYP264A1 converts four substrates (amitriptyline, chlorpromazine, clomipramine, and imipramine) with appropriate yields. The main products of amitriptyline, chlorpromazine, and imipramine formed by CYP264A1 and CYP267B1 are identical. However, none of the P450s were able to convert carbamazepine. In general, CYP260A1 and the CYP267 family show lower conversions for the substrates compared with CYP264A1.

The obtained product patterns were different for each substrate. Besides the expected hydrophilic products, several hydrophobic products were also found. CYP260A1, CYP267A1, and CYP267B1 showed different product patterns for the conversion of promethazine. Four products were observed with CYP260A1 and CYP267A1, whereas CYP267B1 gave five products, in which two products [retention time (RT) = 11.2 and 11.6 minutes] were much more hydrophobic than the substrate (RT = 7.6 minutes). We observed that the most hydrophobic product (RT = 11.6 minutes) showed the same RT as that of phenothiazine (see Fig. 1). The conversion of chlorpromazine by CYP260A1 also forms a hydrophobic product (RT = 11.2 minutes). Likewise, low amounts of a hydrophobic product (RT = 12.4 minutes) were also found using CYP267A1 for thioridazine conversion (RT = 9.0 minutes). All other products were more hydrophilic compared with the substrates.

In accordance with these in vitro results, amitriptyline, chlorpromazine, clomipramine, and imipramine were chosen for the *E. coli*–based whole-cell biotransformation by CYP264A1. Amitriptyline and chlorpromazine were chosen for the conversion by CYP267B1. Thioridazine was chosen for the conversion by CYP267A1 to upscale the production for structure elucidation of the products.

TABLE 2

In vitro conversions of the drugs with the corresponding myxobacterial P450s (the observed products are arranged according to their RTs) Dashes mark that there is no conversion.

Substrate	Conversion by			
	CYP260A1	CYP264A1	CYP267A1	CYP267B1
RT [min]	RT [min]	RT [min]	RT [min]	RT [min]
Amitriptyline 8.2	—	P1: 70%/6.2 P2: 3%/6.8 P3: 18%/7.0	—	P1: 15%/6.2
Carbamazepine 7.7	—	—	—	—
Chlorpromazine 8.5	P1: 9%/11.2	P1: 62%/6.2	—	P1: 39%/6.2
Clomipramine 8.7	—	P1: 69%/7.0 P2: 23%/7.4 P3: 2%/8.5	—	Traces of product
Imipramine 8.0	—	P1: 52%/6.1 P2: 10%/6.5 P3: 4%/7.6	—	P1: 9%/6.1
Iminodibenzyl 12.1	—	P1: 3%/8.4	—	P1: 31%/9.3
Phenothiazine 11.6	—	P1: 4%/6.5	—	P1: 8%/6.5
Promethazine 7.6	—	—	—	P1: 4%/6.5
	P2: 15%/7.4		P2: 2%/7.4	P2: 23%/7.4
	P3: 5%/7.9		P3: 3%/7.9	—
	—		—	P4: 3%/10.8
	P5: 17%/11.2		P5: 4%/11.2	P5: 3%/11.2
	P6: 20%/11.6		P6: 5%/11.6	P6: 3%/11.6
Thioridazine 9.0	—	—	P1: 34%/6.9 P2: 5%/7.9 P3: 4%/12.4	—

Whole-Cell Conversions Using M9CA Medium and Resting Cells. Two different systems for the whole-cell conversions, either using M9CA medium or applying resting cells in buffer, were used to obtain larger amounts of products for NMR characterization. Interestingly, these two systems showed a clear difference concerning substrate conversion. A close correlation between the tested P450s and the conversion of the compounds was not observed (see Fig. 2). CYP264A1 showed higher product yields from amitriptyline, chlorpromazine, and clomipramine with resting cells, whereas a higher yield of the imipramine product was obtained in M9CA medium. In contrast, the yields of the whole-cell conversions with members of the CYP267 family were always higher in M9CA medium. Nevertheless, the ability of CYP267 to convert tricyclic compounds showed their potential pharmaceutical importance to generate derivatives from such compounds.

Product Purification via Preparative HPLC. The products of the corresponding whole-cell conversions were purified via preparative HPLC. The purity of the isolated products was further verified by an additional HPLC measurement before employing it for the NMR measurement. The chromatograms of the purified products and the pure substrates are shown in Supplemental Fig. 1, confirming the successful purifications of the corresponding products. All products were obtained with high purity and sufficient amounts (5–25 mg) for the structure elucidation via NMR spectroscopy.

Structure Elucidation via NMR Spectroscopy and GC-MS. The main products of the CYP264A1-dependent conversion of amitriptyline, chlorpromazine, clomipramine, and imipramine as well as the CYP267A1-dependent conversion of thioridazine were purified and analyzed by NMR spectroscopy. To substantiate the NMR results, the products were additionally analyzed by GC-MS. The ^{1}H NMR,

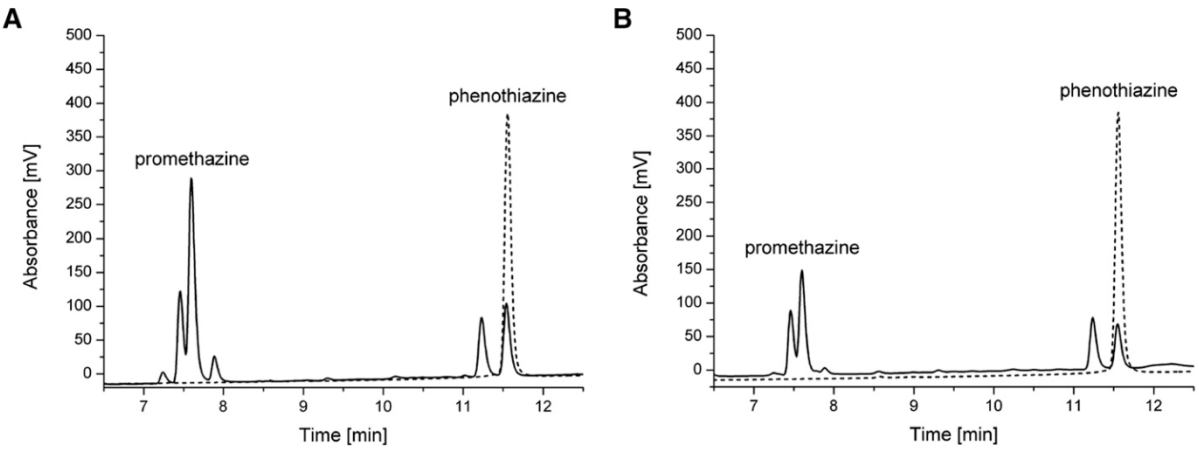

Fig. 1. HPLC chromatograms of the conversions of promethazine (solid lines) with CYP260A1 (A) and CYP267A1 (B) as well as pure phenothiazine (dashed lines). The hydrophobic product at 11.6 minutes shows the same RT as phenothiazine.

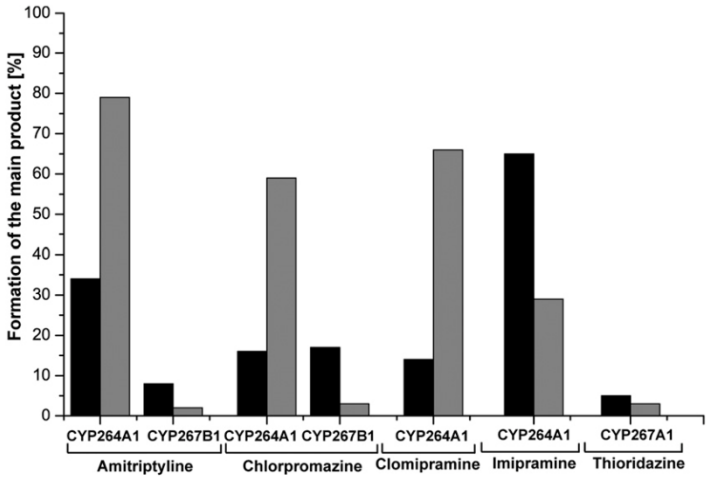

Fig. 2. Conversions of the tricyclic substrates to the corresponding main products. The conversions using M9CA medium (black bar) and resting cells (gray bar) are shown for each substrate.

^{13}C NMR, and GC-MS data are shown in the Supplemental Material (section 2: ^{1}H-NMR, ^{13}CNMR, and GC-MS data).

We observed that the EI-spectra showed a peak with *m/z* of 58, which is correlated to the tertiary ammonium moiety of the dimethylamino propyl group (Frigerio et al., 1972). This peak indicated that the dimethylamino group was intact and a demethylation can be excluded for amitriptyline, chlorpromazine, clomipramine, and imipramine. For clomipramine and imipramine conversion the database comparison of the fragmentation pattern showed the highest identity to the corresponding 10-hydroxy products, whereas chlorpromazine conversion showed the highest identity to chlorpromazine 5-sulfoxide. For the product of thioridazine, an ion with *m/z* of 386 was detected, indicating the insertion of a single oxygen atom. The corresponding 5-sulfoxidated thioridazine product was not available in the NIST database, and therefore it was only elucidated by NMR spectroscopy.

In summary, we showed that the myxobacterial P450s were able to oxidize the heterocyclic ring of the tricyclic compounds (see Fig. 3), in which CYP264A1 and CYP267B1 convert amitriptyline and imipramine to the corresponding 10-hydroxy products, whereas CYP264A1 additionally converts clomipramine to the 10-hydroxy product. In addition, chlorpromazine is sulfoxidated at position 5 by CYP264A1 and CYP267B1. Furthermore, CYP267A1 converts thioridazine to thioridazine 5-sulfoxide. The structures of the products are illustrated in Fig. 3.

Discussion

For the past few years, we have been engaged in the study of novel P450s from myxobacteria, and some P450s from *S. cellulosum* So ce56 have shown a potential for industrial and biotechnological applications (Khatri et al., 2010a,b, 2013, 2014; Ly et al., 2012; Ringle et al., 2013). We were also able to develop an efficient *E. coli*–based whole-cell bioconversion system for some myxobacterial P450s (Ringle et al., 2013). However, the potential applications of those P450s for the production of novel or known drug-related compounds have not yet been studied. Therefore, 10 myxobacterial P450s were investigated concerning their ability to produce human-like or novel drug metabolites from tricyclic psychotherapeutic drugs.

The production of human drug metabolites is an important challenge in the pharmaceutical industry. Drug metabolites formed at greater than 10% of the parent drug systemic exposure at steady state (FDA, 2008) or total drug-related exposure (European Medicines Agency, 2009) need to be tested in toxicological studies, whereby the International Conference on Harmonization guidelines take precedence over the FDA guidelines (Frederick and Obach, 2010; Haglund et al., 2014). For such studies, small (μg) to large quantities (in a gram scale) of these drug metabolites are necessary to provide standards for analytical and toxicological studies, respectively. Utilization of human liver or human liver microsomes is restricted due to limited availability of this human organ. Therefore, alternative ways of producing such metabolites have been investigated. Several approaches, including cell cultures and different microbial systems expressing human P450s as whole-cell biocatalysts to convert drugs, have been described (Crespi et al., 1993; Döhmer, 2001; Drăgan et al., 2011; Geier et al., 2012). However, the low activity and stability of the mammalian P450s compared with the bacterial and fungal P450s are limiting their application at an industrial scale (Julsing et al., 2008; Sakaki, 2012). In addition, the membrane association of the mammalian P450s hinders a simple handling of these enzymes for biotechnological applications, in contrast to the soluble bacterial P450s (Urlacher et al., 2004; Bernhardt and Urlacher, 2014). As a result, bacterial P450s become an alternative method to produce the identical metabolites as those provided by mammalian P450s (Yun et al., 2007; Caswell et al., 2013). Using wild-type microorganisms such as *Cunninghamella* ssp. or *Streptomyces* ssp. for the conversion of drugs is another possibility to obtain sufficient amounts of metabolites (Asha and Vidyavathi, 2009; Murphy, 2015). However, employing such microbial organisms for the production of drug metabolites can be a time-consuming process because of the lack of information regarding the involving enzyme in the biotransformation of the corresponding drug. Therefore, improvements of such a system to obtain higher amounts of a specific product are limited. This can be overcome by the utilization of specific bacterial P450s efficiently expressed in a bacterial whole-cell system as a biocatalyst. In this regard, one of the best characterized bacterial P450s is CYP102A1 (P450BM3) from *Bacillus megaterium*, which has been the target of most engineering efforts to improve activity, selectivity, and the range of substrates (Jung et al., 2011; Whitehouse et al., 2012). However, screening a variety of bacterial P450s for their ability to convert various drugs will certainly lead to a broad range of substrates with high structural diversity to be converted by these P450s. Therefore, we investigated 10 P450s from *S. cellulosum*—a bacterium typically found in soil (Shimkets et al., 2006), where it is exposed to a variety of xenobiotics—for their ability to convert tricyclic drugs.

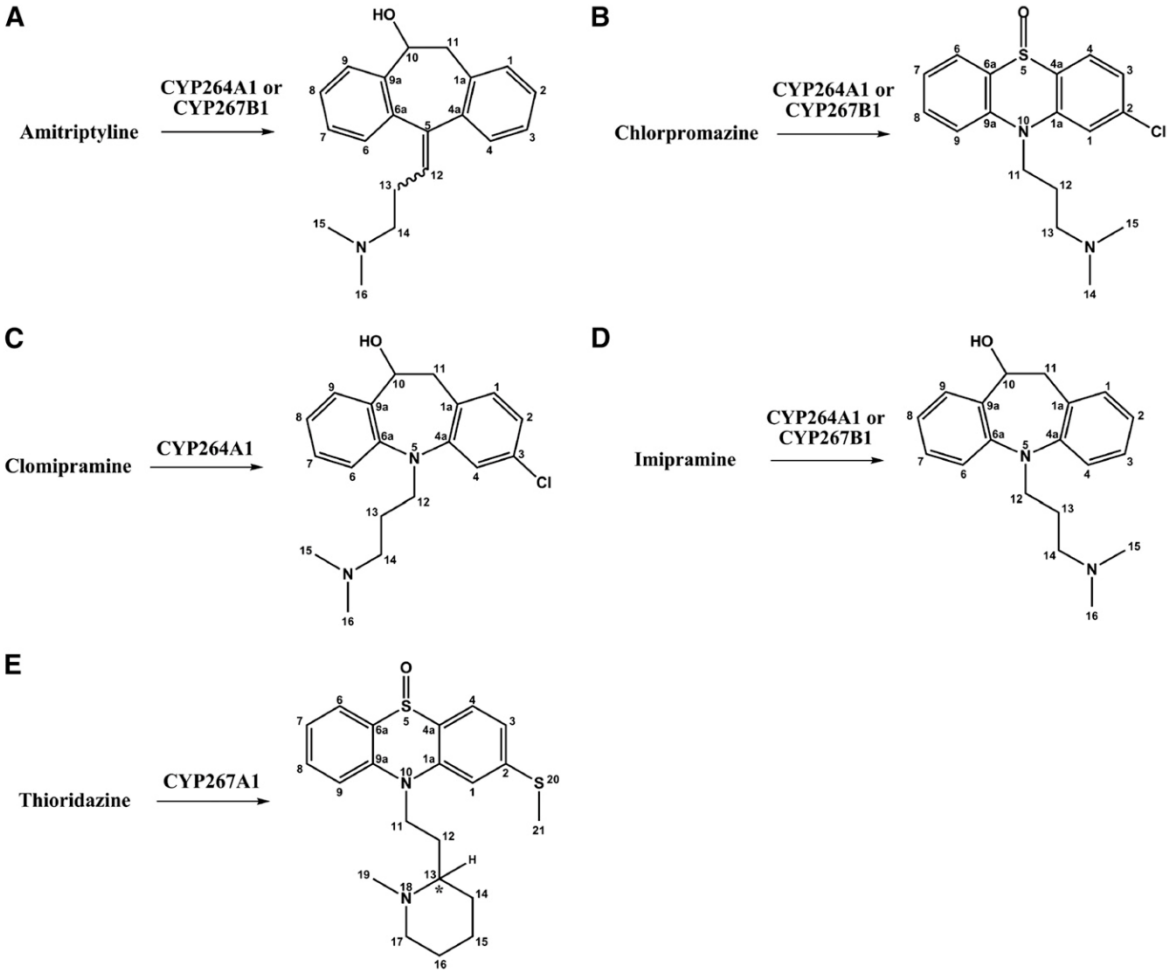

Fig. 3. Conversions of the substrates amitriptyline (A), chlorpromazine (B), clomipramine (C), imipramine (D), and thioridazine (E) by the myxobacterial P450s.

Terpenes and terpenoids as well as fatty acids have already been identified as substrates for these wild-type P450s in previous studies (Khatri et al., 2010a,b, 2014; Ly et al., 2012; Schifrin et al., 2014). Moreover, 4-methyl-3-phenyl-coumarin, a tricyclic molecule, was identified as a substrate for CYP264A1 (Ringle et al., 2013). Here, we can demonstrate that all tricyclic compounds except carbamazepine are converted in vitro by the myxobacterial P450s CYP260A1, CYP264A1, CYP267A1, and CYP267B1. To obtain sufficient amounts of products for structural elucidation, we used an *E. coli*–based whole-cell biotransformation system. The obtained products of amitriptyline, chlorpromazine, clomipramine, imipramine, and thioridazine were purified and characterized by NMR spectroscopy. It is remarkable that these products were indeed the same compounds as those obtained by human liver P450s. The 10-hydroxy products of amitriptyline and imipramine are predominantly formed by CYP2D6, whereas CYP1A2 and CYP3A4 are mainly capable of sulfoxidations of chlorpromazine and thioridazine. Moreover, the myxobacterial P450s show high selectivity for the production of a single major product, whereas the human P450s produce several other side products (see Table 1). Therefore, the ability to produce pure metabolites in a large quantity by the myxobacterial P450s is more suitable compared with the application of human P450s producing several metabolites.

Although 4-methyl-3-phenyl-coumarin has been previously identified as the only substrate for CYP264A1 (Ringle et al., 2013), its product has neither pharmaceutical nor chemical interest. However, the tricyclic moiety of this substrate indicated that CYP264A1 probably needs this structure for substrate recognition. This suggestion was supported by our observation that amitriptyline, chlorpromazine, clomipramine, and imipramine—all containing a tricyclic moiety—were converted by this P450. In addition, CYP264A1 is sensitive to the side chain moiety of the selected tricyclic compounds, since promethazine shows no conversion, whereas chlorpromazine is converted. In this regard, the dimethylamino propyl side chain seems to be necessary for the conversion. In agreement with this assumption, the two precursors, iminodibenzyl and phenothiazine, lacking the side chain, were also nearly not converted. Likewise, thioridazine containing a sterically demanding side chain is also not converted. However, amitriptyline, which possesses a side chain with reduced flexibility caused by the double bond, is converted. Comparing imipramine and clomipramine, there is no significant difference between their conversions, suggesting that the halogen

group at the aromatic ring does not seem to play a notable role in the reaction. Unexpectedly, the homolog of this enzyme from the same strain, CYP264B1, which shows no activity toward the tested tricyclic compounds (see Table 2), acts as a norisoprenoid and sesquiterpene hydroxylase (Ly et al., 2012).

Interestingly, we also observed the formation of products being more hydrophobic than the substrate from the conversion of promethazine by CYP260A1 as well as CYP267A1 and CYP267B1. One single hydrophobic product showing an identical RT as phenothiazine has been identified, suggesting that the side chain of promethazine might have been cleaved. Although the oxidative thermal degradation of promethazine has been previously described (Underberg, 1978), the dealkylation of promethazine by P450s has not yet been described. In addition, CYP260A1 also forms a more hydrophobic product from chlorpromazine. However, the formation of N-oxide products could also lead to more hydrophobic products, although these products are mainly formed by flavin-containing monooxygenases (Ziegler, 1993). In addition, ring-opening products are also unlikely due to the fact that these products are obviously more hydrophilic compared with the substrate. However, because of the very low yield we were not able to characterize these products. Interestingly, although tricyclic substrates for CYP267A1 and CYP267B1 were not known before, we identified the psychotherapeutic drugs as substrates for these P450s for the first time. Despite being homologous to each other, CYP267A1 and CYP267B1 showed quite different affinity for the tested substrates. Promethazine is the only common substrate converted by both P450s. However, the ability of CYP267B1 to convert most of the selected drugs makes this enzyme a promising candidate for the conversion of other drugs or drug-related derivatives. Furthermore, improvements of these P450s by protein engineering could lead to higher yields or an increased substrate range (Gillam, 2008).

We also observed that the conversion of tricyclic compounds by the myxobacterial CYP264A1 showed identical main products as those observed by human CYP2D6. There are no crystal structures for human CYP2D6 with the tested substrates or for the myxobacterial P450s available. Therefore, we performed an alignment of CYP2641 and CYP267A1 with human CYP2D6 to determine the substrate binding residues that have been shown in the crystal structure of CYP2D6 (Rowland et al., 2006) and the recent docking study of imipramine with CYP2D6.1 (Handa et al., 2014). Interestingly, the conserved Phe120 and Val374 of CYP2D6, which control the orientation of the substrate, are conserved as Phe61 and Val279, respectively, in CYP264A1, but not in CYP267A1 (see Supplemental Fig. 2). It is assumed that this observation might be the reason for the similar conversion patterns of both CYP264A1 and CYP2D6.

In our study carbamazepine is the only compound that has not been converted by any of the tested myxobacterial P450s. The presence of a double bond in the middle ring forms a higher electron density, which might subsequently hinder the oxidation at this specific position. In addition, the presence of the urea moiety may influence the hydrogen bonds of the substrate-enzyme interactions, which can lead to an incorrect substrate orientation in the active site of the P450. Taken together, our results showed the potential of the myxobacterial P450s as an efficient source for the production of drug metabolites or their derivatives. The products could be used as analytical standards or for toxicological investigations showing their significance for pharmaceutical studies.

Acknowledgments

The authors thank Birgit Heider-Lips for protein purification, Dr. Michael Ringle for providing the pCDF_dFA vector, and Dr. Josef Zapp for measuring the NMR samples. Special thanks are given to Dr. Stephan Lütz for providing two of the substrates.

Authorship Contributions

Participated in research design: Litzenburger, Kern, Bernhardt.

Conducted experiments: Litzenburger, Kern.

Performed data analysis: Litzenburger, Kern.

Wrote or contributed to the writing of the manuscript: Litzenburger, Kern, Khatri, Bernhardt.

References

Asha S and Vidyavathi M (2009) *Cunninghamella*—a microbial model for drug metabolism studies—a review. *Biotechnol Adv* **27:**16–29.

Bernhardt R (2006) Cytochromes P450 as versatile biocatalysts. *J Biotechnol* **124:**128–145.

Bernhardt R and Urlacher VB (2014) Cytochromes P450 as promising catalysts for biotechnological application: chances and limitations. *Appl Microbiol Biotechnol* **98:**6185–6203.

Caswell JM, O'Neill M, Taylor SJ, and Moody TS (2013) Engineering and application of P450 monooxygenases in pharmaceutical and metabolite synthesis. *Curr Opin Chem Biol* **17:** 271–275.

Crespi CL, Langenbach R, and Penman BW (1993) Human cell lines, derived from AHH-1 TK+/- human lymphoblasts, genetically engineered for expression of cytochromes P450. *Toxicology* **82:**89–104.

Cunningham Owens, D. G.. A Guide to the Extrapyramidal Side-Effects of Antipsychotic Drugs. 2nd ed. Cambridge: Cambridge University Press, 2014. Cambridge Books Online http://dx.doi.org/10.1017/CBO9781139149112.

Daniel WA, Syrek M, Haduch A, and Wójcikowski J (2000) Pharmacokinetics and metabolism of thioridazine during co-administration of tricyclic antidepressants. *Br J Pharmacol* **131:** 287–295.

Demain AL (1999) Pharmaceutically active secondary metabolites of microorganisms. *Appl Microbiol Biotechnol* **52:**455–463.

Döhmer J (2001) [Modern drug development by molecular- and cell-biological methods]. *ALTEX* **18:**9–12.

Drägan CA, Peters FT, Bour P, Schwaninger AE, Schaan SM, Neunzig I, Widjaja M, Zapp J, Kraemer T, and Maurer HH, et al. (2011) Convenient gram-scale metabolite synthesis by engineered fission yeast strains expressing functional human P450 systems. *Appl Biochem Biotechnol* **163:**965–980.

European Medicines Agency (2009) *ICH Guidance M3(R2) on Non-Clinical Safety Studies for the Conduct of Human Clinical Trials and Marketing Authorisation for Pharmaceuticals*, European Medicines Agency, London.

Food and Drug Administration (2008) *Guidance for Industry: Safety Testing of Drug Metabolites*, U.S. Department of Health and Human Services, Food and Drug Administration, Rockville, MD.

Frederick CB and Obach RS (2010) Metabolites in safety testing: "MIST" for the clinical pharmacologist. *Clin Pharmacol Ther* **87:**345–350.

Frigerio A, Belvedere G, De Nadai F, Fanelli R, Pantarotto C, Riva E, and Morselli PL (1972) A method for the determination of imipramine in human plasma by gas-liquid chromatography-mass fragmentography. *J Chromatogr A* **74:**201–208.

Geier M, Braun A, Emmerstorfer A, Pichler H, and Glieder A (2012) Production of human cytochrome P450 2D6 drug metabolites with recombinant microbes—a comparative study. *Biotechnol J* **7:**1346–1358.

Gillam EM (2008) Engineering cytochrome p450 enzymes. *Chem Res Toxicol* **21:**220–231.

Girhard M, Klaus T, Khatri Y, Bernhardt R, and Urlacher VB (2010) Characterization of the versatile monooxygenase CYP109B1 from *Bacillus subtilis*. *Appl Microbiol Biotechnol* **87:** 595–607.

Haglund J, Halldin MM, Brunnström A, Eklund G, Kautiainen A, Sandholm A, and Iverson SL (2014) Pragmatic approaches to determine the exposures of drug metabolites in preclinical and clinical subjects in the MIST evaluation of the clinical development phase. *Chem Res Toxicol* **27:**601–610.

Handa K, Nakagome I, Yamaotsu N, Gouda H, and Hirono S (2014) In silico study on the inhibitory interaction of drugs with wild-type CYP2D6.1 and the natural variant CYP2D6.17. *Drug Metab Pharmacokinet* **29:**52–60.

Hannemann F, Bichet A, Ewen KM, and Bernhardt R (2007) Cytochrome P450 systems—biological variations of electron transport chains. *Biochim Biophys Acta* **1770:**330–344.

Julsing MK, Cornelissen S, Bühler B, and Schmid A (2008) Heme-iron oxygenases: powerful industrial biocatalysts? *Curr Opin Chem Biol* **12:**177–186.

Jung ST, Lauchli R, and Arnold FH (2011) Cytochrome P450: taming a wild type enzyme. *Curr Opin Biotechnol* **22:**809–817.

Kerr BM, Thummel KE, Wurden CJ, Klein SM, Kroetz DL, Gonzalez FJ, and Levy RH (1994) Human liver carbamazepine metabolism. Role of CYP3A4 and CYP2C8 in 10,11-epoxide formation. *Biochem Pharmacol* **47:**1969–1979.

Khatri Y, Girhard M, Romankiewicz A, Ringle M, Hannemann F, Urlacher VB, Hutter MC, and Bernhardt R (2010a) Regioselective hydroxylation of norisoprenoids by CYP109D1 from *Sorangium cellulosum* So ce56. *Appl Microbiol Biotechnol* **88:**485–495.

Khatri Y, Hannemann F, Ewen KM, Pistorius D, Perlova O, Kagawa N, Brachmann AO, Müller R, and Bernhardt R (2010b) The CYPome of *Sorangium cellulosum* So ce56 and identification of CYP109D1 as a new fatty acid hydroxylase. *Chem Biol* **17:**1295–1305.

Khatri Y, Hannemann F, Girhard M, Kappl R, Hutter M, Urlacher VB, and Bernhardt R (2014) A natural heme-signature variant of CYP267A1 from *Sorangium cellulosum* So ce56 executes diverse ω-hydroxylation. *FEBS J* **10:**13104.

Khatri Y, Hannemann F, Girhard M, Kappl R, Même A, Ringle M, Janocha S, Leize-Wagner E, Urlacher VB, and Bernhardt R (2013) Novel family members of CYP109 from *Sorangium cellulosum* So ce56 exhibit characteristic biochemical and biophysical properties. *Biotechnol Appl Biochem* **60:**18–29.

Koeller KM and Wong C-H (2001) Enzymes for chemical synthesis. *Nature* **409:**232–240.

Ly TT, Khatri Y, Zapp J, Hutter MC, and Bernhardt R (2012) CYP264B1 from *Sorangium cellulosum* So ce56: a fascinating norisoprenoid and sesquiterpene hydroxylase. *Appl Microbiol Biotechnol* **95:**123–133.

Murphy CD (2015) Drug metabolism in microorganisms. *Biotechnol Lett* **37:**19–28.

Murray M (2006) Role of CYP pharmacogenetics and drug-drug interactions in the efficacy and safety of atypical and other antipsychotic agents. *J Pharm Pharmacol* **58:**871–885.

Nakamura K, Yokoi T, Inoue K, Shimada N, Ohashi N, Kume T, and Kamataki T (1996) CYP2D6 is the principal cytochrome P450 responsible for metabolism of the histamine H1 antagonist promethazine in human liver microsomes. *Pharmacogenetics* **6:**449–457.
Nelson DR (2011) Progress in tracing the evolutionary paths of cytochrome P450. *Biochim Biophys Acta* **1814:**14–18.
Nielsen KK, Flinois JP, Beaune P, and Brøsen K (1996) The biotransformation of clomipramine in vitro, identification of the cytochrome P450s responsible for the separate metabolic pathways. *J Pharmacol Exp Ther* **277:**1659–1664.
Patel RN (2002) Microbial/enzymatic synthesis of chiral intermediates for pharmaceuticals. *Enzyme Microb Technol* **31:**804–826.
Pearce RE, Vakkalagadda GR, and Leeder JS (2002) Pathways of carbamazepine bioactivation in vitro I. Characterization of human cytochromes P450 responsible for the formation of 2- and 3-hydroxylated metabolites. *Drug Metab Dispos* **30:**1170–1179.
Prox A and Breyer-Pfaff U (1987) Amitriptyline metabolites in human urine. Identification of phenols, dihydrodiols, glycols, and ketones. *Drug Metab Dispos* **15:**890–896.
Ringle M, Khatri Y, Zapp J, Hannemann F, and Bernhardt R (2013) Application of a new versatile electron transfer system for cytochrome P450-based *Escherichia coli* whole-cell bioconversions. *Appl Microbiol Biotechnol* **97:**7741–7754.
Rowland P, Blaney FE, Smyth MG, Jones JJ, Leydon VR, Oxbrow AK, Lewis CJ, Tennant MG, Modi S, and Eggleston DS, et al. (2006) Crystal structure of human cytochrome P450 2D6. *J Biol Chem* **281:**7614–7622.
Sagara Y, Wada A, Takata Y, Waterman MR, Sekimizu K, and Horiuchi T (1993) Direct expression of adrenodoxin reductase in *Escherichia coli* and the functional characterization. *Biol Pharm Bull* **16:**627–630.
Sakaki T (2012) Practical application of cytochrome P450. *Biol Pharm Bull* **35:**844–849.
Schifrin A, Ly TT, Günnewich N, Zapp J, Thiel V, Schulz S, Hannemann F, Khatri Y, and Bernhardt R (2015) Characterization of the gene cluster CYP264B1-geoA from Sorangium cellulosum So ce56: Biosynthesis of (+)-eremophilene and its hydroxylation. *ChemBioChem*, **16**:337–344
Schneiker S, Perlova O, Kaiser O, Gerth K, Alici A, Altmeyer MO, Bartels D, Bekel T, Beyer S, and Bode E, et al. (2007) Complete genome sequence of the myxobacterium *Sorangium cellulosum*. *Nat Biotechnol* **25:**1281–1289.
Shen WW (1999) A history of antipsychotic drug development. *Compr Psychiatry* **40:**407–414.
Shimkets L, Dworkin M, and Reichenbach H (2006) The myxobacteria, in *The Prokaryotes* (Dworkin M, Falkow S, Rosenberg E, Schleifer KH, and Stackebrandt E eds) pp 31–115, Springer, New York.
Singh JK, Solanki A, and Shirsath VS (2012) Comparative in-vitro intrinsic clearance of imipramine in multiple species liver microsomes: human, rat, mouse and dog. *Drug Metab Toxicol* **3:**1000126.
Sono M, Roach MP, Coulter ED, and Dawson JH (1996) Heme-containing oxygenases. *Chem Rev* **96:**2841–2888.
Tanaka E and Hisawa S (1999) Clinically significant pharmacokinetic drug interactions with psychoactive drugs: antidepressants and antipsychotics and the cytochrome P450 system. *J Clin Pharm Ther* **24:**7–16.
Uhlmann H, Kraft R, and Bernhardt R (1994) C-terminal region of adrenodoxin affects its structural integrity and determines differences in its electron transfer function to cytochrome P-450. *J Biol Chem* **269:**22557–22564.
Underberg WJ (1978) Oxidative degradation of pharmaceutically important phenothiazines I: Isolation and identification of oxidation products of promethazine. *J Pharm Sci* **67:**1128–1131.
Urlacher VB and Girhard M (2012) Cytochrome P450 monooxygenases: an update on perspectives for synthetic application. *Trends Biotechnol* **30:**26–36.
Urlacher VB, Lutz-Wahl S, and Schmid RD (2004) Microbial P450 enzymes in biotechnology. *Appl Microbiol Biotechnol* **64:**317–325.
Venkatakrishnan K, Schmider J, Harmatz JS, Ehrenberg BL, von Moltke LL, Graf JA, Mertzanis P, Corbett KE, Rodriguez MC, and Shader RI, et al. (2001) Relative contribution of CYP3A to amitriptyline clearance in humans: in vitro and in vivo studies. *J Clin Pharmacol* **41:**1043–1054.
Weissman KJ and Müller R (2010) Myxobacterial secondary metabolites: bioactivities and modes-of-action. *Nat Prod Rep* **27:**1276–1295.
Whitehouse CJC, Bell SG, and Wong L-L (2012) P450(BM3) (CYP102A1): connecting the dots. *Chem Soc Rev* **41:**1218–1260.
Wójcikowski J, Boksa J, and Daniel WA (2010) Main contribution of the cytochrome P450 isoenzyme 1A2 (CYP1A2) to *N*-demethylation and 5-sulfoxidation of the phenothiazine neuroleptic chlorpromazine in human liver—A comparison with other phenothiazines. *Biochem Pharmacol* **80:**1252–1259.
Yokono A, Morita S, Someya T, Hirokane G, Okawa M, and Shimoda K (2001) The effect of CYP2C19 and CYP2D6 genotypes on the metabolism of clomipramine in Japanese psychiatric patients. *J Clin Psychopharmacol* **21:**549–555.
Yun CH, Kim KH, Kim DH, Jung HC, and Pan JG (2007) The bacterial P450 BM3: a prototype for a biocatalyst with human P450 activities. *Trends Biotechnol* **25:**289–298.
Zanger UM and Schwab M (2013) Cytochrome P450 enzymes in drug metabolism: regulation of gene expression, enzyme activities, and impact of genetic variation. *Pharmacol Ther* **138:**103–141.
Ziegler DM (1993) Recent studies on the structure and function of multisubstrate flavin-containing monooxygenases. *Annu Rev Pharmacol Toxicol* **33:**179–199.

Address correspondence to: Rita Bernhardt, Department of Biochemistry, Saarland University, Campus B2.2, 66123 Saarbruecken, Germany. E-mail: ritabern@mx.uni-saarland.de

Drug metabolism and disposition

"Conversions of tricyclic Antidepressants and Antipsychotics with selected P450s from *Sorangium cellulosum* So ce56"

Martin Litzenburger, Fredy Kern, Yogan Khatri and Rita Bernhardt

Institut für Biochemie, Universität des Saarlandes, Campus B.2.2, 66123, Saarbruecken, Germany

1. Chromatograms of the purified products as well as the pure substrates

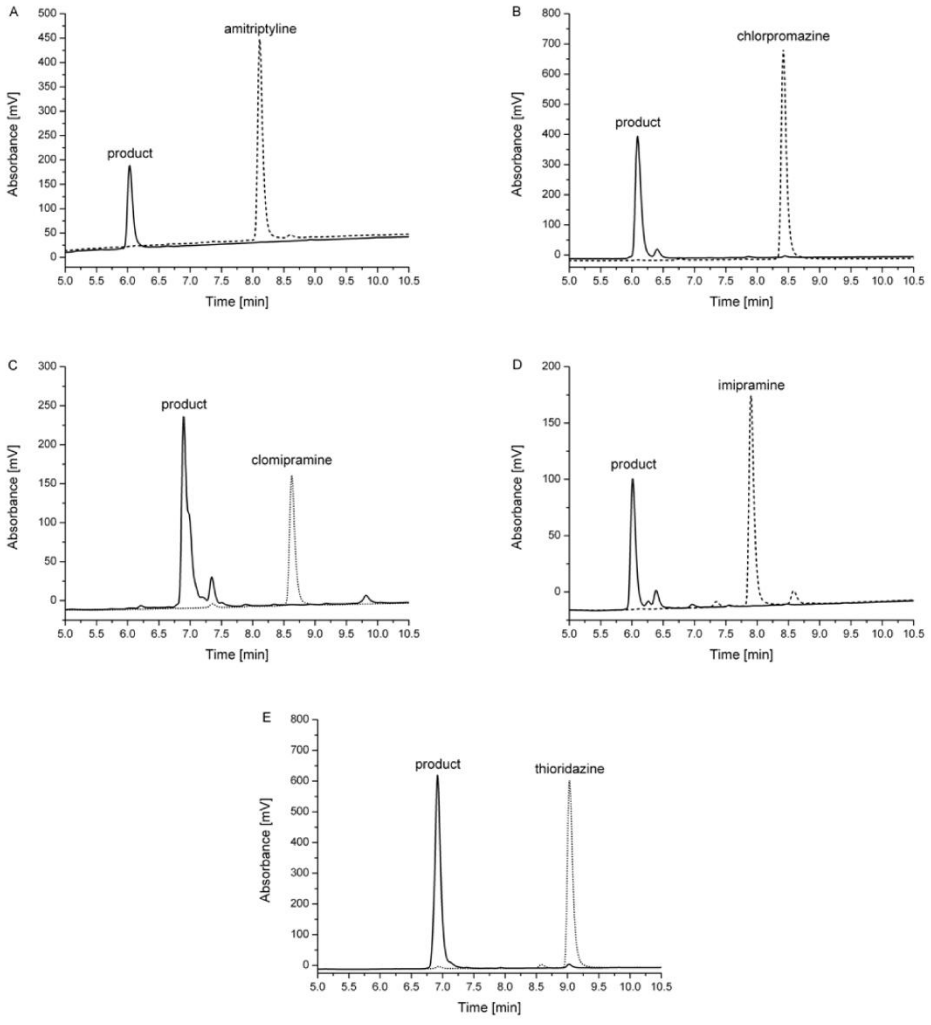

Supplemental Figure 1: Chromatograms of the purified products (solid lines) as well as the pure substrates (dashed lines): amitriptyline (A), chlorpromazine (B), clomipramine (C), imipramine (D) and thioridazine (E).

2. ^{1}H NMR, ^{13}C NMR and GC-MS data

The EI spectra showed a complete fragmentation of the molecules and the relative intensities of the fragments are shown in brackets.

Conversion of amitriptyline by CYP264A1:

NMR-data:

^{1}H NMR ($CDCl_3$, 500 MHz): δ 2.12(s, 6H, H-15 and H-16), 2.21-2.35 (m, 4H, H-13 and H-14), 3.02 (dd, 1H, H-11), 3.59 (dd, 1H, H-11), 5.05 (d, 1H, H-10), 5.89 (t, 1H, H-12), 7.12-7.44 (m, 8H, H-1, H-2, H-3, H-4, H-6, H-7, H-8 and H-9); ^{13}C NMR ($CDCl_3$, 125 MHz): δ 28.08 (C-13), 39.49 (C-11), 45.50 (C-15 and C-16), 59.60 (C-14), 70.27 (C-10), 126.82 (C-7), 127.89 (C-3), 128.12 (C-2), 128.52 (C-8), 128.72 (C-4), 130.26 (C-12), 130.79 (C-1), 131.46 (C-9), 133.99 (C-1a), 138.98 (C-9a), 140.40 (C-6a), 141.34 (C-4a), 142.98 (C-5).

EI mass spectra:

m/z 58.02 (100%), 41.98 (6%), 202.16 (5%), 215.32 (3%), 189.12 (3%), 165.13 (2%), 59.03 (2%) 42.59 (2%), 202.93 (2%), 217.21 (2%).

Conversion of chlorpromazine by CYP264A1:

^{1}H NMR ($CDCl_3$, 500 MHz): δ 1.98-2.08 (m, 2H, H-12), 2.29 (s, 6H, H14 and H15), 2.43 (dt, 2H, H-13), 4.29 (t, 2H, H-11), 7.19 (dd, 1H, H-3), 7.26 (dd, 1H, H-7), 7.50 (d, 1H, H-9), 7.59 (d, 1H, H-1), 7.61 (m, 1H, H-8), 7.84 (d, 1H, H-8), 7.91 (dd, 1H, H-6); ^{13}C NMR ($CDCl_3$, 125 MHz): δ 24.62 (C-12), 45.73 (C-14 and C15), 46.07 (C-11), 56.53 (C-13), 115.98 (C-1), 116.10 (C-9), 121.95 (C-3), 122.28 (C-7), 131.71 (C-6), 132.84 (C-4), 133.04 (C-8), 137.90 (C-9a), 139.02 (C-1a), 142.28 (C-4a), 142.84 (C-6a).

EI mass spectra:

m/z 58.00 (100%), 245.99 (97%), 248.11 (33%), 42.02 (28%), 214.13 (22%), 233.08 (19%), 247.19 (19%), 83.89 (12%), 44.07 (9%), 232.24 (9%).

Conversion of clomipramine by CYP264A1:

^{1}H NMR ($CDCl_3$, 500 MHz): δ 1.67-1.74 (m, 2H, H-13), 2.10 (s, 6H, H-13 and H-14), 2.27 (t, 2H, H-14), 3.15 (dd, 1H, H-11), 3.41 (dd, 1H, H11), 3.75 (t, 2H, C-12), 4.96-5.09 (m, 1H, H-10), 6.89-7.39 (m, 7H, H-1, H-2, H-4, H-6, H-7, H-8, H-9); ^{13}C NMR ($CDCl_3$, 125 MHz): δ 25.95 (C-13), 39.36 (C-11), 45.42 (C-15 and C-16), 48.74 (C-12), 57.49 (C-14), 69.96 (C-10), 118.86 (C-4), 121.02 (C-8), 121.94 (C-2), 123.94 (C-6), 127.12 (C-9), 130.54 (C-7), 132.15 (C-9a), 132.47 (C-1), 133.43 (C-1a), 147.65 (C-6a), 148.48 (C-4a).

EI mass spectra:

m/z 58.09 (100%), 84.78 (26%), 180.21 (20%), 85.32 (19%), 285.02 (18%), 57.45 (17%), 42.22 (15%), 226.92 (14%), 253.71 (14%), 83.90 (12%).

Conversion of imipramine by CYP264A1:

^{1}H NMR ($CDCl_3$, 500 MHz): δ 1.69-1.77 (m, 2H, H-11), 2.11 (s, 6H, H-15 and H-16), 2.29 (t, 2H, H-14), 3.19 (dd, 1H, H-11), 3.45 (dd, 1H, H-11), 3.73-3.84 (m, 2H, H-12), 5.06 (dd, 1H, H-10), 6.94- 7.21 (m, 8H, H-1, H-2, H-3, H-4, H-6,H-7, H-8, H-9); ^{13}C NMR ($CDCl_3$, 125 MHz): δ 26.03 (C-13), 39.81 (C-11), 45.41 (C-15 and C-16), 48.57 (C-12), 57.63 (C-14), 70.48 (C-10), 118.90 (C-8), 120.54 (C-2), 122.25 (C-4), 123.33 (C-6), 126.89 (C-3), 128.04 (C-7), 130.57 (C-9), 130.69 (C-1), 131.97 (C-1a), 134.33 (C-9a), 146.76 (C-6a), 148.76 (C-4a).

EI mass spectra:

m/z 58.00 (100%), 85.10 (29%), 180.09 (27%), 193.11 (27%), 42.02 (23%), 251.22 (19%), 194.14 (16%) 232.22 (15%), 206.23 (12%), 84.04 (12%)

Conversion of thioridazine by CYP267A1:

The use of the racemic mixture of (*R*)- and (*S*)-thioridazine as substrate leads to their respective enantiomeric products. As a consequence, the NMR-signals are duplicated. The enantiomeric signals are labeled as a and b.

^{1}H NMR ($CDCl_3$, 500 MHz): δ 1.33 (m, 2H, H-16a), 1.76 (m, 2H, H-16b), 1.52 (m, 2H, H-15a), 1.65 (m, 2H, H-15b), 1.93 (d, 2H, H-12a), 2.19 (d, 2H, H-12b), 2.11 (m, 2H, H-14a), 2.28 (m, 2H, H-14b), 2.20 (m, 2H, H-17a), 2.27 (s, 2H, H-19a and H-19b), 2.25 (m, 2H, H-13a and H-13b), 2.37 (s, 2H, H-19a and H-19b), 2.72(s, 2H, H-19a and H-19b) 2.91 (m, 2H, H-17b), 2.58 (s, 3H, H-21a), 2.59 (s, 3H, H-21b) 3.96 (m, 2H, H-11a), 4.05 (m, 2H, H-11b), 6.94 (d, 1H, H-4a), 6.98 (t, 1H, H-4b), 7.07 (dd, 1H, H-7a), 7.11 (dt, 1H, H-7b), 7.17 (d, 1H, H-3a), 7.22 (t, 2H, H-3b), 7.24 (d, 1H, H-1a), 7.26 (d, 1H, H-1b), 7.25 (m, 1H, H-9a), 7.28 (m, 1H, H-9b), 7.45 (m, 1H, H-6a), 7.63 (m, 1H, H-6b), 7.83 (m, 1H, H-8a), 7.93 (m, 1H, H-8b); ^{13}C NMR ($CDCl_3$, 125 MHz): δ 15.37 (C-21), 23.85 (C-16a), 30.33 (C-16b), 25.07 (C-15a), 25.10 (C-15b), 29.13 (C-14a), 29.16 (C-14b), 29.61 (C-12a), 29.64 (C-12b), 44.04 (C-11a), 44.70 (C-11b), 56.66 (C-17a), 56.70 (C-17b), 61.95 (C-13a), 62.20 (C-13b), 109.76 (C-9a), 109.83 (C-9b), 115.95 (C-4a and C-4b), 117.25 (C-7a), 119.05 (C-7b), 124.44 (C-2a and C-2b), 127.62 (C-3a), 127.66 (C-3b), 127.85 (C-1a), 127.89 (C-1b), 129.14 (C-6a-a), 129.17 (C-6a-b), 144.35 (C-4a-a and C-4a-b), 144.94 (C-1a-a), 144.96 (C-1a-b), 145.55 (C-9a-a), 145.64 (C-9a-b).

EI mass spectra:

m/z 98.08 (100%), 97.13 (14%), 244.94 (13%), 206.88 (12%), 42.03 (12%), 195.93 (11%), 223.07 (11%), 196.79 (10%), 211.20 (10%), 386.06 (9%)

3. Comparison of CYP264A1 and 267A1 with human CYP2D6

Supplemental Figure 2: Multiple sequence alignment of human CYP2D6 (AFX95842.1), and the S. cellulosum So ce56 CYP264A1 (YP_001616970.1) and CYP267A1 (YP_001611312.1). The amino acid sequences of CYP2D6, CYP264A1 and CYP267A1 were retrieved from EMBL database (http://www.ebi.ac.uk/embl/) and aligned by Clustal W2 (http://www.ebi.ac.uk/Tools/msa/clustalw2/). The absolutely conserved amino-acid residues are highlighted in grey, and the yellow highlight indicates the interacting residues during docking of imipramine as described (Handa et al., 2014).

Handa K, Nakagome I, Yamaotsu N, Gouda H, and Hirono S (2014) In Silico Study on the Inhibitory Interaction of Drugs with Wild-type CYP2D6.1 and the Natural Variant CYP2D6.17. *Drug Metabolism and Pharmacokinetics* 29:52-60.

2.2 New Sesquiterpene Oxidations with CYP260A1 and CYP264B1 from *Sorangium cellulosum* So ce56

Alexander Schifrin, Martin Litzenburger, Michael Ringle, Thuy TB Ly, and Rita Bernhardt

ChemBioChem, December 14, 2015, Volume 16, Issue 18, pages 2624–2632
doi: 10.1002/cbic.201500417

ChemPubSoc Europe

DOI: 10.1002/cbic.201500417

CHEMBIOCHEM Full Papers

New Sesquiterpene Oxidations with CYP260A1 and CYP264B1 from *Sorangium cellulosum* So ce56

Alexander Schifrin,[a] Martin Litzenburger,[a] Michael Ringle,[a] Thuy T. B. Ly,[a, b] and Rita Bernhardt*[a]

Sesquiterpenes are natural products derived from the common precursor farnesyl pyrophosphate (FPP) but are highly diverse in structure and function. Cytochrome P450 enzymes (P450s) exhibit the unique ability to introduce molecular oxygen into non-activated C–H bonds. In plant biosynthetic pathways, P450s commonly derivatize sesquiterpene hydrocarbons. However, the potential of bacterial P450s for terpene derivatization is still underinvestigated. This work compares the substrate specificities and regioselectivities of the sesquiterpene hydroxylases CYP260A1 and CYP264B1 from myxobacterium *Sorangium cellulosum* So ce56. Four tested substrate classes (eremophilanes, humulanes, caryophyllanes, and cedranes) were converted by both P450s. The achievable variety of oxidations is demonstrated on the model substrates (+)-nootkatone and zerumbone. Increasing the number of functionally investigated P450s, this study represents a step towards the selective derivatization of sesquiterpenes.

Introduction

Sesquiterpenes are a group of natural products biosynthesized either through the mevalonate pathway or the methylerythritol pathway.[1] Although all sesquiterpenes contain 15 carbon atoms (C_{15}) and derive from the common precursor farnesyl pyrophosphate (FPP) through bioconversion catalyzed by terpene synthases (TPSs),[2] they display highly diverse branched, mono-, bi-, and tricyclic hydrocarbon skeletons.[3] Physiological derivatization is conducted by other enzymes, most often cytochromes P450 (P450s),[4] so that 89.5% of all known sesquiterpenes are derivatized.[5] P450s are external monooxygenases. They selectively introduce molecular oxygen into non-activated C–H bonds, and this makes them very powerful for applications in synthesis as a complement to chemical methods.[6]

Lightly derivatized sesquiterpenes are volatile and serve for plants as a means of chemical communication either for defense or for attraction of pollinators.[7] Mankind has discovered plant sesquiterpenoids as highly valuable flavors and fragrances,[8] and multiply oxidized derivatives as antitumor[9] or antimalaria agents.[10]

Recently, bacterial sesquiterpenes have been studied more intensely;[11–12] their physiological functions remain a topic of discussion.[12] Nevertheless, bacterial sesquiterpene biosynthesis pathways have been identified as analogous to those in plants, including conversion of FPP by TPSs and derivatization of the hydrocarbons by P450s.[11,13] In a similar way, smaller monoterpenes (C_{10}) and bigger di- (C_{20}) and triterpenes (C_{30}) are synthesized.[1]

Obtaining valuable terpene intermediates is an important challenge, because they often do not accumulate in the host organisms. Chemical synthesis is also often inefficient or unselective. An increasing knowledge of biosynthesis pathways has thus led to the evolution of synthetic biology as a tool for the production of valuable terpene compounds.[14] Crucial steps in the synthesis of oxidized sesquiterpenes are catalyzed by P450s.[5] Consequently, whole-cell biocatalysts are designed for efficient P450-mediated derivatization of sesquiterpenes. The hydrocarbon precursors or low-priced mevalonate pathway intermediates are used as substrates.[15–16] P450s of microbial origin have shown to perform commercially interesting terpene oxidations.[17] For biosynthetic purposes they could represent an efficient alternative to plant P450s, because they show generally high expression rates in *Escherichia coli*, and their combinations with electron-transfer proteins are readily available as bacterial whole-cell catalysts.[17]

Previously, we have identified the CYP106 family from *Bacillus megaterium* as di- and triterpene hydroxylases.[18–20] We have also revealed the biosynthetic potential of CYP105A1 from *Streptomyces griseolus*. It mediates the direct conversion of the diterpene resin abietic acid to its 15-hydroxy derivative, a key precursor of 15-hydroperoxyabietic acid, thus allowing a nine-step chemical synthesis to be avoided.[21]

Because bacterial P450s are able to perform these reactions, we have previously established P450-based *E. coli* whole-cell catalysts for in vivo terpene oxidations,[22–24] and have optimized the electron transfer onto bacterial P450s.[25] Seeking for

[a] *A. Schifrin, M. Litzenburger, Dr. M. Ringle, Dr. T. T. B. Ly, Prof. Dr. R. Bernhardt*
Universität des Saarlandes, Biochemie
Campus B2.2, 66123 Saarbrücken (Germany)
E-mail: ritabern@mx.uni-saarland.de

[b] *Dr. T. T. B. Ly*
Institute of Biotechnology
Vietnam Academy of Science and Technology (VAST)
18-Hoang Quoc Viet, Hanoi (Vietnam)

Supporting information for this article is available on the WWW under http://dx.doi.org/10.1002/cbic.201500417.

ChemPubSoc Europe

CHEMBIOCHEM Full Papers

new versatile sesquiterpene-derivatizing P450s, we turned to the myxobacterial strain *Sorangium cellulosum* So ce56. It is commonly found in upper soil fractions close to plant roots and possesses one of the largest bacterial genomes (13.1 Mbp), including 21 functional P450 genes with great potential for biosynthetic applications.[26]

Among them we found two sesquiterpene-converting enzymes: CYP260A1 oxidizes the grapefruit flavor (+)-nootkatone,[29] whereas CYP264B1 is a native (+)-eremophilene hydroxylase,[27] which was also shown to convert other sesquiterpenes of different parent structures.[30] While further exploiting the sesquiterpene derivatization potential of these P450s, we treated them with a broad range of sesquiterpenes for conversion. The current work reveals CYP260A1 and CYP264B1 to be versatile sesquiterpene oxidases, and compares their substrate specificities and selectivities. As substrates we chose monocyclic humulanes and their bicyclic caryophyllane derivatives, bicyclic eremophilanes, and tricyclic cedranes (Scheme 1). It was demonstrated that CYP260A1 efficiently converts oxygenated sesquiterpenes and that CYP264B1 regioselectively introduces allylic alcohol functions.

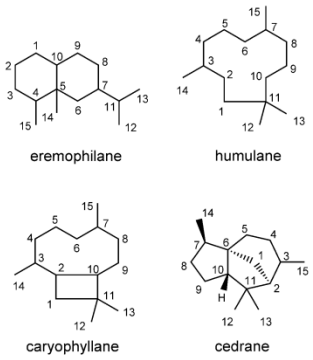

Scheme 1. Hydrocarbon skeletons of the sesquiterpenes tested for CYP260A1- and CYP264B1-mediated derivatization.

Results and Discussion

For conversions of a broad range of sesquiterpene substrates, the (+)-nootkatone oxidase CYP260A1[29] and the native (+)-eremophilene hydroxylase CYP264B1[27] were selected from a range of 21 functional *S. cellulosum* So ce56 cytochromes P450.[26] The readily available *E. coli*-based P450 whole-cell catalysts allow cost-efficient conversions on a milligram scale for structural analysis of the major products by NMR spectroscopy, in addition to GC/MS.[25,27,31]

Four structural classes of sesquiterpene substrates (Scheme 1) were chosen for conversion tests with CYP260A1 and CYP264B1. Pairs of substrates were used from the classes of eremophilanes, humulanes, and cedranes. The eremophilanes (+)-nootkatone (Scheme 2, **1**) and (+)-valencene (**4**), as well as the humulanes zerumbone (**6**) and α-humulene (**12**), represent pairs of hydrocarbons and their corresponding ketones. The cedranes (+)-3(15)-cedren-4-ol (**16**) and α-cedrene (**21**) differ in the hydroxy function at C-4 and in the position of a double bond: between carbon atoms 3 and 4 or 3 and 15, respectively. β-Caryophyllene (**14**) is related to **12**; however, it is less flexible due to the additional intramolecular bond between C-2 and C-10, which forms a strained cyclobutane ring.

CYP260A1-dependent conversion of sesquiterpenes

CYP260A1 converts the sesquiterpene ketones (+)-nootkatone (Scheme 2, **1**) and zerumbone (**6**), as well as the allylic sesquiterpene alcohol (+)-3(15)-cedren-4-ol (**16**). Whereas **1** is 62% consumed, the other two substrates are converted completely under the experimental conditions (Scheme 2, column 2). The tested non-oxidized hydrocarbon sesquiterpenes (compounds **4**, **12**, **14**, and **21**) are not converted by this P450.

The extract from the whole-cell conversion of **1** by CYP260A1 contains six products. Its main product was determined to be 4-hydroxynootkatone (**2**, 61% selectivity; Scheme 2, line 1). Addition of (+)-valencene (**4**) to the whole-cell catalyst gave no conversion. The humulane-type zerumbone (**6**) was converted quantitatively into four different products. Each of these oxidation products bears a hydroxy function at the C-5 atom and an epoxide group between the atoms C-2 and C-3 (compounds **7**–**10**; Scheme 2, line 3). Two of the products, **8** and **9**, are isomers, with a saturated bond between C-6 and C-7. In the fourth product, compound **10**, this initial double bond is epoxidized. The hydrocarbon α-humulene (**12**) and the related β-caryophyllene (**14**) are not oxidized by CYP260A1. From the group of cedrane-type sesquiterpenes, CYP260A1 oxidized (+)-3(15)-cedren-4-ol (**16**) to four products, all hydroxylated at position 9 (compounds **17**–**20**; Scheme 2, line 6). Additionally, the conversion of **16** by CYP260A1 affected the double bond between C-3 and C-15, which was either epoxidized in compound **18** or reduced in compound **20**. The allylic alcohol function of **16** at C-4 can be oxidized to a ketone, in compounds **19** and **20**.

Overall, CYP260A1 catalyzes sesquiterpene conversion for eremophilane-, humulane-, and cedrane-type structures, into a multitude of products in each case. The presence of oxy functions seems to be imperative, because non-derivatized hydrocarbon sesquiterpenes **4**, **12**, **14**, and **21** are not oxidized. Under the defined reaction conditions, the substrates are efficiently converted and often oxidized at different positions (compounds **7**–**10** and **17**–**20**). The selectivities are rather low, with 61% selectivity for the oxidation of **1** to **2** being the high-

Scheme 2. Overview of the sesquiterpene conversions mediated by CYP260A1 and CYP264B1: structures of the tested sesquiterpene substrates (including names) and the determined products (including selectivities). The product structures were determined by NMR and confirmed by GC/MS. Functionalizations introduced by the P450s are represented in bold. The yields and selectivities were calculated on the basis of GC/MS and HPLC UV/Vis peak areas. Pie charts for the degrees of substrate conversion include substrates (white), structurally determined main products (black), and undetermined side products (gray). n.d.: not determined. [a] The substances **3** and another (+)-nootkatone product could not be completely separated by GC/MS: 84% refers to the sum of both products.

ChemPubSoc Europe

CHEMBIOCHEM Full Papers

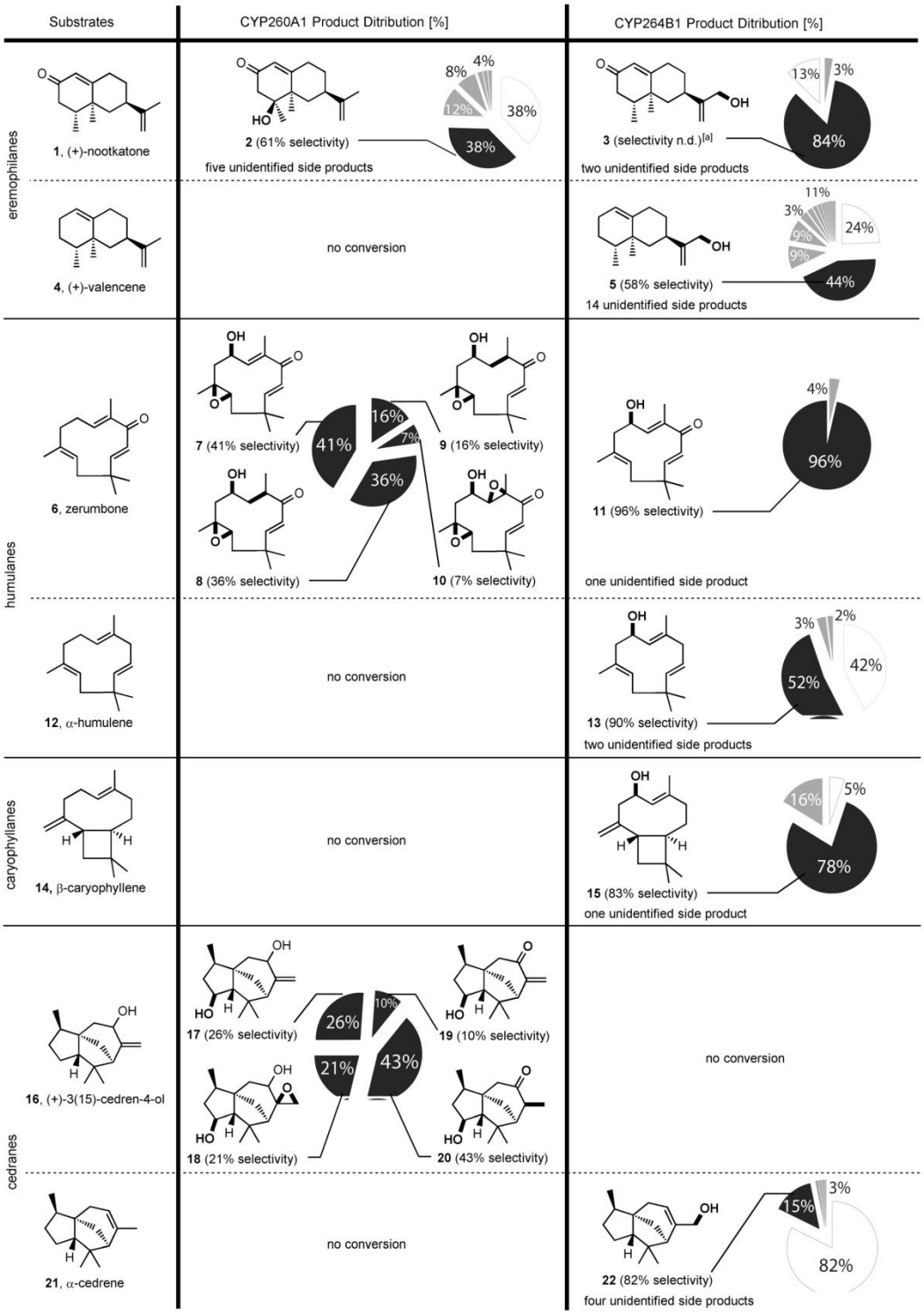

ChemPubSoc Europe

CHEMBIOCHEM Full Papers

est (Scheme 2, column 2). However, it has to be taken into account that the reaction conditions have not been optimized to obtain higher selectivities.

The introduced oxy functions in the humulanes **7**–**10** and the cedranes **17**–**20** are situated at considerable distances from each other. Thus, several binding modes for the substrates and intermediate products seem to be possible. This is also the case for **1**, because four out of its six products are monohydroxylated (results not shown). The conversion of **6** is likely to begin either with hydroxylation at C-5 (compounds **7**–**10**) or with the epoxidation of the C-2=C-3 double bond (also compounds **7**–**10**). It is likely to be completed with saturation of the C-6=C-7 double bond (compounds **8** and **9**) through the epoxide intermediate **10**. Compound **16** is first hydroxylated at C-9 (compounds **17**--**20**); further reaction steps involving oxidation of the 4-hydroxy group (compounds **19** and **20**) as well as epoxidation and reduction of the C-3=C-15 double bond (compounds **18** and **20**) do not seem to be conducted in a defined order.

CYP264B1-dependent conversion of sesquiterpenes

In contrast to the experiments with CYP260A1, each of the tested sesquiterpenes was converted by CYP264B1, with the exception of (+)-3(15)-cedren-4-ol (Scheme 2, **16**). All of the determined products—compounds **3**, **5**, **11**, **13**, **15**, and **22**—contain allylic hydroxy groups.

CYP264B1, a native (+)-eremophilene hydroxylase, oxidized (+)-nootkatone (**1**) and its non-oxygenated precursor (+)-valencene (**4**), the C-7 epimer of (+)-eremophilene (Scheme 3, **23**). In vivo conversions of **1** produced mainly 13-hydroxynootkatone (**3**) along with two side products (Scheme 2, line 1). Compound **4** was oxidized to 15 different products, with 13-hydroxyvalencene (**5**) as the main product (58% selectivity, Scheme 2, line 2). Both of the humulane-type substrates zerumbone (**6**) and α-humulene (**12**) were hydroxylated at position C-5 with selectivities of 96 and 90%, respectively (Scheme 2, lines 3 and 4). The humulane-related β-caryophyllene (**14**) was also selectively converted into its 5-hydroxy derivative **15** (83% selectivity, Scheme 2, line 5). Relative to those of the eremophilanes, the selectivities for humulane and caryophyllane conversions are remarkably high. Even the native CYP264B1 substrate (+)-eremophilene (**23**) is converted into six different products.[27] For products obtained from both eremophilane- and humulane-type substrates, the levels of conversion were higher and more selective for the keto derivatives **1** (97% conversion, three products) and **6** (100%, two products) than for the non-oxidized hydrocarbons **4** (76%, 15 products) and **12** (58%, three products; Scheme 2, column 3). Compound **16** was the only substrate that could not be oxidized by CYP264B1. In contrast, this P450 converted α-cedrene (**21**) into its 15-hydroxy derivative **22**, introducing a primary allylic alcohol function. Steric hindrance in binding of **16** might have been due to the hydroxy group at C-4 or the terminal double bond between C-3 and C-15. This might affect the difference between the conversions of **16** and **21**.

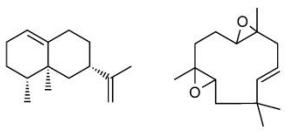

23 **24**

Scheme 3. Sesquiterpene derivatives of the tested substrates. (+)-Eremophilene (**23**) is the native substrate of CYP264B1;[27] (9*E*)-humulene-2,3;6,7-diepoxide (**24**) has been shown to have anti-acetylcholinesterase activity.[28]

Overall, it can be stated that CYP264B1 is a highly selective sesquiterpene hydroxylase. It produces allylic alcohols (at position C-5) from the humulanes **6** and **12** and also from caryophyllene (**14**). In the cases of the eremophilane-type substrates **1** and **4** it shows increased 13-hydroxylation activity, likewise producing allylic alcohols. For these structural sesquiterpene classes, the regioselectivity of the hydroxylation does not seem to be affected by the presence of a carbonyl function or by the higher flexibility of humulanes in relation to caryophyllene. However, a carbonyl group enhances the catalytic activity of CYP264B1 towards eremophilanes and humulanes: hydrocarbon substrates **4** and **12** are converted less efficiently and less selectively than their keto derivatives **1** and **6**. For cedranes, the presence of a 4-hydroxy group and a change in a double bond (**16** in comparison with **21**) abolish the catalytic function of CYP264B1.

Comparison of CYP260A1 and CYP264B1

Both P450s—CYP260A1 and CYP264B1—have shown their versatilities in oxidizing sesquiterpenes. All of the four structural classes of sesquiterpenes employed as substrates (Scheme 1) were converted either by one or by both of the enzymes. This indicates that the active sites of the P450s form cavities large or flexible enough for the binding of these structurally diverse sesquiterpenes.

Sesquiterpenes possessing oxygen-containing functional groups (Scheme 2, compounds **1**, **6**, and **16**) serve as substrates for CYP260A1, whereas the corresponding hydrocarbons are not converted. Thus, this enzyme is likely to bind the substrates through hydrogen bonds. Its oxidation reactions show high promiscuity, producing several products in similar amounts (compounds **7**–**10** from **6**, compounds **17**–**20** from **16**) by oxidizing each substrate at different positions. Wild-type CYP260A1 therefore seems a rather poor candidate for selective sesquiterpene oxidation. However, it does hydroxylate sesquiterpenes at chemically inert positions (compound **1** at C-4, compound **16** at C-9). In analogy to previous studies with CYP106A2,[32] rational mutagenesis of CYP260A1 could be conducted to increase its selectivity. The conversions of **1**, **6**, and **16** demonstrated in this study represent suitable model reactions for this purpose.

CYP264B1 converts all of the employed substances, whether they are oxygenated or non-oxygenated hydrocarbons, except for (+)-3(15)-cedren-4-ol (**16**). The enzyme's active site seems

ChemPubSoc Europe

CHEMBIOCHEM Full Papers

to be governed by hydrophobic residues, able to bind unpolar sesquiterpene hydrocarbons. However, the ketones **1** and **6** are converted more efficiently and more selectively than their non-oxidized parent sesquiterpenes **4** and **12**. This might be explained by hydrogen-bond-directed preorientation of the substrate ketones in the active site. A computational model of **1** bound to CYP264B1 shows binding of the carbonyl group to the backbone amide of Met286.[30] CYP264B1 shows high selectivities for C-5 hydroxylation of the humulanes **6** and **12** as well as for β-caryophyllene (**14**). Therefore, neither the 8-keto function nor the greater flexibility of humulanes in relation to the related caryophyllanes have an effect on the regioselectivity of the hydroxylation. Eremophilane-type substrates are converted into a multitude of products, mainly hydroxylated at C-13 (compounds **3** and **5**). The occurrence of some side products, which has likewise been observed for the physiological substrate (+)-eremophilene,[27] is probably due to reactions taking place in the *E. coli* whole-cell catalyst. CYP264B1-mediated in vitro hydroxylations of **1** and **4** have been shown to produce only one and four side products, respectively.[30] Thus, CYP264B1 is a selective sesquiterpene oxidase, which is able to functionalize a broad range of substrate structures. In general, sesquiterpene olefins of every hydrocarbon skeleton type should be considered as substrates for CYP264B1.

Taken together, both P450s—CYP260A1 and CYP264B1—should be considered for oxidation studies of further sesquiterpene classes. Whereas wild-type CYP264B1 is selective for allylic hydroxylations, CYP260A1 needs to be engineered to perform reactions with higher selectivities.

Filling gaps in the range of sesquiterpene oxidations

Most of the bacterial P450s that have been functionally investigated and found to oxidize sesquiterpenes are contained in biosynthetic clusters of different species,[33–38] including *S. cellulosum* So ce56, close to TPS genes.[27] Sesquiterpene-oxidizing P450s that are not clustered with TPS genes include CYP109B1, which performs the commercially attractive conversion of **4** into **1**,[39] CYP102A1 ($P450_{M3}$) and CYP154E1, which both oxidize **1** to form **3**, **25**, and **26** (Scheme 4), and the cyanobacterial CYP110 family.[40] CYP110E1 hydroxylates **6** to various products, although yielding mainly **27** and **28** (Scheme 5).[41]

Compounds **1** and **6** are the most widely studied sesquiterpenes in terms of bacterial P450-mediated selective oxidations. The existing choice of tools, however, covers only a few oxidation positions of model substrates **1** and **6**. In this study we provide a new product—(4*S*)-hydroxynootkatone (**2**)—through hydroxylation of the chemically inert C-4 of **1**. We also provide another way to access the primary (+)-nootkatone alcohol **3**. Previous studies have shown only allylic hydroxylation products **3** and **26** and the epoxide **25** (Scheme 4).[42–44] Oxidation of **6** leads even to a greater variety of described products. Here, we contribute a new selective hydroxylation by CYP264B1 to yield 5-hydroxyzerumbone (**11**) and the multiply oxidized CYP260A1 products **7**–**10** (Scheme 5). The side products of the CYP260A1- and CYP264B1-catalyzed reactions include new and unidentified structures. Further development

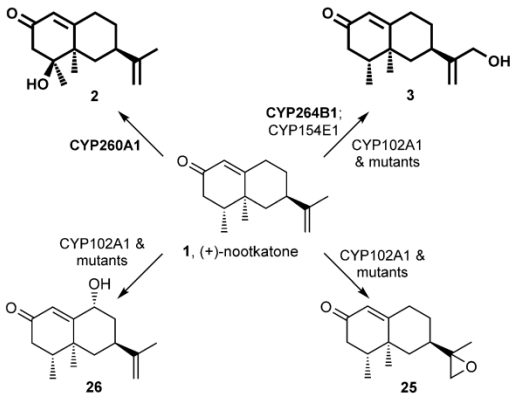

Scheme 4. Oxidation products of (+)-nootkatone (**1**) obtained through conversion with different bacterial P450s. The products identified in this study and the enzymes used are shown in bold. The other derivatization studies of **1** to **3**, **25**, and **26** were conducted by Sowden et al.,[42] by Kolev et al.,[43] and by von Bühler et al.[44]

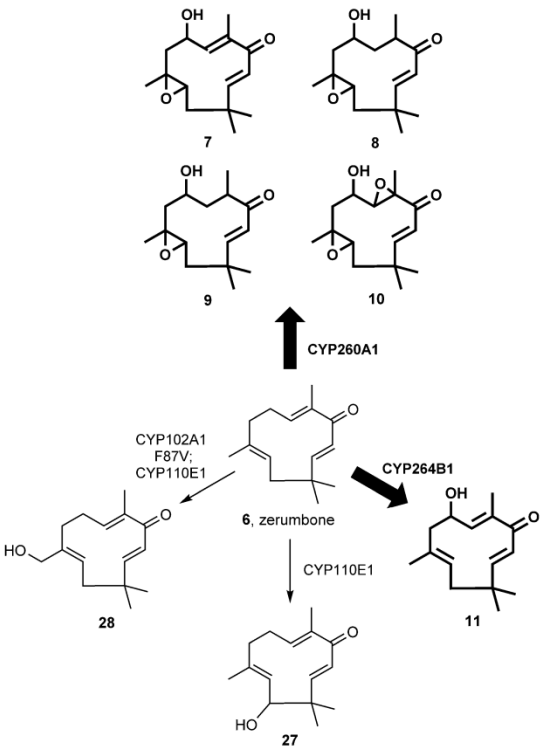

Scheme 5. Oxidation products of zerumbone (**6**) obtained through treatment with different bacterial P450s. The products identified in this study and the enzymes used are shown in bold. The derivatization of **6** by treatment with CYP110E1 and CYP102A1F87V was conducted by Makino et al.[41]

ChemPubSoc Europe

CHEMBIOCHEM Full Papers

based on the previous successful engineering studies of CYP102A1,[41] CYP101,[42] and CYP106A2[32] and including the P450s that have been used in this study should lead to further changes in reaction selectivities, and consequently, to expansion of the range of sesquiterpene products.

Applications of the oxidized sesquiterpene products

Oxidized eremophilane- and humulane-type sesquiterpenes have been shown to exhibit various pharmaceutically interesting activities. Compounds **3** and **11** are inhibitors of NO production in interferon- and lipopolysaccharide-induced RAW264.7 macrophage cells.[45–46] Compound **3** and other oxidized derivatives of (+)-nootkatone (**1**) inhibit proliferation in human cancer cell lines A549 and HL-60.[47] The oxidized zerumbone (**6**) products **7**–**10** are structurally close to (9*E*)-humulene-2,3;6,7-diepoxide (< Scheme 3, **24**), a promising anti-acetylcholinesterase agent for the treatment of Alzheimer's disease.[28] Compounds **7**–**10** could thus be tested for similar functions. Generally, the introduction of functional groups by P450s paves the way for further derivatizations. Selectively oxidized sesquiterpenes might serve as lead structures for the development of compound libraries for screening for biological activities.

Another important field of application for oxidized sesquiterpenes is that of flavors and fragrances. Introducing an alcohol or keto function significantly alters the olfactory properties of natural terpene hydrocarbons and artificial sesquiterpene-like ketones.[48] Selectively oxidized sesquiterpenes could thus serve for structure–odor relationship studies.[49]

Conclusion

The increasing industrial demand for oxidized sesquiterpenoids as pharmaceuticals, flavors, and fragrances requires synthetic methods for selective oxidation of their hydrocarbon precursors.[39,50] The methods of organic synthesis are often not able to meet this need, due to low efficiencies and selectivities. Cytochromes P450 from plants are known as native terpene oxidases.[5,13] However, bacterial P450s have been little studied for sesquiterpene derivatization until now. In this study we have focused on conversions of a structural variety of sesquiterpenes by the two P450s CYP260A1 and CYP264B1 from *S. cellulosum* So ce56. Three structural sesquiterpene types—eremophilanes, humulanes, and cedranes (Scheme 1)—were converted by both of the enzymes. The humulane-related caryophyllene (Scheme 2, **14**) was selectively hydroxylated by CYP264B1. Using the model substrates (+)-nootkatone (**1**) and zerumbone (**6**), we were able to produce the new oxidized derivatives **2** and **7**–**11**, complementary to products formed by other P450s (Schemes 4 and 5).

We also observed side products in the conversion analyses (Scheme 2), but these were not produced in sufficient amounts for structural analysis by NMR spectroscopy. The activity of CYP264B1 might be improved and the selectivities of both CYP260A1 and CYP264B1 increased by engineering through different mutagenesis techniques.[42–43,51] In this way, new oxidation positions could be accessible, to build up a toolbox for selective sesquiterpene derivatization with the aid of P450s. P450 expression can be efficiently coupled with the MVA pathway and TPS genes in terpene-producing strains to test CYP260A1 and CYP264B1 for oxidations of commercially unavailable sesquiterpenes.[15,52] Cadinane- and cubebane-type sesquiterpenes, which have recently been discovered as products of a *S. cellulosum* So ce56 TPS,[53] represent potential new substrates for CYP260A1 and CYP264B1.

Overall, CYP260A1 and CYP264B1 have been shown to be versatile oxidases, able to convert various structural sesquiterpene classes. Therefore, both P450s are promising oxidases for other sesquiterpene types. CYP264B1 is a highly selective allylic hydroxylase, derivatizing oxidized and non-oxidized substrates. CYP260A1 exclusively converts oxy-sesquiterpenes, producing unselective product mixtures. It is, however, valuable for its ability to hydroxylate chemically inert carbon atoms (compound **1** at C-4, compound **16** at C-9), and could be engineered to achieve higher selectivities.

The oxidized sesquiterpenes obtained in this study have been shown to exhibit antiproliferative (compound **3**)[47] and NO-synthesis-inhibiting (compounds **3** and **11**) abilities.[45–46] The products **7–10** are structurally close to the acetylcholinesterase-inhibiting agent **24**[28] and, therefore, likely to show similar properties. The oxidized sesquiterpenes can serve as precursors for compound libraries for the improvement of these pharmaceutically interesting properties. Because oxidation can change the odor of a fragrance compound,[48] the obtained products should be tested for their qualities as flavors and fragrances, and they could be used for structure–odor relationship studies.

Experimental Section

Enzymes and chemicals: The substrate α-cedrene was provided by Dr. Fanny Lambert (V. Mane & Fils, Bar-Sur-Loup, France), and β-caryophyllene was provided by Prof. Dr. Danièle Werck-Reichhart (University of Strasbourg, France). Isopropyl β-D-1-thiogalactopyranoside (IPTG) and 5-aminolevulinic acid were purchased from Carbolution chemicals (Saarbrücken, Germany). Bacterial media were purchased from Becton Dickinson (Heidelberg, Germany). All other chemicals were obtained from standard sources in the highest purity available.

Strains: The *E. coli* strain BL21-Gold(DE3) for the whole-cell conversions was purchased from Agilent Technologies, and the *E. coli* strain C43(DE3) was purchased from Lucigen Corp. (Middleton, USA).

Expression vectors: The redox partners Fpr and Adx_{4-108} were used for the *E. coli*-based whole-cell conversions. CYP260A1 (pET17b) was applied with the duet vector (pCDF dFA) coding for Fpr and Adx_{4-108},[31] whereas a tricistronic vector (pETC4oFA) coding for CYP264B1, Fpr and Adx_{4-108} was used for the CYP264B1-dependent conversions.[27]

Media: Terrific broth medium consisted of (per liter H_2O) yeast extract (24 g), peptone (12 g), glycerol (4 mL), K_2HPO_4 (2.31 g), and KH_2PO_4 (12.54 g).

ChemPubSoc Europe

CHEMBIOCHEM Full Papers

M9CA medium consisted of (per liter H_2O) Na_2HPO_4 (6 g), KH_2PO_4 (3 g), NaCl (0.5 g), NH_4Cl (1 g), casamino acids (4 g), glucose (4 g), $CaCl_2$ (1 M, 50 μL), $MgSO_4$ (1 M, 2 mL), and trace elements solution [2 mL, trace elements solution contained (per 50 mL H_2O) EDTA (2.5 g), $FeSO_4$ (250 mg), $ZnCl_2$ (25 mg), and $CuSO_4$ (5 mg)].

***E. coli*-based whole-cell conversions with CYP260A1**: The experiments were performed with *E. coli* BL21(DE3) gold cells. The cells were transformed with two plasmids, one for CYP260A1 (pET17b) and the other for the redox partners Fpr and Adx_{4-108} (pCDF dFA). The overnight culture was prepared in nutrient broth containing ampicillin (100 μg mL^{-1}) and streptomycin (50 μg mL^{-1}). The main culture with M9CA medium was inoculated with the overnight culture (dilution 1:100) and incubated at 37 °C in sealed baffled flasks. The induction of the corresponding genes was initiated by adding IPTG (1 mM) and 5-aminolevulinic acid (0.5 mM) when the optical density reached ≈0.9, and the culture was grown further at 28 °C. After 21 h of expression, the temperature was set to 30 °C, and the substrates (50 mM stock solution in EtOH) were added to a final concentration of 200 μM. The reaction was carried out for 48 h under the same conditions, quenched by addition of the same volume of ethyl acetate, and extracted twice. The organic phases were collected, pooled, and concentrated to dryness. The obtained extracts were stored at −20 °C until purification.

***E. coli*-based whole-cell conversions with CYP264B1**: *E. coli* C43(DE3) cells were transformed with the tricistronic vector pET-C4oFA and grown overnight in nutrient broth containing ampicillin (100 μg mL^{-1}) at 37 °C. Terrific Broth medium containing ampicillin (100 μg mL^{-1}) was inoculated with the overnight culture (dilution 1:100) and grown under the same conditions until the optical density reached ≈0.9. The expression was induced with isopropyl β-D-1-thiogalactopyranoside (1 mM) and 5-aminolevulinic acid (0.5 mM). After shaking for 24 h at 30 °C, the cells were harvested by centrifugation (4000 *g*) and resuspended in potassium phosphate buffer (50 mM, pH 7.4) containing glycerol (4%). The substrates (200 μM), IPTG (1 mM), and 5 aminolevulinic acid (0.5 mM) were added, and the conversion was carried out at 30 °C for a further 24 h in sealed baffled flasks. The reactions were stopped by cooling at 4 °C for 30 min, and then the same volume of ethyl acetate was added. The products were extracted twice, and the organic phases were pooled and concentrated to dryness. The extracts were kept at −20 °C until purification.

Purification of the products: The extracts of α-cedrene, β-caryophyllene, (+)-3(15)-cedren-4-ol, α-humulene, and (+)-valencene zerumbone (CYP260A1-dependent conversion) were dissolved in ethyl acetate and loaded on a silica gel column. Mixtures of ethyl acetate and hexane were used as mobile phase. The ratios of these solvents are substrate-dependent: β-caryophyllene (ethyl acetate/hexane 1:9), α-cedrene (1:99), (+)-3(15)-cedren-4-ol (8:2), α-humulene (1:9), (+)-valencene (5:95), and zerumbone (8:2 for the CYP260A1-dependent conversion). The collected fractions were analyzed by thin-layer chromatography (silica gel on PET) with the same solvent mixture as the mobile phase. The separated compounds were stained with *p*-anisaldehyde for detection.[31] The obtained products were pooled, concentrated to dryness, and prepared for the analysis by GC/MS or NMR spectroscopy.

The extracts of (+)-nootkatone (CYP260A1-dependent conversion) and zerumbone (CYP264B1-dependent conversion) were purified by preparative HPLC. A system consisting of a PU-2080 HPLC pump, an AS-2059-SF autosampler, and a MD-2010 multi-wavelength detector (Jasco, Gross-Umstadt, Germany) was used. The products of (+)-nootkatone were purified with a reversed-phase Nucleodur 100–5 C18 column (250×5 mm, Macherey–Nagel, Düren, Germany) and use of A) water containing acetonitrile (10%), and B) pure acetonitrile as mobile phase. A gradient from 30% to 90% B was used for the separation of the corresponding products. The product of CYP264B1-dependent zerumbone conversions were purified with an unmodified VP Nucleodur 100–5 column (250×10 mm, Macherey–Nagel) and use of hexane and ethyl acetate as mobile phase. The zerumbone product was separated under isocratic conditions (ethyl acetate/hexane 2:8). The product-containing fractions were pooled, concentrated to dryness, and prepared for further analysis by GC/MS or NMR spectroscopy.

GC/MS analysis of the products: GC/MS analysis was performed with a system consisting of an AI/AS 3000 autosampler, a DSQII quadrupole, a Focus GC column oven (Thermo Scientific), and a HP-5 ms capillary column (25 m×0.32 mm i.d., 0.52 μm film, Agilent Technologies). The compounds were analyzed under the following conditions: inlet pressure 50 kPa, column flow 10 mL min^{-1}, injection volume 1 μL, transfer line 280 °C, electron energy 70.5 eV, splitless mode. The starting oven temperature was 50 °C for 1 min; then the temperature was increased by 10 °C min^{-1} to 310 °C and held for 5 min. The carrier gas was He with a flow of 1 mL min^{-1}. Mass spectra were recorded in a *m/z* range of 20–350.

HPLC analysis of the (+)-nootkatone conversion by CYP260A1: HPLC analysis was performed with a system consisting of a PU-2080 HPLC pump, an AS-2059-SF autosampler, and a MD-2010 multi-wavelength detector (Jasco). A Nucleodur 100–5 C_{18} column (125×4 mm, Macherey–Nagel) was used at 40 °C. The mobile phase consisted of A) a mixture of water and acetonitrile (90:10), and B) pure acetonitrile. The samples were dissolved in a mixture of water and acetonitrile (70:30) and separated by use of the following gradient with a flow rate of 0.8 mL min^{-1}: 30% solvent B for 1 min, linear increase to 90% for 8 min, maintained for 1 min, immediate decrease to 30%, maintained for 5 min. (+)-Nootkatone and its oxidation products were detected at 254 nm.

NMR analysis and data for the obtained products: NMR spectra were recorded in $CDCl_3$ with a Bruker DRX 500 spectrometer (Institut für Pharmazeutische Biologie, Universität des Saarlandes). The 2D NMR spectra were recorded as gs-HH-COSY, gs-HSQC, and gs-HMBC. All chemical shifts are relative to $CHCl_3$ or $CDCl_3$ (δ = 77.00 ppm for ^{13}C NMR, δ = 7.24 ppm for ^{1}H NMR) with use of the standard δ notion.

(4*S*)-Hydroxynootkatone (2): ^{1}H NMR (500 MHz, $CDCl_3$): δ = 1.24 (s, 3H; H-14), 1.26 (s, 3H; H-15), 1.36 (m, 1H; H-8a), 1.62 (ddd, *J* = 13.0, 3.0 and 3.0 Hz, 1H; H-6a), 1.73 (s, 3H; H-13), 1.85 (m, 1H; H-8b), 1.96 (dd, *J* = 13.0, 13.0 Hz, 1H; H-6b), 2.31 (dddd, *J* = 15.5, 13.0, 3.0, 3.0 Hz, 1H; H-7), 2.42 (dd, *J* = 17.0, 1.0 Hz, 1H; H-3a), 2.43 (m, 1H; H-9a), 2.51 (m, 1H; H-9b), 2.76 (d, *J* = 17 Hz, 1H; H-3b), 4.73 (s, 2H; H-12), 5.83 ppm (br s, H-1); ^{13}C NMR (125 MHz, $CDCl_3$): δ = 20.8 (C-13), 22.4 (C-14), 23.4 (C-15), 30.8 (C-8), 33.1, (C-9), 35.9 (C-6), 40.4 (C-7), 44.5 (C-5), 49.0 (C-3), 75.9 (C-4), 109.4 (C-12), 124.5 (C-1), 149.1 (C-11), 167.0 (C-10), 197.3 ppm (C-2).

13-Hydroxynootkatone (3): The NMR data for this compound are presented in Ly et al.[30]

13-Hydroxyvalencene (5): ^{1}H NMR (500 MHz, $CDCl_3$): δ = 0.85 (d, *J* = 6.4 Hz, 3H; H-15), 0.93 (s, 3H; H-14), 0.97 (d, *J* = 12.8 Hz, 1H; H-6a), 1.19 (m, 1H; H-8a), 1.40 (m, 3H; H-3, H-4), 1.80 (m, 1H; H-8b), 1.89 (m, 1H; H-6b), 1.92 (m, 1H; H-2a), 2.05 (m, 1H; H-9a), 2.08 (m, 1H; H-2b), 2.29 (m, 2H; H-7, H-9b), 4.11 (d, *J* = 6.1 Hz, 2H; H-13), 4.86 (s, 1H; H-12a), 5.00 (s, 1H; H-12b), 5.32 ppm (m, 1H; H-1); ^{13}C NMR (125 MHz, $CDCl_3$): δ = 15.6 (C-15), 18.5 (C-14), 25.9 (C-2),

ChemPubSoc Europe

CHEMBIOCHEM Full Papers

27.1 (C-3), 32.7, (C-9), 33.6 (C-8), 36.7 (C-7), 37.9 (C-5), 40.9 (C-4), 45.4 (C-6), 65.3 (C-13), 107.9 (C-12), 120.4 (C-1), 142.7 (C-10), 154.1 ppm (C-11).

2,3-Epoxy-5-hydroxyzerumbone (7): ^{1}H NMR (500 MHz, $CDCl_3$): $\delta = 1.06$ (s, 3H; H-12, H-13), 1.28 (s, 3H; H-12, H-13), 1.21 (s, 3H; H-14), 1.29 (m, 1H; H-4a), 1.42 (m, 1H; H-1a), 1.91 (m, 1H; H-1b), 1.97 (d, $J = 1.5$ Hz, 3H; H-15), 2.63 (m, 1H; H-4b), 2.74 (dd, $J = 11.2$, 1.7 Hz, 1H; H-2), 4.58 (m, 1H; H-5), 5.92 ppm (d, $J = 9.7$, 1.5 Hz, 1H; H-6), H-9 and H-10 were not present; ^{13}C NMR (125 MHz, $CDCl_3$): $\delta = 12.6$ (C-15), 16.8 (C-14), 24.0 and 29.7 (C-12 and C-13), 35.9 (C-11), 42.6 (C-1), 47.6 (C-4), 59.3 (C-3), 62.7 (C-2), 64.9 (C-5), 128.7 (C-9), 142.5 (C-7), 144.4 (C-6), 161.3 (C-10), 202.7 ppm (C-8).

6,7-Dihydro-2,3-epoxy-5-hydroxyzerumbone (8): ^{1}H NMR (500 MHz, $CDCl_3$): $\delta = 1.13$ (s, 3H; H-12, H-13), 1.24 (s, 3H; H-12, H-13), 1.18 (s, 3H; H-14), 1.18 (d, $J = 6.8$ Hz, 3H; H-15), 1.33 (m, 2H; H-4a, H-1a), 1.89 (m, 2H; H-6a, H-1b), 2.08 (d, $J = 13.3$ Hz, 1H; H-4b), 2.16 (dd, $J = 15.7$, 3.3 Hz, 1H; H-6b), 2.63 (m, 1H; H-2), 2.79 (m, 1H; H-7), 3.33 (dd, $J = 10.2$, 6.9 Hz, 1H; H-5), 6.25 (d, $J = 16.0$ Hz, 1H; H-9), 6.29 ppm (d, $J = 16.0$ Hz, 1H; H-10); ^{13}C NMR (125 MHz, $CDCl_3$): $\delta = 12.6$ (C-15), 17.5 (C-14), 23.4 and 29.6 (C-12 and C-13), 36.1 (C-11), 40.4 (C-1), 42.7 (C-6), 44.7 (C-7), 51.1 (C-4), 59.1 (C-3), 60.5 (C-2), 66.3 (C-5), 128.0 (C-9), 150.4 (C-10), 204.0 ppm (C-8).

6,7-Dihydro-2,3-epoxy-5-hydroxyzerumbone (9): ^{1}H NMR (500 MHz, $CDCl_3$): $\delta = 1.13$ (s, 3H; H-12, H-13), 1.25 (s, 3H; H-12, H-13), 1.21 (d, $J = 7.0$ Hz, 3H; H-15), 1.22 (s, 3H; H-14), 1.31 (m, 1H; H-4a), 1.34 (m, 1H; H-1a), 1.70 (m, 1H; H-6a), 1.80 (dd, $J = 15.1$, 11.7 Hz, 1H; H-6b), 1.86 (m, 1H; H-1b), 2.13 (d, $J = 13.5$ Hz, 1H; H-4b), 2.61 (m, 1H; H-2), 2.63 (m, 1H; H-7), 3.32 (m, 1H; H-5), 6.25 (d, $J = 16.1$ Hz, 1H; H-10), 6.33 ppm (d, $J = 16.1$ Hz, 1H; H-9); ^{13}C NMR (125 MHz, $CDCl_3$): $\delta = 16.7$ (C-15), 17.5 (C-14), 23.5 and 29.7 (C-12 and C-13), 36.3 (C-11), 39.8 (C-1), 45.4 (C-6), 46.4 (C-7), 50.2 (C-4), 59.3 (C-3), 60.1 (C-2), 68.1 (C-5), 124.9 (C-9), 151.2 (C-10), 206.5 ppm (C-8).

2,3:6,7-Diepoxy-5-hydroxyzerumbone (10): ^{1}H NMR (500 MHz, $CDCl_3$): $\delta = 1.15$ (s, 3H; H-12, H-13), 1.25 (s, 3H; H-12, H-13), 1.37 (s, 3H; H-14), 1.37 (m, 1H; H-4b), 1.51 (dd, $J = 14.3$, 11.2 Hz, 1H; H-1a), 1.69 (s, 3H; H-15), 1.97 (m, 1H; H-1b), 2.60 (m, 1H; H-4b), 2.65 (dd, $J = 11.3$, 1.5 Hz, 1H; H-2), 2.78 (d, $J = 9.0$ Hz, 1H; H-6), 3.74 (m, 1H; H-5), 5.95 (d, $J = 17.2$ Hz, 1H; H-9), 6.83 ppm (d, $J = 17.2$ Hz, 1H; H-10); ^{13}C NMR (125 MHz, $CDCl_3$): $\delta = 16.6$ (C-15), 17.6 (C-14), 25.1 and 30.1 (C-12 and C-13), 35.3 (C-11), 41.6 (C-1), 44.7 (C-4), 58.1 (C-3), 61.7 (C-2), 65.2 (C-5), 65.9 (C-6), 66.7 (C-7), 126.4 (C-9), 160.0 (C-10), 197.2 ppm (C-8).

5-Hydroxyzerumbone (11): ^{1}H NMR (500 MHz, $CDCl_3$): $\delta = 1.06$ (s, 3H; H-12, H-13), 1.18 (s, 3H; H-12, H-13), 1.54 (s, 3H; H-14), 1.90 (s, 3H; H-15), 1.90 (m, 1H; H-1a), 2.13 (m, 1H; H-4a), 2.34 (t, $J = 12.8$ Hz, 1H; H-1b), 2.74 (m, 1H; H-4b), 4.62 (m, 1H; H-5), 5.28 (br d, $J = 10.9$ Hz, 1H; H-2), 5.79 (d, $J = 9.8$ Hz, 1H; H-6), 5.88 (d, $J = 16.5$ Hz, 1H; H-10), 5.98 ppm (d, $J = 16.5$ Hz, 1H; H-9); ^{13}C NMR (125 MHz, $CDCl_3$): $\delta = 12.2$ (C-15), 16.5 (C-14), 24.2 and 29.3 (C-12 and C-13), 38.5 (C-11), 42.5 (C-1), 49.3 (C-4), 64.9 (C-5), 126.7 (C-2), 127.3 (C-9), 133.0 (C-3), 140.6 (C-7), 145.6 (C-6), 162.4 (C-10), 204.2 ppm (C-8).

5-Hydroxyhumulene (13): ^{1}H NMR (500 MHz, $CDCl_3$): $\delta = 1.02$ (s, 3H; H-12, H-13), 1.07 (s, 3H; H-12, H-13), 1.45 (s, 3H; H-14), 1.70 (s, 3H; H-14), 1.80 (dd, $J = 13.5$, 5.2 Hz, 1H; H-1a), 1.98 (dd, $J = 13.5$,d 10.0 Hz, 1H; H-1b), 2.05 (dd, $J = 12.0$, 8.2 Hz, 1H; H-4a), 2.31 (m, 1H; H-8a), 2.46 (dd, $J = 12.0$, 5.2 Hz, 1H; H-4b), 2.71 (dd, $J = 13.8$, 8.3 Hz, 1H; H-8b), 4.54 (m, 1H; H-5), 4.94 (dd, $J = 9.7$, 5.3 Hz, 1H; H-2), 5.00, dt, $J = 9.6$, 1.4 Hz, 1H; H-6), 5.14 (d, $J = 16.0$ Hz, 1H; H-10), 5.58 ppm (m, 1H; H-9); ^{13}C NMR (125 MHz, $CDCl_3$): $\delta = 16.7$ (C-14), 19.1 (C-15), 25.5 and 28.7 (C-12 and C-13), 36.9 (C-11), 39.4 (C-8), 41.7 (C-1), 49.3 (C-4), 67.0 (C-5), 126.5 (C-2), 127.5 (C-9), 130.0 (C-6), 131.7 (C-3), 141.5 (C-10), 141.9 ppm (C-7).

5-Hydroxycaryophyllene (15): ^{1}H NMR (500 MHz, $CDCl_3$): $\delta = 0.94$ (s, 3H; H-12, H-13), 0.95 (s, 3H; H-12, H-13), 1.41 (t, $J = 9.7$ Hz, 1H; H-10), 1.53–1.58 (m, 3H; H-1a, H-8a, H-9a), 1.60 (s, 3H; H-14), 1.67 (m, 1H; H-9b), 1.78 (m, 1H; H-1b), 1.92 (t, $J = 10.6$ Hz, 1H; H-4a), 2.25 (dd, $J = 9.7$, 8.9 Hz, 1H; H-2), 2.51 (dd, $J = 13.7$, 6.7 Hz, 1H; H-8), 2.76 (dd, $J = 11.5$, 6.6 Hz, 1H; H-4b), 4.58 (m, 1H; H-5), 4.89 (s, 1H; H-15a), 4.98 (s, 1H; H-15b), 5.24 ppm (d, $J = 10.2$ Hz, 1H; H-6); ^{13}C NMR (125 MHz, $CDCl_3$): $\delta = 21.8$ and 22.9 (C-12 and C-13), 29.8 (C-14), 31.2 (C-9), 32.7 (C-11), 34.7 (C-8), 42.2 (C-1), 48.9 (C-2), 49.2 (C-4), 55.5 (C-10), 70.8 (C-5), 112.4 (C-15), 127.8 (C-6), 136.9 (C-7), 150.0 ppm (C-3).

4,9-Dihydroxy-3(15)-cedrene (17): ^{1}H NMR (500 MHz, $CDCl_3$): $\delta = 0.92$ (d, $J = 7.1$ Hz, 3H; H-14), 1.00 (s, 3H; H-12, H-13), 1.11 (s, 3H; H-12, H-13), 1.18 (dd, $J = 11.9$, 10.2 Hz, 1H; H-5a), 1.31 (d, $J = 11.6$ Hz, 1H; H-1a), 1.50 (m, 1H; H-8a), 1.65 (d, $J = 8.3$ Hz, 1H; H-10), 1.72 (m, 1H; H-1b), 1.78 (m, 1H; H-7), 2.08 (m, 1H; H-8b), 2.20 (m, 1H; H-5b), 2.35 (d, $J = 4.2$ Hz, 1H; H-2), 4.10 (m, 1H; H-9), 4.35 (m, 1H; H-4), 4.74 (t, $J = 2.1$ Hz, 1H; H-15a), 4.98 ppm (t, $J = 2.1$ Hz, 1H; H-15b); ^{13}C NMR (125 MHz, $CDCl_3$): $\delta = 15.2$ (C-14), 26.4 and 26.5 (C-12 and C-13), 39.0 (C-7), 41.1 (C-11), 45.0 (C-5), 45.6 (C-1), 46.6 (C-8), 53.5 (C-6), 60.8 (C-2), 65.8 (C-10), 69.7 (C-4), 73.6 (C-9), 107.0 (C-15), 153.4 ppm (C-3).

3,15-Epoxy-4,9-dihydroxycedrane (18): ^{1}H NMR (500 MHz, $CDCl_3$): $\delta = 0.93$ (d, $J = 7.1$ Hz, 3H; H-14), 1.10 (s, 3H; H-12, H-13), 1.17 (s, 3H; H-12, H-13), 1.22 (m, 1H; H-5a), 1.39 (m, 1H; H-2), 1.50 (AB q, $J = 2.0$ Hz, $\Delta\nu = 5.2$ Hz, 1H H-8a), 1.62 (m, 2H; H-1), 1.72 (d, $J = 8.2$ Hz, 1H; H-10), 1.80 (m, 1H; H-7), 2.08 (m, 1H; H-8b), 2.22 (m, 1H; H-5b), 2.61 (d, $J = 4.7$ Hz, 1H; H-15a), 3.05 (d, $J = 4.7$ Hz, 1H; H-15b), 4.10 (m, 1H; H-4), 4.11 ppm (m, 1H; H-9); ^{13}C NMR (125 MHz, $CDCl_3$): $\delta = 15.1$ (C-14), 25.9 and 26.4 (C-12 and C-13), 39.1 (C-7), 40.3 (C-11), 42.3 (C-1), 43.2 (C-5), 46.5 (C-8), 51.7 (C-15), 52.9 (C-6), 58.1 (C-2), 61.5 (C-3), 65.1 (C-10), 65.3 (C-4), 73.5 ppm (C-9).

9-Hydroxy-4-keto-3(15)-cedrene (19): ^{1}H NMR (500 MHz, $CDCl_3$): $\delta = 0.93$ (d, $J = 7.1$ Hz, 3H, H-14), 0.93 (s, 3H; H-12, H-13), 1.14 (s, 3H; H-12, H-13), 1.52 (AB q, $J = 2.2$ Hz, $\Delta\nu = 5.5$ Hz, 1H; H-8a), 1.59 (d, $J = 7.8$ Hz, 1H; H-10), 1.69 (d, $J = 12.2$ Hz, 1H; H-1a), 1.91 (m, 1H; H-7), 1.93 (m, 1H; H-1b), 2.11 (m, 1H; H-8b), 2.32 (dd, $J = 17.5$, 1.0 Hz, 1H; H-5a), 2.53 (dd, $J = 17.5$, 3.2 Hz, 1H; H-5b), 2.57 (d, $J = 4.2$ Hz, 1H; H-2), 4.15 (m, 1H; H-9), 5.04 (d, $J = 2.0$ Hz, 1H; H-15a), 5.90 ppm (d, $J = 2.0$ Hz, 1H; H-15b); ^{13}C NMR (125 MHz, $CDCl_3$): $\delta = 15.4$ (C-14), 25.8 and 28.9 (C-12 and C-13), 39.3 (C-7), 42.2 (C-11), 42.8 (C-1), 46.3 (C-8), 51.6 (C-5), 53.1 (C-6), 58.3 (C-2), 67.9 (C-10), 73.5 (C-9), 121.1 (C-15), 148.2 (C-3), 201.1 ppm (C-4).

9-Hydroxy-4-ketocedrane (20): ^{1}H NMR (500 MHz, $CDCl_3$): $\delta = 0.91$ (d, $J = 7.1$ Hz, 3H, H-14), 1.05 (s, 3H; H-12, H-13), 1.09 (s, 3H; H-12, H-13), 1.16 (d, $J = 7.0$ Hz, 3H, H-15), 1.45 (AB q, $J = 1.9$ Hz, $\Delta\nu = 5.1$ Hz, 1H; H-8a), 1.57 (d, $J = 8.4$ Hz, 1H; H-10), 1.78 (m, 1H; H-1a), 1.90 (m, 1H; H-7), 1.97 (m, 1H; H-2), 1.97 (m, 1H; H-1b), 2.10 (m, 1H; H-8b), 2.31 (d, $J = 14.5$ Hz, 1H; H-5a), 2.40 (dd, $J = 14.7$, 2.6 Hz, 1H; H-5b), 2.50 (m, 1H; H-3), 4.07 ppm (m, 1H; H-9). ^{13}C NMR (125 MHz, $CDCl_3$): $\delta = 14.5$ (C-15), 15.4 (C-14), 27.8 and 28.8 (C-12 and C-13), 38.5 (C-7), 43.5 (C-11), 46.5 (C-8), 47.1 (C-1), 51.7 (C-5), 51.8 (C-3), 55.3 (C-6), 56.7 (C-2), 67.7 (C-10), 73.4 (C-9), 212.5 ppm (C-4).

15-Hydroxy-3(4)-cedrene (22): ^{1}H NMR (500 MHz, $CDCl_3$): $\delta = 0.84$ (d, $J = 7.1$ Hz, 3H, H-14), 0.95 (s, 3H; H-12, H-13), 0.98 (s, 3H; H-12,

ChemPubSoc Europe

CHEMBIOCHEM Full Papers

H-13), 1.34–1.38 (m, 3H; H-1a, H-8a, H-9a), 1.57 (m, 1H; H-9b), 1.66–1.78 (m, 3H; H-1b, H-2, H-7b), 1.82–1.87 (m, 2H; H-5a, H-8b), 1.93 (d, $J=3.8$ Hz, 1H; H-10), 2.23 (dd, $J=17.2$ and 1.4 Hz, 1H; H-7), 3.99 (AB q, $J=13.5$ Hz, $\Delta\nu=41.4$ Hz, 1H; H-15), 5.50 ppm (m, 1H; H-1); ^{13}C NMR (125 MHz, $CDCl_3$): $\delta=15.4$ (C-14), 24.8 (C-9), 25.5 (C-13), 27.7 (C-12), 36.1, (C-8), 38.6 (C-5), 40.6 (C-1), 41.4 (C-7), 48.4 (C-11), 50.4 (C-10), 54.3 (C-6), 59.1 (C-2), 67.2 (C-15), 120.4 (C-4), 144.1 ppm (C-3).

Acknowledgements

This work was supported by a grant from the Deutsche Forschungsgemeinschaft to R.B. (Be1343/23-1) and from the DAAD (Deutscher Akademischer Austauschdienst), as well as from the Vietnam National Foundation for Science and Technology Development (NAFOSTED) under grant number 106-NN.02–2013.57 to T.T.B.L. We want to express our gratitude to Dr. Fanny Lambert (V. Mane & Fils, Bar-Sur-Loup, France) and to Prof. Dr. Danièle Werck-Reichhart (University of Strasbourg, France) for the kind gifts of α-cedrene and β-caryophyllene. Furthermore, we wish to thank Dr. Josef Zapp, Reiner Wintringer, and Dr. Gerardine Pereira (Universität des Saarlandes) for conducting the NMR measurements, for help with GC/MS measurements, and for helpful comments on the manuscript, respectively.

Keywords: cytochromes · enzyme catalysis · hydroxylation · regioselectivity · terpenoids

[1] Y. Gao, R. B. Honzatko, R. J. Peters, *Nat. Prod. Rep.* **2012**, *29*, 1153 – 1175.
[2] D. J. Miller, R. K. Allemann, *Nat. Prod. Rep.* **2012**, *29*, 60 – 71.
[3] D. Joulain, W. A. König, *The Atlas of Spectral Data of Sesquiterpene Hydrocarbons*, E. B.-Verlag, Hamburg, **1998**.
[4] C. Weitzel, H. T. Simonsen, *Phytochem. Rev.* **2015**, *14*, 7 – 24.
[5] I. Pateraki, A. M. Heskes, B. Hamberger in *Biotechnology of Isoprenoids, Vol. 148* (Eds.: J. Schrader, J. Bohlmann), Springer, Berlin, **2015**, pp. 107 – 139.
[6] R. Bernhardt, V. Urlacher, *Appl. Microbiol. Biotechnol.* **2014**, *98*, 6185 – 6203.
[7] J. Gershenzon, N. Dudareva, *Nat. Chem. Biol.* **2007**, *3*, 408 – 414.
[8] E. Breitmaier in *Terpene*, Wiley, Weinheim, **2008**, pp. 23 – 50.
[9] G. Schneider, H. Anke, O. Sterner, *Nat. Prod. Lett.* **1997**, *10*, 133 – 138.
[10] C. J. Paddon, J. D. Keasling, *Nat. Rev. Microbiol.* **2014**, *12*, 355 – 367.
[11] D. E. Cane, H. Ikeda, *Acc. Chem. Res.* **2012**, *45*, 463 – 472.
[12] S. Schulz, J. S. Dickschat, *Nat. Prod. Rep.* **2007**, *24*, 814 – 842.
[13] B. Hamberger, S. Bak, *Phil. Trans. R. Soc. Lond. B* **2013**, *368*, 20120426.
[14] N. Kitaoka, X. Lu, B. Yang, R J. Peters, *Mol. Plant* **2015**, *8*, 6 – 16.
[15] H. Harada, F. Yu, S. Okamoto, T. Kuzuyama, R. Utsumi, N. Misawa, *Appl. Microbiol. Biotechnol.* **2009**, *81*, 915 – 925.
[16] J. Kirby, J. D. Keasling, *Annu. Rev. Plant Biol.* **2009**, *60*, 335 – 355.
[17] S. Janocha, D. Schmitz, R. Bernhardt in *Biotechnology of Isoprenoids, Vol. 148* (Eds.: J. Schrader, J. Bohlmann), Springer, Berlin Heidelberg, **2015**, pp. 215 – 250.
[18] S. Bleif, F. Hannemann, M. Lisurek, J. P. von Kries, J. Zapp, M. Dietzen, I. Antes, R. Bernhardt, *ChemBioChem* **2011**, *12*, 576 – 582.
[19] D. Schmitz, J. Zapp, R. Bernhardt, *FEBS J.* **2012**, *279*, 1663 – 1674.
[20] E. Brill, F. Hannemann, J. Zapp, G. Brüning, J. Jauch, R. Bernhardt, *Appl. Microbiol. Biotechnol.* **2014**, *98*, 1703 – 1717.
[21] S. Janocha, J. Zapp, M. Hutter, M. Kleser, J. Bohlmann, R. Bernhardt, *ChemBioChem* **2013**, *14*, 467 – 473.
[22] D. Zehentgruber, F. Hannemann, S. Bleif, R. Bernhardt, S. Lütz, *ChemBioChem* **2010**, *11*, 713 – 721.
[23] S. Bleif, F. Hannemann, J. Zapp, D. Hartmann, J. Jauch, R. Bernhardt, *Appl. Microbiol. Biotechnol.* **2012**, *93*, 1135 – 1146.
[24] S. Janocha, R. Bernhardt, *Appl. Microbiol. Biotechnol.* **2013**, *97*, 7639 – 7649.
[25] M. Ringle, Y. Khatri, J. Zapp, F. Hannemann, R. Bernhardt, *Appl. Microbiol. Biotechnol.* **2013**, *97*, 7741 – 7754.
[26] Y. Khatri, F. Hannemann, K. M. Ewen, D. Pistorius, O. Perlova, N. Kagawa, A. O. Brachmann, R. Müller, R. Bernhardt, *Chem. Biol.* **2010**, *17*, 1295 – 1305.
[27] A. Schifrin, T. T. B. Ly, N. Günnewich, J. Zapp, V. Thiel, S. Schulz, F. Hannemann, Y. Khatri, R. Bernhardt, *ChemBioChem* **2015**, *16*, 337 – 344.
[28] P. Chen, P.-P. Wang, Z.-Z. Jiao, L. Xiang, *Helv. Chim. Acta* **2014**, *97*, 388 – 397.
[29] K. M. Ewen, F. Hannemann, Y. Khatri, O. Perlova, R. Kappl, D. Krug, J. Hüttermann, R. Müller, R. Bernhardt, *J. Biol. Chem.* **2009**, *284*, 28590 – 28598.
[30] T. B. Ly, Y. Khatri, J. Zapp, M. Hutter, R. Bernhardt, *Appl. Microbiol. Biotechnol.* **2012**, *95*, 123 – 133.
[31] M. Litzenburger, F. Kern, Y. Khatri, R. Bernhardt, *Drug Metab. Dispos.* **2015**, *43*, 392 – 399.
[32] K. T. Nguyen, C. Virus, N. Günnewich, F. Hannemann, R. Bernhardt, *ChemBioChem* **2012**, *13*, 1161 – 1166.
[33] D. Zhu, M.-J. Seo, H. Ikeda, D. E. Cane, *J. Am. Chem. Soc.* **2011**, *133*, 2128 – 2131.
[34] B. Zhao, X. Lin, L. Lei, D. C. Lamb, S. L. Kelly, M. R. Waterman, D. E. Cane, *J. Biol. Chem.* **2008**, *283*, 8183 – 8189.
[35] B. Zhao, L. Lei, D. G. Vassylyev, X. Lin, D. E. Cane, S. L. Kelly, H. Yuan, D. C. Lamb, M. R. Waterman, *J. Biol. Chem.* **2009**, *284*, 36711 – 36719.
[36] B. Zhao, M. R. Waterman, *IUBMB Life* **2011**, *63*, 473 – 477.
[37] S. C. Moody, B. Zhao, L. Lei, D. R. Nelson, J. G. L. Mullins, M. R. Waterman, S. L. Kelly, D. C. Lamb, *FEBS J.* **2012**, *279*, 1640 – 1649.
[38] R. Quaderer, S. Omura, H. Ikeda, D. E. Cane, *J. Am. Chem. Soc.* **2006**, *128*, 13036 – 13037.
[39] M. Girhard, K. Machida, M. Itoh, R. Schmid, A. Arisawa, V. Urlacher, *Microb. Cell Fact.* **2009**, *8*, 36.
[40] H. Harada, K. Shindo, K. Iki, A. Teraoka, S. Okamoto, F. Yu, J.-i. Hattan, R. Utsumi, N. Misawa, *Appl. Microbiol. Biotechnol.* **2011**, *90*, 467 – 476.
[41] T. Makino, T. Otomatsu, K. Shindo, E. Kitamura, G. Sandmann, H. Harada, N. Misawa, *Microb. Cell Fact.* **2012**, *11*, 95.
[42] R. J. Sowden, S. Yasmin, N. H. Rees, S. G. Bell, L. L. Wong, *Org. Biomol. Chem.* **2005**, *3*, 57 – 64.
[43] J. N. Kolev, J. M. Zaengle, R. Ravikumar, R. Fasan, *ChemBioChem* **2014**, *15*, 1001 – 1010.
[44] C. von Bühler, P. Le-Huu, V. B. Urlacher, *ChemBioChem* **2013**, *14*, 2189 – 2198.
[45] J. Xu, J. Su, Y. Li, N. Tan, *Chem. Nat. Compd.* **2013**, *49*, 457 – 461.
[46] H.-Y. Min, M. S. Kim, D. S. Jang, E.-J. Park, E.-K. Seo, S. K. Lee, *Int. Immunopharmacol.* **2009**, *9*, 844 – 849.
[47] A. Gliszczyńska, A. Łysek, T. Janeczko, M. Świtalska, J. Wietrzyk, C. Wawrzeńczyk, *Bioorg. Med. Chem.* **2011**, *19*, 2464 – 2469.
[48] B. Schilling, R. Kaiser, A. Natsch, M. Gautschi, *Chemoecology* **2010**, *20*, 135 – 147.
[49] C. Delasalle, C. A. de March, U. J. Meierhenrich, H. Brevard, J. Golebiowski, N. Baldovini, *Chem. Biodiversity* **2014**, *11*, 1843 – 1860.
[50] C. Gavira, R. Höfer, A. Lesot, F. Lambert, J. Zucca, D. Werck-Reichhart, *Metab. Eng.* **2013**, *18*, 25 – 35.
[51] A. Glieder, E. T. Farinas, F. H. Arnold, *Nat. Biotechnol.* **2002**, *20*, 1135 – 1139.
[52] M. C. Chang, R. A. Eachus, W. Trieu, D. K. Ro, J. D. Keasling, *Nat. Chem. Biol.* **2007**, *3*, 274 – 277.
[53] Y. Yamada, T. Kuzuyama, M. Komatsu, K. Shin-ya, S. Omura, D. E. Cane, H. Ikeda, *Proc. Natl. Acad. Sci. USA* **2015**, *112*, 857 – 862.

Manuscript received: August 17, 2015
Accepted article published: October 9, 2015
Final article published: November 10, 2015

2.3 Selective oxidation of carotenoid-derived aroma compounds by CYP260B1 and CYP267B1 from *Sorangium cellulosum* So ce56

Martin Litzenburger and Rita Bernhardt

Applied Microbiology and Biotechnology [Epub ahead of print]

doi: 10.1007/s00253-015-7269-7

Appl Microbiol Biotechnol
DOI 10.1007/s00253-015-7269-7

BIOTECHNOLOGICALLY RELEVANT ENZYMES AND PROTEINS

Selective oxidation of carotenoid-derived aroma compounds by CYP260B1 and CYP267B1 from *Sorangium cellulosum* So ce56

Martin Litzenburger[1] · **Rita Bernhardt**[1]

Received: 11 September 2015 / Revised: 17 December 2015 / Accepted: 23 December 2015

Abstract Due to their bioactive properties as well as their application as precursors in chemical synthesis, hydroxylated isoprenoids and norisoprenoids are very valuable compounds. The efficient hydroxylation of such compounds remains a challenge in organic chemistry caused by the formation of a variety of side products and lack of overall regio- and stereoselectivity. In contrast, cytochromes P450 are known for their selective oxidation under mild conditions. Here, we demonstrate for the first time the ability of myxobacterial CYP260B1 and CYP267B1 from *Sorangium cellulosum* So ce56 to oxidize such carotenoid-derived aroma compounds. A focused library of 14 substrates such as ionones, damascones, as well as some of their isomers and derivatives was screened in vitro. Both P450s were capable of an efficient oxidation of all tested compounds. CYP260B1-dependent conversions mainly formed multiple products, whereas conversions by CYP267B1 resulted predominantly in a single product. To identify the main products by NMR spectroscopy, an *Escherichia coli*-based whole-cell system was used. CYP267B1 showed a hydroxylase activity towards the formation of allylic alcohols. Likewise, CYP260B1 performed the allylic hydroxylation of β-damascone [(E)-1-(2,6,6-trimethylcyclohex-1-enyl)but-2-en-1-one] and δ-damascone [(E)-1-(2,6,6-trimethylcyclohex-3-enyl)but-2-en-1-one]. Moreover, CYP260B1 showed an epoxidase activity towards β-ionone [(E)-4-(2,6,6-trimethylcyclohex-1-enyl)but-3-en-2-one] as well as the methyl-substituted α-ionone derivatives raldeine [(E)-1-(2,6,6-trimethylcyclohex-2-enyl)pent-1-en-3-one] and isoraldeine [(E)-3-methyl-4-(2,6,6-trimethylcyclohex-2-enyl)but-3-en-2-one]. In addition, to known products, also novel products such as 2-OH-δ-damascone [(E)-1-(5-hydroxy-2,6,6-trimethylcyclohex-3-enyl)but-2-en-1-one], 3-OH-allyl-α-ionone [(E)-1-(4-hydroxy-2,6,6-trimethylcyclohex-2-enyl)hepta-1,6-dien-3-one], and 4-OH-allyl-β-ionone [(E)-1-(3-hydroxy-2,6,6-trimethylcyclohex-1-enyl)hepta-1,6-dien-3-one] were identified during our studies.

Keywords Cytochromes P450 · Ionone · Damascone · CYP260B1 · CYP267B1 · Norisoprenoids

Introduction

Cytochromes P450 (P450s) are heme-containing monooxygenases that are present in all domains of life (Nelson 2011). They catalyze the oxidation of various classes of compounds such as xenobiotics, steroids, terpenes, fatty acids, and others (Bernhardt 2006). The activation of non-activated C-H bonds by the insertion of a single oxygen atom from molecular oxygen is catalyzed by these enzymes. Besides that hydroxylation, they are able to perform diverse reactions including epoxidation, alcohol oxidation, *N*-, *S*-, and *O*-dealkylation or the cleavage of C–C bonds (Sono et al. 1996). The electrons, required for such reactions, are provided by NAD(P)H and delivered via an electron transfer chain (Hannemann et al. 2007).

Mammalian P450s are mainly involved in the degradation of xenobiotics and drugs as well as in the metabolism of steroids and lipids (Bernhardt and Urlacher 2014). In contrast, the physiological role of many microbial P450s is not characterized yet. However, it is known that they play an important role in the production of secondary metabolites (Urlacher et al. 2004). For that reason, the discovery of their functions and

✉ Rita Bernhardt
ritabern@mx.uni-saarland.de

[1] Institut für Biochemie, Universität des Saarlandes, Campus B.2.2, 66123 Saarbruecken, Germany

Published online: 15 January 2016

activities is a promising field of research (Kelly and Kelly 2013). Myxobacteria are top producers of microbial secondary metabolites which attract the attention of the pharmaceutical industry (Weissman and Müller 2010). The genome of the myxobacterium *Sorangium cellulosum* So ce56 was sequenced in 2007 (Schneiker et al. 2007) and 21 P450s were identified (Khatri et al. 2010b). Since that time, various exogenous substrates like terpenes, fatty acids, or drugs were characterized for these P450s (Khatri et al. 2015; Litzenburger et al. 2015; Schifrin et al. 2015). Likewise, α- and β-ionones were identified as substrates of CYP109D1 and CYP264B1 (Khatri et al. 2010a; Ly et al. 2012).

Ionones and their regioisomers damascones (or the so-called rose ketones) belong to the group of norisoprenoids (carotenoid-derived aroma compounds). These secondary metabolites of carotenoids occur in many essential oils and play an important role for the flavor and fragrance industry due to their olfactory properties as well as their low odor threshold. Several derivatives of ionones such as dihydro-ionones, ionols, or irones occur in nature. Besides their natural derivatives, there are also some synthetic derivatives like allyl-α-ionone, isomethyl-α-ionone (isoraldeine), or n-methyl-α-ionone (raldeine) which are commercially of even greater importance. From a structural point of view, all compounds possess a megastigmane carbon skeleton as shown in Scheme 1 (Ohloff et al. 2012; Winterhalter and Rouseff 2002).

Hydroxylated and epoxidized derivatives of ionones and related compounds are of significant interest since they are used as precursors for chemical syntheses (Barakat et al. 2008; Brenna et al. 2002; Tu et al. 2014), for pharmaceutical applications (Gerhäuser et al. 2009; Zhou et al. 2009), or for the investigation of their potential allelopathic properties (Kato-Noguchi et al. 2010a, b; Macias et al. 2008; Macias et al. 2004). Furthermore, these oxyfunctionalized compounds are of interest due to their olfactory properties as reported for 3-hydroxy-α-ionone and its tobacco-like odor (Yamazaki et al. 1988). In addition, such compounds might be used as fly attractants (Ishida et al. 2008).

The first production of oxidized ionones was described in 1950 by isolating 4-oxo-β-ionone and 4-oxo-β-ionol from rabbit urine after feeding the animals with β-ionone (Prelog and Meier 1950). Since the 1980s and 1990s, there are several studies showing the formation of oxyfunctionalized products by microorganisms like *Streptomyces*, *Botrytis cinera*, *Lasiodiplodia theobromae*, or *Aspergillus niger* (Krasnobajew and Helmlinger 1982; Lutz-Wahl et al. 1998; Mikami et al. 1981; Mikami et al. 1978; Schoch et al. 1991; Yamazaki et al. 1988). However, such approaches lack the information on which specific enzyme is capable of the desired reaction. Several studies about specific bacterial P450s able to perform the regio- and stereoselective hydroxylation of α-ionone and β-ionone were published in the last decade (Celik et al. 2005; Girhard et al. 2010; Hall and Bell 2015; Ma et al. 2011; Zhang et al. 2015), likewise CYP109D1 and CYP264B1 from *Sorangium cellulosum* So ce56 (Khatri et al. 2010a; Ly et al. 2012). However, CYP260B1 and CYP267B1 from So ce56 were never tested for their ability to convert such substrates. Hence, we screened these P450s concerning the conversion of α-ionone (**1**), β-ionone (**2**), α-irone (**3**), 7,8-dihydro-α-ionone (**4**), 7,8-dihydro-β-ionone (**5**), α-ionol (**6**), β-ionol (**7**), α-damascone (**8**), β-damascone (**9**), δ-damascone (**10**), β-damascenone (**11**), as well as the synthetic derivatives isomethyl-α-ionone (**12**), *n*-methyl-α-ionone (**13**), and allyl-α-ionone (**14**). Those substrates showing a high selective product formation during our in vitro screening were further investigated in an *Escherichia coli*-based whole-cell system to obtain sufficient amounts for product identification via NMR spectroscopy.

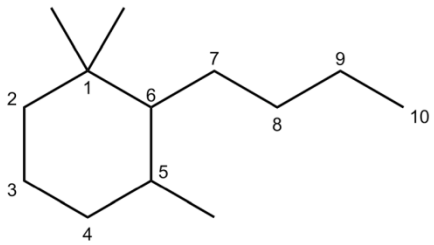

Scheme 1 Structure and numbering of the megastigmane carbon skeleton

Material and methods

Chemicals

Isoraldeine (isomethyl-α-ionone), α-damascone, β-damascone, δ-damascone, and β-damascenone were provided by Bell Flavors and Fragrances (Leipzig, Germany). Isopropyl β-D-1-thiogalactopyranoside and 5-aminolevulinic acid were purchased from Carbolution Chemicals (Saarbruecken, Germany). Bacterial media were purchased from Becton Dickinson (Heidelberg, Germany). All other chemicals were obtained from standard sources in the highest purity available.

Expression and purification of the enzymes

CYP260B1 and CYP267B1 were expressed and purified by a method previously described (Khatri et al. 2010b). The electron transfer partners $Adx_{4\text{-}108}$ and AdR from *Bos taurus* were expressed and purified as described elsewhere (Sagara et al. 1993; Uhlmann et al. 1994).

In vitro screening

A reconstituted in vitro system containing the corresponding P450 (0.5 μM), AdR (1.5 μM), $Adx_{4\text{-}108}$ (10 μM), $MgCl_2$

(1 mM), and a cofactor regenerating system with glucose-6-phosphate (5 mM) and glucose-6-phosphate dehydrogenase (1 U) in a final volume of 250 μl of potassium phosphate buffer (20 mM, pH 7.4) was used. All substrates were dissolved in EtOH (50 mM) and added to a final concentration of 200 μM. The reaction was started by the addition of NADPH (500 μM). After 1 h at 30 °C, the reaction was quenched by adding ethyl acetate (500 μl). The aqueous phase was extracted twice with ethyl acetate (2 × 500 μl). A negative control in the absence of cytochrome P450 in the reaction sample was employed for each substrate to verify the P450-dependent reaction.

Whole-cell experiments

All experiments were performed with *E. coli* BL21(DE3) gold cells (Agilent Technologies; Santa Clara, USA). The cells were transformed with two plasmids, one for the corresponding P450 (pET17b for CYP260B1 or pET22b for CYP267B1) and the other one for the redox partners Fpr and $Adx_{4\text{-}108}$. The overnight culture was prepared in nutrient broth containing ampicillin (100 μg/ml) and streptomycin (50 μg/ml). The main culture was carried out in 5 × 1 l sealed baffled flasks containing 200 ml modified M9CA medium (Litzenburger et al. 2015). The medium was inoculated with 1 % (*v*/*v*) of the overnight culture and incubated at 37 °C. The induction of the corresponding genes was initiated by adding 1 mM isopropyl β-D-1-thiogalactopyranoside and 0.5 mM 5-aminolevulinic acid when the optical density reached 0.8–1.0 and the culture was grown further at 28 °C. After 21 h of expression, the temperature was set to 30 °C and the substrates (stock solution 50 mM in EtOH) were added to a final concentration of 200 μM. After 48 h, the reaction was quenched with the same volume of ethyl acetate and extracted twice. Organic phases were collected and pooled, and the organic solvent was removed by vacuum distillation. The extracts were stored in a dark refrigerator at 4 °C until purification.

Analysis of the conversions via HPLC-DAD

HPLC analyses were performed on a system consisting of a PU-2080 HPLC pump, an AS-2059-SF autosampler, and a MD-2010 multi wavelength detector (Jasco, Gross-Umstadt, Germany). A Nucleodur 100–5 C18 column (125 × 4 mm, Macherey–Nagel, Düren, Germany) was used at 40 °C. The mobile phases consisted of water with 10 % acetonitrile (A) and pure acetonitrile (B). A gradient from 20 to 80 % of B with a flow rate of 1 ml/min was used for the separation of the compounds.

Analysis of the conversions and products via GC-MS

Gas chromatography mass spectrometry (GC-MS) analyses were performed on a system consisting of an AI/AS 3000 autosampler, a DSQII quadrupole, a Focus GC column oven (Thermo scientific, Waltham, USA), and a DB-5 column (Agilent) with a length of 25 m, 0.32 mm ID, and 0.52 μm film thickness. The compounds were analyzed in a *m*/*z* range of 20–350. The starting oven temperature was 50 °C for 1 min and then the temperature was ramped to 220 °C by 10 °C/min and held for 3 min with a flow rate of 1 ml/min. The EI-mass spectra were compared with the NIST mass spectral library (version 2.0).

Purification of the products

The extracts were purified using silica gel chromatography. Mixtures of hexane and ethyl acetate either 8:2 (epoxidized products) or 6:4 (hydroxylated products) were used as a mobile phase. Fractions were collected and analyzed via thin-layer chromatography (TLC). TLC plates were stained with anisaldehyde (4-methoxybenzaldehyde (0.5 % *v*/*v*) in sulfuric acid, acetic acid, and MeOH 5:10:85) for visualization of the products. Fractions containing single products were pooled, evaporated, and prepared for NMR analysis.

NMR analysis

NMR spectra were recorded on a Bruker (Rheinstetten, Germany) 500 NMR spectrometer. A combination of ^{1}H, ^{13}C, COSY, HSQC, and HMBC experiments was used for structure elucidation. The *cis*/*trans*-configuration of the products between H3 and H6 was carried out by NOESY experiments. All chemical shifts are relative to $CHCl_3$ (δ = 7.24 for ^{1}H NMR) or $CDCl_3$ (δ = 77.00 for ^{13}C NMR) using the standard δ notion in parts per million (ppm).

NMR and GC-MS data

Data for 5,6-epoxy-β-ionone (15) *m*/*z* = 208.3; ^{1}H NMR ($CDCl_3$, 500 MHz): δ = 6.99 (*d*, *J* = 15.6 Hz, 1H, H7), 6.26 (*d*, *J* = 15.6 Hz, 1H, H8), 2.25 (*s*, 3H, Me5), 1.92–1.84 (*m*, 1H, H4a), 1.77–1.70 (*m*, 1H, H4b), 1.48–1.37 (*m*, 3H, H3; H2a), 1.12 (*s*, 3H, Me5), 1.11 (*s*, 3H, Me1a), 1.08–1.02 (*m*, 1H, H2b), 0.91 (*s*, 3H, Me1b); ^{13}C NMR ($CDCl_3$, 125 MHz): δ = 197.53 (C9), 142.63 (C7), 132.44 (C8), 70.59 (C6), 65.86 (C5), 35.46 (C2), 33.53 (C1), 29.74 (C4), 28.26 (C10), 25.87 (Me1a), 25.81 (Me1b), 20.81 (Me5), 16.85 (C3).

Data for 7,11-epoxymegastigma-5,6-en-9-one (17) *m*/*z* = 208.1; ^{1}H NMR ($CDCl_3$, 500 MHz): δ = 5.22–5.16 (*m*, 1H, H7), 4.49 (ddt, *J* = 12.0; 5.2; 1.3 Hz, 1H, H11a), 4.37–4.33 (*m*, 1H, H11b), 2.69 (dd, *J* = 2.9; 14.8 Hz, 1H, H8a), 2.58

(dd, J = 9.8; 14.8 Hz, 1H, H8b), 2.20 (s, 3H, H10), 1.96–1.84 (*m*, 2H, H4), 1.73–1.65 (*m*, 2H, H3), 1.50–1.44 (*m*, 1H, H2a), 1.40–1.32 (*m*, 1H, H2b), 1.03 (*s*, 3H, Me1a), 1.02 (*s*, 3H, Me1b); ^{13}C NMR ($CDCl_3$, 125 MHz): δ = 207.46 (C9), 139.16 (C5), 132.27 (C6), 82.48 (C7), 76.27 (C11), 50.54 (C8), 40.07 (C2), 31.05 (C1), 30.91 (C10), 27.95 (Me1a), 27.93 (Me1b), 22.25 (C4), 19.06 (C3).

Data for 4,5-epoxy-isomethyl-α-ionone (20) m/z = 222.2; ^{1}H NMR ($CDCl_3$, 500 MHz): δ = 6.63 (dq, J = 10.9; 1.35 Hz, 1H, H7), 3.07 (*q*, J = 1.6 Hz, 1H, H4), 2.46 (*d*, J = 10.9 Hz, 1H, H6), 2.34 (*s*, 3H, H10), 2.01–1.95 (*m*, 1H, H3a), 1.93–1.85 (*m*, 1H, H3b), 1.82 (*d*, J = 1.4 Hz, 3H, Me8), 1.45–1.38 (*m*, 1H, H2a), 1.21 (*s*, 3H, Me5), 1.02–0.96 (*m*, 1H, H2b), 0.92 (*s*, 3H, Me1a), 0.72 (*s*, 3H, Me1b); ^{13}C NMR ($CDCl_3$, 125 MHz): δ = 200.23 (C9), 141.89 (C7), 138.89 (C8), 59.79 (C4), 59.43 (C5), 47.62 (C6), 31.89 (C1), 28.96 (C2), 28.37 (Me1a), 26.64 (Me1b), 25.73 (C10), 24.30 (Me5), 21.74 (C3), 11.95 (Me8).

Data for 4,5-epoxy-*n*-methyl-α-ionone (21) m/z = 222.3; ^{1}H NMR ($CDCl_3$, 500 MHz): δ = 6.72 (dd, J = 16.1; 10.2 Hz, 1H, H7), 6.09 (*d*, J = 16.1 Hz, 1H, H8), 3.07 (*t*, J = 1.9 Hz, 1H, H4), 2.63 (*q*, J = 7.3 Hz, 2H, H10), 2.05 (*d*, J = 10.2 Hz, 1H, H6), 2.01–1.94 (*m*, 1H, H2a), 1.92–1.84 (*m*, 1H, H2b), 1.44–1.36 (*m*, 1H, H2a), 1.23 (*s*, 3H, Me5), 1.09 (*t*, J = 7.3, 3H, H11), 1.02–0.96 (*m*, 1H, H2b), 0.90 (*s*, 3H, Me1a), 0.73 (*s*, 3H, Me1b); ^{13}C NMR ($CDCl_3$, 125 MHz): δ = 201.33 (C9), 144.94 (C7), 133.00 (C8), 59.44 (C4), 58.79 (C5), 52.46 (C6), 32.38 (C10), 31.19 (C1), 28.54 (C2), 27.89 (Me1a), 27.41 (Me1b), 24.01 (Me5), 21.73 (C3), 8.23 (C11).

Data for 4-hydroxy-β-damascone (22) m/z = 208.1; ^{1}H NMR ($CDCl_3$, 500 MHz): δ = 6.75 (dq, J = 6.9; 15.8 Hz, 1H, H9), 6.13 (dq, J = 1.7; 15.7 Hz, 1H, H8), 3.97 (*t*, J = 4.9 Hz, 1H, H4), 2.01–1.93 (*m*, 1H, H3a), 1.90 (dd, J = 1.6; 4.8 Hz, 3H, H10), 1.77–1.70 (*m*, 1H, H3b), 1.67–1.62 (*m*, 1H, H2a), 1.62 (*s*, 3H, Me5), 1.45–1.39 (*m*, 1H, H2b), 1.01 (*s*, 6H, Me1a; Me1b); ^{13}C NMR ($CDCl_3$, 125 MHz): δ = 200.90 (C7), 146.47 (C9), 143.55 (C5), 133.90 (C8), 130.97 (C6), 68.98 (C4), 34.61 (C2), 33.95 (C1), 28.79 (Me1a), 28.60 (C3), 27.61 (Me1b), 18.43 (C10), 17.93 (Me5).

Data for *trans*-2-hydroxy-δ-damascone (23) m/z = 208.4; ^{1}H NMR ($CDCl_3$, 500 MHz): δ = 6.87 (dq, J = 6.9; 15.6 Hz, 1H, H9), 6.22 (dq, J = 1.7; 15.6 Hz, 1H, H8), 5.76 (ddd, J = 2.4; 5.1; 9.9 Hz, 1H, H3), 5.70 (dd, J = 2.0; 10.0 Hz, 1H, H4), 3.43 (*d*, J = 5.0 Hz, 1H, H2), 2.79 (*d*, J = 10.5 Hz, 1H, H6), 2.63–2.54 (*m*, 1H, H5), 1.89 (dd, J = 1.6; 6.9 Hz, 3H, H10), 0.96 (*s*, 3H, Me1a), 0.86 (*s*, 3H, Me1b), 0.86 (*d*, J = 7.0 Hz, 3H, Me5); ^{13}C NMR ($CDCl_3$, 125 MHz): δ = 203.44 (C7), 142.29 (C9), 136.93 (C4), 134.76 (C8), 125.40 (C3), 73.27 (C2), 53.65 (C6), 37.62 (C1), 31.72 (C5), 25.07 (Me1a), 20.14 (Me1b), 19.39 (Me5), 18.27 (C10).

Data for 3-hydroxy-α-irone (24a) m/z = 222.1; ^{1}H NMR ($CDCl_3$, 500 MHz): δ = 6.59 (dd, J = 16.0; 9.8 Hz, 1H, H7), 6.03 (*d*, J = 15.9 Hz, 1H, H8), 5.62–5.58 (*m*, 1H, H4), 4.14–4.09 (*m*, 1H, H3), 2.41 (*d*, J = 9.6, 1H, H6), 2.22 (*s*, 3H, H10), 1.76–1.70 (*m*, 1H, H2), 1.59 (*t*, J = 1.1 Hz, 3H, Me5), 0.95 (*s*, 3H, Me1a), 0.94 (*d*, J = 7.7, 3H, Me2), 0.85 (*s*, 3H, Me1b); ^{13}C NMR ($CDCl_3$, 125 MHz): δ = 198.18 (C9), 147.05 (C7), 135.41 (C5), 133.18 (C8), 125.50 (C4), 68.58 (C3), 54.90 (C6), 39.10 (C2), 35.86 (C1), 27.12 (C10), 25.92 (Me1a), 24.37 (Me1b), 22.61 (Me5), 9.77 (Me2).

Data for 3-hydroxy-α-irone (24b) m/z = 222.2; ^{1}H NMR ($CDCl_3$, 500 MHz): δ = 6.56 (dd, J = 16.1; 10.9 Hz, 1H, H7), 6.11 (*d*, J = 15.5 Hz, 1H, H8), 5.56–5.53 (*m*, 1H, H4), 3.76–3.71 (*m*, 1H, H3), 2.58 (*d*, J = 9.9, 1H, H6), 2.24 (*s*, 3H, H10), 1.54 (*q*, J = 3.0; 1.4 Hz, 3H, Me5), 1.30–1.26 (*m*, 1H, H2), 1.01 (*d*, J = 6.8 Hz, 3H, Me2), 0.85 (*s*, 3H, Me1a), 0.72 (*s*, 3H, Me1b); ^{13}C NMR ($CDCl_3$, 125 MHz): δ = 197.88 (C9), 147.58 (C7), 134.76 (C8), 134.35 (C5), 126.83 (C4), 71.41 (C3), 55.86 (C6), 47.02 (C2), 37.83 (C1), 27.00 (C10), 26.46 (Me1a), 22.53 (Me5), 15.24 (Me1b), 10.86 (Me2).

Data for *trans*-3-hydroxy-α-damascone (25) m/z = 208.2; ^{1}H NMR ($CDCl_3$, 500 MHz): δ = 6.87 (dq, J = 6.9; 15.5 Hz, 1H, H9), 6.20 (dq, J = 1.6, 15.4 Hz, 1H, H8), 5.69–5.66 (*m*, 1H, H4), 4.34–4.29 (*m*, 1H, H3), 3.10 (*s*, 1H, H6), 1.91 (dd, J = 5.8; 13.7 Hz, 1H, H2a), 1.88 (dd, J = 1.6; 6.9 Hz, 3H, H10), 1.60 (*s*, 3H, Me5), 1.37 (dd, J = 5.4; 13.6 Hz, 1H, H2a), 1.09 (*s*, 3H, Me1a), 0.85 (*s*, 3H, Me1b); ^{13}C NMR ($CDCl_3$, 125 MHz): δ = 200.50 (C7), 142.91 (C9), 134.16 (C5), 132.57 (C8), 126.64 (C4), 65.43 (C3), 60.95 (C6), 43.56 (C2), 33.30 (C1), 30.50 (Me1a), 25.80 (Me1b), 22.71 (Me5), 18.29 (C10).

Data for *trans*-3-hydroxy-7,8-dihydro-α-ionone (26) m/z = 210.1; ^{1}H NMR ($CDCl_3$, 500 MHz): δ = 5.43 (*t*, J = 1.2 Hz, 1H, H4), 4.17–4.12 (*m*, 1H, H3), 2.55–2.37 (*m*, 2H, H8), 2.10 (*s*, 3H, H10), 1.79–1.71 (*m*, 2H, H2a; H7a), 1.70 (*s*, 3H, Me5), 1.59 (*t*, J = 5.1 Hz, 1H, H6), 1.51–1.43 (*m*, 1H, H7b), 1.32 (dd, J = 5.2, 13.7 Hz, 1H, H2b), 0.99 (*s*, 3H, Me1a), 0.86 (*s*, 3H, Me1b); ^{13}C NMR ($CDCl_3$, 125 MHz): δ = 208.69 (C9), 139.17 (C5), 124.53 (C4), 65.38 (C3), 48.56 (C6), 43.95 (C8), 43.79 (C2), 33.39 (C1), 29.97 (C10), 29.74 (Me1a), 24.89 (Me1b), 23.18 (Me5), 22.63 (C7).

Data for 4-hydroxy-7,8-dihydro-β-ionone (27) m/z = 210.1; ^{1}H NMR ($CDCl_3$, 500 MHz): δ = 3.87 (*t*, J = 4.5 Hz, 1H, H4), 2.48 (*t*, J = 8.3 Hz, 2H, H8), 2.31–2.18 (*m*, 2H, H7), 2.11 (*s*, 3H, H10), 1.86–1.79 (*m*, 1H, H3a), 1.68 (*s*, 3H, Me5), 1.66–1.54 (*m*, 2H, H2a; H3b), 1.36–1.30 (*m*, 1H, H2b), 0.99 (*s*, 3H,

Me1a), 0.93 (*s*, 3H, Me1b); ^{13}C NMR ($CDCl_3$, 125 MHz): δ = 208.47 (C9), 140.98 (C6), 129.42 (C5), 70.04 (C4), 43.75 (C6), 35.47 (C1), 34.45 (C2), 29.75 (C10), 28.54 (C3), 28.33 (Me1a), 26.83 (Me1b), 22.28 (C7), 16.69 (Me5).

Data for *trans*-3-hydroxy-isomethyl-α-ionone (28) *m/z* = 222.1; ^{1}H NMR ($CDCl_3$, 500 MHz): δ = 6.31 (dd, *J* = 1.3; 10.2 Hz, 1H, H7), 5.56 (*s*, 1H, H4), 4.28–4.22 (*m*, 1H, H3), 2.86 (dd, *J* = 0.5; 11.2 Hz, 1H, H6), 2.28 (*s*, 3H, H10), 1.84 (dd, *J* = 5.7; 13.1 Hz, 1H, H2a), 1.81 (*d*, *J* = 1.4 Hz, 3H, Me8), 1.54 (br *s*, 3H, Me5), 1.39 (dd, *J* = 7.4; 13.1 Hz, 1H, H2b), 0.95 (*s*, 3H, Me1a), 0.84 (*s*, 3H, Me1b); ^{13}C NMR ($CDCl_3$, 125 MHz): δ = 199.74 (C9), 143.06 (C7), 139.41 (C5), 136.09 (C8), 125.58 (C4), 65.54 (C3), 49.94 (C6), 44.77 (C2), 34.86 (C1), 29.59 (Me1a), 25.68 (C10), 23.62 (Me1b), 22.36 (Me5), 11.62 (Me8).

Data for *trans*-3-hydroxy-*n*-methyl-α-ionone (29) *m/z* = 222.1; ^{1}H NMR ($CDCl_3$, 500 MHz): δ = 6.54 (dd, *J* = 10.2; 15.8 Hz, 1H, H7), 6.09 (*d*, *J* = 15.7 Hz, 1H, H8), 5.59 (br *m*, 1H, H4), 4.26–4.21 (*m*, 1H, H3), 2.55 (*q*, *J* = 7.3 Hz, 2H, H10), 2.45 (*d*, *J* = 10.2 Hz, 1H, H6), 1.81 (dd, *J* = 6.2; 13.3 Hz, 1H, H2a), 1.60–1.57 (br *s*, 3H, Me5), 1.37 (dd, *J* = 13.5; 6.4 Hz, 1H, H2b), 1.08 (*t*, *J* = 7.3 Hz, 3H, H11), 0.99 (*s*, 3H, Me1a), 0.85 (*s*, 3H, Me1b); ^{13}C NMR ($CDCl_3$, 125 MHz): δ = 200.60 (C9), 145.76 (C7), 135.51 (C5), 132.48 (C8), 125.71 (C4), 65.46 (C3), 54.26 (C6), 43.87 (C2), 33.83 (C1), 33.49 (C10), 29.28 (Me1a), 24.56 (Me1b), 22.62 (Me5), 8.09 (C11).

Data for *trans*-3-hydroxy-allyl-α-ionone (31) *m/z* = 248.1; ^{1}H NMR ($CDCl_3$, 500 MHz): δ = 6.55 (dd, *J* = 10.2; 15.8 Hz, 1H, H7), 6.10 (*d*, *J* = 15.8 Hz, 1H, H8), 5.86–5.76 (*m*, 1H, H12), 5.59 (br *s*, 1H, H12), 4,99 (ddq, *J* = 1.5; 8.9; 23.7 Hz, 2H, H13), 4.26–4.21 (*m*, 1H, H3), 2.63 (*t*, *J* = 7.7 Hz, 2H, H10), 2.46 (*d*, *J* = 10.0 Hz, 1H, H6), 2.38–2.29 (*m*, 2H, H11), 1.81 (dd, *J* = 6.0; 13.4 Hz, 1H, H2a), 1.59 (*s*, 3 H, Me5), 1.37 (dd, J = 6.5; 13.5 Hz, 1 H, H2b), 0.99 (s, 3 H, Me1a), 0.86 (s, 3 H, Me1b); ^{13}C NMR ($CDCl_3$, 125 MHz): δ = 199.26 (C9), 146.24 (C7), 137.13 (C12), 135.49 (C5), 132.66 (C8), 125.69 (C4), 115.26 (C13), 65.49 (C3), 54.26 (C6), 43.82 (C2), 39.36 (C10), 33.86 (C1), 29.28 (Me1a), 28.13 (C11), 24.59 (Me1b), 22.66 (Me5).

Data for 4-hydroxy-allyl-β-ionone (32) *m/z* = 248.1; ^{1}H NMR ($CDCl_3$, 500 MHz): δ = 7.20 (*d*, *J* = 16.3 Hz, 1H, H7) 6.13 (*d*, *J* = 16.3 Hz, 1H, H8), 5.88–5.78 (*m*, 1H, H12), 5.01 (ddq, *J* = 1.3; 10.2; 26.8 Hz, 2H, H13), 4.00 (*t*, *J* = 4.9 Hz, 1H, H4), 2.67 (*t*, *J* = 7.7 Hz, 2H, H10), 2.42–2.36 (*m*, 2H, H11), 1.94–1.86 (*m*, 1H, H3a), 1.82 (*s*, 3H, Me5), 1.74–1.66 (*m*, 2H, H2a; H3b), 1.46–1.40 (*m*, 1H, H2b), 1.04 (*s*, 3H, Me1a), 1.02 (*s*, 3H, Me1b); ^{13}C NMR ($CDCl_3$, 125 MHz): δ = 199.57 (C9), 141.78 (C7), 139.61 (C6), 137.17 (C12), 133.66 (C5), 132.04 (C8), 115.28 (C13), 69.94 (C4), 39.83 (C10), 34.65 (C1), 34.56 (C2), 28.83 (C3), 28.25(C11), 28.23(Me1a), 27.43 (Me1b), 18.51 (Me5).

Results

In vitro screening with CYP260B1 and CYP267B1

CYP260B1 and CYP267B1 were screened for their ability to convert the substrates α-ionone (**1**), β-ionone (**2**), α-irone (**3**), dihydro-α-ionone (**4**), dihydro-β-ionone (**5**), α-ionol (**6**), β-ionol (**7**), α-damascone (**8**), β-damascone (**9**), δ-damascone (**10**), β-damascenone (**11**), isomethyl-α-ionone (**12**), *n*-methyl-α-ionone (**13**), and allyl-α-ionone (**14**).The conversions were analyzed by HPLC-DAD as well as GC-MS. **4**–**6** were solely analyzed by GC-MS, due to their low UV absorbance. Both P450s were able to catalyze the conversion of all tested substrates. CYP260B1 converted most of the substrates by 90–95 % under the conditions applied, whereas CYP267B1 converted most of them by 80–95 %, with the exception of damascones (**8**–**10**) and allyl-α-ionone (**14**). These compounds were converted in lower amounts by both P450s (50–75 %). CYP267B1 showed a high selectivity for the formation of a single product (except for **11**) as exemplified in Fig. 1b. The side-products were formed to less than 10 % of the total conversion, except for **10** (~15 %). In contrast, CYP260B1 was able to perform the selective conversions of **2** (including two side products), **9**, and **10** (including one side product), whereas the other CYP260B1-dependent conversions showed multiple products (see Fig. 1a). Nevertheless, the main products of the conversions of **9** and **10** were identical for both P450s. The CYP260B1-dependent conversion of **2** resulted in one main product (~75 %) as well as two side products (~15 % in total). The main product of this conversion showed an absorption maximum shifted to shorter wavelengths indicating the lack of a conjugated double bond. One of the side products had an identical retention time as the main product of the CYP267B1-dependent conversion. GC-MS analyses identified all products as mono-oxidized products, and the database comparison of the fragment patterns showed the highest probabilities for 5,6-epoxy-β-ionone (**15**) as the main product as well as 7,11- epoxymegastigma-5,6-en-9-one (**17**) and 3-hydroxy-β-ionone (**19**) as the side products. 3-Hydroxy-α-ionone (**18**), 3-hydroxy-β-ionone (**19**), and 4-hydroxy-β-ionone (**16**) were available as standards, since these products were characterized during previous studies in our group (Khatri et al. 2010a; Ly et al. 2012). The comparison of the retention times and mass spectra identified the side product of the CYP260B1-dependent conversion of **2**, therefore, as **16**. Further database comparisons of CYP260B1-dependent conversions indicated the most apolar product (~20 %) of the conversion of **12** as the corresponding 4,5-

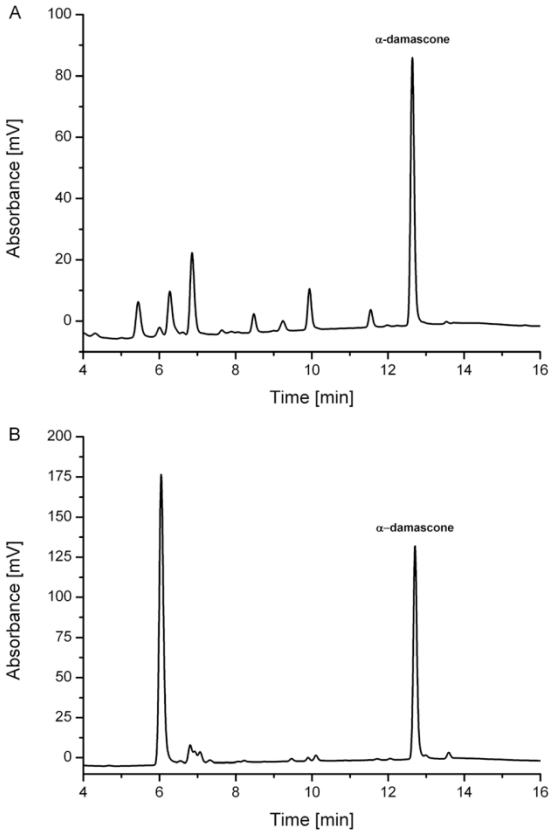

Fig. 1 HPLC chromatograms of in vitro conversions of α-damascone (8) by CYP260B1 (**a**) and CYP267B1 (**b**). CYP260B1 shows an unselective product formation, whereas the CYP267B1-dependent conversion results predominantly in one main product

epoxy isomethyl-α-ionone (**20**). The other products did not show a reliable hit. Likewise, the main products of CYP267B1-dependent conversions were not further characterized by database comparisons. However, the main products of the conversions of **1** and **2** by CYP267B1 were compared with the standards and, therefore, identified as **16** and **18**, respectively.

Whole-cell conversions with CYP260B1 and CYP267B1

Higher amounts of products are required for structure elucidation via NMR spectroscopy. Therefore, an *E. coli*-based whole-cell system harboring the corresponding P450 as well as the electron transfer proteins $Adx_{4\text{-}108}$ and Fpr was applied. **9** and **10** were used in the whole-cell system harboring CYP260B1 to characterize the corresponding products. Additionally, **2**, **12**, and **13** were investigated to verify the epoxidase activity of CYP260B1. The remaining substrates were not further investigated due to the formation of multiple products by CYP260B1. In contrast, CYP267B1 showed a high selectivity for the formation of a single product, except for **11** which formed multiple products. In addition, the conversion of **14** resulted in two products. **1** and **2** were not investigated since the corresponding products were elucidated by GC-MS via standards. The other substrates were applied to the whole-cell system to obtain sufficient amounts of products for NMR characterization. **6** and **7** showed different main products during the whole-cell conversions compared with the in vitro reactions. This observation might be explained by the higher reactivity of the ionols caused by their alcohol group. As a result, the formation of such products is P450-independent or an *E. coli* caused consecutive reaction occurred. For that reason, these products were not further characterized. The remaining nine substrates were applied to the whole-cell system and sufficient amounts of products (2–20 mg/l) were obtained after purification. All purified products were analyzed via GC-MS and the mass spectra indicated all compounds as mono-oxidized products.

Scheme 2 Structures of the purified products formed by CYP260B1 and CYP267B1. The structures were elucidated by NMR spectroscopy; except for (16) and (18), which were elucidated by GC-MS via standards ▶

Product identification via NMR spectroscopy

The structures of the corresponding products were identified by different NMR techniques like ^{1}H, ^{13}C, COSY, HSQC, and HMBC. The main products of **9** and **10** formed by CYP260B1-dependent conversions were identified as compounds hydroxylated in allylic position (**22** and **23**). The conversion of **2** resulted in three products. **16** was elucidated via comparison with a standard and the formation of **15** as well as **17** was verified by NMR analyses. The conversion of the methyl-substituted α-ionone derivatives **12** and **13** led to the 4,5-epoxy products **20** and **21** proving an epoxidase activity of CYP260B1 for α-ionone derivatives. The other products of the CYP260B1-dependent conversions were not further characterized. The CYP267B1-dependent conversions resulted predominantly in a single main product. All products formed by this enzyme were identified as allylic alcohols (**16**, **18**, **22**–**29**, **31**, **32**). The structures of the products are illustrated in Scheme 2.

However, the conversion of **14** resulted in two products. The product obtained in higher amounts was identified as 3-hydroxy-allyl-α-ionone (**31**), whereas the side product was identified as 4-hydroxy-allyl-β-ionone (**32**). This observation can be explained by the composition of the substrate. Allyl-β-ionone (**30**) is mentioned as major impurity (13 %) by Sigma Aldrich and, therefore, served as potential substrate for CYP267B1 in our experiments. As shown for the other substrates, **30** was hydroxylated in allylic position at C4.

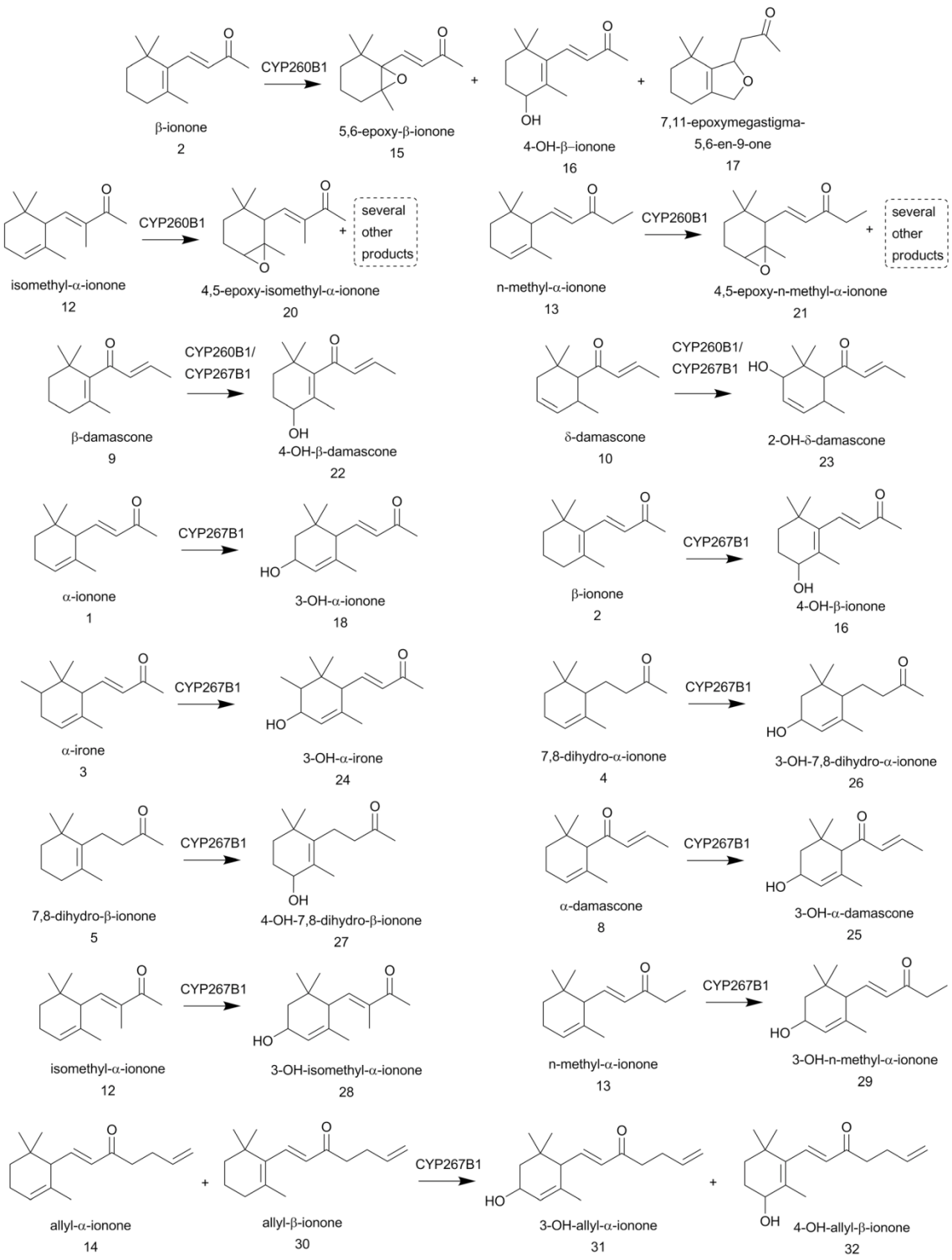
β-ionone
2
CYP260B1
5,6-epoxy-β-ionone
15
4-OH-β–ionone
16
7,11-epoxymegastigma-
5,6-en-9-one
17
isomethyl-α-ionone
12
CYP260B1
4,5-epoxy-isomethyl-α-ionone
20
several
other
products
n-methyl-α-ionone
13
CYP260B1
4,5-epoxy-n-methyl-α-ionone
21
several
other
products
β-damascone
9
CYP260B1/
CYP267B1
4-OH-β-damascone
22
δ-damascone
10
CYP260B1/
CYP267B1
2-OH-δ-damascone
23
α-ionone
1
CYP267B1
3-OH-α-ionone
18
β-ionone
2
CYP267B1
4-OH-β-ionone
16
α-irone
3
CYP267B1
3-OH-α-irone
24
7,8-dihydro-α-ionone
4
CYP267B1
3-OH-7,8-dihydro-α-ionone
26
7,8-dihydro-β-ionone
5
CYP267B1
4-OH-7,8-dihydro-β-ionone
27
α-damascone
8
CYP267B1
3-OH-α-damascone
25
isomethyl-α-ionone
12
CYP267B1
3-OH-isomethyl-α-ionone
28
n-methyl-α-ionone
13
CYP267B1
3-OH-n-methyl-α-ionone
29
allyl-α-ionone
14
allyl-β-ionone
30
CYP267B1
3-OH-allyl-α-ionone
31
4-OH-allyl-β-ionone
32

The *cis*/*trans*-geometry of known products was elucidated by comparison with published data (Barakat et al. 2008; Schwab and Schreier 1991; Yamazaki et al. 1988), whereas those products where no data are available were elucidated by NOESY experiments. The epoxides **20** and **21** produced by CYP260B1 show *trans*-geometry between Me5 and the corresponding side chain at position C6. Moreover, the CYP260B1-dependent conversion of **10** resulted in the 2-hydroxy-*trans*-product (**23**). CYP267B1 showed a high regio- and diastereoselectivity for such compounds, since all 3-hydroxy-α-products formed by this enzyme were identified as *trans*-isomers. Likewise, **23** resulted in a *trans*--configuration as shown for CYP260B1. Interestingly, none of the substrates led to *cis*-configurated products despite their application as racemic mixtures.

HPLC and GC analyses of pure α-irone (**3**) showed two peaks which represent the diastereomers of this compound (methyl at C2 and butenone at C6). The conversion of **3** by CYP267B1 resulted in two main products despite the introduction of a third stereogenic center caused by the hydroxylation at position C3. These two compounds were not successfully separated; nevertheless, the corresponding structures were identified by 2D-NMR techniques and their data matched those in the literature (Yamazaki et al. 1986). As shown in Scheme 3, one product (**24a**) shows *cis*-geometry between H2 and H3, whereas the other product (**24b**) shows *trans*-geometry. However, both compounds show *trans*-geometry between H3 and H6 verifying the high diastereoselectivity of CYP267B1 for the formation of 3,6-*trans*-products.

Discussion

Since a couple of years, we are investigating the functions, properties, and activities of P450s from *Sorangium cellulosum* So ce56. An efficient *E. coli*-based whole-cell system for some of these P450s was established (Ringle et al. 2013), and several substrate classes like terpenes, drugs, or fatty acids were already identified (Khatri et al. 2015; Litzenburger et al. 2015; Schifrin et al. 2015). Likewise, α- and β-ionone (**1**, **2**) serve as substrates for CYP109D1 and CYP264B1 (Khatri et al. 2010a; Ly et al. 2012). In contrast, about potential substrates for CYP260B1 and CYP267B1, which are members of new P450 families found in this myxobacterium, only little is known. However, knowledge about substrates is necessary to characterize these enzymes in more detail. For that reason, we screened their ability to convert carotenoid-derived aroma compounds like ionones, damascones, as well as some of their isomers and derivatives (**1**–**14**). As shown here, both P450s are capable of the efficient in vitro conversions of all tested substrates. CYP267B1 shows a high selectivity towards the formation of a single product, whereas CYP260B1 mainly forms multiple products. Furthermore, based on our whole-cell experiments, we were able to identify several main products formed by these P450s. CYP267B1 is mostly responsible for the regioselective hydroxylation in allylic position. Likewise, CYP260B1 hydroxylates **9** and **10** as well as small quantities of **2** in this specific position. The formation of allylic alcohols is preferred by many P450s as shown by several studies (Celik et al. 2005; Hall and Bell 2015; Khatri et al. 2010a; Ly et al. 2012; Ma et al. 2011; Venkataraman et al. 2012; Zhang et al. 2015). This observation can be explained by the bond strength of the C–H bonds. The bond strength of the allylic C–H bond is about 10 kcal/mol lower than that of a secondary C–H bond (Ortiz de Montellano 2010). As a result, the allylic position is more reactive and, therefore, preferred for hydroxylation. Moreover, free energy-related calculations of the stereoselective hydroxylation of α-ionone (**1**) by P450 BM3 mutants revealed that the *trans*-isomers show the most favorable free energies in solution (de Beer et al. 2012). As shown here, CYP267B1 predominantly forms such energetically preferred diastereomers, despite the application of racemic mixtures as substrate. Previous studies of the conversion of **1** by *Streptomyces* strains also revealed the formation of *trans*-isomers out of a racemic mixture (Lutz-Wahl et al.

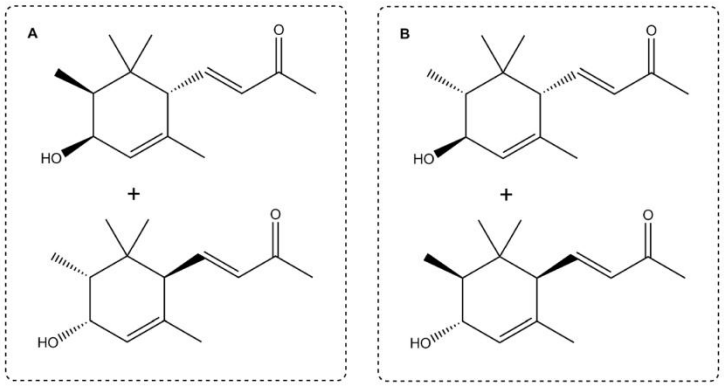

Scheme 3 Relative geometry of the 3-hydroxy-α-irone main products 24a (**a**, *left side*) and 24b (**b**, *right side*) formed by CYP267B1

1998). In contrast, several other bacterial P450s produce mixtures of *cis*- and *trans*-isomers (Hall and Bell 2015; Ma et al. 2011; Venkataraman et al. 2012). The selectivity for the production of a specific isomer is, therefore, considerably lower. As a result, CYP267B1 is a suitable candidate for the diastereoselective production of several norisoprenoids.

Interestingly, during all previous studies published in the literature, only **1**, **2**, and **9** were applied as substrates for P450s, and none of their isomers or derivatives was investigated. Both P450s investigated in this study were able to convert all tested substrates in vitro. Thereby, the selectivity of CYP260B1 towards a single product is lower compared with CYP267B1. The formation of multiple compounds hinders, therefore, the product characterization. Nevertheless, **2**, **9**, and **10** are converted by CYP260B1 with high selectivity, whereby the main products of **9** and **10** are identical to those obtained with CYP267B1. In addition, CYP260B1 shows an epoxidase activity towards **2** as well as the methyl-substituted α-ionone derivatives **12** and **13**, albeit in lower amounts. CYP260B1 hydroxylates **9** in the allylic position at C4, whereas **2** is mainly epoxidized between C5 and C6. This shows that the keto-group either at position C7 (damascones) or C9 (ionones) seems to alter the substrate orientation in the active site of this enzyme and, hence, the regioselectivity as well as the type of reaction. In addition, the location of the double bond in the cyclohexene ring has also a high impact on the product formation. The conversions of **9** and **10** by CYP260B1 lead predominantly to single products of allylic alcohols, whereas the conversion of **8** resulted in multiple products. The location of the double bond is thereby responsible for the conformation of the cyclohexene ring in the active site, and this way affects the hydroxylation selectivities. This sensitivity towards the moieties of these compounds might be explained by a low flexibility of the active site. On the contrary, CYP267B1 selectively hydroxylates all tested substrates in allylic position. Its active site might be more flexible and allows the required substrate orientation for allylic hydroxylation. In addition, the catalyzed reactions seem to be thermodynamically controlled, since predominantly 3,6-*trans*-products were formed. The conversion of **3** is an interesting example which substantiates this assumption due to the formation of the thermodynamically most stable products (**24a** and **24b**). A more detailed assertion about the conformation of the active site or substrate orientation can only be given after the crystal data of these enzymes become available. Furthermore, improved analytical methods to elucidate the absolute configuration of the products as well as computational methods to estimate the binding affinities are necessary to understand the detailed mechanistic of the stereoselectivity. Nevertheless, this study gives first insights in the substrate range as well as variety of reactions catalyzed by theses P450s. CYP267B1 shows the typical for P450s allylic hydroxylase activity, whereas CYP260B1 is additionally able to epoxidize some of the substrates. This epoxidase activity is of interest, since neither CYP109D1 nor CYP264B1 or CYP267B1 from So ce56 are known for such an activity. Hence, CYP260B1 expands the "toolbox" towards oxyfunctionalized norisoprenoids, a group of valuable compounds known for their wide range of applications.

Hydroxylated and epoxidized norisoprenoids are utilized as building blocks for the organic chemistry, like for the syntheses of odorants (Fráter et al. 1998) or carotenoids (Brenna et al. 2002) and their derivatives (Tu et al. 2014). Furthermore, they are investigated for their potential medical applications (Gerhäuser et al. 2009) or used as precursors for pharmaceuticals (Colombo et al. 1992; Zhou et al. 2009). There are several studies indicating the potential growth inhibiting and allelopathic properties of such compounds, especially those with a keto- or hydroxyl-function at position C3 (Walter and Strack 2011). Aside from these examples, there are several other possible applications for these products including their utilization as standard (Venkataraman et al. 2012). This wide range of applications proves the significance of such products for diverse fields of research and novel compounds with altered properties are very valuable and might provide new possibilities for application. During our studies, we were able to identify several known as well as some novel products like **23**, **31**, and **32**. These novel compounds might be investigated for their olfactory properties or used as standards to simplify the product characterization of other P450s. However, higher amounts of these products in a multimillgram to gram scale are required to apply them as building blocks for synthetic routes. The whole-cell system used in this study yielded up to 20 mg/l under non-optimized conditions. Improvements, such as the utilization of alternative redox partners, applying resting cells in buffer or protein engineering towards higher activities can be used to establish a system towards preparative scale.

Taken together, the carotenoid-derived aroma compounds were identified as substrates for CYP260B1 and CYP267B1 for the first time. The utilization of a whole-cell system facilitates the product identification via NMR spectroscopy and provides, therefore, first insights in the substrate range and reaction diversity of these myxobacterial P450s. The high regio- and diastereoselectivity of CYP267B1 as well as the epoxidase activity of CYP260B1 reveal the potential of these P450s for the oxyfunctionalization of norisoprenoids.

Acknowledgments The authors thank Birgit Heider-Lips for the purification of AdR and Adx_{4-108} and Dr. Joseph Zapp for the measurement of the NMR samples. This work is supported by a grant of the Deutsche Forschungsgemeinschaft (Be1343/23) to R.B.

Compliance with ethical standards This article does not contain any studies with human participants or animals performed by any of the authors.

Conflict of interest The authors declare that they have no competing interests.

References

Barakat A, Brenna E, Fuganti C, Serra S (2008) Synthesis, olfactory evaluation and determination of the absolute configuration of the β- and γ-Iralia® isomers. Tetrahedron: Asymmetry 19:2316–2322. doi:10.1016/j.tetasy.2008.09.028

Bernhardt R (2006) Cytochromes P450 as versatile biocatalysts. J Biotechnol 124:128–145. doi:10.1016/j.jbiotec.2006.01.026

Bernhardt R, Urlacher VB (2014) Cytochromes P450 as promising catalysts for biotechnological application: chances and limitations. Appl Microbiol Biotechnol 98:6185–6203. doi:10.1007/s00253-014-5767-7

Brenna E, Fuganti C, Serra S, Kraft P (2002) Optically active ionones and derivatives: preparation and olfactory properties. Eur J Org Chem 2002:967–978. doi:10.1002/1099-0690(200203)2002:6<967::aid-ejoc967>3.0.co;2-e

Celik A, Flitsch SL, Turner NJ (2005) Efficient terpene hydroxylation catalysts based upon P450 enzymes derived from actinomycetes. Org Biomol Chem. 3:2930–2934. doi:10.1039/B506159H

Colombo MI, Zinczuk J, Rúveda EA (1992) Synthetic routes to forskolin. Tetrahedron 48:963–1037. doi:10.1016/S0040-4020(01)88199-0

de Beer SB, Venkataraman H, Geerke DP, Oostenbrink C, Vermeulen NP (2012) Free energy calculations give insight into the stereoselective hydroxylation of alpha-ionones by engineered cytochrome P450 BM3 mutants. J Chem Inf Model. 52:2139–2148. doi:10.1021/ci300243n

Fráter G, Bajgrowicz JA, Kraft P (1998) Fragrance chemistry. Tetrahedron 54:7633–7703. doi:10.1016/S0040-4020(98)00199-9

Gerhäuser C, Klimo K, Hummer W, Holzer J, Petermann A, Garreta-Rufas A, Bohmer FD, Schreier P (2009) Identification of 3-hydroxy-beta-damascone and related carotenoid-derived aroma compounds as novel potent inducers of Nrf2-mediated phase 2 response with concomitant anti-inflammatory activity. Mol Nutr Food Res. 53:1237–1244. doi:10.1002/mnfr.200800492

Girhard M, Klaus T, Khatri Y, Bernhardt R, Urlacher VB (2010) Characterization of the versatile monooxygenase CYP109B1 from *Bacillus subtilis*. Appl Microbiol Biotechnol. 87:595–607. doi:10.1007/s00253-010-2472-z

Hall EA, Bell SG (2015) The efficient and selective biocatalytic oxidation of norisoprenoid and aromatic substrates by CYP101B1 from *Novosphingobium aromaticivorans* DSM12444. RSC Adv. 5:5762–5773. doi:10.1039/c4ra14010a

Hannemann F, Bichet A, Ewen KM, Bernhardt R (2007) Cytochrome P450 systems—biological variations of electron transport chains. Biochim Biophys Acta 3:330–344. doi:10.1016/j.bbagen.2006.07.017

Ishida T, Enomoto H, Nishida R (2008) New attractants for males of the solanaceous fruit fly *Bactrocera latifrons*. J Chem Ecol. 34:1532–1535. doi:10.1007/s10886-008-9562-8

Kato-Noguchi H, Seki T, Shigemori H (2010a) Allelopathy and allelopathic substance in the moss *Rhynchostegium pallidifolium*. J Plant Physiol. 167:468–471. doi:10.1016/j.jplph.2009.10.018

Kato-Noguchi H, Yamamoto M, Tamura K, Teruya T, Suenaga K, Fujii Y (2010b) Isolation and identification of potent allelopathic substances in rattail fescue. Plant Growth Regul 60:127–131. doi:10.1007/s10725-009-9428-2

Kelly SL, Kelly DE (2013) Microbial cytochromes P450: biodiversity and biotechnology. Where do cytochromes P450 come from, what do they do and what can they do for us? Phil Trans R Soc B 368:19. doi:10.1098/rstb.2012.0476

Khatri Y, Girhard M, Romankiewicz A, Ringle M, Hannemann F, Urlacher VB, Hutter MC, Bernhardt R (2010a) Regioselective hydroxylation of norisoprenoids by CYP109D1 from *Sorangium cellulosum* So ce56. Appl Microbiol Biotechnol 88:485–495. doi:10.1007/s00253-010-2756-3

Khatri Y, Hannemann F, Ewen KM, Pistorius D, Perlova O, Kagawa N, Brachmann AO, Müller R, Bernhardt R (2010b) The CYPome of *Sorangium cellulosum* So ce56 and identification of CYP109D1 as a new fatty acid hydroxylase. Chem Biol 17:1295–1305. doi:10.1016/j.chembiol.2010.10.010

Khatri Y, Hannemann F, Girhard M, Kappl R, Hutter M, Urlacher VB, Bernhardt R (2015) A natural heme-signature variant of CYP267A1 from *Sorangium cellulosum* So ce56 executes diverse Ω-hydroxylation. FEBS J 282:74–88. doi:10.1111/febs.13104

Krasnobajew V, Helmlinger D (1982) Fermentation of fragrances: biotransformation of β-ionone by *Lasiodiplodia theobromae* Helv. Chim Acta. 65:1590–1601. doi:10.1002/hlca.19820650532

Litzenburger M, Kern F, Khatri Y, Bernhardt R (2015) Conversions of tricyclic antidepressants and antipsychotics with selected P450s from *Sorangium cellulosum* So ce56. Drug Metab Dispos. 43:392–399. doi:10.1124/dmd.114.061937

Lutz-Wahl S, Fischer P, Schmidt-Dannert C, Wohlleben W, Hauer B, Schmid RD (1998) Stereo- and Regioselective hydroxylation of Alpha-Ionone by Streptomyces Strains. Appl Environ Microbiol 64:3878–3881

Ly TT, Khatri Y, Zapp J, Hutter MC, Bernhardt R (2012) CYP264B1 from *Sorangium cellulosum* So ce56: a fascinating norisoprenoid and sesquiterpene hydroxylase. Appl Microbiol Biotechnol 95:123–133. doi:10.1007/s00253-011-3727-z

Ma M, Bell SG, Yang W, Hao Y, Rees NH, Bartlam M, Zhou W, Wong LL, Rao Z (2011) Structural Analysis of CYP101C1 from *Novosphingobium aromaticivorans* DSM12444. ChemBioChem. 12:88–99. doi:10.1002/cbic.201000537

Macias FA, Lacret R, Varela RM, Nogueiras C, Molinillo JM (2008) Bioactive apocarotenoids from *Tectona grandis*. Phytochemistry. 69:2708–2715. doi:10.1016/j.phytochem.2008.08.018

Macias FA, Lopez A, Varela RM, Torres A, Molinillo JM (2004) Bioactive apocarotenoids annuionones F and G: structural revision of annuionones A. B and E Phytochemistry 65:3057–3063. doi:10.1016/j.phytochem.2004.08.048

Mikami Y, Fukunaga Y, Arita M, Kisaki T (1981) Microbial transformation of β-ionone and β-methylionone. Appl Environ Microbiol 41:610–617

Mikami Y, Watanabe E, Fukunaga Y, Kisaki T (1978) Formation of 2S-hydroxy-β-ionone and 4ξ-hydroxy-β-ionone by microbial hydroxylation of β-ionone. Agric Biol Chem 42:1075–1077

Nelson DR (2011) Progress in tracing the evolutionary paths of cytochrome P450 BBA-Proteins. Proteom 1814:14–18. doi:10.1016/j.bbapap.2010.08.008

Ohloff G, Pickenhagen W, Kraft P (2012) Scent and chemistry. The molecular world of odors. Wiley Online Library, Zürich

Ortiz de Montellano PR (2010) Hydrocarbon hydroxylation by cytochrome P450 enzymes. Chem Rev. 110:932–948. doi:10.1021/cr9002193

Prelog V, Meier HL (1950) Untersuchungen über Organextrakte und Harn. 18. Mitteilung. Über die Biochemische Oxydation von β-Jonon im Tierkörper Helv Chim Acta 33:1276–1284. doi:10.1002/hlca.19500330523

Ringle M, Khatri Y, Zapp J, Hannemann F, Bernhardt R (2013) Application of a new versatile electron transfer system for cytochrome P450-based *Escherichia coli* whole-cell bioconversions. Appl Microbiol Biotechnol 97:7741–7754. doi:10.1007/s00253-012-4612-0

Sagara Y, Wada A, Takata Y, Waterman MR, Sekimizu K, Horiuchi T (1993) Direct expression of adrenodoxin reductase in *Escherichia coli* and the functional characterization. Biol Pharm Bull 16:627–630

Schifrin A, Ly TTB, Günnewich N, Zapp J, Thiel V, Schulz S, Hannemann F, Khatri Y, Bernhardt R (2015) Characterization of

the gene cluster CYP264B1-geoA from *Sorangium cellulosum* So ce56: biosynthesis of (+)-Eremophilene and its hydroxylation. ChemBioChem 16:337–344. doi:10.1002/cbic.201402443

Schneiker S, Perlova O, Kaiser O, Gerth K, Alici A, Altmeyer MO, Bartels D, Bekel T, Beyer S, Bode E, Bode HB, Bolten CJ, Choudhuri JV, Doss S, Elnakady YA, Frank B, Gaigalat L, Goesmann A, Groeger C, Gross F, Jelsbak L, Kalinowski J, Kegler C, Knauber T, Konietzny S, Kopp M, Krause L, Krug D, Linke B, Mahmud T, Martinez-Arias R, McHardy AC, Merai M, Meyer F, Mormann S, Munoz-Dorado J, Perez J, Pradella S, Rachid S, Raddatz G, Rosenau F, Ruckert C, Sasse F, Scharfe M, Schuster SC, Suen G, Treuner-Lange A, Velicer GJ, Vorholter FJ, Weissman KJ, Welch RD, Wenzel SC, Whitworth DE, Wilhelm S, Wittmann C, Blocker H, Puhler A, Müller R (2007) Complete genome sequence of the myxobacterium *Sorangium cellulosum*. Nat Biotechnol. 25:1281–1289. doi:10.1038/nbt1354

Schoch E, Benda I, Schreier P (1991) Bioconversion of alpha-Damascone by *Botrytis cinerea*. Appl Environ Microbiol. 57:15–18

Schwab E, Schreier P (1991) Conformational studies of 3-hydroxy-alpha-damascone by nuclear overhauser effect nuclear magnetic resonance experiments. J Agric Food Chem 39:1641–1642. doi:10.1021/jf00009a021

Sono M, Roach MP, Coulter ED, Dawson JH (1996) Heme-containing oxygenases. Chem Rev 96:2841–2888. doi:10.1021/cr9500500

Tu VA, Kaga A, Gericke K-H, Watanabe N, Narumi T, Toda M, Brueckner B, Baldermann S, Mase N (2014) Synthesis and characterization of quantum dot nanoparticles bound to the plant volatile precursor of hydroxy-apo-10′-carotenal. J Org Chem 79:6808–6815. doi:10.1021/jo500605c

Uhlmann H, Kraft R, Bernhardt R (1994) C-terminal region of adrenodoxin affects its structural integrity and determines differences in its electron transfer function to cytochrome P-450. J Biol Chem. 269:22557–22564

Urlacher VB, Lutz-Wahl S, Schmid RD (2004) Microbial P450 enzymes in biotechnology. Appl Microbiol Biotechnol 64:317–325. doi:10.1007/s00253-003-1514-1

Venkataraman H, de Beer SB, Geerke DP, Vermeulen NP, Commandeur JN (2012) Regio- and stereoselective hydroxylation of optically active α-ionone enantiomers by engineered cytochrome P450 BM3 mutants. Adv Synth Catal. 354:2172–2184. doi:10.1002/adsc.201200067

Walter MH, Strack D (2011) Carotenoids and their cleavage products: biosynthesis and functions. Nat Prod Rep 28:663–692. doi:10.1039/c0np00036a

Weissman KJ, Müller R (2010) Myxobacterial secondary metabolites: bioactivities and modes-of-action. Nat Prod Rep 27:1276–1295. doi:10.1039/c001260m

Winterhalter P, Rouseff RL (2002) Carotenoid-derived aroma compounds. American Chemical Society, Washington, D.C.

Yamazaki Y, Hayashi Y, Arita M, Hieda T, Mikami Y (1988) Microbial conversion of alpha-ionone, alpha-methylionone, and alpha-isomethylionone. Appl Environ Microbiol 54:2354–2360

Yamazaki Y, Hori N, Fukunaga Y, Mikami Y (1986) Manufacture of hydroxyirons as tobacco flavorant, Patent, JP61167638A

Zhang A, Zhang T, Hall EA, Hutchinson S, Cryle MJ, Wong L-L, Zhou W, Bell SG (2015) The crystal structure of the versatile cytochrome P450 enzyme CYP109B1 from *Bacillus subtilis*. Mol Biosyst. 11:869–881. doi:10.1039/c4mb00665h

Zhou J, Geng G, G B, JH W (2009) Syntheses and potential anti-prostate cancer activities of ionone-based chalcones. Bioorg Med Chem 19:1183–1186. doi:10.1016/j.bmcl.2008.12.089

2.4 CYP267A1 and CYP267B1 from *Sorangium cellulosum* So ce56 are highly versatile drug metabolizers

Fredy Kern, Yogan Khatri, Martin Litzenburger, and Rita Bernhardt

Submitted to Drug Metabolism and Disposition

CYP267A1 and CYP267B1 from *Sorangium cellulosum* So ce56 are highly versatile drug metabolizers

Fredy Kern, Yogan Khatri, Martin Litzenburger and Rita Bernhardt

Department of Biochemistry, Saarland University, 66123 Saarbruecken, Germany

Abstract

The guidelines of the Food and Drug Administration (FDA) and International Conference on Harmonization (ICH) have highlighted the importance of drug metabolites in clinical trials. As a result, an authentic source for the production of them is of great interest, both for their potential application as analytical standards and for required toxicological testing. Since we showed promising biotechnological potential of cytochromes P450 from the soil bacterium *Sorangium cellulosum* So ce56 before, herein we investigated the CYP267 family and its application for the conversion of commercially available drugs including nonsteroidal anti-inflammatory, antitumor and antihypotensive drugs. The CYP267 family, especially CYP267B1, revealed the interesting ability to convert a broad range of substrates. We established substrate-dependent extraction protocols and also optimized the reaction conditions for the *in vitro* experiments and *E. coli* based whole-cell bioconversions. We were able to detect activity of CYP267A1 towards 7 out of 22 drugs and the ability of CYP267B1 to convert 14 out of 22 drugs. In our established whole-cell system using CYP267B1 and expressing the autologous redox partners Fdx8 and FdR_B, moderate to high conversions (up to 85% yield) were observed. With our existing setup, we present a system capable of producing reasonable quantities of the human drug metabolites 4-hydroxydiclofenac, 2-hydroxyibuprofen and omeprazole sulfone. Due to the great potential of converting a broad range of substrates, wild-type CYP267B1 offers a wide scope for the screening of further substrates, which will draw further attention to a future biotechnological usage of CYP267B1 from *S. cellulosum* So ce56.

Introduction

The emergence of new diseases, rising concerns about drug resistance and the decreasing efficacy of the existing drugs are of great pharmaceutical concerns. As a result, drug research during the past century, driven by chemistry, pharmacology and clinical science, has shown an increasing contribution to the development of new therapeutic agents (Drews, 2000). Despite the success in combating the majority of genetic, infectious and bacterial diseases, novel drugs and drug derivatives are consistently demanded. However, the efficacy of such drugs and their related metabolites need to be tested and approved. The guidelines published by the Food and Drug Administration (FDA) and the International Conference on Harmonization (ICH) highlight the importance of qualifying metabolite exposure in clinical trials, in which a metabolite formed greater than 10% needs to be specifically tested for toxicity (FDA, 2008; ICH, 2009, 2012). Due to the frequent introduction of novel drugs and drug candidates with new or modified chemical structure, implementation of costly multi-step chemical syntheses may not be sufficient enough to overcome the demand of the respective metabolites (Rushmore *et al.*, 2000).

Although the purification of major metabolites from urine is relatively easy and cheap (Gao *et al.*, 2012), a large scale production of drug metabolites, for instance with the usage of human liver, is hindered by a very limited availability. To circumvent such limitations, alternative approaches of using microorganisms have been practiced, in which several microorganisms like the fungus *Cunninghamella* sp. or bacterial variants of *Streptomyces* strains were shown to transform drugs and xenobiotics to mammalian metabolites (Zhang *et al.*, 1996; Asha and Vidyavathi, 2009; Bright *et al.*, 2011; Murphy and Sandford, 2012; Diao *et al.*, 2013). However, because of the release of side-products and the difficulty on handling the microbes during such biotransformation process, there is now a great interest in cytochrome P450 enzymes (P450s) for the production of drug metabolites. In general, P450s are versatile, heme-containing enzymes, which catalyze a variety of reactions highlighting them as essential candidates for biotechnological and pharmaceutical researches (Bernhardt and Urlacher, 2014). It has been shown that the utilization of human P450s enables the sufficient production of human drug metabolites employing baculovirus infected insect cells expressing CYP3A4 or CYP2D9 (Rushmore *et al.*, 2000), fission yeast expressing CYP2D6 (Peters *et al.*, 2007) or CYP2C9 (Drăgan *et al.*, 2011; Neunzig *et al.*, 2012) and *E. coli* cells expressing CYP3A4, CYP2C9 and CYP1A2 (Vail *et al.*, 2005). Since it is not mandatory to employ associated human P450s to synthesize human drug metabolites (Schroer *et al.*, 2010; Geier *et al.*, 2015), microbial, especially bacterial, P450s serve as a good alternative as they are convenient to handle and usually hold higher expression levels and activities, recommending the possibility to employ them as useful biocatalysts (Bernhardt, 2006). The genetic manipulation of bacterial P450s towards a drug metabolizing activity has been successfully demonstrated for several P450s including the most studied $P450_{BM3}$ (CYP102A1) (Whitehouse *et al.*, 2012; Ren *et al.*, 2015). However, the engineering of enzymes against their native, narrow substrate range or, in general, the screening for enzymes to produce certain drug metabolites is time-consuming and complex, which can be overcome by employing versatile wild-type P450s showing an untypically broad substrate range (Yin *et al.*, 2014).

During our recent investigations on P450s from the myxobacterium *Sorangium cellulosum* So ce56, several interesting enzymes displaying new properties and substrate specificities have been discovered, which lead us to investigate the potential of these P450s for an application as drug metabolizing biocatalysts (Khatri *et al.*, 2010, 2013; Litzenburger and Bernhardt, 2015; Schifrin *et al.*, 2015). Therefore, we used bioinformatics analysis to identify myxobacterial P450s which are closely related to drug metabolizing P450s. Among others, the two

members of the CYP267 family, CYP267A1 and CYP267B1, were found to be potential candidates. Although the purified CYP267A1 and CYP267B1 were shown before to convert certain drugs (Kern *et al.*, 2015; Litzenburger *et al.*, 2015) and CYP267A1 was found to catalyze the hydroxylation of fatty acids (Khatri *et al.*, 2015), a broader analysis of their substrate spectrum has never been tested. Therefore, in this study, we have tested the *in vitro* and whole-cell conversion of 22 widely used drugs (see Figure 1) by CYP267A1 and CYP267B1 for the first time. Compounds showing a significant *in vitro* conversion were further chosen for a whole-cell biotransformation to upscale the metabolite production for the structural elucidation of the product(s) via NMR spectroscopy. We demonstrate that 7 out of 14 drugs can be converted by CYP267A1 and CYP267B1 shows activity towards 14 out of 22 drugs.

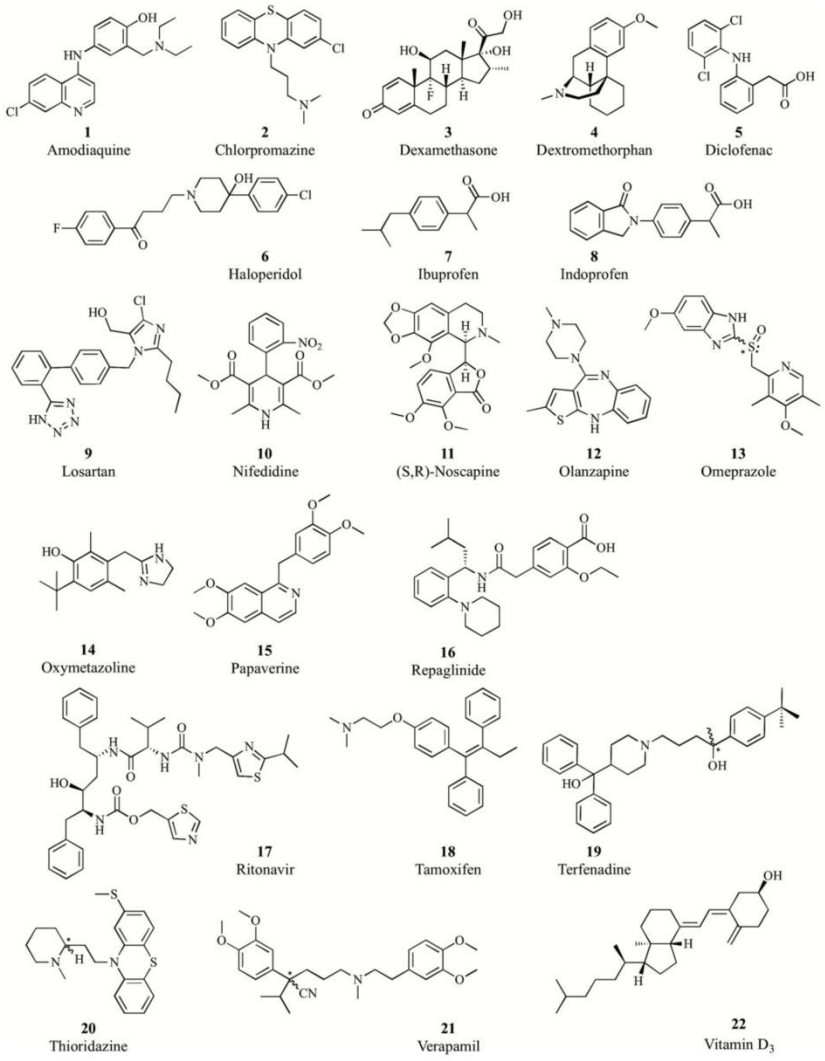

Figure 1: Structural illustration of the tested drugs. In the case of **13**, **19**, **20** and **21**, racemic mixtures were used in all experiments.

Materials and methods

Chemicals

Amitriptyline, amodiaquine, haloperidol, losartan, olanzapine, quinine, repaglinide, ritonavir, tamoxifen and thioridazine were kindly provided by Dr. Stephan Lütz (Novartis, Basel, Switzerland). Isopropyl-β-D-1-thiogalactopyranoside and δ-aminolevulinic acid were purchased from Carbolution Chemicals (Saarbruecken, Germany). Bacterial media were purchased from Becton Dickinson (Heidelberg, Germany). All other chemicals were obtained from standard sources in the highest purity available.

Strains

The *E. coli* strains Top 10 and NovaBlue Singles™ Competent Cells for cloning purpose were obtained from Invitrogen (San Diego, CA) and Merck (Duesseldorf, Germany). The *E. coli* strains BL21-Gold(DE3) for the heterologous expression of CYP267A1 and C43(DE3) for the heterologous expression of CYP267B1 were purchased from Agilent Technologies (Santa Clara, CA), whereby C43(DE3) was also used for whole-cell conversions.

Plasmids

The genes of CYP267A1 and CYP267B1 were cloned into a pET22b plasmid (Novagen) as described elsewhere (Litzenburger *et al.*, 2015). The pKKHC plasmids for the heterologous expression of the autologous redox partners Fdx8 and FdR_B originate from previous work done in our lab (Ewen *et al.*, 2009).

For the expression of the redox partners in the whole-cell system, the pCDF_dFA plasmid from (Litzenburger *et al.*, 2015) was used and changed as follows. The gene encoding Fpr was excised using the restriction enzymes *Nde*I and *Kpn*I and substituted with the FdR_B gene obtained from pKKHC_FdR_B using the same restriction enzymes. The ligation reactions were performed with the Fast-Link DNA Ligase Kit (Biozym Scientific GmbH, Hessisch Oldendorf, Germany). From the resulting plasmid pCDF_AFB containing *bovine* $Adx_{4\text{-}108}$ and ferredoxin-$NADP^+$ reductase FdR_B from *S. cellulosum* So ce56, the gene of $Adx_{4\text{-}108}$ was excised with *Nco*I and *Hind*III. The resulting open plasmid was ligated with the gene of Fdx8 previously obtained from pKKHC_Fdx8 using the mentioned restriction enzymes. The resulting plasmid pCDF_F8B contains the genes for expressing the autologous ferredoxin Fdx8 and the ferredoxin-$NADP^+$ reductase FdR_B from *S. cellulosum* So ce56 (see also Figure S 1).

Expression and purification

CYP267A1 and CYP267B1 have been expressed and purified as previously described (Khatri *et al.*, 2015) using the T7 promoter based expression construct of CYP267A1 and CYP267B1 (pET22b_CYP267A1 and pET22b_CYP267B1).

The electron transfer partners Fdx8 and FdR_B were expressed and purified as noted elsewhere (Ewen *et al.*, 2009).

Media and buffers

For the heterologous expression of CYP267A1 and CYP267B1, terrific broth medium (24 g yeast extract, 12 g peptone, 4 ml glycerol, 2.31 g K_2HPO_4 and 12.54 g KH_2PO_4 per liter H_2O) was used. The whole-cell conversions

were performed in M9CA medium (6 g Na_2HPO_4, 3 g KH_2PO_4, 0.5 g NaCl, 1 g NH_4Cl, 4 g Bacto Casamino Acids, 4 g glucose, 50 µl 1M $CaCl_2$, 2 ml 1 M $MgSO_4$, 2 ml of trace elements solution per liter H_2O; Trace elements solution contained 2.5 g EDTA, 250 mg $FeSO_4$, 25 mg $ZnCl_2$ and 5 mg $CuSO_4$ per 50 ml H_2O).

Spectral characterization of the CYP267 family

UV-visible spectra for the purified P450s were recorded at room temperature on a double-beam spectrophotometer (UV-2101PC, SHIMADZU, Kyoto, Japan). The enzyme solution (2 µM) in 10 mM potassium phosphate buffer, pH 7.4, was dosed with a few grains of sodium dithionite to reduce the heme-iron and the sample was split into two cuvettes. The baseline was recorded between 400 and 700 nm. The sample cuvette was bubbled gently with carbon monoxide (CO) for 1 min and a spectrum was recorded. The concentration of the P450s was estimated by CO-difference spectroscopy assuming ε(450-490 nm) = 91 mM^{-1} cm^{-1} according to the method of Omura and Sato (Omura and Sato, 1964).

***In vitro* conversions**

A reconstituted *in vitro* system containing the corresponding P450 (0.5 µM), FdR_B (1.5 µM), Fdx8 (10 µM) and a cofactor regenerating system with glucose-6-phosphate (5 mM) and glucose-6-phosphate dehydrogenase (2 U ml^{-1}) in potassium phosphate buffer (20 mM, pH 7.4, 1% glycerin) was used. The potential substrates, except olanzapine and omeprazole (both dissolved in DMSO), were dissolved in ethanol (10 mM) and added to an end-concentration of 200 µM. The total volume of the reaction was 250 µl. The reaction was started by the addition of NADPH (800 µM) and carried out for 3 h at 30°C. For the substrates **1**, **9**, **11**-**15** and **18**-**21**, 1 M glycine buffer (pH 11) or acetate buffer (pH 4) were added after reaction to enable improved recovery of the analytes. The reaction was, therefore, stopped by adding buffer (300 µl) or organic solvent (500 µl). The extraction was performed twice with 500 µl of the appropriate solvent (see supplemental Table S 0). A negative control without P450 was implemented for each substrate to verify the P450 dependent reaction.

Whole-cell conversions

The experiments were performed with C43(DE3) cells, which were transformed with two plasmids, one encoding CYP267A1 (pET22b_CYP267A1) or CYP267B1 (pET22b_CYP267B1) and the second one encoding the redox partners Fdx8 and FdR_B (pCDF_F8B). For the main culture, 50 ml M9CA medium containing ampicillin (100 µg/ml) and streptomycin (50 µg/ml), inoculated with the corresponding overnight culture in LB medium (dilution 1:100), was used. At an optical density of 0.9-1, the induction was initiated by adding 1 mM IPTG and 0.5 mM δ-Ala and the temperature was set to 28°C. After 21 h of expression, the temperature was set to 30°C and the substrate was added to a final concentration of 200 µM. To enable higher substrate conversion, EDTA (20 mM) or polymyxin B (32 µg/l) were added to increase permeability and substrate uptake of the *E. coli* cells (Janocha and Bernhardt, 2013). After 48 h at 30°C, a 500 µl sample was removed, quenched with adding buffer or organic solvent and extracted two times with 500 µl of organic solvent (see supplemental Table S 0). The organic phases were collected and evaporated to dryness. The extracts were stored at -20°C until analysis. All experiments were done twice including a negative control (cells only transformed with pCDF_F8B).

Analysis of the *in vitro* and whole-cell conversions via HPLC

The HPLC analysis was performed on a Jasco HPLC 2000 system consisting of a PU-2080 Plus Pump, a AS-2050 Plus Sampler and a UV-2075 Plus UV/Vis-Detector. For the HPLC analysis, samples of **3**, **10**, **13** and **22** were dissolved in 75 µl acetonitrile and 75 µl Milli-Q water. The remaining substrates were dissolved in the same volumes of solvents containing 0.1% trifluoroacetic acid (TFA). Analyses were performed on a reversed phase column (125/4 Nucleodur 100-5 C18ec; Macherey Nagel, Düren, Germany) at a flow rate of 1 ml min^{-1} and a temperature of 40°C. The injection volume was set to 30 µl. Due to the amount of different substrates, the HPLC methods (including detection wavelengths) were substrate-dependent and are presented in the supplemental data (Table S 1).

Upscaling of the whole-cell biotransformation system and purification of the products

To obtain sufficient amounts of products for structure elucidation via NMR analysis, the previously described whole-cell conversions were up-scaled to a total volume of 2.5 L. After 48 h, the reaction was stopped with the same volume of the appropriate solvent (see supplemental Table S 0). Before extraction of the product of **13**, the culture was set to a pH of 11 using 2 M KOH and subsequently purified as described previously (Litzenburger *et al.*, 2015). The purification of the product **13a** was done in the absence of TFA.

NMR Analysis

The structures of the products were analyzed by NMR spectroscopy (Institute for Pharmaceutical Biology, Saarland University, Germany). The ^{1}H- and ^{13}C-NMR were recorded on a Bruker (Rheinstetten, Germany) 500 MHz NMR spectrometer. Two-dimensional NMR spectra were recorded as gs-HH-COSY, gs-HSQC, and gs-HMBC. All chemical shifts are relative to $CDCl_3$ (d = 77.00 for ^{13}C-NMR; d =7.24 for ^{1}H-NMR) or CD_3OD (d = 49.00 for ^{13}C-NMR; d = 3.31 for ^{1}H-NMR) using the standard δ notion in parts per million.

MS/MS Analysis

The product **13a** was additionally characterized by MS/MS analysis (Institute of Bioanalytical Chemistry, Saarland University, Germany) with a API 2000 Qtrap (ABSciex, Darmstadt, Germany). Detailed settings of the MS/MS experiments can be found in the supplemental data (section 8: MS/MS settings).

Results

Bioinformatics studies and comparison of CYP267A1 with CYP267B1

In order to identify homologues of potentially drug metabolizing P450s from *S. cellulosum* So ce56, all of the 21 P450s (Khatri *et al.*, 2010) from this bacterium were aligned with the known bacterial drug metabolizing P450s (supplemental Table S 2). We observed that CYP265A1, CYP266A1 and the CYP267 family of this bacterium clustered within the same clan of the drug metabolizing P450s like CYP107E4 from *Actinoplanes* sp, CYP105 and CYP256 from *Rhodococcus jostii* RHA1, showing an amino acid sequence identity of 38.9%, 34.2% and 33.4%, respectively (Figure 2, supplemental Table S 2). These bacterial P450s are considered as active drug metabolizers for several drugs including amitriptyline, chlorpromazine (**2**) and diclofenac (**5**) (Prior *et al.*, 2010; Kulig *et al.*, 2015). In addition, we have already shown that CYP264A1 was able to convert tricyclic drug molecules (Litzenburger *et al.*, 2015), and CYP265A1 and CYP266A1 were able to hydroxylate the antitumor drug epothilone D (Kern *et al.*, 2015). As a result, our homology study with the drug metabolizing bacterial P450s suggested that the two members of the CYP267 family (in addition to CYP265A1 and CYP266A1) are potential candidates for metabolizing certain drugs. The amino acid sequence alignment of CYP267A1 and CYP267B1 showed an identity of 38%. CYP267B1 possesses a conserved heme-binding domain ($_{347}$**F**GG**G**IHF**C**L**G**$_{356}$), the conserved threonine in the I-helix ($_{243}$AGHE**T**T$_{248}$), and glutamic acid and arginine in the K-helix ($_{281}$E**E**AL**R**$_{285}$), whereas in CYP267A1 the conserved phenylalanine in the heme-domain is replaced by Leucine (L366) (Khatri *et al.*, 2015).

Amino acid sequence alignment of the CYP267 family with human P450s demonstrated that CYP267B1 showed the highest identities of 20.7%, 20.2%, 19.6%, 19.3% and 19.0% with CYP2W1, CYP2C8, CYP2A6, CYP2D6 and CYP3A4, respectively (supplemental Table S 2), which are considered as efficient drug metabolizers (Wrighton and Stevens, 1992; Guengerich, 1999).

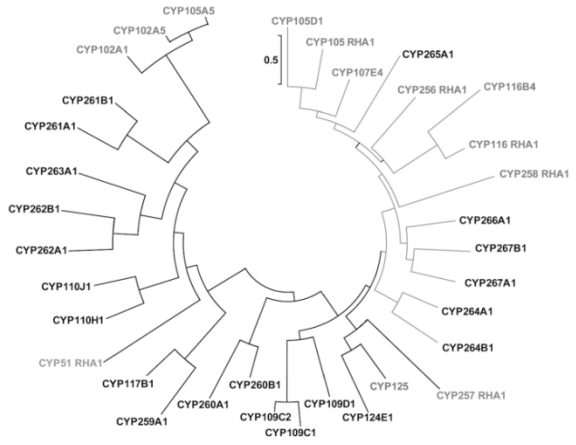

Figure 2: The radial view of an unrooted phylogenetic tree obtained by MEGA4 (version 4.0) analysis for the determination of relatedness of the 21 P450s from *S. cellulosum* So ce56 (in black) with respect to drug metabolizing bacterial P450s CYP105D1 [P26911.1] from *Streptomyces griseus*, CYP51_RHA1 [Q0S7M9], CYP105_RHA1 [Q0SDH7], CYP116_RHA1 [Q0RUR9], CYP125_RHA1 [Q0S7N3], CYP256_RHA1 [Q0RXF8] and CYP257_RHA1 [Q0RVH0] from *Rhodococcus jostii* RHA1, CYP107E4 [ACN71221.1] from *Actinoplanes* sp. ATCC 53771, CYP116B4 [EAV41564.1] from *Labrenzia aggregate* (in grey). The cluster of drug metabolizing P450s is shown in grey clan. The bar in the tree indicates 0.5 amino acid substitutions per amino acid for the branch length.

Expression, purification and characterization of the CYP267 family members

First expression studies for CYP267B1 were realized using the vector pCWori$^+$. However, the yield of CYP267B1 using the pCWori$^+$ based expression construct was very low (<20 nmol/L *E. coli* culture after the purification). Therefore, the protein has been expressed and purified using a T7 based expression construct (pET22b_CYP267B1) (Litzenburger *et al.*, 2015), in which the protein yield was increased five fold (100 nmol/L).

As shown in Figure 3, the UV-visible absorption spectrum of the oxidized CYP267B1 showed the presence of the Soret band (γ) at 416 nm, and the *Q*-bands at 567 nm (*β*) and 533 nm (*α*). The reduction of CYP267B1 with sodium dithionite showed a slightly diminished absorption peak for the Soret band at 410 nm and a single peak in the *Q*-region (538 nm). The reduced CO-complex of CYP267B1 showed a typical peak maximum at 449 nm. The purified CYP267A1 showed the same spectroscopic features as previously described (Khatri *et al.*, 2015), with the characteristic peak maximum at 448 nm in the CO-difference spectroscopy experiment and a peak maximum at 418 nm in the oxidized form of CYP267A1.

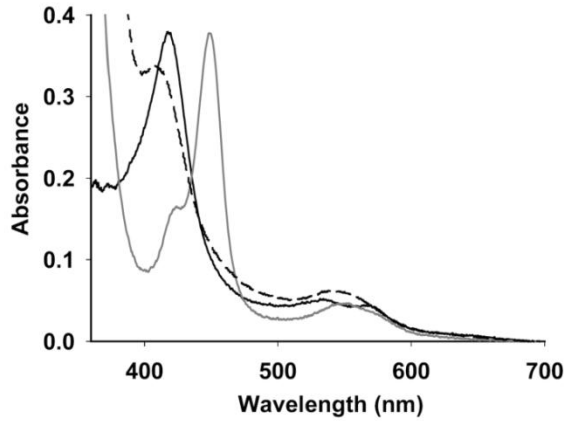

Figure 3: Spectroscopic characterization of CYP267B1. The UV-visible spectra of oxidized (black line), dithionite reduced (dashed line) and CO-bound (gray line) CYP267B1 were recorded in 10 mM potassium phosphate buffer, pH 7.5.

Optimization of the *in vitro* conversion

Since P450s are monooxygenases, they require electrons from NAD(P)H, which are transferred by autologous or heterologous redox partners (Hannemann *et al.*, 2007). The substrate turnover also depends on the coupling and the efficiency of the redox partner proteins. In the case of the CYP267 family we observed limited *in vitro* conversions (Kern *et al.*, 2015; Litzenburger *et al.*, 2015) when using the bovine redox partners $Adx_{4\text{-}108}$/AdR. Therefore, we substituted the heterologous $Adx_{4\text{-}108}$ and AdR with the autologous redox partners Fdx8 and FdR_B from *S. cellulosum* So ce56, which were previously shown to increase the CYP267B1-dependent epothilone D conversion (Kern *et al.*, 2015). In our earlier studies on the conversion of tricyclic antipsychotics and antidepressants (Litzenburger *et al.*, 2015), thioridazine (**20**) could be identified as substrate for CYP267A1 and amitriptyline as well as chlorpromazine (**2**) for CYP267B1, however, with a low *in vitro* and whole-cell conversion. The substitution of $Adx_{4\text{-}108}$/AdR with the autologous redox partners Fdx8/FdR_B showed increased

thioridazine-5-sulfoxide (**20a**) formation (from 43% to 50%) during the *in vitro* conversion of **20**. Likewise, the *in vitro* conversion of amitriptyline by CYP267B1 showed a significant enhancement of 10-hydroxyamitriptyline formation (from 15% to 60%), whereas the *in vitro* conversion of chlorpromazine (**2**) showed no difference.

Optimization of the *E. coli* based whole-cell bioconversion system

Since we observed a significant increase in the product formation when using the autologous redox partners, we investigated the coexpression of the autologous redox partners Fdx8 and FdR_B for our whole-cell bioconversion experiments. For comparison, a whole-cell system co-expressing Adx_{4-108} and Fpr was used, since it has been shown previously that the whole-cell conversion of 4-methyl-3-phenyl-coumarin by CYP264A1 from *S. cellulosum* So ce56 increased when Fpr instead of AdR was used (Ringle *et al.*, 2013). However, when substituting Adx_{4-108}/Fpr with the autologous redox partners Fdx8/FdR_B, the yield of the product was even further increased. In case of CYP267A1, a nine times higher conversion of **20** was observed (from 5% to 45% thioridazine-5-sulfoxide **20a**, Table 1). Likewise, the formation of chlorpromazine sulfoxide (**2a**) was nearly doubled by the CYP267B1-Fdx8-FdR_B whole-cell bioconversion system compared with CYP267B1-Adx_{4-108}-Fpr (from 18% to 30% **2a**, Table 1). In addition, we also observed a higher yield (from 7.5% to 26%) of the product 10-hydroxyamitriptyline from amitriptyline (Table 1). On the basis of these results, all further drug conversions were performed using Fdx8/FdR_B as redox partners in all *in vitro* and *E. coli* based whole-cell bioconversion experiments.

When establishing a whole-cell system for P450s, the indole-dependent inhibition should also be considered. It was observed that indole acts as an inhibitor of CYP264A1 from *S. cellulosum* So ce56 (Ringle *et al.*, 2013) and CYP109B1 from *Bacillus subtilis* (Girhard *et al.*, 2010). In addition, some P450s are known to convert indole, this way competing with the normal substrate (Gillam *et al.*, 2000). The metabolism of tryptophan by the tryptophanase TnaA of *E. coli* results in the formation of indole (Li and Young, 2013). Since tryptophan is present in TB medium, a concentration of over 600 µM indole was detected after 72 h (Ringle *et al.*, 2013). In case of the two members of the CYP267 family, the presence of 600 µM indole decreases the product formation *in vitro* up to 40% for CYP267B1 and up to 85% in the case of CYP267A1 (supplemental Figure S 3). Therefore, we performed the whole-cell bioconversions in a defined M9CA minimal medium, which was previously shown to exhibit a very low amount of indole when using *E. coli* as a host (<5 µM) (Ringle *et al.*, 2013).

Furthermore, the effect of the additives EDTA and polymyxin B was also investigated during the whole-cell conversions, since it has been shown previously that the presence of EDTA or polymyxin B enhances substrate uptake of *E. coli* cells for resin acid diterpenoid conversion by a CYP105A1-based whole-cell biocatalyst (Janocha and Bernhardt, 2013). We observed that the highest product formation was obtained when 20 mM EDTA for **1**, **2**, **5**, **7**, **9**, **15**, **16** and 32 µg ml^{-1} polymyxin B for **11**, **13**, **18**, **19**, **20** were applied in the whole-cell system. Higher concentrations of both additives did not alter the product pattern for the tested drugs.

Table 1: Comparison of the whole-cell conversions with CYP267A1 and CYP267B1 using different redox partners (* taken from (Litzenburger *et al.*, 2015)).

Model substrate	CYP267	Conversion [%] with		Product
		Heterologous Adx_{4-108}/Fpr*	Autologous Fdx8/FdR_B	
Amitriptyline	B1	7.5%	26%	10-Hydroxyamitriptyline*
Chlorpromazine (**2**)	B1	18%	30%	Chlorpromazine sulfoxide* (**2a**)
Thioridazine (**20**)	A1	5%	45%	Thioridazine-5-sulfoxide* (**20a**)

Optimization of product extraction and HPLC conditions for the investigation of drug conversions

Due to the diverse chemical structures and functional groups of the tested drug molecules, we established a substrate-dependent extraction protocol to improve our experimental conditions for efficient analyses and for product purification (supplemental Table S 0). We also optimized the HPLC conditions and listed them in the supplemental Table S 1.

CYP267-dependent substrate conversion

***In vitro* and whole-cell conversions by CYP267A1**

The *in vitro* conversions revealed that 7 out of 22 drugs were converted by CYP267A1. In comparison with CYP267B1, the product pattern of CYP267A1 differs only for chlorpromazine (**2**; 2.4%) for which only one product was observed. For ibuprofen (**7**), tamoxifen (**18**) and terfenadine (**19**) the yields of the product formation were significantly lower compared with the respective CYP267B1-dependent conversions (**7**: 1.5%, **18**: 3.7%, **19**: 2.1%). Despite having lower conversions with CYP267A1, five new substrates for CYP267A1 were identified (**4**, **6**, **7**, **18** and **19**, Figure 4 A). However, during *in vitro* conversion of **18** and **20**, one side product for **18** (1.9 ±1.1%) and in the case of **20** two minor side products (3.7 ±0.3% and 2.6 ±0.1%) have also been observed.

Only dextromethorphan (**4**), haloperidol (**6**) and thioridazine (**20**) were further employed for the investigation in the whole-cell system with CYP267A1-Fdx8-FdR_B, in which compounds **4** and **6** showed no conversion. Due to the higher *in vitro* conversion of **2**, **18** and **19** with CYP267B1, these substrates were only tested in the CYP267B1-Fdx8-FdR_B whole-cell system. However, using CYP267A1, **20** was successfully converted to **20a** yielding in a 44.7% product formation in our *E. coli* based whole-cell bioconversion (Figure 4 A).

***In vitro* and whole-cell conversions by CYP267B1**

It is very interesting to note that the *in vitro* conversions of the 22 tested drugs showed that CYP267B1 was able to convert 14 out of 22 compounds (Figure 4 B), seven more than CYP267A1. The highest *in vitro* yield was observed for oxymetazoline (**14**; 77.7%) and moderate *in vitro* conversions were also detected for chlorpromazine (**2**; 37%), diclofenac (**5**; 37.5%), ibuprofen (**7**; 31.1%) and repaglinide (**16**; 41.4%). In addition, amodiaquine (**1**, 10.2%), losartan (**9**; 8.9%), noscapine (**11**; 12.1%), olanzapine (**12**; 16.5%), omeprazole (**13**;

13.7%), papaverine (**15**; 12.6%) and tamoxifen (**18**; 15%) were also converted by CYP267B1. Very low conversion was observed for ritonavir (**17**; 1.4%) and terfenadine (**19**; 4.1%). However, one minor side product was observed for **7** (2.2 ±0.1%), **9** (1.9 ±0.4%), **11** (1.85 ±0.45%), **12** (2 ±0.1%), **13** (7 ±0.4%), **15** (2.2 ±0.1%), **16** (7.8 ±1.4%) and **18** (2.55 ±0.45%). In the case of **14**, two minor side products were observed (5.1 ±1.0% and 3 ±0.5%) during the *in vitro* experiments.

The 14 drugs identified as substrate for CYP267B1 during the *in vitro* experiments were further investigated in the corresponding whole-cell experiments. Thereby, the highest yield was observed for omeprazole (**13**; 78.1%). The compounds **2** (30.3%), **5** (38%) and **7** (44.1%) showed similar yields compared to their corresponding *in vitro* experiments. Due to their high conversion in the whole-cell experiments, **2**, **5**, **7** and **13** were further chosen for upscale and product characterization. However, the CYP267B1-Fdx8-FdR_B whole-cell system was also able to convert **1**, **11**, **15**, **16**, **18** and **19** in lower yields (≤10%). In the CYP267B1-dependent whole-cell experiments, minor side products were only formed in the case of **11** (1.25±0.15%), **13** (5.3 ±0.2), **15** (5.4 ±0.5%) and **16** (5.2 ±0.4%), showing identical retention time to those observed in the *in vitro* experiments. For the compounds **12** and **14**, all the attempts of utilizing them in the whole-cell conversion system were unsuccessful, despite having high *in vitro* conversions (16.5% for **12** and 83% for **14**). For the substrates which are not converted (**3**, **4**, **6**, **8**, **10**, **20**, **21**, **22**) or showed poor conversion (**17**) during the *in vitro* assay, attempts of investigating these drugs within the whole-cell system were discarded. Despite these CYP267B1-dependent conversions, we observed a high conversion of losartan (**9**) to one product, without expressing CYP267B1 in the whole-cell experiment. This observation leads to the assumption that **9** is oxidized by *E. coli* C43 (DE3) to losartan carboxy acid. Due to the limited availability of this reference standard, we were not able to further investigate our assumption.

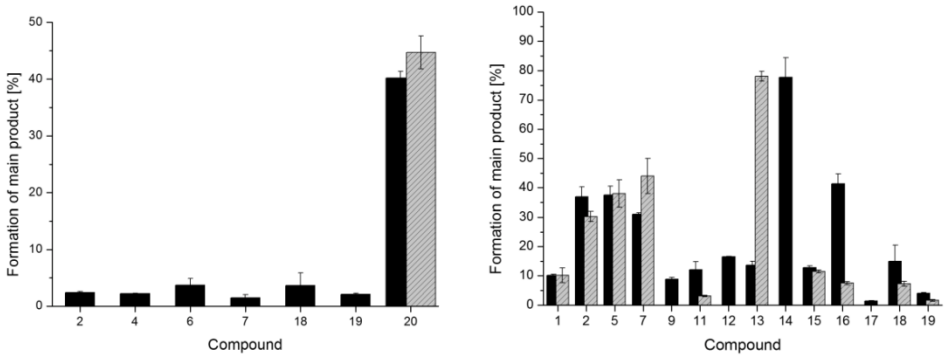

Figure 4: The main metabolite formation in vitro (black bar) and in the whole-cell (grey bar) system by CYP267A1-Fdx8-FdR_B (A) and CYP267B1-Fdx8-FdR_B (B).

A: The compounds 1, 3, 5, 8-17 and 21-22 were not converted by CYP267A1 and are therefore not shown. Only the substrates 4, 6 and 20 were further tested in the whole-cell system, whereby compound 4 and 6 showed no conversion. The highest whole-cell conversion for 20 was achieved with the supplement of polymyxin B (32 µg ml^{-1}).

B: The highest yields for the whole-cell conversions of 1, 2, 5, 7, 9, 15 and 16 by CYP267B1 were achieved in the presence of 20 mM EDTA. In case of 11, 13, 18 and 19, the highest conversions were observed with the addition of polymyxin B (32 µg ml^{-1}). Despite the in vitro conversions of 12 and 14 by CYP267B1, no conversion was observed in the corresponding whole-cell experiments. Due to the absence of conversion in the in vitro experiments, compounds 3, 4, 6, 8, 10 and 20-22 are not presented in this diagram.

Production of drug metabolites using an *E. coli* based whole-cell bioconversion system and purification of products via preparative HPLC

The whole-cell system of CYP267B1-Fdx8-FdR_B was up-scaled to 2.5 L of M9CA medium for the substrates **2**, **5**, and **7**. For the compound **13**, an upscaling to 500 ml was sufficient enough to produce 5 mg of **13a**. In case of the whole-cell system CYP267A1-Fdx8-FdR_B and the substrate **20**, the conversion was also up-scaled to 2.5 L M9CA medium. For the compounds converted in a larger scale, comparable yields as previously described (Figure 4 A and B) were observed, revealing a great potential of the established bioconversion system for future biotechnological upscaling. The products were purified via preparative HPLC and the purity of the isolated products was further verified by an additional HPLC measurement. The chromatograms of the purified products (**5a**, **7a** and **13a**) and the pure substrates (**5**, **7**, and **13**) are shown in the supplemental data (Figure S 2) confirming the high purity of the corresponding products. For **2a** and **20a**, the chromatograms coincide with previous data and can be found in the supplement (Litzenburger *et al.*, 2015).

Drug metabolites formed by the CYP267 family

As previously presented, CYP267A1 is able to convert 7 out of 22 drugs and CYP267B1 catalyzes the conversion of 14 out of 22 drugs *in vitro*. However, only drug **20** for CYP267A1 and 10 drugs (**1**, **2**, **5**, **7**, **11**, **12**, **15**, **16**, **18**, **19**) for CYP267B1 were successfully converted in our whole-cell system. For the drugs **2**, **5**, **7**, **13** and **20** showing high yields after whole-cell biotransformation, the respective metabolites were additionally elucidated with an up-scaled production and via NMR measurements. A comprehensive overview of the analyzed drugs, and the human metabolites produced by the two members of the CYP267 family, is presented in supplemental Figure S 6. CYP267B1 is able to catalyze an aromatic hydroxylation of **5** to the human metabolite 4-hydroxydiclofenac (**5a**) and an aliphatic hydroxylation of **7** to 2-hydroxyibuprofen (**2a**). Furthermore, the sulfoxidation of **2** and **13** is catalyzed by CYP267B1 and the sulfoxidation of **20** by CYP267A1. All products were obtained with high purity and sufficient amounts (5-10 mg) for the structure elucidation via NMR spectroscopy. The NMR (^{1}H and ^{13}C) data for **5a**, **7a** and **13a** are shown in the supplemental data. In the case of **13a**, an additional MS/MS measurement provided an unambiguous assignment to omeprazole sulfone (Figure S 5). The NMR data of the products **2a** and **20a** were identical to those we have described before (Litzenburger *et al.*, 2015) and match the corresponding reference standards (Zhang *et al.*, 1996; Morrow *et al.*, 2005). However, we achieved significantly increased yields in this study by our new whole-cell constructs (see supplemental data Figure S 1), which also gave better access to high product amounts for characterization of the respective products.

Discussion

In recent years, the number of publications about the potential applications of P450s for the production of a drug or drug-related compounds of pharmaceutical interest are continuously growing (Julsing *et al.*, 2008). This progress can directly be of use for the efficient and time-saving production of human drug metabolites. Thereby, high yields and conversion rates can already be achieved by using corresponding human (Rushmore *et al.*, 2000; Vail *et al.*, 2005; Schroer *et al.*, 2010; Geier *et al.*, 2012; Schiffer *et al.*, 2015) or suitable non-human (Taylor *et al.*, 1999; Otey *et al.*, 2006; Sawayama *et al.*, 2009; Reinen *et al.*, 2011; Di Nardo and Gilardi, 2012; Kiss *et al.*, 2015; Ren *et al.*, 2015) P450s in a whole-cell system to produce respective metabolites. The majority of published bacterial P450s used for the conversion of drugs are mutants of CYP102A1(BM3) from *Bacillus megaterium*. We investigated the native myxobacterial cytochromes P450 from *S. cellulosum* So ce56 for their application as drug metabolizers, since soil bacteria should be able to convert and metabolize different xenobiotics present in their environment. Thereby, special attention was given to the CYP267 family.

It is interesting to note that CYP267B1 revealed the remarkable ability to accept substrates with completely different chemical structures and functions. In addition to the capability of converting tricyclic compounds (Litzenburger *et al.*, 2015), the large 16-membered macrolide epothilone D (Kern *et al.*, 2015) and small structures like apocarotenoids (Litzenburger and Bernhardt, 2015), herein CYP267B1 showed activity towards the conversion of 14 out of 22 different drugs. In contrast, CYP267A1 was only able to convert 7 out of 22 drugs. The drugs converted by CYP267A1 and CYP267B1 feature a variety of chemical structures like heterocyclic aromatics, morphinan class compounds and alkaloids this way increasing both the known substrate spectrum for this P450 family and the conceivable fields of their application. The metabolism of a drug molecule by a human P450 usually results in the formation of several side products (Table 2), since the main aspect of drug metabolism is the excretion out of the body. Hence, the application of myxobacterial P450s is favorable to enable the production of a single human drug metabolite, highlighting their ability for biotechnological processes in order to produce a metabolite in large quantity.

However, an important bottleneck for the application of cytochrome P450 enzymes in biotechnological processes is often the efficiency of the redox system (Bernhardt and Urlacher, 2014). Concerning this, we first identified efficient autologous redox partners to transfer electrons to the CYP267 family. Even though the autologous redox system Fdx8/FdR_B from *S. cellulosum* So ce56 was already shown to transfer electrons to myxobacterial CYP109D1, CYP260A1 and CYP264A1 (Khatri *et al.*, 2010; Ringle *et al.*, 2013), the heterologous *bovine* adrenodoxin ($Adx_{4\text{-}108}$) with adrenodoxin reductase (AdR) or the *E. coli* reductase (Fpr) were shown to be more efficient (Khatri *et al.*, 2013; Ringle *et al.*, 2013). However, in this study, the substitution of $Adx_{4\text{-}108}$/Fpr by Fdx8/FdR_B showed a significant increase of product yields for drug molecules (Table 1) when using the members of the CYP267 family. As a result, an *E. coli* based whole-cell bioconversion system has been established containing the autologous redox partners of the CYP267 family.

Another bottleneck for the whole-cell conversions we faced during our studies, was the substrate uptake and indole inhibition. As a result, we established a substrate-dependent protocol, where EDTA and polymyxin B, which were shown to enhance substrate uptake into *E. coli* cells (Janocha and Bernhardt, 2013), significantly increased the limited whole-cell conversions (Figure 4 A and B). To overcome inhibition of CYP267A1 and CYP267B1 by indole (Supplemental Figure S 3), we performed the whole-cell experiments in defined M9CA medium. However, for the substrates **2**, **11**, **14**, **16**, **18** and **19** the CYP267B1-dependent whole-cell conversion

showed lower yields compared with the *in vitro* assay, which might be a limitation caused by the low permeability of the the *E. coli* cells for these substrates during the whole-cell conversion. In contrast, **7** and **13** showed higher yields in the whole-cell system compared with the *in vitro* conversion, suggesting that the conditions established for these substrates support an efficient metabolite production with our whole-cell system.

It has been shown recently that several members of a P450 fusion library, constructed by P450s and their autologous redox system RhfRED from *Rhodococcus jostii* RHA1, are able to convert 5 out of 48 selected drugs (Kulig *et al.*, 2015). Compared with our system consisting of the wild-type CYP267B1 and its autologous redox partners Fdx8 and FdR_B, we observed a larger substrate range (14 out of 22 drugs) and significantly higher activity towards the conversion of drugs. This leads to the suggestion that CYP267B1 features a great potential for the biotechnological production of various drug metabolites when using bacterial P450s. Our so far not optimized whole-cell system was able to convert 38% of 160 mg of diclofenac (**5**) within 48 h, which is a good starting point for the production of 4-hydroxydiclofenac (**5a**). Concerning this, the production of **5a** was previously shown by an optimized fermentation process. The recombinant expression of CYP2C9 in fission yeast strain CAD68 resulted in an efficient formation of **5a** (468 mg L^{-1}) after the optimization of the pH value, the glucose concentration and the establishment of a favorable host organism for the hydroxylation of **5** (Drăgan *et al.*, 2011). The engineering of BM3 towards the metabolism of drugs resulted in the BM3 mutant Asp251Gly/Gln307His capable of the metabolism of **5** to **5a** *in vitro* (Tsotsou *et al.*, 2012). This BM3 mutant was also shown to produce 2-hydroxyibuprofen (**7a**) from ibuprofen (**7**) (Tsotsou *et al.*, 2012), but experiments were only done *in vitro* or in a microtiter plate. Likewise, the production of **7a** in a preparative *in vitro* scale was described yielding 74.3 mg of **7a** (96% conversion) (Rentmeister *et al.*, 2011). However, in this study, we were able to produce **7a** in a more relevant, biotechnological way using an *E. coli* based whole-cell bioconversion system for CYP267B1 consisting of autologous redox partners and necessary cofactors within the cells. In this regard, the conversion of 115 mg **7** to **7a** giving 44% product yield by the wild-type CYP267B1 demonstrated a promising scope for further optimization, since we have not focused on the optimization or the engineering of the respective P450 towards higher space time yields yet. In addition, our CYP267B1-Fdx8-FdR_B whole-cell system also presents the first method to produce omeprazole sulfone (**13a**) using a biotechnological approach with a high conversion yield (nearly 80%, 68 mg of **13** L^{-1}) and high selectivity (<5% formation of unknown side product). Although CYP3A4 is responsible for the formation of omeprazole sulfone (**13a**) in the human body (Yamazaki *et al.*, 1997), to the best of our knowledge, the biotechnological production of **13a** with CYP3A4 (Table 2) or another P450 has not been described so far.

Table 2: Comprehensive overview of human drug metabolites formed by the members of the CYP267 family from *S. cellulosum* So ce56 and the corresponding human P450s. Metabolites marked with # and * are selectively formed by CYP267A1 and CYP267B1, respectively. The order of the listed metabolites is not representative for the product distribution.

Drug	Human P450	Desired metabolite	Expected side products of human P450s	Reference
Chlorpromazine (**2**)	CYP2D6, CYP3A4	Chlorpromazine sulfoxide (**2a**) *	7-Hydroxychlorpromazine, Chlorpromazine-N-oxide	(Cashman *et al.*, 1993)
Diclofenac (**5**)	CYP1A2	4-Hydroxydiclofenac (**5a**) *	-	(Bort *et al.*, 1999)
	CYP2C8, CYP2C18, CYP2C19		5-Hydroxydiclofenac, 4,5-Dihydroxydiclofenac	
	CYP2C9		3-Hydroxydiclofenac, 5-Hydroxydiclofenac	
Ibuprofen (**7**)	CYP2C8, CYP2C9	2-Hydroxyibuprofen (**7a**) *	3-Hydroxyibuprofen, Carboxyibuprofen	(Hamman *et al.*, 1997; Neunzig *et al.*, 2012)
Omeprazole (**13**)	CYP3A4	Omeprazole sulfone (**13a**) *	5-Hydroxyomeprazole	(Yamazaki *et al.*, 1997; Äbelö *et al.*, 2000)
Thioridazine (**20**)	CYP2D6	Thioridazine-5-sulfoxide (**20a**) #	N-desmethylthioridazine, 7-Hydroxythioridazine, Mesoridazine	(Daniel *et al.*, 2000)

The established CYP267-Fdx8-FdR_B whole-cell systems are an excellent starting point for further optimizations in view of biotechnological upscaling and optimization (Bernhardt and Urlacher, 2014). Optimizations like changing expression and reaction conditions or engineering the P450 could be potential topics of interests. Several approaches for increasing the performance of the whole-cell system were published describing that an increased number of ferredoxin gene copies (Schiffer *et al.*, 2015) or co-expressing a NADPH regenerating system (Zehentgruber *et al.*, 2010) could enhance the product formation. In a recent review, numerous approaches and examples were presented to enhance the catalytic activity of P450s towards potential practical purposes (Gillam, 2008). It is remarkable that the wild-type CYP267B1 is already able to catalyze three different reaction types (hydroxylation, sulfoxidation and epoxidation) without any directed or evolutionary modification. In fact, the catalyzed hydroxylation reactions can be diversified to aliphatic (in the case of **7**), allylic (as described for sesquiterpenes (Litzenburger and Bernhardt, 2015)) and aromatic (as shown for **5**) hydroxylations, whereby the aromatic hydroxylation has not been described for a myxobacterial P450 before.

Although the previous studies on the bioconversion of drugs and xenobiotics were performed using biotransformation (Zhang *et al.*, 1996; Asha and Vidyavathi, 2009; Bright *et al.*, 2011; Murphy and Sandford, 2012; Diao *et al.*, 2013), they are not selective and side products are usually observed, and the non-optimized

media condition could also interfere the detailed product identification. However, in this study, for the conversion of widely used therapeutically important drugs and xenobiotics, we established a whole-cell biocatalyst depending on two P450s (CYP267A1 and CYP267B1) and also optimized an *E. coli* based whole-cell system, in addition to the unambiguous product isolation and identification by NMR and MS/MS. In addition, the substrate spectrum of the CYP267 family, and thereby especially for CYP267B1, was also extended to commercially used drugs and their associated diverse chemical structures to show the potential of myxobacterial P450s as a drug metabolizer. Due to the great potential of catalyzing a broad range of substrates, it can be concluded that CYP267B1 is an efficient and promising candidate for further substrate screening and protein engineering, particularly with regard to its biotechnological applicability.

Acknowledgements

Special thanks are given to Dr. Stephan Lütz, Novartis (Basel, Switzerland), for providing some of the substrates and Dr. Josef Zapp, Institute of Pharmaceutical Biology (Saarland University, Germany), for measuring the NMR samples. We are grateful to Tobias Dier, Institute of Bioanalytical Chemistry (Saarland University, Germany) for the MS/MS measurement of omeprazole and omeprazole sulfone.

References

Äbelö A, Andersson TB, Antonsson M, Naudot AK, Skånberg I, and Weidolf L (2000) Stereoselective Metabolism of Omeprazole by Human Cytochrome P450 Enzymes. *Drug Metab Dispos* **28**:966–972.

Asha S, and Vidyavathi M (2009) Cunninghamella – A microbial model for drug metabolism studies – A review. *Biotechnol Adv* **27**:16–29.

Bernhardt R (2006) Cytochromes P450 as versatile biocatalysts. *J Biotechnol* **124**:128–145.

Bernhardt R, and Urlacher VB (2014) Cytochromes P450 as promising catalysts for biotechnological application: Chances and limitations. *Appl Microbiol Biotechnol* **98**:6185–6203.

Bort R, Macé K, Boobis A, Gómez-Lechón M-J, Pfeifer A, and Castell J (1999) Hepatic metabolism of diclofenac: role of human CYP in the minor oxidative pathways. *Biochem Pharmacol* **58**:787–796.

Bright T V, Clark BR, O'Brien E, and Murphy CD (2011) Bacterial production of hydroxylated and amidated metabolites of flurbiprofen. *J Mol Catal B Enzym* **72**:116–121.

Cashman JR, Yang Z, Yang L, and Wrighton SA (1993) Stereo- and regioselective N- and S-oxidation of tertiary amines and sulfides in the presence of adult human liver microsomes. *Drug Metab Dispos* **21**:492–501.

Daniel W a, Syrek M, Haduch a, and Wójcikowski J (2000) Pharmacokinetics and metabolism of thioridazine during co-administration of tricyclic antidepressants. *Br J Pharmacol* **131**:287–295.

Di Nardo G, and Gilardi G (2012) Optimization of the bacterial cytochrome P450 BM3 system for the production of human drug metabolites. *Int J Mol Sci* **13**:15901–15924.

Diao X, Deng P, Xie C, Li X, Zhong D, Zhang Y, and Chen X (2013) Metabolism and Pharmacokinetics of 3-n-Butylphthalide (NBP) in Humans: The Role of Cytochrome P450s and Alcohol Dehydrogenase in Biotransformation. *Drug Metab Dispos* **41**:430–444.

Drăgan CA, Peters FT, Bour P, Schwaninger AE, Schaan SM, Neunzig I, Widjaja M, Zapp J, Kraemer T, Maurer HH, and Bureik M (2011) Convenient gram-scale metabolite synthesis by engineered fission yeast strains expressing functional human P450 systems. *Appl Biochem Biotechnol* **163**:965–980, Humana Press Inc.

Drews J (2000) Drug discovery: a historical perspective. *Science* **287**:1960–1964.

Ewen KM, Hannemann F, Khatri Y, Perlova O, Kappl R, Krug D, Hütterman J, Müller R, and Bernhardt R (2009) Genome mining in Sorangium cellulosum So ce56: Indentification characterization of the homologous electron transfer proteins of a Myxobacterial cytochrome P450. *J Biol Chem* **284**:28590–28598.

FDA (2008) *Guidance for Industry Safety Testing of Drug Metabolites* (FDA MD R ed).

Gao R, Li L, Xie C, Diao X, Zhong D, and Chen X (2012) Metabolism and pharmacokinetics of morinidazole in humans: Identification of diastereoisomeric morpholine N +-glucuronides catalyzed by UDP glucuronosyltransferase 1A9. *Drug Metab Dispos* **40**:556–567.

Geier M, Bachler T, Hanlon SP, Eggimann FK, Kittelmann M, Weber H, Lütz S, Wirz B, and Winkler M (2015) Human FMO2-based microbial whole-cell catalysts for drug metabolite synthesis. *Microb Cell Fact* **14**:82.

Geier M, Braun A, Emmerstorfer A, Pichler H, and Glieder A (2012) Production of human cytochrome P450 2D6 drug metabolites with recombinant microbes – a comparative study. *Biotechnol J* **7**:1346–1358, WILEY-VCH Verlag.

Gillam EMJ (2008) Engineering Cytochrome P450 Enzymes. *Chem Res Toxicol* **21**:220–231, American Chemical Society.

Gillam EMJ, Notley LM, Cai H, De Voss JJ, and Guengerich FP (2000) Oxidation of Indole by Cytochrome P450 Enzymes †. *Biochemistry* **39**:13817–13824.

Girhard M, Klaus T, Khatri Y, Bernhardt R, and Urlacher VB (2010) Characterization of the versatile monooxygenase CYP109B1 from Bacillus subtilis. *Appl Microbiol Biotechnol* **87**:595–607.

Guengerich FP (1999) Cytochrome P-450 3A4: regulation and role in drug metabolism. *Annu Rev Pharmacol Toxicol* **39**:1–17.

Hamman MA, Thompson GA, and Hall SD (1997) Regioselective and stereoselective metabolism of ibuprofen by human cytochrome P450 2C. *Biochem Pharmacol* **54**:33–41.

Hannemann F, Bichet A, Ewen KM, and Bernhardt R (2007) Cytochrome P450 systems-biological variations of electron transport chains. *Biochim Biophys Acta* **1770**:330–344.

ICH (2009) Guidance of Nonclinical safety studies for the conduct of human clinical trials and marketing authorization for pharmaceuticals M3 (R2).

ICH (2012) ICH guideline M3 (R2) - questions and answers.

Janocha S, and Bernhardt R (2013) Design and characterization of an efficient CYP105A1-based whole-cell biocatalyst for the conversion of resin acid diterpenoids in permeabilized Escherichia coli. *Appl Microbiol Biotechnol* **97**:7639–7649.

Julsing MK, Cornelissen S, Bühler B, and Schmid A (2008) Heme-iron oxygenases: powerful industrial biocatalysts? *Curr Opin Chem Biol* **12**:177–186.

Kern F, Dier TKF, Khatri Y, Ewen KM, Jacquot J-P, Volmer DA, and Bernhardt R (2015) Highly Efficient CYP167A1 (EpoK) dependent Epothilone B Formation and Production of 7-Ketone Epothilone D as a New Epothilone Derivative. *Sci Rep* **5**:14881.

Khatri Y, Hannemann F, Ewen KM, Pistorius D, Perlova O, Kagawa N, Brachmann AO, Müller R, and Bernhardt R (2010) The CYPome of sorangium cellulosum so ce56 and identification of CYP109D1 as a new fatty acid hydroxylase. *Chem Biol* **17**:1295–1305.

Khatri Y, Hannemann F, Girhard M, Kappl R, Hutter M, Urlacher VB, and Bernhardt R (2015) A natural heme-signature variant of CYP267A1 from Sorangium cellulosum So ce56 executes diverse ω-hydroxylation. *FEBS J* **282**:74–88.

Khatri Y, Hannemann F, Girhard M, Kappl R, Même A, Ringle M, Janocha S, Leize-Wagner E, Urlacher VB, and Bernhardt R (2013) Novel family members of CYP109 from Sorangium cellulosum so ce56 exhibit characteristic biochemical and biophysical properties. *Biotechnol Appl Biochem* **60**:18–29.

Kiss FM, Lundemo MT, Zapp J, Woodley JM, and Bernhardt R (2015) Process development for the production of 15β-hydroxycyproterone acetate using Bacillus megaterium expressing CYP106A2 as whole-cell biocatalyst. *Microb Cell Fact* **14**:1–13, BioMed Central.

Kulig JK, Spandolf C, Hyde R, Ruzzini AC, Eltis LD, Grönberg G, Hayes M a., and Grogan G (2015) A P450

fusion library of heme domains from Rhodococcus jostii RHA1 and its evaluation for the biotransformation of drug molecules. *Bioorg Med Chem* **23**:5603–5609.

Li G, and Young KD (2013) Indole production by the tryptophanase TnaA in Escherichia coli is determined by the amount of exogenous tryptophan. *Microbiology* **159**:402–10, Microbiology Society.

Litzenburger M, and Bernhardt R (2015) Selective oxidation of carotenoid-derived aroma compounds by CYP260B1 and CYP267B1 from Sorangium cellulosum So ce56. *Appl Microbiol Biotechnol* **submitted**.

Litzenburger M, Kern F, Khatri Y, and Bernhardt R (2015) Conversions of Tricyclic Antidepressants and Antipsychotics with Selected P450s from Sorangium cellulosum So ce56. *Drug Metab Dispos* **43**:392–399.

Morrow RJ, Millership JS, and Collier PS (2005) Facile Syntheses of the Three Major Metabolites of Thioridazine. *Helv Chim Acta* **88**:962–967, WILEY-VCH Verlag.

Murphy CD, and Sandford G (2012) Fluorinated drug metabolism in microorganisms. *Chim Oggi/Chemistry Today* **30**:16–19.

Neunzig I, Göhring A, Drăgan CA, Zapp J, Peters FT, Maurer HH, and Bureik M (2012) Production and NMR analysis of the human ibuprofen metabolite 3-hydroxyibuprofen. *J Biotechnol* **157**:417–420.

Omura T, and Sato R (1964) the Carbon Monoxide-Binding Pigment of Liver Microsomes. I. Evidence. *J Biol Chem* **239**:2370–2378.

Otey CR, Bandara G, Lalonde J, Takahashi K, and Arnold FH (2006) Preparation of human metabolites of propranolol using laboratory-evolved bacterial cytochromes P450. *Biotechnol Bioeng* **93**:494–499.

Peters FT, Drăgan C a., Wilde DR, Meyer MR, Zapp J, Bureik M, and Maurer HH (2007) Biotechnological synthesis of drug metabolites using human cytochrome P450 2D6 heterologously expressed in fission yeast exemplified for the designer drug metabolite 4′-hydroxymethyl-α-pyrrolidinobutyrophenone. *Biochem Pharmacol* **74**:511–520.

Prior JE, Shokati T, Christians U, and Gill RT (2010) Identification and characterization of a bacterial cytochrome P450 for the metabolism of diclofenac. *Appl Microbiol Biotechnol* **85**:625–633.

Reinen J, Van Leeuwen JS, Li Y, Sun L, Grootenhuis PDJ, Decker CJ, Saunders J, Vermeulen NPE, and Commandeur JNM (2011) Efficient screening of cytochrome P450 BM3 mutants for their metabolic activity and diversity toward a wide set of drug-like molecules in chemical space. *Drug Metab Dispos* **39**:1568–1576.

Ren X, Yorke J a., Taylor E, Zhang T, Zhou W, and Wong LL (2015) Drug Oxidation by Cytochrome P450 $_{BM3}$: Metabolite Synthesis and Discovering New P450 Reaction Types. *Chem - A Eur J* n/a–n/a.

Rentmeister A, Brown TR, Snow CD, Carbone MN, and Arnold FH (2011) Engineered Bacterial Mimics of Human Drug Metabolizing Enzyme CYP2C9. *ChemCatChem* **3**:1065–1071, WILEY-VCH Verlag.

Ringle M, Khatri Y, Zapp J, Hannemann F, and Bernhardt R (2013) Application of a new versatile electron transfer system for cytochrome P450-based Escherichia coli whole-cell bioconversions. *Appl Microbiol Biotechnol* **97**:7741–7754.

Rushmore TH, Reider PJ, Slaughter D, Assang C, and Shou M (2000) Bioreactor systems in drug metabolism: synthesis of cytochrome P450-generated metabolites. *Metab Eng* **2**:115–125.

Sawayama AM, Chen MMY, Kulanthaivel P, Kuo MS, Hemmerle H, and Arnold FH (2009) A panel of cytochrome P450 BM3 variants to produce drug metabolites and diversify lead compounds. *Chem - A Eur J* **15**:11723–11729.

Schiffer L, Anderko S, Hobler A, Hannemann F, Kagawa N, and Bernhardt R (2015) A recombinant CYP11B1 dependent Escherichia coli biocatalyst for selective cortisol production and optimization towards a preparative scale. *Microb Cell Fact* **14**.

Schifrin A, Ly TTB, Günnewich N, Zapp J, Thiel V, Schulz S, Hannemann F, Khatri Y, and Bernhardt R (2015) Characterization of the Gene Cluster CYP264B1- geo A from Sorangium cellulosum So ce56: Biosynthesis of (+)-Eremophilene and Its Hydroxylation. *ChemBioChem* **16**:337–344, WILEY-VCH Verlag.

Schroer K, Kittelmann M, and Lütz S (2010) Recombinant human cytochrome P450 monooxygenases for drug metabolite synthesis. *Biotechnol Bioeng* **106**:699–706.

Taylor M, Lamb DC, Cannell R, Dawson M, and Kelly SL (1999) Cytochrome P450105D1 (CYP105D1) from Streptomyces griseus: heterologous expression, activity, and activation effects of multiple xenobiotics. *Biochem Biophys Res Commun* **263**:838–842.

Tsotsou GE, Sideri A, Goyal A, Di Nardo G, and Gilardi G (2012) Identification of Mutant Asp251Gly/Gln307His of Cytochrome P450 BM3 for the Generation of Metabolites of Diclofenac, Ibuprofen and Tolbutamide. *Chem – A Eur J* **18**:3582–3588, WILEY-VCH Verlag.

Vail RB, Homann MJ, Hanna I, and Zaks A (2005) Preparative synthesis of drug metabolites using human cytochrome P450s 3A4, 2C9 and 1A2 with NADPH-P450 reductase expressed in Escherichia coli. *J Ind Microbiol Biotechnol* **32**:67–74, Springer-Verlag.

Whitehouse CJC, Bell SG, and Wong L-L (2012) P450BM3 (CYP102A1): connecting the dots. *Chem Soc Rev* **41**:1218–1260, The Royal Society of Chemistry.

Wrighton SA, and Stevens JC (1992) The Human Hepatic Cytochromes P450 Involved in Drug Metabolism. *Crit Rev Toxicol* **22**:1–21, Taylor & Francis.

Yamazaki H, Inoue K, Shaw PM, Checovich WJ, Guengerich FP, and Shimada T (1997) Different Contributions of Cytochrome P450 2C19 and 3A4 in the Oxidation of Omeprazole by Human Liver Microsomes: Effects of Contents of These Two Forms in Individual Human Samples. *J Pharmacol Exp Ther* **283**:434–442.

Yin Y-C, Yu H-L, Luan Z-J, Li R-J, Ouyang P-F, Liu J, and Xu J-H (2014) Unusually Broad Substrate Profile of Self-Sufficient Cytochrome P450 Monooxygenase CYP116B4 from *Labrenzia aggregata*. *ChemBioChem* **15**:2443–2449.

Zehentgruber D, Hannemann F, Bleif S, Bernhardt R, and Lütz S (2010) Towards preparative scale steroid hydroxylation with cytochrome P450 monooxygenase CYP106A2. *ChemBioChem* **11**:713–721.

Zhang D, Freeman JP, Sutherland JB, Walker AE, Yang Y, and Cerniglia CE (1996) Biotransformation of chlorpromazine and methdilazine by Cunninghamella elegans. *Appl Environ Microbiol* **62**:798–803, Am Soc Microbiol.

SUPPORTING INFORMATION

CYP267A1 and CYP267B1 from *Sorangium cellulosum* So ce56 are highly versatile drug metabolizers

Fredy Kern, Yogan Khatri, Martin Litzenburger and Rita Bernhardt

Department of Biochemistry, Saarland University, 66123 Saarbruecken, Germany

To whom correspondence should be addressed: Rita Bernhardt, Department of Biochemistry, Saarland University, 66123 Saarbrücken, Germany, Tel.: +49 (0)681 302 4241; Fax: +49 (0)681 302 4739; Email: ritabern@mx.uni-saarland.de

Optimized extraction procedure **-** Due to the different substrates, and thus, the diversity of chemical structures and functional groups, we established a substrate-dependent extraction protocol as shown in Table S 0 accompanied by substrate-dependent HPLC methods listed in Table S 1.

Table S 0. The optimized extraction procedure for the tested drugs and respective metabolites. To improve the extraction efficiency, the addition of acidic (pH 4) or basic (pH 11) buffer before extraction is needed.

#	Substrate	Added before extraction	Solvent used for extraction
1	Amodiaquine	Glycine buffer	Chloroform
2	Chlorpromazine	-	Chloroform
3	Dexamethasone	-	Chloroform
4	Dextromethorphan	-	Chloroform
5	Diclofenac	-	Ethyl acetate
6	Haloperidol	-	Ethyl acetate
7	Ibuprofen	-	Ethyl acetate
8	Indoprofen	-	Ethyl acetate
9	Losartan	Acetic acid/Acetate buffer	Hexane 95%/ 5% Isopropyl alcohol
10	Nifedepine	-	Ethyl acetate
11	Noscapine	Glycine buffer	Ethyl acetate
12	Olanzapine	Glycine buffer	Chloroform
13	Omeprazole	Glycine buffer	Ethyl acetate
14	Oxymetazoline	Glycine buffer	Ethyl acetate
15	Papaverine	Glycine buffer	Chloroform
16	Repaglinide	-	Chloroform
17	Ritonavir	-	Chloroform
18	Tamoxifen	Glycine buffer	Hexane 95%/ 5% Isopropyl alcohol
19	Terfenadine	Glycine buffer	Chloroform
20	Thioridazine	Glycine buffer	Ethyl acetate
21	Verapamil	Glycine buffer	Chloroform
22	Vitamin D3	-	Chloroform

HPLC methods – The HPLC analysis of the substrates **3**, **10**, **13**, and **22** were performed using 20% acetonitrile/80% Milli-Q water (*v/v*) as solvent A and 100% acetonitrile as solvent B. All other substrates (**1**, **2**, **4-9**, **11**, **12** and **14-21**) were analyzed by using 100% Milli-Q water containing 0.1% TFA as solvent A and 100% acetonitrile containing 0.1% TFA as solvent B. Unless otherwise specified, the flow rate for all methods was set as 1 ml min^{-1} and the oven temperature as 40°C.

Table S 1. HPLC Methods for the tested compounds.

#	Substrate	Molecular weight [g mol^{-1}]	Wavelength [nm]	Method [minutes / % of solvent A]
1	Amodiaquine	464.81	344	0/90 5/90 10/60 13/60 13.1/20 14/20 14.1/90 16/90
2	Chlorpromazine	318.86	256	0/80 1/80 9/20 12/20 12.1/80 14/80
3	Dexamethasone	392.47	240	0/90 7/90 13/50 13.1/90 15/90
4	Dextromethorphan	271.40	280	Same method as **3**
5	Diclofenac	318.10	276	0/70 1/70 12/20 14/20 14.5/70 15/70
6	Haloperidol	375.86	244	0/80 2/80 8/50 12/50 12.1/80 14/80 1.2 ml min^{-1}
7	Ibuprofen	229.28	224	0/80 4/80

				13/20 15/20 15.1/80 17/80
8	Indoprofen	281.31	284	Same method as **7**
9	Losartan	461.91	244	0/90 2/90 10/40 12/40 12.1/20 14/20 14.1/90 16/90
10	Nifedepine	346.34	236	Same method as **7**
11	Noscapine	413.42	232	Same method as **7**
12	Olanzapine	312.43	260	0/90 12/70 12.1/50 13.5/50 13.6/90 16/90
13	Omeprazole	345.42	300	Same method as **3**
14	Oxymetazoline	296.84	228	Same method as **7**
15	Papaverine	375.75	252	0/90 2/90 7/60 10/60 10.1/20 11/20 11.1/90 13/90
16	Repaglinide	452.59	244	0/90 1/90 10/10 12/10 12.5/90 15/90
17	Ritonavir	720.94	240	0/70 1/70 9/10 10/10 10.1/70 13/70 0.8 ml min^{-1}

3/11

18	Tamoxifen	371.51	240	0/60 3/60 10/20 13/20 13.1/60 15/60
19	Terfenadine	471.67	228	Same method as **7**
20	Thioridazine	407.04	264	Same method as **7**
21	Verapamil	491.06	232	Same method as **11**
22	Vitamin D_3	384.64	265	0/40 15/0 26/0 30/40

Phylogenetic analysis of CYP267B1 with drug metabolizing P450s of human and bacterial origin – In addition to the phylogenetic analysis of CYP267B1 with respect to drug metabolizing human and bacterial P450s as depicted in Figure 2, we performed pairwise alignments with EMBOSS Needle and present the identities and similarities in Table S 2.

Table S 2. Overview of identities and similarities of drug metabolizing human and bacterial P450s with respect to CYP267B1 from *Sorangium cellulosum* So ce56.

CYP267B1 to	P450	UniProtKB	Identity	Similarity
human	CYP1A1	P04798.1	96/612 (15.7%)	152/612 (24.8%)
	CYP1A2	P05177.3	107/572 (18.7%)	166/572 (29.0%)
	CYP1B1	Q16678.2	96/600 (16.0%)	167/600 (27.8%)
	CYP2A6	P11509.3	105/537 (19.6%)	181/537 (33.7%)
	CYP2A7	P20853.2	99/592 (16.7%)	160/592 (27.0%)
	CYP2A13	Q16696.3	103/540 (19.1%)	175/540 (32.4%)
	CYP2B6	P20813.1	100/570 (17.5%)	164/570 (28.8%)
	CYP2C8	P10632.2	106/524 (20.2%)	173/524 (33.0%)
	CYP2C9	P11712.3	97/554 (17.5%)	168/554 (30.3%)
	CYP2C18	P33260.3	89/583 (15.3%)	159/583 (27.3%)
	CYP2C19	P33261.3	101/559 (18.1%)	172/559 (30.8%)
	CYP2D6	P10635.2	110/569 (19.3%)	164/569 (28.8%)
	CYP2E1	P05181.1	101/567 (17.8%)	160/567 (28.2%)
	CYP2F1	P24903.2	90/605 (14.9%)	138/605 (22.8%)
	CYP2J2	P51589.2	106/552 (19.2%)	160/552 (29.0%)
	CYP2R1	Q6VVX0.1	91/599 (15.2%)	150/599 (25.0%)
	CYP2S1	Q96SQ9.2	91/568 (16.0%)	154/568 (27.1%)
	CYP2U1	Q7Z449.1	93/615 (15.1%)	155/615 (25.2%)
	CYP2W1	Q8TAV3.2	112/540 (20.7%)	169/540 (31.3%)
	CYP3A4	P08684.4	95/565 (16.8%)	164/565 (29.0%)
	CYP3A5	P20815.1	102/536 (19.0%)	184/536 (34.3%)
	CYP3A7	P24462.2	92/565 (16.3%)	164/565 (29.0%)
	CYP3A43	Q9HB55.1	97/536 (18.1%)	168/536 (31.3%)
Streptomyces griseus	P450-SOY	P26911.1	147/433 (33.9%)	200/433 (46.2%)
Actinoplanes sp. ATCC 53771	CYP107E4	ACN71221.1	163/419 (38.9%)	216/419 (51.6%)
Labrenzia aggregate	CYP116B4	EAV41564.1	129/819 (15.8%)	189/819 (23.1%)
Bacillus cereus	CYP102A5	Q81BF4	100/1141 (8.8%)	169/1141 (14.8%)
Rhodococcus jostii RHA1	CYP51_RHA1	Q0S7M9	104/481 (21.6%)	176/481 (36.6%)
	CYP105_RHA1	Q0SDH7	144/434 (33.2%)	209/434 (48.2%)
	CYP116_RHA1	Q0RUR9	135/460 (29.3%)	202/460 (43.9%)
	CYP125_RHA1	Q0S7N3	139/429 (32.4%)	207/429 (48.3%)
	CYP256_RHA1	Q0RXF8	131/446 (29.4%)	205/446 (46.0%)
	CYP257_RHA1	Q0RVH0	122/445 (27.4%)	195/445 (43.8%)
	CYP258_RHA1	Q0RUW2	130/451 (28.8%)	194/451 (43.0%)
Sorangium cellulosum So ce56	CYP264A1	CAN96490.1	147/430 (34.2%)	207/430 (48.1%)
	CYP267A1	CAN90832.1	173/453 (38.2%)	235/453 (51.9%)

Whole-cell biotransformation construct – The established pCDF_dFA plasmid[1] (Figure S 1 A) containing the genes for an expression of bovine adrenodoxin (Adx_{4-108}) and Fpr reductase from *E. coli* was optimized with the substitution of the mentioned genes with Fdx8 and FdR_B from *Sorangium cellulosum* So ce56 as described in the materials and methods section. The resulting plasmid was named as pCDF_F8B and is presented in Figure S 1 B.

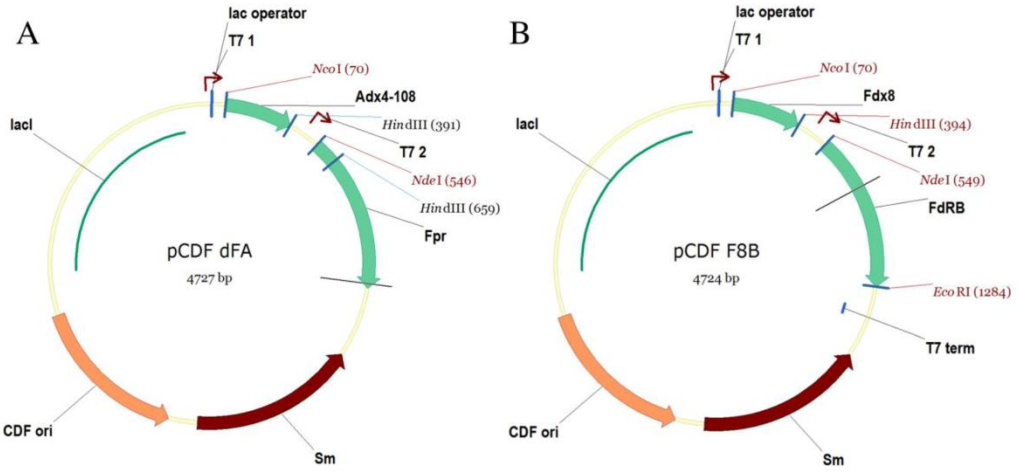

Figure S 1. Vector map of pCDF_dFA plasmid (A) and the optimized pCDF_F8B plasmid (B).

[1] Litzenburger M, Kern F, Khatri Y, and Bernhardt R (2015) Conversions of Tricyclic Antidepressants and Antipsychotics with Selected P450s from Sorangium cellulosum So ce56. *Drug Metab Dispos* **43**:392–399.

HPLC chromatograms of the purified products – To validate the purity of the metabolites produced by the whole-cell system CYP267B1-Fdx8-FdR_B, all purified products were analyzed via preparative HPLC and compared with the respective substrate as presented in Figure S 2.
For **13**, we detected an additional peak at 7 min in the chromatogram of the pure substrate (red line, 11.8 min, Figure S 2 C). As described by Brändström et al. in 1989, omeprazole is able to form a more hydrophilic positively charged intermediate in a reversible chemical equilibrium[2], which explains a second peak (red line, 7 min, Figure S 2 C) in the pure substrate chromatogram.
However, for the purified product **13a**, only a minor amount of the substrate peak at 11.8 min was observed indicating a high purity of the product (blue line, 4 min, Figure S 2 C).

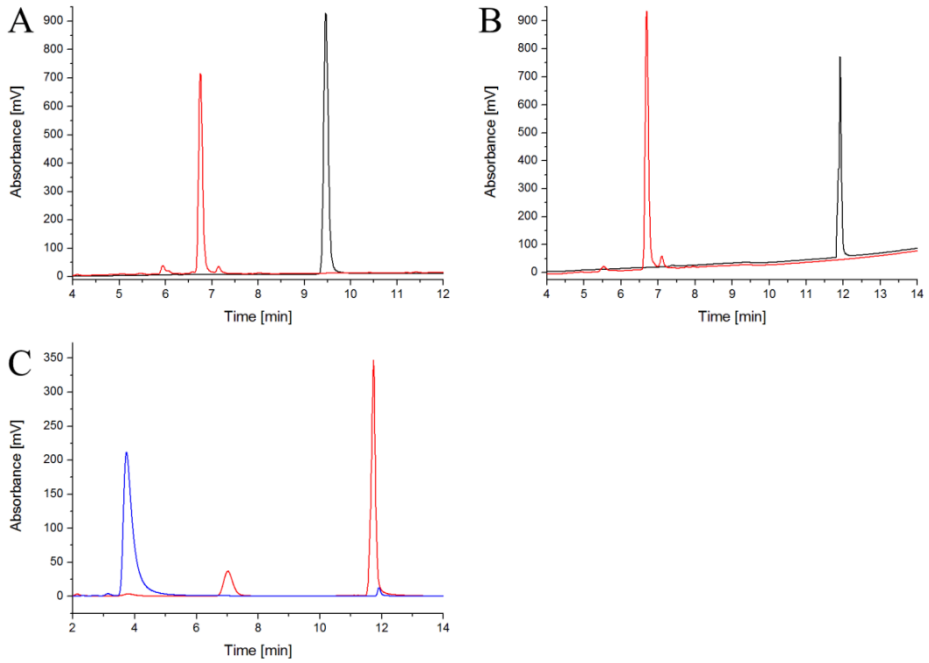

Figure S 2. HPLC chromatograms of the substrates and products. A: diclofenac (**5**, black line), 4-hydroxydiclofenac (**5a**, red line); B: ibuprofen (**7**, black line), 2-hydroxyibuprofen (**7a**, red line); C: omeprazole (**13**, red line) and omeprazole sulfone (**13a**, blue line).

[2] A. Brändström et al. (1989) Chemical Reactions of Omeprazole and Omeprazole Analogues. VI. The Reactions of Omeprazole in the Absence of 2-Mercaptoethanol. *Acta Chem. Scand.* **43**, 595-611

Determination of inhibition of CYP267 family by indole – To validate the necessity to use a defined minimal medium (M9CA) in our whole-cell system, we performed *in vitro* conversions of 200 µM β-ionone with increasing concentrations of indole (Figure S 3). The conditions of this assay were chosen analogous to our previous work[3] with a shorter reaction time of 20 min.

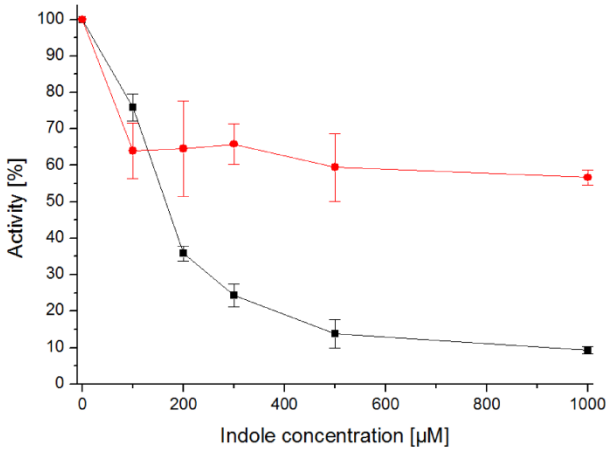

Figure S 3. Inhibition of product formation by increased indole concentration. The data were produced with the conversion of β-ionone. The results of the product inhibition catalyzed by CYP267A1 (black line) and CYP267B1 (red line) in the presence of increasing concentrations of indole is shown.

[3] Litzenburger M, and Bernhardt R (2015) Selective oxidation of carotenoid-derived aroma compounds by CYP260B1 and CYP267B1 from *Sorangium cellulosum* So ce56. *Appl. Microbiol. Biotechnol.* **in press**

NMR data of the purified products 5a, 7a and 13a – The chemical structures of the products (inclusive numbering) are presented in Figure S 4.

4-Hydroxydiclofenac (**5a**):
^{1}H-NMR ($CDCl_3$, 500 MHz): δ 3.63 (s, 2H, CH_2), 6.11 (d, 1H, ArH-3), 6.73 (t, 1H, ArH-5), 6.94 (s, 2H, ArH-3' and ArH-5'), 6.99 (t, 1H, ArH-4), 7.12 (d, 1H, ArH-6).
^{13}C-NMR ($CDCl_3$, 125 MHz): δ 40.43 (C-a), 113.64 (C-3), 115.80 (C-3' and C-5'), 118.92 (C-5), 127.46 (C-4), 128.06 (C-1), 129.10 (C-2), 130.72 (C-6), 132.94 (C-1'), 144.12 (C-2' and C-6'), 155.34 (C-4'), 173.10 (COOH).

2-Hydroxyibuprofen (**7a**):
^{1}H-NMR ($CDCl_3$, 500 MHz): δ 1.19 (s, 6H, H-3), 1.45 (d, 3H, H-b), 2.78 (s, 2H, H-a), 3.65 (q, 1H, H-1), 7.28 (m, 4H, ArH-1 to ArH-4).
^{13}C-NMR ($CDCl_3$, 125 MHz): δ 17.6 (C-3), 27.7 (C-b), 45.0 (C-1), 48.2 (C-a), 71.8 (C-2), 127.2 (C-2', C-6'), 131.3 (C-3', C-5'), 137.3 (C-4'), 138.9 (C-1').

Omeprazole sulfone (**13a**):
^{1}H-NMR (CD_3OD, 500 MHz): δ 1.86 (s, 3H, $ArCH_3$), 1.89 (s, 3H, $ArCH_3$), 3.19 (s, 3H, OCH_3), 3.70 (s, 3H, OCH_3) 4.30 (s, 2H, CH_2), 6.74 (dd, 1H, ArH-6), 6.87 (s, 1H, ArH-4), 7.27 (s, 1H, ArH-7), 7.47 (s, 1H, ArH-13).

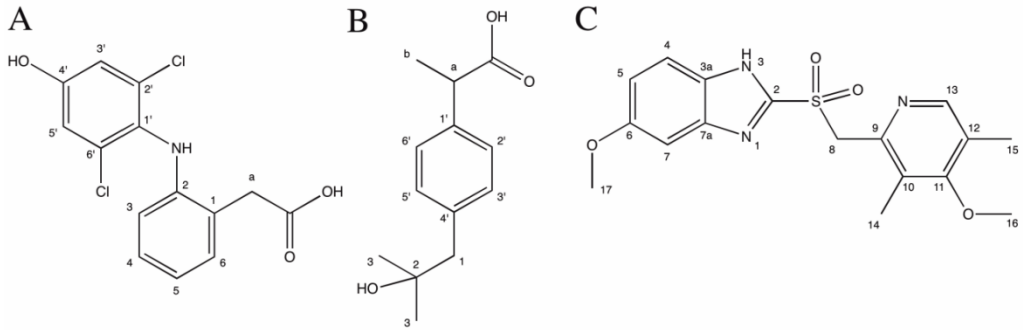

Figure S 4. Chemical formula of 4-hydroxydiclofenac (A), 2-hydroxyibuprofen (B) and omeprazole sulfone (C).

Settings of the MS/MS measurements of omeprazole (13) and omeprazole sulfone (13a) **–** The MS/MS experiments were performed on an API 2000 Qtrap (ABSciex, Darmstadt, Germany) in positive mode (*m/z* 100-400) with a flow rate of 4.0 µL min^{-1} using a syringe pump with ID 4.6 mm. Additional settings are presented in Table S 3.

Table S 3. Detailed settings for the MS/MS measurements of **13** and **13a**.

Name	Value	Name	Value
Curtain Gas (CUR)	20.0 psi	Collision Potential	25 V
Ion Spray Voltage (IS)	5500.0 V	Declustering Potential (DP)	80.0 V
Ion Source Gas 1 (GS1)	25.0 psi	Entrance Potential (EP)	10.0 V
Ion Source Gas 2 (GS2)	0.0 psi	Temperature (TEM)	230.0 C

MS data of omeprazole sulfone (13a) **–** Clear elucidation of product **13a** exclusively by NMR was unsatisfactory since no ^{33}S NMR was measured. We therefore performed MS/MS analysis (Figure S 5**)** and compared the results with the MS/MS spectrum from 5'-hydroxyomeprazole published by Woolf et al.[4] to exclude a hydroxylation of **13** by CYP267B1 in 5' position. The fragmentation of the precursor ion **13a** (*m/z* 362) results in four characteristic fragments, which is related to the fragment pattern published for 5'-hydroxyomeprazole [4]. The characteristic fragment for **13** (*m/z* 198) can be found as *m/z* 214 fragment in the product spectrum of **13a** indicating the insertion of an oxygen (*m/z* +16) to the pyridine part of the compound resulting in $[SO_2\text{-}CH_2\text{-}C_8H_{10}ON]^+$. However, taken the results of the mass spectrometric analysis (precursor *m/z* 362, fragment *m/z* 214) and the NMR data into account, we were able to conclusively assign the product **13a** as omeprazole sulfone.

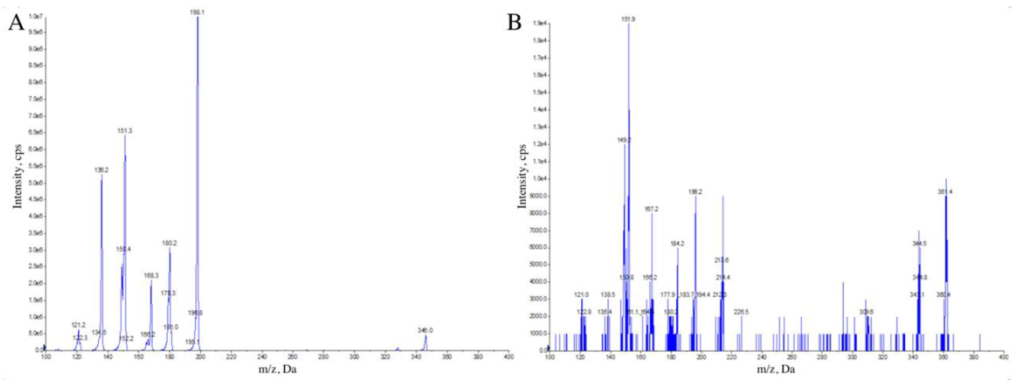

Figure S 5. Positive product ion mass spectra of the protonated substrate omeprazole (**13**, A) and omeprazole sulfone (**13a**, B).

[4] E. J. Woolf, B. K. Matuszewski. (1998) Simultaneous determination of omeprazole and 5'-hydroxyomeprazole in human plamsa by liquid chromatography - tandem mass spectrometry. *J. Chromatogr. A.* **828**, 229-238.

Overview of drugs metabolized by the CYP267 family - A comprehensive overview of the analyzed drugs, and the human metabolites produced by the two members of the CYP267 family, is presented in supplemental Figure S 6.

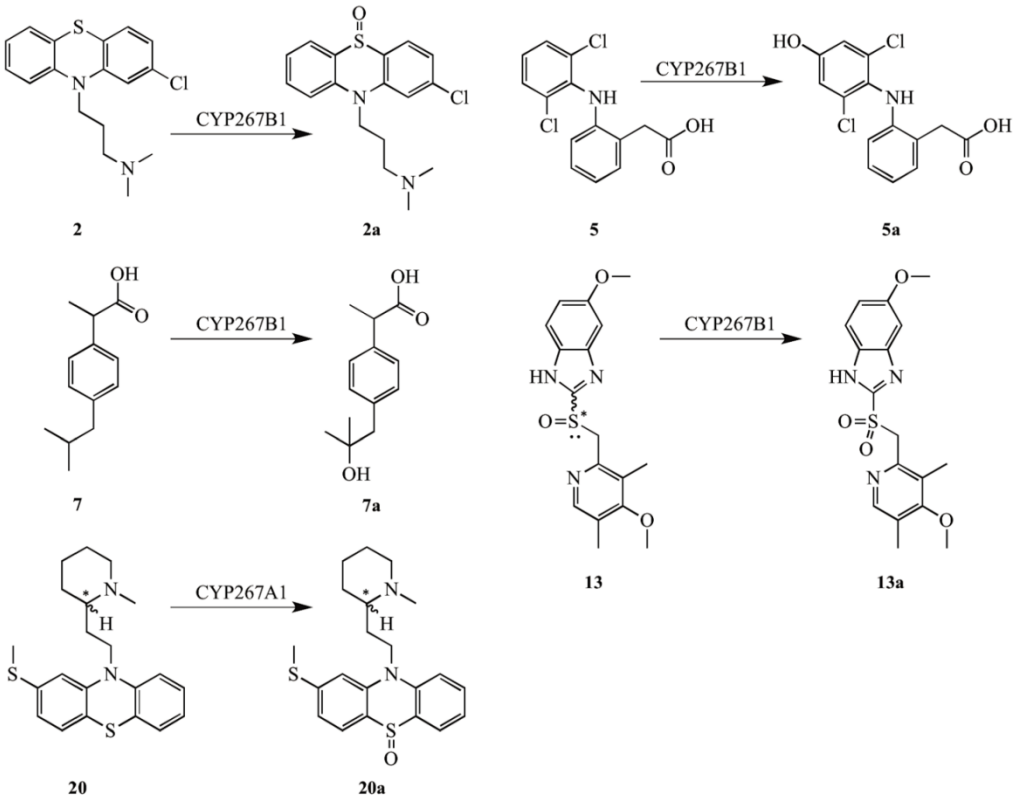

Figure S 6. Overview of drugs converted by the CYP267 family: Conversion of **20** to thioridazine-5-sulfoxide (**20a**) by CYP267A1 and conversion of **2** to chlorpromazine sulfoxide (**2a**), **5** to 4-hydroxydiclofenac (**5a**), **7** to 2-hydroxyibuprofen (**7a**) and **13** to omeprazole sulfone (**13a**) by CYP267B1.

3 Discussion and Conclusions

The aim of this work was the determination of novel substrates for P450s from *Sorangium cellulosum* So ce56 as well as the elucidation of their corresponding products. Hence, several classes of compounds were chosen to test their ability to serve as substrate. The investigation of substrates as well as their products is essential to obtain insights in the substrate range and selectivity of the P450s. In addition, knowledge about substrates is necessary to investigate these P450s in more detail, like for the crystallization in a substrate-bound form, determination of the activity or to test the influence of inhibitors. For that reason, the investigation of substrates as well as their corresponding products is of interest to further characterize these promising P450s. Carotenoid-derived aroma compounds, terpenes, terpenoids, small aromatic compounds as well as drugs are known to serve as substrates for other P450s and, therefore, seem to be a good starting point for finding novel substrates of orphan P450s. Oxygenated products of these compounds are of interest for different kind of applications. Terpenoids may act as flavors and fragrances as shown for the conversion of valencene to the grapefruit flavor nootkatone (Schulz *et al.* 2015) or used as building blocks for the synthesis of chemically and pharmaceutically important compounds (Wang *et al.* 2005). Carotenoid-derived aroma compounds are already applied as material in perfumery and their oxyfunctionalization alters the odor properties as well as the odor threshold as shown for the 3-hydroxy derivatives of α-ionone and their tobacco-like odor (Yamazaki *et al.* 1988). Furthermore, functionalized carotenoid-derived aroma compounds can also be used as precursors for some synthetic routes (Brenna *et al.* 2002). Drugs are predominantly metabolized by liver P450s and their respective metabolites need several safety tests before they can be administered and, as a result, alternative ways for their production are requested by the pharmaceutical industry. A further application for all these products is their utilization as authentic standard to simplify the product characterization for other P450-based conversions.

3.1 Carotenoid-derived aroma compounds as substrates

Many carotenoid-derived aroma compounds (apocarotenoids, norisoprenoids or norterpenoids) used in these studies belong to the most widespread class of C13 norisoprnoids such as ionones (see Figure 7 B [R=H]) and damascones (see Figure 7 A). Synthetic methyl-substituted ionones like n-methyl-α-ionone (see Figure 7 B [R=Me]) and isomethyl-α-ionone belong to the C14 norisoprenoids and are of high importance for the perfumery. On the other side, α-irone is a naturally occurring C14 norisoprenoid, however, its higher price limits the application in perfumery. Additionally, allyl-α-ionone (a synthetic C16 norisoprenoid, see Figure 7 B [R=allyl])

was tested in our studies, a compound of less importance for the flavor and fragrance industry, though, its sterically demanding side chain gives more insights into the substrate diversity of the myxobacterial P450s. As shown in the supplemental data (4.1.1.1), several more P450s from So ce56, as published in 2.3, were tested for their conversions of the selected apocarotenoids. Interestingly, CYP109C1 is the only P450, which is not converting any of these compounds. All remaining P450s convert at least one compound, albeit in low amounts. This class of substrates might be structurally similar to some of their natural substrates, which are not known yet. However, it is described that So ce56 contains a putative carotenoid gene cluster and, hence, there is a strong probability that the P450s are exposed to carotenoids as well as their corresponding degraded products (Schneiker *et al.* 2007). Another explanation might be the structural valuable properties of these compounds. Such molecules can access the active site of most P450s, due to their small size. Furthermore, they possess several functional groups such as the α-,β-unsaturated ketone and the cyclohexene moiety (see Figure 7 A and B), which enable diverse docking positions. Moreover, the rigid side chain and more flexible ring structure might simplify the correct substrate orientation turning such compounds into promising substrates. Previous studies with myxobacterial P450s have shown that the amino acids of the active site form a hydrogen bond with the keto-group of the substrate (either His94 for CYP109D1 or Thr285 for CYP264B1), whereby the required substrate orientation is created (Khatri *et al.* 2010a; Ly *et al.* 2012). However, the alignment of the most valuable P450s tested in this study (CYP260B1 and CYP267B1) with CYP264B1 and CYP109D1 do not show high sequence identities. There is only a maximum of 33% and the corresponding residues are not highly conserved in these myxobacterial P450s (see supplemental 4.1.1.3 and 4.1.1.4). As a result, the sequences of these P450s cannot be taken into account and separate homology models need to be created. In the case of CYP260B1, the substrate-free crystal structure will be available soon and docking studies might give details about the amino acids involved in the substrate orientation.

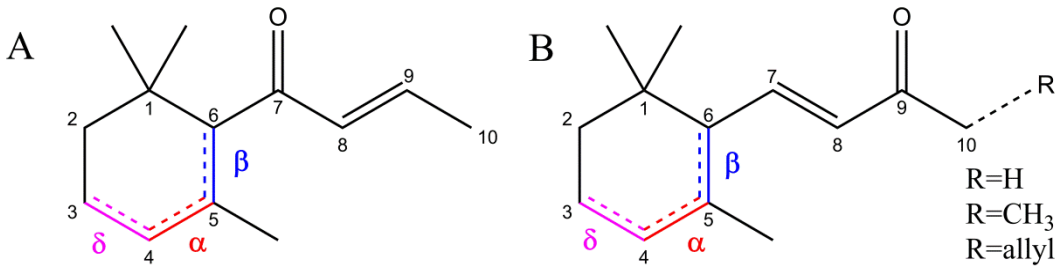

Figure 7: Structures and numbering of damascones (A) and ionones (B). The location of the double bond is represented by a greek letter (as shown in red, blue and magenta).

CYP260B1, CYP264A1 and CYP267B1 are capable of the conversion of all tested norisoprenoids. However, only CYP267B1 showed a high selectivity for nearly all tested compounds towards a single product. In contrast, CYP260B1 showed the highest yields of all P450s during this study but a high selectivity was just achieved towards β-ionone, β-damascone and δ-damascone. CYP264A1 showed the lowest yields and selectivities out of these three P450s and was, therefore, not further investigated.

The steric of the side chain in position 6 influences the conversion significantly as shown for the methyl-substituted compounds being less converted than their non-substituted counterparts (see supplemental 4.1.1.1). Allyl-α-ionone (see Figure 7B [R=allyl]) demonstrates this observation even better, since most of the P450-dependent conversions show only traces of products. This compound is only converted by CYP260B1 and CYP267B1 in higher amounts. As a result, CYP260B1, CYP267B1 as well as CYP267A1 (known for its conversion of sterically demanding compounds like thioridazine) were chosen for the conversion of retinol (vitamin A1). This sterically more demanding compound (polyunsaturated side chain at position C6) is not converted by any P450 indicating the sensitivity of the P450s towards the length of the side chain. Besides the steric effects, the location of the keto group influences the conversion as shown for the damascones (see Figure 7 A). CYP109C2, for example accepts only compounds with a keto-group at position C7 as substrate. In contrast, most of the tested P450s prefer the substrates of the ionone-type with a keto-group at position C9 (see supplemental 4.1.1.1). An increased distance between the keto moiety and the ring seems to facilitate the correct substrate orientation, since all known products show an endocyclic oxyfunctionalization. Most myxobacterial P450s showed the hydroxylation at allylic position as main catalytic activity (data not shown). Such hydroxylations are preferred by many P450s, since C-H bonds in this specific position are very reactive caused by their low bond-dissociation energy (Ortiz de Montellano 2010). The endocyclic epoxidation of β-ionone as main catalytic activity of CYP260B1 is thereby an exception. Those epoxy-products are not of high interest for biotechnological applications, since the corresponding compounds are easily formed by autoxidation processes under light exposure (Gagarina *et al.* 1984) or by chemical synthesis with mCPBA (*meta*-chloroperoxybenzoic acid) (Barakat *et al.* 2008). However, the question about the factors effecting the allylic hydroxylation versus the epoxidation of the double bond is not clarified in detail and still topic of researches (de Visser *et al.* 2002; Ilie *et al.* 2015). CYP260B1 catalyzes both reactions, hydroxylation and epoxidation, whereby the epoxidation is formed predominantly. Further studies about the substrate orientation of β-ionone in CYP260B1 as well as protein engineering towards a high selectivity of a certain reaction type might give deeper insights in this topic. Moreover, to the best of our knowledge, this is the first report of a specific P450 capable of the

epoxidation of an ionone-type structure (see Figure 8, right side), even $P450_{BM3}$ mutants are not known for this type of reaction towards α- and β-ionone (Watanabe *et al.* 2007).

Taken together, the myxobacterial P450s from So ce56 represent a promising tool for the oxyfunctionalization of carotenoid-derived aroma compounds. Figure 8 shows a toolbox towards the selective oxyfunctionalization of β-ionone. CYP109D1 and CYP267B1 form the endocyclic allylic alcohol, CYP260B1 forms predominantly the epoxy product and CYP264B1 forms the 3-hydroxy product.

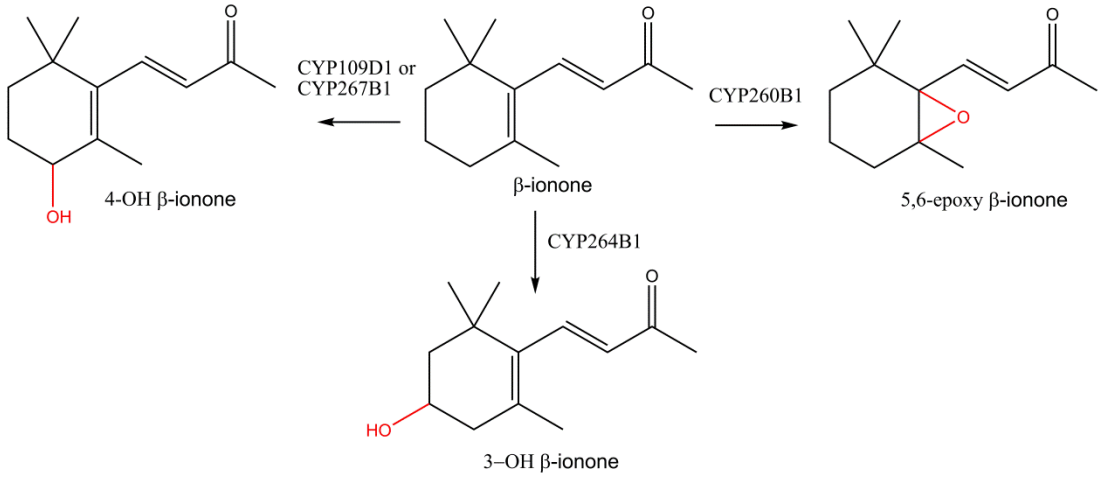

Figure 8: Toolbox of myxobacterial P450s towards the selective oxyfunctionalization of β-ionone. The 3-OH-β-ionone and 4-OH-β-ionone products formed by CYP264B1 and CYP109D1 were identified in previous studies by our group (Khatri *et al.* 2010a; Ly *et al.* 2012).

3.2 Terpenes and terpenoids as substrates

Terpenes and terpenoids represent the largest class of natural products with over 40,000 known compounds (Withers and Keasling 2007). Most of them were isolated from plants but also from animals and microorganisms. They are classified as primary metabolites necessary for cellular functions and maintenance as shown for gibberellins, carotenoids and sterols as well as secondary metabolites known for their use as flavor and color enhancers, agricultural chemicals or pharmaceuticals (Roberts 2007; Rasool and Mohamed 2015). Their selective oxyfunctionalization is difficult to achieve with chemical syntheses caused by the complex structure of the substrates and the resulting low regio-, and stereoselectivity. The involvement of P450s in the biosynthesis of terpenoids is already studied for several mono- and sesquiterpenes, thus, P450s are an efficient alternative for the production of oxygenated terpenes (Weitzel and Simonsen 2015). Employing plant P450s for such an approach has the advantage that the natural

P450 capable of the desired reaction is used. However, the membrane-anchor of these P450s needs to be removed to solubilize them and to simplify, therefore, their expression in prokaryotes (Pateraki *et al.* 2015). Bacterial P450s represent a valuable substitute concerning their solubility and higher activity. There are several examples of terpenoids produced by bacterial P450s such as camphor, vitamin D3 or pravastatin (Janocha *et al.* 2015). In our studies, two P450s were investigated with four different sesquiterpene structures of the eremophilane-, humulane-, caryophyllane- and cedrane-type (see 2.2). CYP264B1 was chosen because of its function as terpene hydroxylase and CYP260A1 was selected, since it is known for the conversion of nootkatone (Ewen *et al.* 2009; Schifrin *et al.* 2015). Interestingly, CYP260A1 accepts only oxygenated compounds as substrates, whereas CYP264B1 accepts all kinds of substrates. CYP264B1 is located close to a terpene synthase in the genome of So ce56 and its natural function is the hydroxylation of eremophilene (Schifrin *et al.* 2015). Thus, it is not surprising that non-oxygenated compounds act as substrates. Furthermore, CYP264B1 shows a higher selectivity towards a single main product compared with CYP260A1, which is capable of the formation of a variety of products. The main products formed by CYP264B1 were identified as compounds predominantly hydroxylated in allylic position. In contrast, CYP260A1 did not show a main reaction type; hydroxylation, epoxidation and reduction of the double bond were identified, whereby the reduction may be caused by a consecutive reaction formed by enzymes from *E. coli.* Taken together, CYP264B1 is a potent enzyme for the oxyfunctionalization of terpenes and CYP260A1 might be a promising candidate for the introduction of additional oxygen atoms into terpenoids.

Besides CYP260A1 and CYP264B1, several other myxobacterial P450s were tested with the terpenes τ-muurolol and β-phellandrene, whereby some of them were able to convert these substrates (see supplemental 4.1.2). However, none of the P450s showed a high selectivity towards a single main product and hence, the products were not available in sufficient amounts for structure elucidation. In addition, CYP267A1 and CYP267B1 were tested for their ability to convert nootkatone. The *in vitro* reactions showed that CYP267A1 was capable of the production of a single compound, whereas CYP267B1 formed predominantly two main products. However, the corresponding products were not scaled up by the utilization of the whole-cell system nor identified due to the time limit of this work. Nevertheless, those examples indicate the potential of the myxobacterial P450s to act as terpene/terpenoid oxidase and these first results might serve as good starting point for further experiments towards this large class of substrates.

3.3 Drugs as substrates

Drugs are mainly metabolized in the liver by diverse P450s, whereby CYP1A2, CYP2C9, CYP2C19, CYP2D6, and CYP3A4 play the most important roles. Studies about the excretion of the drugs and the formation of metabolites are essential for the development, establishment and approval of novel drugs. Furthermore, drug metabolites formed greater than 10 % at steady state or total drug exposure need to be investigated in toxicological tests according to the Food and Drug administration or European Medicines agency guidelines, respectively (FDA 2008; ICH 2009). To obtain sufficient amounts of metabolites for such tests, efficient ways for the selective production of certain metabolites are requested. Liver P450s can be applied for this purpose but they are often capable of the formation of a variety of compounds. Furthermore, the activities and expression levels of mammalian P450s are often limited in a reconstituted system. In contrast, bacterial P450s have the benefits of a high activity and high expression levels. Moreover, the solubility and high stability simplifies their handling for biotechnological applications (Bernhardt 2006). Hence, there are several reports of bacterial P450s performing the production of specific drug metabolites, whereby $P450_{BM3}$ represents the best studied one (Julsing *et al.* 2008; Fasan 2012; Whitehouse *et al.* 2012; Kang *et al.* 2014; Kulig *et al.* 2015; Ren *et al.* 2015). Myxobacterial P450s are known to be involved in the formation of secondary metabolites of structurally complex compounds such as epothilones and might, therefore, act as drug metabolizers. For that reason, several classes of drugs, which are known to be converted by mammalian P450s, were chosen (see 2.4 and supplemental 4.1.4) for an initial *in vitro* screening, since spin shift experiments are often not significant because nitrogen containing compounds often lead to a type-II shift besides acting as substrate (Locuson *et al.* 2007). During the *in vitro* experiments, the CYP267 family, CYP260A1 and CYP264A1 were identified as potential drug metabolizers. The CYP267 family represents the most promising P450s with a very high substrate range, however, their activity is low and, therefore, the product identification is hindered (see 2.1 and 2.4). Likewise, CYP260A1 acts as drug metabolizer but its activity is also very low towards most of these compounds. On the other hand, CYP264A1 showed higher yields towards the conversion of some tricyclic psychotherapeutics. Since 4-methyl-3-phenyl-coumarin (also a tricyclic compound) was known so far as sole substrate, it seems that this P450 prefers cyclic compounds as substrate. To verify this assumption, several other tricyclic antidepressants and antipsychotics as well as their corresponding precursors were tested (see 2.1). Some of these compounds were converted by CYP264A1, whereby the side chain plays an important role. The dimethyl-amino-propyl group seems to be necessary for an efficient conversion, since the precursors lacking the side chain were not converted in higher amounts. Promethazine possessing a dimethyl-amino-isopropyl side chain is also not converted, verifying the high

sensitivity of CYP264A1 towards the side chain of these compounds. Besides the typical production of more hydrophilic compounds, CYP260A1 was capable of the formation of several compounds more hydrophobic than the substrate. One of the products formed by the conversion of promethazine showed the same retention time as phenothiazine leading to the assumption that the side chain was degraded or cleaved, respectively. A dealkylation of the side chain of such drugs is to the best of our knowledge not described yet. However, this product was not obtained in higher amounts by the whole-cell system, so that the product identification was not verified by NMR spectroscopy and further analyses by HRMS or MS^n-experiments are necessary to characterize the product in detail.

Other groups also tried to find bacterial drug metabolizing P450s besides $P450_{BM3}$. For example, Kulig *et al.* fused diverse P450s from *Rhodococcus jostii* RHA1 with the P450 reductase domain (RhfRED) of cytochrome $P450_{Rhf}$ from *Rhodococcus* sp. NCIMB 9784 and tested them as drug metabolizers. One fusion protein, named Ro07-RhfRED, showed a demethylation activity towards imipramine and related compounds and might be used to produce the corresponding demethylated metabolites (Kulig *et al.* 2015). Interestingly, CYP264A1- and CYP267B1-dependent reactions achieved the 10-hydroxy derivatives of imipramine and some of its analogs. Additionally, CYP267A1 was able to convert the sterically more demanding thioridazine, albeit in lower amounts. The regioselectivity is, thereby, the same for CYP267A1, CYP267B1 and CYP264A1, since all tested P450s functionalized the middle ring. CYP264A1 was capable of the production of these metabolites in a milligram per liter scale during the whole-cell processes, whereas CYP267B1-dependent conversions showed considerably lower yields. However, optimizations of the whole-cell systems led to higher yields for the CYP267 family (see 2.4) but further improvements like protein engineering are required to apply these P450s for biotechnological applications. Nevertheless, these examples substantiate the potential of bacterial P450s for the production of specific drug metabolites.

3.4 Establishment of a whole-cell system for myxobacterial P450s towards a preparative scale

The whole-cell system previously developed by our laboratory enables the production in a more preparative scale and is suitable for some of the myxobacterial P450s (Ringle *et al.* 2013). However, our studies demonstrated that further improvements for several P450s are needed to produce sufficient amounts of products for structure elucidation via NMR spectroscopy. Furthermore, a higher productivity towards a preparative scale of several hundred milligrams per liter is requested for biotechnological processes. To reach such a goal, several optimization strategies can be applied, whereby improvements can be performed by altering the properties of the proteins as well as changing the conditions of the whole-cell system.

3.4.1 Improvements of the gene expression, P450 activity and electron transfer

Since we are working with wild type enzymes, protein engineering would be a good starting point to optimize the productivity. Site directed mutagenesis and laboratory evolution are very common methods to improve the properties of P450s (Gillam 2008). Wild type enzymes often show a low activity towards their non-natural substrates and, therefore, optimizations towards their activity are essential for biotechnological relevant processes. Furthermore, improvements concerning the regioselectivity and reaction type would be necessary for some of the myxobacterial P450s. CYP260B1 for example, is very unselective for several norisoprenoid substrates (see 2.3) and improvements towards a higher selectivity are necessary to produce a single compound. The crystal structure of this P450 will be available soon and as a result, site directed mutagenesis might be the most promising approach to achieve a higher selectivity. The crystal structures of CYP260A1 and CYP109D1 are also close to be finished, however, resolving the crystal structures of the other P450s is not in progress yet. Nevertheless, computer aided mutagenesis approaches or laboratory evolution can be used for proteins, whose three-dimensional structures are not known. Low concentrations of the corresponding P450 in the whole-cell system might also be critical, whereby altering the cells lines or expression plasmids can lead to higher expression levels of the P450s (Zelasko *et al.* 2013). Additionally, the genes encoding the P450 might be improved by codon optimization, which was already successfully done for CYP264B1, leading to an improved expression level (Schifrin *et al.* 2015). The availability of sufficient amounts of the cofactor might be another problematic issue, especially for conversions with a lower coupling efficiency. The expression of a dehydrogenase capable of the recycling of NAD(P)H can, therefore, lead to an increased product formation (Schewe *et al.* 2008). Furthermore, the efficiency of the redox partners need to be optimized for each P450

individually, since not all P450s prefer the same redox partners as shown for CYP267B1 and CYP260A1. CYP267B1 shows a higher efficiency with the natural electron transfer partners Fdx8 and Fdr_B, whereas CYP260A1 prefers the heterologous redox partners Adx_{4-108} and AdR (Ewen *et al.* 2009; Khatri *et al.* 2010b; Kern *et al.* 2015). The influence of the electron transfer partners was also demonstrated for the CYP21A2-dependent whole-cell process for the production of premedrol by our labrartory (Brixius-Anderko *et al.* 2015). As a result, the selection of redox partners is a critical factor for the optimization of a whole-cell system. Furthermore, the electron transfer from the ferredoxin to the P450 is known as rate limiting step in the electron transport chain and the expression of additional ferredoxin by introducing two or more copies of the ferredoxin cDNA into the plasmid can lead to improved yields (Ewen *et al.* 2012; Schiffer *et al.* 2015b).

3.4.2 Improvements of the conditions for the whole-cell system

The substrate uptake of the cells is often a limiting step in the establishment of a whole-cell system. Cell permeabilizing compounds like EDTA, polymyxin B, toluol, Tween 20 or CTAB (N-cetyl-N,N,N-trimethylammonium bromide) can be applied to ensure the substrate availability in the cells (Janocha and Bernhardt 2013). This problem was also shown for the conversion of the tricyclic drugs, which was solved by the addition of EDTA increasing the substrate availability (see 2.1). Another common issue in *E. coli* based whole-cell systems is the occurrence of indole, an inhibitor for many P450s as shown for CYP267A1 and CYP267B1 (see 2.4). In *E. coli*, the enzyme tryptophanase produces indole from tryptophan decreasing the efficiency of biocatalytic P450 processes dramatically (Li and Young 2013). For that reason, complex media are often not suitable for *E. coli* based whole-cell systems harboring P450s. There are two common approaches to overcome this problem by either using medium, which only contains a minimum of tryptophan, or applying resting cells in buffer. As shown in 2.1, both approaches enable the production of the drug metabolites, however, there are significant differences in the productivity of both systems. A close correlation between the tested P450s and the conversion of the compounds was not observed. Hence, the application of resting cells in buffer or growing cells in medium need to be tested for each system individually. An additional bottleneck for P450-based bioconversions is the solubility of the substrates caused by their strong hydrophobic character. Several solvents like ethanol, DMSO or derivatives of β-cyclodextrin (complexing of substrates) might be tested for their influence on the conversion (Schulz *et al.* 2015). Furthermore, a biphasic system consisting of water containing the cells and a layer of organic solvent as reservoir for the substrates can be used. Thereby, the organic phase allows the accumulation of oxygenated products and hinders overoxidation. Moreover, inhibitory and toxic effects of the substrates as

well as products are minimized in a biphasic system. The efficiency of such an approach was already demonstrated for the conversion of terpenes and steroids (Girhard *et al.* 2009; Braun *et al.* 2012). Besides all these examples, there are several additional bottlenecks for the development and implementation of a whole-cell system. A recently published review by Lundemo and Woodley describes the most common challenges and solutions for the establishment of whole-cell P450 catalyzed reactions in more detail (Lundemo and Woodley 2015).

3.5 Potential natural functions

In this study, compounds out of different classes of substrates such as apocarotenoids, sesquiterpenes, aromatic compounds and drugs were tested with nine of the myxobacterial P450s. Thereby, we found ionones, damascones, cedrenol, zerumbone, cinnamaldehyde as well as several drugs such as the tricyclic psychotherapeutics as novel substrates for some of the P450s. Moreover, we identified several products and got a first overview of the substrate ranges and selectivities for these P450s (see Table 1) leading to some speculations about their physiological roles.

The CYP109 family consists of three members, which are clustered with carbohydrate-metabolism related genes (CYP109C1), regulatory elements (CYP109C2) or unique proteins (CYP109D1), respectively (Khatri *et al.* 2011). These P450s are known for the binding and conversion of fatty acids and, in addition, CYP109D1 is known for the conversion of α- and β-ionone (Khatri *et al.* 2010a; Khatri *et al.* 2013). Due to their low substrate range, it is not surprising that for CYP109C1 no novel substrates were found, for CYP109C2 only damascones act as substrate and just CYP109D1 converted several carotenoid-derived aroma compounds as well as cinnamaldehyde. CYP109B1 from *Bacillus subtilis* revealed also a small substrate range, since only fatty acids, ionones, indole and nootkatone were identified as substrates (Girhard *et al.* 2010). This observation indicates that the CYP109 family seems to have a specific function in the metabolism of a certain compound and might not be capable of the degradation of xenobiotics. Thereby, the preference towards small cyclic compounds and fatty acids of the CYP109 family might lead to the conclusion that they are involved in the biosynthesis of such compounds.

The CYP260 family shows a much broader substrate diversity, ranging from terpenoids (see 2.2) and apocarotenoids (see 2.3) to drugs (see 2.1 and supplemental 4.1.4) and steroids (Khatri *et al.* 2015). However, all compounds need to be oxygenated to act as substrate for this family as shown during all studies. Interestingly, besides belonging to the same family, both P450s differ very much in their substrate range. CYP260B1 converts apocarotenoids with a high yield,

whereas CYP260A1 produces only low amounts of products. In contrast, CYP260A1 is more potent towards drugs, albeit the activity is very low. The aromatic compound cinnamaldehyde is converted by CYP260B1 producing the corresponding acid, whereas CYP260A1 only shows a very low activity towards this compound. The formation of cinnamic acid out of cinnamaldehyde is an uncommon reaction, since the structurally similar apocarotenoids are oxygenated at the ring moiety by CYP260B1. This reaction also occurs after the exposure to air and during all conversions, low amounts of cinnamic acid were detected. However, CYP260B1 converted most of the aldehyde to the acid and we presumed that the formation of hydrogen peroxide might be responsible for the reaction. However, the addition of H_2O_2 to the reaction mixture did not result in a conversion, disproving the assertion of a H_2O_2-driven reaction. Furthermore, cinnamyl alcohol, also known for its autoxidation (Niklasson *et al.* 2013), did not show any product formation verifying that the reaction is H_2O_2 independent. Spectral analyses showed a typical type-I shift for the aldehyde, whereas the alcohol and the acid did not show any shifts (data not shown). Therefore, this reaction is of interest for studying the interaction between the amino acids of the active site and the moieties of the substrate. The crystal structures of CYP260A1 and CYP260B1 will be available soon and docking studies of cinnamylaldehyde might give more details about this uncommon reaction. The comparison of the interactions of cinnamaldehyde, the apocarotenoids as well as some of the drugs with both P450s might identify the differences in the SRSs of this family and, therefore, their diverse substrate range. The physiological roles of the CYP260 family might be related to the degradation of xenobiotics due to their broad substrate range. Moreover, they could be involved in the functionalization of secondary metabolites. Since only oxygenated compounds are accepted as substrates, the functionalization would be more probably in a late state of the biosynthesis.

The CYP264 family consists of two members, CYP264A1 and CYP264B1, which show a diverse substrate range. CYP264B1 is clustered to a terpene synthase in the genome of So ce56 and hence, its natural function is presumed as terpene hydroxylase (Khatri *et al.* 2011). Previous studies by our laboratory proved this assumption by identifying CYP264B1 as efficient hydroxylase for the sesquiterpene (+)-eremophilene (Schifrin *et al.* 2015). The conversion of further sequiterpenes based on eremophilane, humulane, caryophyllane and cedrane resulted predominantly in a main product hydroxylated in allylic position as well as some unknown side products (see 2.2). In contrast, the physiological role of CYP264A1 is not known and cannot be hypothesized, since it is clustered in open reading frames (ORFs) encoding hypothetical proteins (Khatri *et al.* 2011). During previous studies, only a derivative of coumarin was identified as substrate (Ringle *et al.* 2013). In this study, several novel substrates such as tricyclic drugs and apocarotenoids were identified (see 2.1 and supplemental 4.1.1.1). Only cyclic compounds seem

to act as substrate for this enzyme, whereby tricyclic compounds showed a higher selectivity towards a single main product. Homocyclic and heterocyclic compounds are both accepted by this P450 and hydroxylation as well as sulfoxidation is observed as catalytic activity towards the tricyclic drugs. In contrast, CYP264B1 did not show any activity towards the tricyclic drugs, although, having a similar size than sesquiterpenes. The low flexibility of the aromatic rings in the drugs might hinder the binding and, therefore, the conversion compared to the non-aromatic terpene structures possessing a more flexible structure. Interestingly, all tested carotenoid-derived aroma compounds were converted by CYP264A1, whereby β-damascenone showed the highest yields. This observation shows the preference of CYP264A1 towards cyclic substrates with a less flexibility leading to the assumption that CYP264A1 is involved in the biosynthesis of cyclic or particularly tricyclic compounds with a rigid structure.

The CYP267 family showed the widest substrate range of all tested myxobacterial P450s and is, therefore, a promising enzyme family for different kinds of biotechnological approaches. The tested substrates range from structurally diverse drugs (see 2.1 and 2.4) to simple structures like the carotenoid-derived aroma compounds (see 2.3). Although showing a broad substrate range and high selectivity, these family members show a quite low activity towards most of the substrates. Thereby, CYP267B1 converts more substrates and shows a higher activity compared to CYP267A1. Nearly all tested apocarotenoids are converted to the allylic alcohols by CYP267B1, whereas CYP267A1 did not show high activities and selectivities towards most of these compounds. Interestingly, CYP267A1 was capable of the sulfoxidation of thioridazine, a sterically more demanding compound that was not converted by CYP267B1. However, another study by our laboratory identified epothilone D as substrate for CYP267B1 indicating that both enzymes have the ability to convert sterically more demanding compounds (Kern *et al.* 2015). Thus, this family is capable of the conversion of small (like ionones and damascones) and large molecules (like thioridazine or epothilone D) as well as structurally diverse compounds (see 2.4) making it difficult to assume about the physiological role. Moreover, the diverse reaction types such as aliphatic hydroxylation, aromatic hydroxylation, alcohol oxidation and sulfoxidation do not give a hint about their natural functions (see 2.1, 2.3 and 2.4) (Kern *et al.* 2015). In the genome, CYP267A1 is clustered with carbohydrate-metabolism related genes, so its natural function might be bound up with using different carbon sources for growth. In contrast, CYP267B1 is clustered with some hypothetical proteins, which does not give any clue about its physiological role (Khatri *et al.* 2011). However, such a broad substrate range and variety of reaction types might indicate that these P450s are involved in the degradation of xenobiotics similar to the liver P450s CYP3A4 or CYP2D6. Interestingly, there is only a low number of bacterial P450s showing a similar broad substrate range like $P450_{BM3}$ or CYP116B4 from *Labrenzia aggregata* (Whitehouse *et al.* 2012; Yin

et al. 2014). These specific properties turn this family into promising biocatalysts for the development of biotechnological processes.

Table 1: Investigated myxobacterial P450s, their substrate range, novel substrates identified in this study as well as their performed reaction types.

P450	Substrate range	Novel substrates found during this work	Main reaction types
CYP109C1	No substrate known	-	-
CYP109C2	Small cyclic compounds	Damascones	n.d.
CYP109D1	Small cyclic compounds	Derivatives of ionones, damascones as well as cinnamaldehyde	Allylic hydroxylation
CYP260A1	Oxygenated compounds	Oxygenated drugs and sesquiterpenes	Hydroxylation, epoxidation
CYP260B1	Oxygenated compounds	Ionones and derivatives of them, damascones as well as cinnamaldehyde	Hydroxylation, epoxidation, aldehyde oxidation
CYP264A1	Cyclic compounds	Ionones and derivatives of them, damascones as well as tricyclic drugs	Hydroxylation, sulfoxidation
CYP264B1	Terpenes and terpenoids	Ionones and derivatives of them as well as damascones	Allylic hydroxylation
CYP267A1	Drugs, terpenes, terpenoids and apocarotenoids	Ionones and derivaties of them, damascones, diverse drugs, terpenes and terpenoids	Allylic hydroxylation, sulfoxidation
CYP267B1	Drugs, terpenes, terpenoids and apocarotenoids	Ionones and derivaties of them, damascones, diverse drugs, terpenes and terpenoids	Aliphatic and aromatic hydroxylation, allylic hydroxylation, sulfoxidation

Taken together, several classes of potential substrates for the myxobacterial P450s were screened in this work. Those systems showing a highly selective *in vitro* conversion towards a single main product were scaled up in an *E. coli* based whole-cell system and the purified products were analyzed by NMR spectroscopy. During these studies, apocarotenoids were identified as substrates efficiently converted by CYP260B1, CYP264A1 and CYP267B1, whereby several products of the CYP260B1- and CYP267B1-dependent conversions were characterized. CYP267B1 showed the typical allylic hydroxylase activity, whereas CYP260B1 showed an additional epoxidase activity towards some of the tested compounds. Such an epoxidase activity towards β-ionone as well as the methyl-substituted derivatives of α-ionone is to the best of our knowledge not known for any specific P450. Moreover, some novel products such as 2-OH-δ-damascone, 3-OH-allyl-α-ionone and 4-OH-allyl-β-ionone were identified. Aromatic compounds (see supplemental 4.1.3) were also tested in this study but did not serve as substrates for most of the P450s. Cinnamaldehyde was the only compound out of this class, which acts as substrate for CYP109D1 and CYP260B1, whereby the activity of CYP109D1 was too low to characterize the corresponding product. In contrast, the product formed by CYP260B1 was obtained in sufficient amounts for NMR analysis and thereby, elucidated as cinnamic acid. Furthermore, several structural diverse drugs were tested as potential substrates, whereby CYP260A1, CYP264A1, CYP267A1 as well as CYP267B1 were identified to act as drug metabolizers. CYP260A1 accepted only oxygenated drugs as substrates but its activity was too low to characterize the corresponding products. However, the comparison of the retention times with phenothiazine as standard gave a first clue about the possible degradation of the side chain of promethazine. Additionally, the CYP267 family was identified as highly versatile drug metabolizers. Moreover, CYP264A1 converted the tricyclic psychotherapeutic drugs amitriptyline, clomipramine, chlorpromazine and imipramine in a milligram per liter scale. Thereby, the same metabolites as those formed by human liver P450s were obtained. This was the first report about the production of pharmaceutically important compounds by a myxobacterial P450 from So ce56. The largest class of substrates tested in this study belongs to the terpenes and terpenoids. The sesquiterpenes cedrenol and zerumbone were identified as novel substrates for CYP260A1. The selectivity of this P450 was not high, however, several new products were characterized. Moreover, some other terpenes and terpenoids such as nootkatone, τ-muurolol or β-phellandrene were identified as substrates for CYP267A1 and CYP267B1. The products were not elucidated during this study due to the time limit of this thesis, nevertheless, this preliminary work might serve as good starting point for further studies.

3.6 Outlook

The obtained results demonstrate the substrate range and catalytic activity of the selected myxobacterial P450s. During this work, 9 out of the 21 P450s from So ce56 were investigated, whereas the remaining 12 P450s are still not characterized. Most of the latter ones show a low expression rate and hence, the expression and purification of these P450s is not efficient. Increasing the expression rate by optimization of the expression conditions or the change to a pET-system might lead to sufficient amounts of pure protein for further characterization. These unknown P450s may also reveal unique and novel activities. A high throughput screening towards a ligand library checking the spectral shifts would be helpful to identify potential substrates for these P450s as demonstrated for CYP260A1 (Khatri *et al.* 2015). New P450s with novel properties are valuable as shown for their increasing importance in the field of biotransformation (Meyer *et al.* 2013).

Some of the products identified in this study are of biotechnological interest such as the drug metabolites or the functionalized apocarotenoids, however, the optimization of the whole-cell system towards a preparative scale is required. Drug metabolites are often used in toxicological tests or as authentic standard for analytical studies, whereby amounts from a low milligram to gram scale are needed. Fine chemicals such as the functionalized apocarotenoids are used as building blocks and, therefore, amounts in a gram scale are required. To achieve this goal, optimizations like protein engineering or exchange of the redox partners are necessary. Higher amounts of products would enable diverse synthetic routes or chemoenzymatic approaches for the development of novel compounds with altered characteristics. Nevertheless, the already obtained products might be applied for some further characterization like testing the odor properties of the apocarotenoid-products, which only requires a few milligrams of substance.

The identified substrates can also be used to characterize the P450s in more detail. Crystallization of the P450s in a substrate-bound form will now be available for several more P450s. The structural analyses would give detailed insights in the active sites of the P450s. The crystallization of the CYP267 members with structurally diverse substrates would be of high interest, since these P450s show a broad substrate range. Such an approach might be useful to explore the flexibility of the active site as well as the SRSs. Another interesting issue would be the crystallization of CYP260B1 with β-ionone as substrate. The crystal structure may be used to identify the amino acids and docking positions responsible for the reaction type. Site directed mutagenesis of these specific amino acids could help to investigate the question about the factors influencing the epoxidation versus the allylic hydroxylation.

Furthermore, testing several more substrates or substrate classes may identify some more interesting reactions and products. Some terpenes and terpenoids were already tested in this study, however, their corresponding products were not elucidated due to the time limit of this thesis. These initial tests identified activities of the CYP267 family members towards nootkatone, τ-muurolol or β-phellandrene. As a result, CYP267A1 and CYP267B1 may be promising candidates to act as terpene/terpenoid-oxidase. This preliminary work might be used for further studies towards this large class of substrates that is of particular interest for the production of flavor and fragrance as well as pharmaceutical compounds.

The identification of their physiological roles is another important topic, which should be investigated in more detail. Analyses of the genomic context were already done but potential functions are just presumed and need to be proven (Khatri *et al.* 2011). The reconstitution of the biosynthetic gene clusters involved in the secondary metabolite formation might elucidate the physiological roles of the P450s. However, such an approach is only feasible for the P450s CYP263A1 and CYP265A1, since solely these P450s are clustered with genes potentially involved in the secondary metabolite formation. Another approach could be the knockout of specific P450s to check if their biodiversity is bound up with using different carbon sources for growth. CYP109C1 and CYP267A1 are clustered with carbohydrate-metabolism related genes. The knockout of their corresponding genes might influence the growth of the bacterium on diverse carbon sources. Moreover, improved analytic studies concerning the metabolomics might lead to the identification of diverse secondary metabolites as well as their intermediates. A comparison of those metabolites with the substrates and products characterized in this study may identify structurally similar compounds. Such an approach could be used to specify their physiological roles.

4 Appendix

4.1 Supplemental data

4.1.1 Carotenoid-derived aroma compounds as substrates

4.1.1.1 Screening of carotenoid-derived aroma compounds

The carotenoid-derived aroma compounds were screened with CYP109C1, CYP109C2, CYP109D1, CYP260A1, CYP264A1, CYP264B1 and CYP267A1 and analyzed by GC-MS as shown before (see 2.3).

Table 2: Screening of carotenoid-derived aroma compounds with selected P450s from So ce56. Conversions are marked with – (no conversion), + (<10%), ++ (<50%), +++ (>50%), us (unselective product formation, 3 or more products) and s (selective, maximum of 2 products).

substrate	CYP109C1	CYP109C2	CYP109D1	CYP260A1	CYP264A1	CYP264B1	CYP267A1
α-ionone	-	-	++ (s) (Khatri *et al.* 2010a)	+ (us)	+ (us)	++ (s) (Ly *et al.* 2012)	++ (us)
β-ionone	-	-	++ (s) (Khatri *et al.* 2010a)	++ (s)	++ (s)	++ (s) (Ly *et al.* 2012)	++ (s)
Dihydro-α-ionone	-	-	+ (s)	+ (us)	++ (us)	+ (us)	++ (us)
Dihydro-β-ionone	-	-	+ (s)	++ (s)	++ (s)	-	++ (s)
Methyl-α-ionone	-	-	+ (s)	+ (us)	+ (us)	+ (us)	+ (us)
Isomethyl-α-ionone	-	-	+ (s)	Traces of product	+ (us)	+ (s)	Traces of product
Allyl-α-ionone	-	-	Traces of product	Traces of product	+ (s)	Traces of product	Traces of product
α-ionol	-	-	+ (s)	+ (us)	+ (us)	Traces of product	+ (us)
β-ionol	-	-	+ (us)	+ (us)	+ (us)	+ (s)	++ (us)
α-irone (diastereomeric mixture -> No selectivity determined)	-	-	+	+	++	+	+
α-damascone	-	+ (s)	+ (s)	+ (us)	++ (us)	-	+ (s)
β-damascone	-	+ (s)	+ (s)	+ (s)	++ (s)	+ (s)	+ (s)
δ-damascone	-	+ (s)	+ (us)	+ (us)	+++ (s)	+ (us)	+ (us)
β-damascenone	-	+ (s)	+ (s)	+ (s)	+++ (us)	++ (s)	+ (s)
	CYP260B1	CYP267A1	CYP267B1				
Retinol*	-	-	-				

* *In vitro* reactions were performed as described before (see 2.3), with the exception that retinol was dissolved in Tween80, ascorbic acid was added as radical scavenger and that the reaction was analyzed by HPLC-DAD.

4.1.1.2 Whole-cell conversions of carotenoid-derived aroma compounds

During the whole-cell conversion of n-methyl-α-ionone by CYP267B1, an additional product was isolated in sufficient amounts for NMR-characterization and characterized as 3-keto-n-methyl α-ionone:

^{1}H NMR ($CDCl_3$): 6.68 (dd, 1H, H7), 6.18 (dd, 1H, H8), 5,96 (br s, 1H, H4), 2.69 (d, 1H, H6), 2.57 (q, 2H, H10), 2.36-2.30 (m, 1H, H2a), 2.01 (d, 1H, H2b), 1.87 (d, 3H, Me5), 1.50 (s, 3H, Me1a), 0.98 (s, 3H, Me1b); ^{13}C NMR ($CDCl_3$): 200.32 (C9), 198.32 (C3), 159.49 (C5), 142.58 (C7), 132.88 (C8), 55.67 (C6), 47.60 (C2), 34.94 (C1), 33.84 (C10), 28.17 (Me1a), 27.54 (Me1b), 23.74 (Me5), 8.17 (C11).

The whole-cell conversion of α-ionone by CYP260B1 led to a variety of compounds. The purification of the products was not sufficient to characterize all compounds by NMR spectroscopy. Nevertheless, the epoxy product was also identified for non-substituted α-ionone:

^{1}H NMR ($CDCl_3$): 6.65 (dd, 1H, H7), 6.08 (d, 1H, H8), 3.08 (t, 1H, H4), 2.28 (s, H3, Me10), 2.06 (d, 1H, H6), 1.90-1.83 (m, 2H, H3), 1.47-1.43 (m, 1H, H1a), 1.26 (s, 3H, Me5), 1.02-0.99 (m, 1H, H1b), 0.91 (s, 3H, Me1a), 0.73 (s, 3H, H1b); ^{13}C NMR ($CDCl_3$): 197.78 (C9), 145.20 (C7), 134.07 (C8), 59.49 (C4), 58.83 (C5), 52.44 (C6), 28.65 (C2), 28.44 (C1), 27.90 (Me1a), 27.48 (Me1b), 26.39 (C10), 22.68 (C11), 21.70 (C3).

4.1.1.3 Comparison of CYP260B1 and CYP267B1 with CYP109D1

```
CYP260B1      ----------------------MLPRKNLFSFTSKDPSAFGIHLAAAAREH-SVYFDEG
CYP109D1      -METETAPSPSPEQIDLSAPSVIADPYPAYRALRGRSPVLYARV-PAGGAAG-LGEP---
CYP267B1      MVDQDA-------FPELFHPSSRAEPH-----------AIYARM-RAAGRLHRLVHPRLD

CYP260B1      LGVPVVLRGADVVAVLRDSETFSTRT--------------YDTGIMKGALVTLGGEAHTR
CYP109D1      IRAYALLRHAEVLAALRDPQTFS------SNVTD------KIRVLPRITLLHDDPPRHTH
CYP267B1      VPIWVAVRYDDCVELLKDPRLIRDFRKLPDEVRRRYFPLSDRTTFMDQHMLDADPPDHTR

CYP260B1      MRRLFNAVLSPRVISRYEEATVTPVARRVVERLVRKERAELFDDFAISMPMGVTSALFGL
CYP109D1      LRRLVSRSFTPRRIAELEP-WIGRLAASLLEATGD-GPSDLMGAYAMPLPMMVIATLLGI
CYP267B1      LRAIVQRAFSPRMMEGLRP-RIQEIADGLIDAVIDRRRMELIADFAFPLPTAVIAELLGL

CYP260B1      PEERIAENDALIRKMIRSVVMPQDPVVVAEGRSAHAAMEAQLREIAEREVAHPSDTLLGE
CYP109D1      PAERYVQFRSWSESVMS---YSGIPA--EERASRGKAMVDFFAAELEARRRAPSGDLISA
CYP267B1      PVEDRGRFRRWTKILLA---PAKDREFVERAQPVVEEFAAYFRALADARRKAPRDDLISG

CYP260B1      IARAIVAEGLGGVEACEGVVLTLILGSYETTSWMLANLLVALLAHPDAMNQLRQQPSLLP
CYP109D1      LVEAEIDGARLDTPEAVGFCVGLLVAGNDTTTNLIGNMAHLLSERPELYRRAQQDRSLVG
CYP267B1      LLLAEEQEHKLSPAELSSMVFLLLVAGHETTVHLIASGMLLLLSHPAERRRLDEDPGLVG

CYP260B1      QAIEESTRWCSSAAG-IVRFVEREATIGGETLAAGTILYLSLIARHYDEEIYPRPETFDI
CYP109D1      PIIEETLRHSSPVQR-LLRVTTRPVDVSGVMIPAGHLVDVVFGAANRDPAVFEEPDAFRL
CYP267B1      SAVEEALRCEGPAELSTIRWSLEDIELFGARVPAGEGVAAGLLAANRDPQHFPDPDRFDI

CYP260B1      HRRPVGMLNFGGGLHYCVGAPLARMEARVGVSLLLERFPALRADPTVQP-TFSTAP--RG
CYP109D1      DRPPAEHLAFGQGTHFCIGAALARMEARIALNALLDCYESITPGE---------APPLRQ
CYP267B1      GRSPNRHIGFGGGIHFCLGAMLARIEAAIAFSTLLRRLPRIELATSTRDIVWSEWPTIRG

CYP260B1      A---AAFGPDQIPALLV------           ->28% identity
CYP109D1      TRAIMPLGFESLPLVLRRSRATA
CYP267B1      -PAAVPVVF--------------           ->33% identity
```

4.1.1.4 Comparison of CYP260B1 and CYP267B1 with CYP264B1

```
CYP260B1      ---MLPRKNLFSFTS-KDPSAFGIHLAAAAREHSVY-FDEGLGVPVVLRGADVVAVLRDS
CYP264B1      ----MTRLNLFAPEVRENPYPFYAALRRESPVCQ----VDPNGMWVVTRYDDIVAAFKNT
CYP267B1      MVDQDAFPELFHPSSRAEPHAIYARMRAAGRLHRLVHPRLDVPIWVAVRYDDCVELLKDP

CYP260B1      ETFSTRT--------------YDTGIMKGALVTLGGEAHTRMRRLFNAVLSPRVISRYEE
CYP264B1      QVFSSAGLR-M---ATEPPYLRRQNPLSGSMILADPPRHGQLRSISSRAFTANMVSTLEH
CYP267B1      RLIRDFRKLPDEVRRRYFPLSDRTTFMDQHMLDADPPDHTRLRAIVQRAFSPRMMEGLRP

CYP260B1      ATVTPVARRVVERLVRKERAELFDDFAISMPMGVTSALFGLPEERIAENDALIRKMI-RS
CYP264B1      -HMRSMAVRLTDDLVHRRVVEFISEFASRAQVSVLAKLIGFDPGLEGHFKRWATDLVIVG
CYP267B1      -RIQEIADGLIDAVIDRRRMELIADFAFPLPTAVIAELLGLPVEDRGRFRRWTKILLA--

CYP260B1      VVMPQDPVVVAEGRSAHAAMEAQLREIAEREVAHPSDTLLGEIARAIVAEGLGGVEACEG
CYP264B1      VIPPEDHARIAEVRRTIDEMEQYMLGLLASRRRHLENDLVSELLRSRRDDDGITDQDLVS
CYP267B1      --PAKDREFVERAQPVVEEFAAYFRALADARRKAPRDDLISGLLLAEEQEHKLSPAELSS

CYP260B1      VVLTLILGSYETTSWMLANLLVALLAHPDAMNQLRQQPSLLPQAIEESTRWCSSAA-GIV
CYP264B1      LLSLLLVAGLETSTSLMTHMVLILAQRPMWMDRLRAEPALIPHFIEEVMRFEAPVH-ATM
CYP267B1      MVFLLLVAGHETTVHLIASGMLLLLSHPAERRRLDEDPGLVGSAVEEALRCEGPAELSTI

CYP260B1      RFVEREATIGGETLAAGTILYLSLIARHYDEEIYPRPETFDIHRRPVGMLNFGGGLHYCV
CYP264B1      RLTVTETELGGTRLPAHAVVALLISSGLRDEARFQEPDRFNPERGDQANLAFGHGAHFCL
CYP267B1      RWSLEDIELFGARVPAGEGVAAGLLAANRDPQHFPDPDRFDIGRSPNRHIGFGGGIHFCL

CYP260B1      GAPLARMEARVGVSLLLERFPALRADPTVQ-PTFSTAPRGAAAFGPDQIPALLV------
CYP264B1      GVFLARVQARIVLEELLRRCHRIVLRT--DRLEWQAAL---NTRSPVALPIEVIPVSTTA
CYP267B1      GAMLARIEAAIAFSTLLRRLPRIELATSTRDIVWSEWP---TIRGPAAVPVVF-------

CYP260B1      -----------     ->24% identity
CYP264B1      ARESPVVQGIW
CYP267B1      -----------     ->33% identity
```

4.1.2 Screening of terpenes and terpenoids

Table 3: Screening of terpenes and terpenoids by selected P450s from So ce56. Conversions are marked with – (no conversion), + (<10%), ++ (<50%), +++ (> 50%) and n.d. (not determined).

substrate	CYP 109C1	CYP 109C2	CYP 109D1	CYP 260A1	CYP 260B1	CYP 264A1	CYP 264B1	CYP 267A1	CYP 267B1
τ-muurolol	-	-	-	+	-	+	-	+	++
β-phellandrene	-	-	-	-	-	-	-	++	++
nootkatone	n.d.	n.d.	-*	+++	+++*	-*	+++	+++	+++

* Tested by Michael Ringle

In vitro reactions were performed as shown before (see 2.3). The temperature profile for the measurements was adjusted for these substances; the starting temperature was 50°C and then the temperature was ramped to 300°C with a rate of 10°C/min.

4.1.3 Screening of aromatic compounds

Table 4: Screening of aromatic compounds by selected P450s from So ce56. Conversions are marked with – (no conversion), + (<10%), ++ (<50%), +++ (> 50%) and n.d. (not determined).

substrate	CYP109C1	CYP109C2	CYP109D1	CYP260A1	CYP260B1	CYP264A1	CYP264B1
4-allylanisole	-	-	-	-	-	-	-
eugenol	-	-	-	-	-	-	-
4-ethylphenol	-	-	-	-	-	-	-
4-picoline	-	-	-	-	-	-	-
cinnamyl alcohol	n.d.	n.d.	n.d.	n.d.	-	n.d.	n.d.
cinnamaldehyde	Traces of product	Traces of product	+	Traces of product	+++	Traces of product	Traces of product
cinnamic acid	n.d.	n.d.	n.d.	n.d.	-	n.d.	n.d.

In vitro reactions were performed as shown before (see 2.3) with small modifications. After extraction, the solvent was removed to a total volume of about 40 µl and then analyzed by GC-MS. The temperature profile for the measurements was also adjusted for these substances; the starting temperature was 40°C and then the temperature was ramped to 170°C with a rate of 10°C/min.

Cinnamaldehyde and derivatives were solely analyzed by HPLC-DAD. The whole-cell conversion of cinnamaldehyde by CYP260B1 as well as extraction and purification of the product was done as described previously (see 2.3). The product was characterized by NMR spectroscopy and identified as cinnamic acid (see Figure 9).

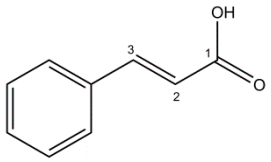

Figure 9: Structure of cinnamic acid.

NMR data:

^{1}H NMR ($CDCl_3$): 7.62 (d, J=16.0 Hz, H3), 7.40-7.00 (Ar-H, 5x), 6.29 (d, J= 16.0, H2); ^{13}C NMR ($CDCl_3$): 172.06 (C1), 147.00 (C3), 130.72 (Ar), 128.94 (Ar, 2x), 128.25 (Ar, 2x), 126.45 (Ar), 117.29 (C2).

4.1.4 Screening of drugs

In addition to the published data (see 2.4), some drugs were additionally screened with CYP109C1, CYP109C2, CYP109D1, CYP260A1, CYP260B1, CYP264A1 and CYP264B1.

Table 5: Screening of drugs with selected myxobacterial P450s. Conversions are marked with – (no conversion) or the value for the total conversion in [%].

substrate	CYP109C1	CYP109C2	CYP109D1	CYP260A1	CYP260B1	CYP264A1	CYP264B1
amodiaquine	-	-	-	-	-	-	-
papaverine	-	-	-	Traces of product	-	-	-
diclofenac	-	-	-	Traces of product	-	Traces of product	Traces of product
diltiazem	-	-	-	Traces of product	-	-	-
haloperidol	-	-	-	~5%	Traces of product	-	-
losartan	-	-	-	-	-	-	-
piroxicam	-	-	-	-	-	-	-
quinine	-	-	-	~30% (2 products)	-	-	-
repaglinide	-	-	-	-	-	Traces of product	-
ritonavir	-	-	-	-	-	Traces of product	-
tamoxifen	-	-	-	-	-	-	-

4.2 Abbreviations

AdR	Adrenodoxin reductase
Adx	Adrenodoxin
°C	Degree Celcius
CYP	Cytochrome P450
δ	Chemical shift [ppm]
CPR	Cytochrome P450 reductase
Da	Dalton
DAD	Diode array detector
DMSO	Dimethyl sulfoxide
E. coli	Escherichia coli
EDTA	Ethylenediaminetetraacetate
FAD	Flavine adenine dinucleotide
FDA	Food and drug administration
FMN	Flavine mononucleotide
g	Gram
GC	Gas chromatogaphy
GPP	Geranyl pyrophosphate
h	Hour
HPLC	High performance liquid chromatography
Hz	Hertz
J	Coupling constant
l	Liter
M	Molar
m	Meter
MS	Mass spectrometry
min	Minute
n.d.	Not determined
NADPH	Nicotinamide adenine dinucleotide phosphate
NMR	Nuclear magnetic resonance spectroscopy
NRPS	Nonribosomal polypeptide synthase
ORF	Open reading frame
P450	Cytochrome P450

PKS	Polyketide synthase
ppm	Parts per million
rpm	Rounds per minute
s	Second
SRS	Substrate recognition site
T	Temperature
UV/Vis	Ultraviolet–visible spectroscopy

Abbreviations for amino acids

A	Alanine	M	Methionine
C	Cysteine	N	Asparagine
D	Aspartate	P	Proline
E	Glutamate	Q	Glutamine
F	Phenylalanine	R	Arginine
G	Glycine	S	Serine
H	Histidine	T	Threonine
I	Ispleucine	V	Valine
K	Lysine	W	Tryptophan
L	Leucine	Y	Tyrosine

5 References

Agematu, H., N. Matsumoto, Y. Fujii, H. Kabumoto, S. Doi, K. Machida, J. Ishikawa and A. Arisawa (2006). "Hydroxylation of testosterone by bacterial cytochromes P450 using the Escherichia coli expression system." Bioscience, biotechnology and biochemistry **70**(1): 307-311.

Ajikumar, P. K., W. H. Xiao, K. E. Tyo, Y. Wang, F. Simeon, E. Leonard, O. Mucha, T. H. Phon, B. Pfeifer and G. Stephanopoulos (2010). "Isoprenoid pathway optimization for Taxol precursor overproduction in Escherichia coli." Science **330**(6000): 70-74.

Alonso-Gutierrez, J., R. Chan, T. S. Batth, P. D. Adams, J. D. Keasling, C. J. Petzold and T. S. Lee (2013). "Metabolic engineering of Escherichia coli for limonene and perillyl alcohol production." Metabolic engineering **19**: 33-41.

Appleby, A. C. (1967). "A soluble haemoprotein P 450 from nitrogen-fixing Rhizobium bacteroids." Biochimica et biophysica acta **147**(2): 399-402.

Barakat, A., E. Brenna, C. Fuganti and S. Serra (2008). "Synthesis, olfactory evaluation and determination of the absolute configuration of the β- and γ-Iralia® isomers." Tetrahedron: Asymmetry **19**(19): 2316-2322.

Bernhardt, R. (2006). "Cytochromes P450 as versatile biocatalysts." Journal of biotechnology **124**(1): 128-145.

Bernhardt, R. and V. B. Urlacher (2014). "Cytochromes P450 as promising catalysts for biotechnological application: chances and limitations." Applied microbiology and biotechnology **98**(14): 6185-6203.

Bhatti, H. N. and R. A. Khera (2012). "Biological transformations of steroidal compounds: a review." Steroids **77**(12): 1267-1290.

Braun, A., M. Geier, B. Buhler, A. Schmid, S. Mauersberger and A. Glieder (2012). "Steroid biotransformations in biphasic systems with Yarrowia lipolytica expressing human liver cytochrome P450 genes." Microbial cell factories **11**(106): 1475-2859.

Brenna, E., C. Fuganti, S. Serra and P. Kraft (2002). "Optically Active Ionones and Derivatives: Preparation and Olfactory Properties." European Journal of Organic Chemistry **2002**(6): 967-978.

Brixius-Anderko, S., L. Schiffer, F. Hannemann, B. Janocha and R. Bernhardt (2015). "A CYP21A2 based whole-cell system in Escherichia coli for the biotechnological production of premedrol." Microbial cell factories **14**(135): 015-0333.

Coelho, P. S., Z. J. Wang, M. E. Ener, S. A. Baril, A. Kannan, F. H. Arnold and E. M. Brustad (2013). "A serine-substituted P450 catalyzes highly efficient carbene transfer to olefins in vivo." Nature chemical biology **9**(8): 485-487.

de Visser, S. P., F. Ogliaro, P. K. Sharma and S. Shaik (2002). "What factors affect the regioselectivity of oxidation by cytochrome p450? A DFT study of allylic hydroxylation and double bond epoxidation in a model reaction." Journal of American Chemical Society **124**(39): 11809-11826.

Denisov, I. G., T. M. Makris, S. G. Sligar and I. Schlichting (2005). "Structure and chemistry of cytochrome P450." Chemical reviews **105**(6): 2253-2277.

Donova, M. V. and O. V. Egorova (2012). "Microbial steroid transformations: current state and prospects." Applied microbiology and biotechnology **94**(6): 1423-1447.

Estabrook, R. W., D. Y. Cooper and O. Rosenthal (1963). "The Light Reversible Carbon Monoxide Inhibition of the Steroid C21-Hydroxylase System of the Adrenal Cortex." Biochemische Zeitschrift **338**: 741-755.

Ewen, K. M., F. Hannemann, Y. Khatri, O. Perlova, R. Kappl, D. Krug, J. Huttermann, R. Müller and R. Bernhardt (2009). "Genome mining in Sorangium cellulosum So ce56: identification and characterization of the homologous electron transfer proteins of a myxobacterial cytochrome P450." Journal of biological chemistry **284**(42): 28590-28598.

Ewen, K. M., M. Ringle and R. Bernhardt (2012). "Adrenodoxin--a versatile ferredoxin." IUBMB Life **64**(6): 506-512.

Fasan, R. (2012). "Tuning P450 Enzymes as Oxidation Catalysts." ACS Catalysis **2**(4): 647-666.

FDA (2008). "Food and Drug Adminitration: Guidance for Industry: Safety Testing of Drug Metabolites, U.S. Department of Health and Human Services, Food and Drug Administration, Rockville, MD."

Gagarina, A. B., N. M. Evteena, W. Pritzkow, A. Shabanova, L. Willecke, V. Voerckel and W. Schmidt-Renner (1984). "Elucidation of two Main Autoxidation Products of β-Ionone." Journal für Praktische Chemie **326**(4): 686-688.

Garfinkel, D. (1958). "Studies on pig liver microsomes. I. Enzymic and pigment composition of different microsomal fractions." Archives of biochemistry and biophysics **77**(2): 493-509.

Gerth, K., N. Bedorf, G. Hofle, H. Irschik and H. Reichenbach (1996). "Epothilons A and B: antifungal and cytotoxic compounds from Sorangium cellulosum (Myxobacteria). Production, physico-chemical and biological properties." Journal of antibiotics **49**(6): 560-563.

Gillam, E. M. (2008). "Engineering cytochrome p450 enzymes." Chemical research in toxicology **21**(1): 220-231.

Girhard, M., T. Klaus, Y. Khatri, R. Bernhardt and V. B. Urlacher (2010). "Characterization of the versatile monooxygenase CYP109B1 from Bacillus subtilis." Applied microbiology and biotechnology **87**(2): 595-607.

Girhard, M., K. Machida, M. Itoh, R. D. Schmid, A. Arisawa and V. B. Urlacher (2009). "Regioselective biooxidation of (+)-valencene by recombinant E. coli expressing CYP109B1 from Bacillus subtilis in a two-liquid-phase system." Microbial cell factories **8**(36): 1475-2859.

Gotoh, O. (1992). "Substrate recognition sites in cytochrome P450 family 2 (CYP2) proteins inferred from comparative analyses of amino acid and coding nucleotide sequences." Journal of biological chemistry **267**(1): 83-90.

Graham, S. E. and J. A. Peterson (1999). "How similar are P450s and what can their differences teach us?" Archives of biochemistry and biophysics **369**(1): 24-29.

Guengerich, F. P. (2001). "Common and uncommon cytochrome P450 reactions related to metabolism and chemical toxicity." Chemical research in toxicology **14**(6): 611-650.

Guengerich, F. P. and Q. Cheng (2011). "Orphans in the human cytochrome P450 superfamily: approaches to discovering functions and relevance in pharmacology." Pharmacological reviews **63**(3): 684-699.

Gunsalus, I. C., T. C. Pederson and S. G. Sligar (1975). "Oxygenase-catalyzed biological hydroxylations." Annual review of biochemistry **44**: 377-407.

Hannemann, F., A. Bichet, K. M. Ewen and R. Bernhardt (2007). "Cytochrome P450 systems--biological variations of electron transport chains." Biochimica et biophysica acta **3**: 330-344.

Hlavica, P. (2015). "Mechanistic basis of electron transfer to cytochromes p450 by natural redox partners and artificial donor constructs." Advances in experimental medicine and biology **851**: 247-297.

ICH (2009). "European Medicines Agency: ICH Guidance M3(R2) on Non-Clinical Safety Studies for the Conduct of Human Clinical Trials and Marketing Authorisation for Pharmaceuticals, European Medicines Agency, London."

Ilie, A., R. Lonsdale, R. Agudo and M. T. Reetz (2015). "A diastereoselective P450-catalyzed epoxidation reaction: anti versus syn reactivity." Tetrahedron Letters **56**(23): 3435-3437.

Janocha, S. and R. Bernhardt (2013). "Design and characterization of an efficient CYP105A1-based whole-cell biocatalyst for the conversion of resin acid diterpenoids in permeabilized Escherichia coli." Applied microbiology and biotechnology **97**(17): 7639-7649.

Janocha, S., D. Schmitz and R. Bernhardt (2015). "Terpene hydroxylation with microbial cytochrome P450 monooxygenases." Advances in biochemical engineering/biotechnology **148**: 215-250.

Julien, B. and S. Shah (2002). "Heterologous expression of epothilone biosynthetic genes in Myxococcus xanthus." Antimicrobial agents and chemotherapy **46**(9): 2772-2778.

Julsing, M. K., S. Cornelissen, B. Buhler and A. Schmid (2008). "Heme-iron oxygenases: powerful industrial biocatalysts?" Current opinion in chemical biology **12**(2): 177-186.

Jung, S. T., R. Lauchli and F. H. Arnold (2011). "Cytochrome P450: taming a wild type enzyme." Current opinion in biotechnology **22**(6): 809-817.

Kang, J. Y., S. H. Ryu, S. H. Park, G. S. Cha, D. H. Kim, K. H. Kim, A. W. Hong, T. Ahn, J. G. Pan, Y. H. Joung, H. S. Kang and C. H. Yun (2014). "Chimeric cytochromes P450 engineered by domain swapping and random mutagenesis for producing human metabolites of drugs." Biotechnology and bioengineering **111**(7): 1313-1322.

Katagiri, M., B. N. Ganguli and I. C. Gunsalus (1968). "A soluble cytochrome P-450 functional in methylene hydroxylation." Journal of biological chemistry **243**(12): 3543-3546.

Kelly, S. L. and D. E. Kelly (2013). "Microbial cytochromes P450: biodiversity and biotechnology. Where do cytochromes P450 come from, what do they do and what can they do for us?" Philosophical transactions of the Royal Society of London. Series B, Biological sciences. **368**(1612): 19.

Kelly, S. L., D. C. Lamb, C. J. Jackson, A. G. Warrilow and D. E. Kelly (2003). "The biodiversity of microbial cytochromes P450." Advances in microbial physiology **47**: 131-186.

Kern, F., T. K. Dier, Y. Khatri, K. M. Ewen, J. P. Jacquot, D. A. Volmer and R. Bernhardt (2015). "Highly Efficient CYP167A1 (EpoK) dependent Epothilone B Formation and Production of 7-Ketone Epothilone D as a New Epothilone Derivative." Scientific reports **5**(14881).

Khatri, Y., M. Girhard, A. Romankiewicz, M. Ringle, F. Hannemann, V. B. Urlacher, M. C. Hutter and R. Bernhardt (2010a). "Regioselective hydroxylation of norisoprenoids by CYP109D1 from Sorangium cellulosum So ce56." Applied microbiology and biotechnology **88**(2): 485-495.

Khatri, Y., F. Hannemann, K. M. Ewen, D. Pistorius, O. Perlova, N. Kagawa, A. O. Brachmann, R. Müller and R. Bernhardt (2010b). "The CYPome of Sorangium cellulosum So ce56 and identification of CYP109D1 as a new fatty acid hydroxylase." Chemistry & biology **17**(12): 1295-1305.

Khatri, Y., F. Hannemann, M. Girhard, R. Kappl, A. Même, M. Ringle, S. Janocha, E. Leize-Wagner, V. B. Urlacher and R. Bernhardt (2013). "Novel family members of CYP109 from Sorangium cellulosum So ce56 exhibit characteristic biochemical and biophysical properties." Biotechnology and Applied Biochemistry **60**(1): 18-29.

Khatri, Y., F. Hannemann, O. Perlova, R. Müller and R. Bernhardt (2011). "Investigation of cytochromes P450 in myxobacteria: excavation of cytochromes P450 from the genome of Sorangium cellulosum So ce56." FEBS Letters **585**(11): 1506-1513.

Khatri, Y., M. Ringle, M. Lisurek, J. P. Kries, J. Zapp and R. Bernhardt (2015). "Substrate hunting for the myxobacterial CYP260A1 revealed novel 1alpha-hydroxylated products from C-19 steroids." Chembiochem **19**(10): in press.

Kiss, F. M., Y. Khatri, J. Zapp and R. Bernhardt (2015). "Identification of new substrates for the CYP106A1-mediated 11-oxidation and investigation of the reaction mechanism." FEBS Letters **589**(18): 2320-2326.

Klingenberg, M. (1958). "Pigments of rat liver microsomes." Archives of biochemistry and biophysics **75**(2): 376-386.

Koeller, K. M. and C. H. Wong (2001). "Enzymes for chemical synthesis." Nature **409**(6817): 232-240.

Kraft, P., J. A. Bajgrowicz, C. Denis and G. Frater (2000). "Odds and Trends: Recent Developments in the Chemistry of Odorants " Angewandte Chemie (International Edition) **39**(17): 2980-3010.

Kulig, J. K., C. Spandolf, R. Hyde, A. C. Ruzzini, L. D. Eltis, G. Gronberg, M. A. Hayes and G. Grogan (2015). "A P450 fusion library of heme domains from Rhodococcus jostii RHA1 and its evaluation for the biotransformation of drug molecules." Bioorganic & medicinal chemistry **23**(17): 5603-5609.

Kumar, S. (2010). "Engineering cytochrome P450 biocatalysts for biotechnology, medicine and bioremediation." Expert opinion on drug metabolism & toxicology **6**(2): 115-131.

Lamb, D. C., L. Lei, A. G. Warrilow, G. I. Lepesheva, J. G. Mullins, M. R. Waterman and S. L. Kelly (2009). "The first virally encoded cytochrome p450." Journal of virology **83**(16): 8266-8269.

Lebeault, J. M., E. T. Lode and M. J. Coon (1971). "Fatty acid and hydrocarbon hydroxylation in yeast: role of cytochrome P-450 in Candida tropicalis." Biochemical and biophysical research communications **42**(3): 413-419.

Li, G. and K. D. Young (2013). "Indole production by the tryptophanase TnaA in Escherichia coli is determined by the amount of exogenous tryptophan." Microbiology **159**(Pt 2): 402-410.

Liu, S., C. Li, X. Fang and Z. a. Cao (2004). "Optimal pH control strategy for high-level production of long-chain α,ω-dicarboxylic acid by Candida tropicalis." Enzyme and Microbial Technology **34**(1): 73-77.

Locuson, C. W., J. M. Hutzler and T. S. Tracy (2007). "Visible spectra of type II cytochrome P450-drug complexes: evidence that "incomplete" heme coordination is common." Drug metabolism and disposition **35**(4): 614-622.

Lundemo, M. T. and J. M. Woodley (2015). "Guidelines for development and implementation of biocatalytic P450 processes." Applied microbiology and biotechnology **99**(6): 2465-2483.

Luthra, A., I. G. Denisov and S. G. Sligar (2011). "Spectroscopic features of cytochrome P450 reaction intermediates." Archives of biochemistry and biophysics **507**(1): 26-35.

Ly, T. T., Y. Khatri, J. Zapp, M. C. Hutter and R. Bernhardt (2012). "CYP264B1 from Sorangium cellulosum So ce56: a fascinating norisoprenoid and sesquiterpene hydroxylase." Applied microbiology and biotechnology **95**(1): 123-133.

Matsuoka, T., S. Miyakoshi, K. Tanzawa, K. Nakahara, M. Hosobuchi and N. Serizawa (1989). "Purification and characterization of cytochrome P-450sca from Streptomyces carbophilus. ." European journal of biochemistry **184**(3): 707-713.

Meunier, B., S. P. de Visser and S. Shaik (2004). "Mechanism of Oxidation Reactions Catalyzed by Cytochrome P450 Enzymes." Chemical reviews **104**(9): 3947-3980.

Meyer, H.-P., E. Eichhorn, S. Hanlon, S. Lutz, M. Schurmann, R. Wohlgemuth and R. Coppolecchia (2013). "The use of enzymes in organic synthesis and the life sciences: perspectives from the Swiss Industrial Biocatalysis Consortium (SIBC)." Catalysis Science & Technology **3**(1): 29-40.

Munro, A. W., D. G. Leys, K. J. McLean, K. R. Marshall, T. W. Ost, S. Daff, C. S. Miles, S. K. Chapman, D. A. Lysek, C. C. Moser, C. C. Page and P. L. Dutton (2002). "P450 BM3: the very model of a modern flavocytochrome." Trends in biochemical sciences **27**(5): 250-257.

Nebert, D. W., M. Adesnik, M. J. Coon, R. W. Estabrook, F. J. Gonzalez, F. P. Guengerich, I. C. Gunsalus, E. F. Johnson, B. Kemper, W. Levin and et al. (1987). "The P450 gene superfamily: recommended nomenclature." DNA **6**(1): 1-11.

Nelson, D. R. (1999). "Cytochrome P450 and the individuality of species." Archives of biochemistry and biophysics **369**(1): 1-10.

Nelson, D. R. (2011). "Progress in tracing the evolutionary paths of cytochrome P450." Biochimica et biophysica acta **1**: 14-18.

Newman, D. J. and G. M. Cragg (2012). "Natural Products As Sources of New Drugs over the 30 Years from 1981 to 2010." Journal of Natural Products **75**(3): 311-335.

Niklasson, I. B., T. Delaine, M. N. Islam, R. Karlsson, K. Luthman and A.-T. Karlberg (2013). "Cinnamyl alcohol oxidizes rapidly upon air exposure." Contact Dermatitis **68**(3): 129-138.

Omura, T., E. Sanders, R. W. Estabrook, D. Y. Cooper and O. Rosenthal (1966). "Isolation from adrenal cortex of a nonheme iron protein and a flavoprotein functional as a reduced triphosphopyridine nucleotide-cytochrome P-450 reductase." Archives of biochemistry and biophysics **117**(3): 660-673.

Omura, T. and R. Sato (1962). "A New Cytochrome in Liver Microsomes." Journal of Biological Chemistry **237**(4): PC1375-PC1376.

Omura, T. and R. Sato (1964a). "The Carbon Monoxide-Binding Pigment of Liver Microsomes. I. Evidence for Its Hemoprotein Nature." Journal of Biological Chemistry **239**: 2370-2378.

Omura, T. and R. Sato (1964b). "The Carbon Monoxide-Binding Pigment of Liver Microsomes. Ii. Solubilization, Purification, and Properties." Journal of Biological Chemistry **239**: 2379-2385.

Ortiz de Montellano, P. R. (2010). "Hydrocarbon hydroxylation by cytochrome P450 enzymes." Chemical reviews **110**(2): 932-948.

Paddon, C. J., P. J. Westfall, D. J. Pitera, K. Benjamin, K. Fisher, D. McPhee, M. D. Leavell, A. Tai, A. Main, D. Eng, D. R. Polichuk, K. H. Teoh, D. W. Reed, T. Treynor, J. Lenihan, M. Fleck, S. Bajad, G. Dang, D. Dengrove, D. Diola, G. Dorin, K. W. Ellens, S. Fickes, J. Galazzo, S. P. Gaucher, T.

Geistlinger, R. Henry, M. Hepp, T. Horning, T. Iqbal, H. Jiang, L. Kizer, B. Lieu, D. Melis, N. Moss, R. Regentin, S. Secrest, H. Tsuruta, R. Vazquez, L. F. Westblade, L. Xu, M. Yu, Y. Zhang, L. Zhao, J. Lievense, P. S. Covello, J. D. Keasling, K. K. Reiling, N. S. Renninger and J. D. Newman (2013). "High-level semi-synthetic production of the potent antimalarial artemisinin." Nature **496**(7446): 528-532.

Pateraki, I., A. M. Heskes and B. Hamberger (2015). "Cytochromes P450 for terpene functionalisation and metabolic engineering." Advances in biochemical engineering/biotechnology **148**: 107-139.

Picataggio, S., T. Rohrer, K. Deanda, D. Lanning, R. Reynolds, J. Mielenz and L. D. Eirich (1992). "Metabolic Engineering of Candida Tropicalis for the Production of Long-Chain Dicarboxylic Acids." Nature biotechnology **10**(8): 894-898.

Podust, L. M. and D. H. Sherman (2012). "Diversity of P450 enzymes in the biosynthesis of natural products." Natural product reports **29**(10): 1251-1266.

Poulos, T. L., B. C. Finzel, I. C. Gunsalus, G. C. Wagner and J. Kraut (1985). "The 2.6-A crystal structure of Pseudomonas putida cytochrome P-450." Journal of biological chemistry **260**(30): 16122-16130.

Rasool, S. and R. Mohamed (2015). "Plant cytochrome P450s: nomenclature and involvement in natural product biosynthesis." Protoplasma **12**: 12.

Reichenbach, H. and G. Hofle (1993). "Biologically active secondary metabolites from myxobacteria." Biotechnology advances **11**(2): 219-277.

Ren, X., J. A. Yorke, E. Taylor, T. Zhang, W. Zhou and L. L. Wong (2015). "Drug Oxidation by Cytochrome P450BM3 : Metabolite Synthesis and Discovering New P450 Reaction Types." Chemistry **21**(42): 15039-15047.

Rendic, S. P. and F. P. Guengerich (2014). "Survey of Human Oxidoreductases and Cytochrome P450 Enzymes Involved in the Metabolism of Chemicals." Chemical research in toxicology **8**: 8.

Rentmeister, A., F. H. Arnold and R. Fasan (2009). "Chemo-enzymatic fluorination of unactivated organic compounds." Nature chemical biology **5**(1): 26-28.

Ringle, M., Y. Khatri, J. Zapp, F. Hannemann and R. Bernhardt (2013). "Application of a new versatile electron transfer system for cytochrome P450-based Escherichia coli whole-cell bioconversions." Applied microbiology and biotechnology **97**(17): 7741-7754.

Roberts, S. C. (2007). "Production and engineering of terpenoids in plant cell culture." Nature chemical biology **3**(7): 387-395.

Roiban, G. D. and M. T. Reetz (2015). "Expanding the toolbox of organic chemists: directed evolution of P450 monooxygenases as catalysts in regio- and stereoselective oxidative hydroxylation." Chemical communications **51**(12): 2208-2224.

Ruhmann, A. G. and D. L. Berliner (1967). "Influence of Steroids on Fibroblasts. II. The Fibroblast as an Assay System for Topical Anti-Inflammatory Potency of Corticosteroids1." The Journal of Investigative Dermatology **49**(2): 123-130.

Rylott, E. L., R. G. Jackson, J. Edwards, G. L. Womack, H. M. B. Seth-Smith, D. A. Rathbone, S. E. Strand and N. C. Bruce (2006). "An explosive-degrading cytochrome P450 activity and its targeted application for the phytoremediation of RDX." Nature biotechnology **24**(2): 216-219.

Schewe, H., B. A. Kaup and J. Schrader (2008). "Improvement of P450(BM-3) whole-cell biocatalysis by integrating heterologous cofactor regeneration combining glucose facilitator and dehydrogenase in E. coli." Applied microbiology and biotechnology **78**(1): 55-65.

Schiffer, L., S. Anderko, F. Hannemann, A. Eiden-Plach and R. Bernhardt (2015a). "The CYP11B subfamily." Journal of steroid biochemistry and molecular biology **151**: 38-51.

Schiffer, L., S. Anderko, A. Hobler, F. Hannemann, N. Kagawa and R. Bernhardt (2015b). "A recombinant CYP11B1 dependent Escherichia coli biocatalyst for selective cortisol production and optimization towards a preparative scale." Microbial cell factories **14**(25): 015-0209.

Schifrin, A., T. T. Ly, N. Gunnewich, J. Zapp, V. Thiel, S. Schulz, F. Hannemann, Y. Khatri and R. Bernhardt (2015). "Characterization of the gene cluster CYP264B1-geoA from Sorangium

cellulosum So ce56: biosynthesis of (+)-eremophilene and its hydroxylation." Chembiochem **16**(2): 337-344.

Schneiker, S., O. Perlova, O. Kaiser, K. Gerth, A. Alici, M. O. Altmeyer, D. Bartels, T. Bekel, S. Beyer, E. Bode, H. B. Bode, C. J. Bolten, J. V. Choudhuri, S. Doss, Y. A. Elnakady, B. Frank, L. Gaigalat, A. Goesmann, C. Groeger, F. Gross, L. Jelsbak, J. Kalinowski, C. Kegler, T. Knauber, S. Konietzny, M. Kopp, L. Krause, D. Krug, B. Linke, T. Mahmud, R. Martinez-Arias, A. C. McHardy, M. Merai, F. Meyer, S. Mormann, J. Munoz-Dorado, J. Perez, S. Pradella, S. Rachid, G. Raddatz, F. Rosenau, C. Ruckert, F. Sasse, M. Scharfe, S. C. Schuster, G. Suen, A. Treuner-Lange, G. J. Velicer, F. J. Vorholter, K. J. Weissman, R. D. Welch, S. C. Wenzel, D. E. Whitworth, S. Wilhelm, C. Wittmann, H. Blocker, A. Puhler and R. Müller (2007). "Complete genome sequence of the myxobacterium Sorangium cellulosum." Nature biotechnology **25**(11): 1281-1289.

Schulz, S., M. Girhard, S. K. Gaßmeyer, V. D. Jäger, D. Schwarze, A. Vogel and V. B. Urlacher (2015). "Selective Enzymatic Synthesis of the Grapefruit Flavor (+)-Nootkatone." ChemCatChem **7**(4): 601-604.

Shaik, S., S. P. de Visser, F. Ogliaro, H. Schwarz and D. Schroder (2002). "Two-state reactivity mechanisms of hydroxylation and epoxidation by cytochrome P-450 revealed by theory." Current opinion in chemical biology **6**(5): 556-567.

Shimkets, L., M. Dworkin and H. Reichenbach (2006). The myxobacteria, in The Prokaryotes. New York, Springer**:** 31-115.

Urlacher, V. B. and S. Eiben (2006). "Cytochrome P450 monooxygenases: perspectives for synthetic application." Trends in Biotechnology **24**(7): 324-330.

Urlacher, V. B. and M. Girhard (2012). "Cytochrome P450 monooxygenases: an update on perspectives for synthetic application." Trends in biotechnology **30**(1): 26-36.

Urlacher, V. B., S. Lutz-Wahl and R. D. Schmid (2004). "Microbial P450 enzymes in biotechnology." Applied microbiology and biotechnology **64**(3): 317-325.

Wang, G., W. Tang and R. R. Bidigare (2005). Terpenoids as therapeutic drugs and pharmaceutical agents. Natural products, Springer**:** 197-227.

Wang, M., D. L. Roberts, R. Paschke, T. M. Shea, B. S. S. Masters and J.-J. P. Kim (1997). "Three-dimensional structure of NADPH–cytochrome P450 reductase: Prototype for FMN- and FAD-containing enzymes." Proceedings of the National Academy of Sciences of the United States of America **94**(16): 8411-8416.

Watanabe, Y., S. Laschat, M. Budde, O. Affolter, Y. Shimada and V. B. Urlacher (2007). "Oxidation of acyclic monoterpenes by P450 BM-3 monooxygenase: influence of the substrate E/Z-isomerism on enzyme chemo- and regioselectivity." Tetrahedron **63**(38): 9413-9422.

Weitzel, C. and H. Simonsen (2015). "Cytochrome P450-enzymes involved in the biosynthesis of mono- and sesquiterpenes." Phytochemistry Reviews **14**(1): 7-24.

Werck-Reichhart, D. and R. Feyereisen (2000). "Cytochromes P450: a success story." Genome biology **1**(6): 8.

Whitehouse, C. J., S. G. Bell and L. L. Wong (2012). "P450(BM3) (CYP102A1): connecting the dots." Chemical Society reviews **41**(3): 1218-1260.

Withers, S. T. and J. D. Keasling (2007). "Biosynthesis and engineering of isoprenoid small molecules." Applied microbiology and biotechnology **73**(5): 980-990.

Yamazaki, Y., Y. Hayashi, M. Arita, T. Hieda and Y. Mikami (1988). "Microbial Conversion of alpha-Ionone, alpha-Methylionone, and alpha-Isomethylionone." Applied and environmental microbiology **54**(10): 2354-2360.

Yin, Y.-C., H.-L. Yu, Z.-J. Luan, R.-J. Li, P.-F. Ouyang, J. Liu and J.-H. Xu (2014). "Unusually Broad Substrate Profile of Self-Sufficient Cytochrome P450 Monooxygenase CYP116B4 from Labrenzia aggregata." Chembiochem **15**(16): 2443-2449.

Zelasko, S., A. Palaria and A. Das (2013). "Optimizations to achieve high-level expression of cytochrome P450 proteins using Escherichia coli expression systems." Protein expression and purification **92**(1): 77-87.

Zhang, W., Y. Liu, J. Yan, S. Cao, F. Bai, Y. Yang, S. Huang, L. Yao, Y. Anzai, F. Kato, L. M. Podust, D. H. Sherman and S. Li (2014). "New reactions and products resulting from alternative interactions between the P450 enzyme and redox partners." Journal of american Chemical Society **136**(9): 3640-3646.

Acknowledgements

I would like to express my deepest gratitude to my supervisor, Prof. Dr. Rita Bernhardt, for giving me the opportunity to work in this interesting field of research. I am grateful for her patient guidance, enthusiastic encouragement and useful critiques of this research work.

I would also like to thank Prof. Dr. Andreas Speicher for reviewing this thesis and being the second supervisor.

Special thanks to the members of the “Myxo group” Fedy Kern, Alexander Schifrin and Yogan Khatri for their great support and helpful advices during the last years.

I would also like to extend my thanks to Birgit Heider-Lips and Wolfgang Reinle for the protein purifications.

I also want to show my gratitude to Dr. Josef Zapp for measuring all the NMR samples.

Special acknowledgements go to all the current and former members of this working group for their scientific support and the great moments during the last three years.

Last but not least, i wish to thank my family for their support and encouragement throughout my study.